Study of the Electron-Transfer properties of phenolics and their relationship with the biological activity on cancer cells

Anna Carreras Cardona

UNIVERSITAT DE BARCELONA

CSIC
Consejo Superior de Investigaciones Científicas

iQAC

Study of the Electron-Transfer properties of phenolics and their relationship with the biological activity on cancer cells.

Anna Carreras Cardona, 2012

7. Annexes

Annex 1. IR spectra of HNTTM, TNPTM and DPPH.

A. HNTTM (**4**)

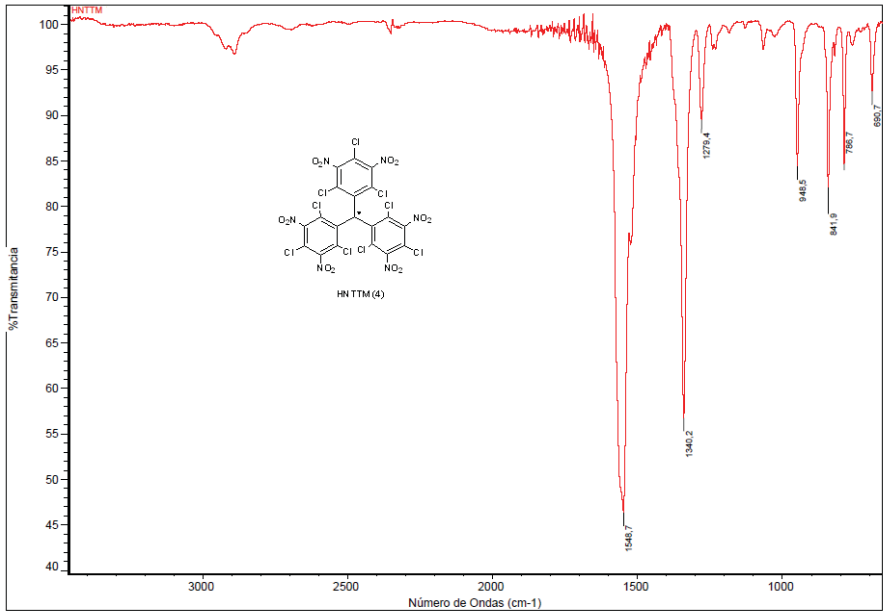

B. TNPTM (**8**)

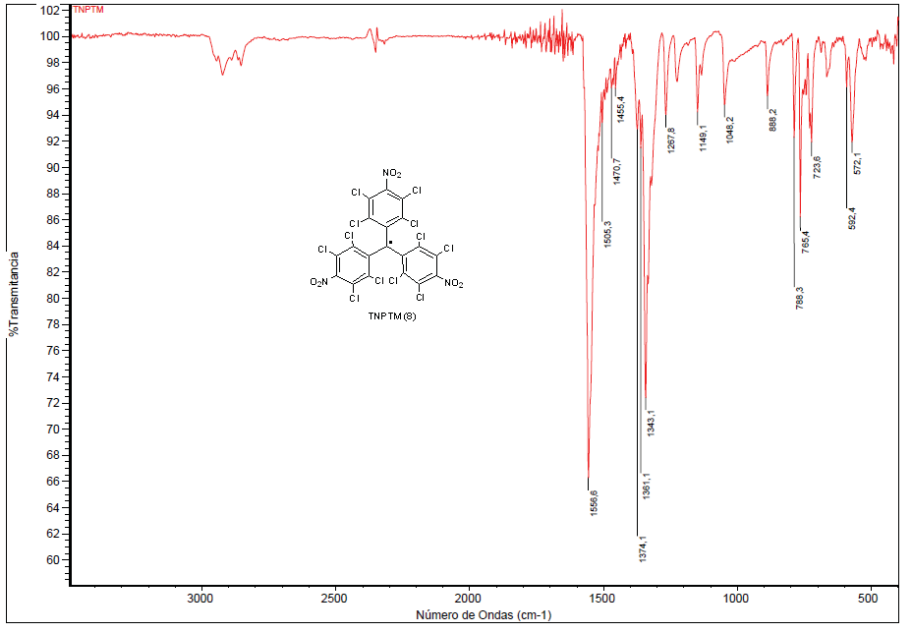

C. DPPH (**9**)

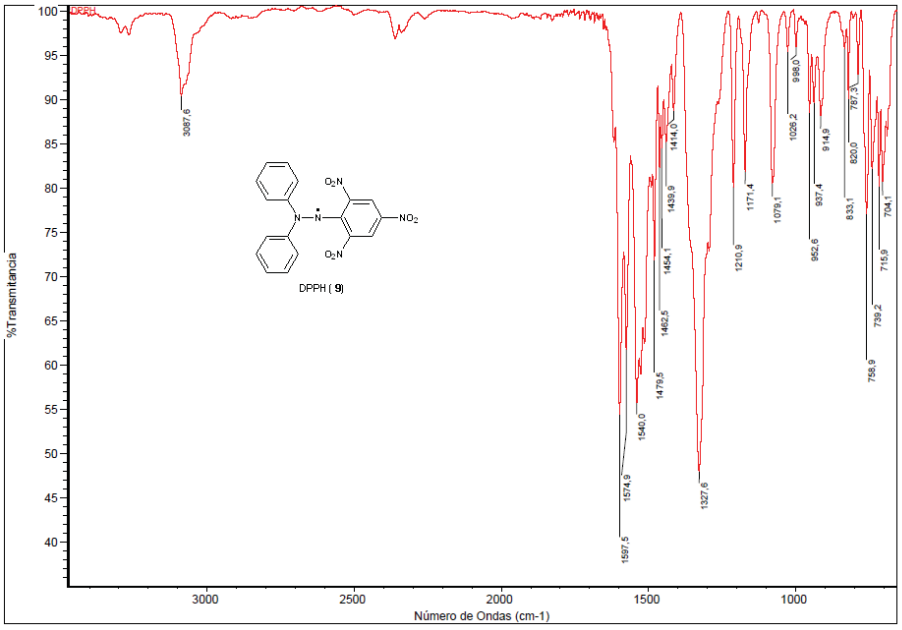

Annex 2. IR spectra of the products of HNTTM, TNPTM and DPPH in toluene

A. IR spectrum of the HNTTM product obtained after reflux of **4** in toluene.

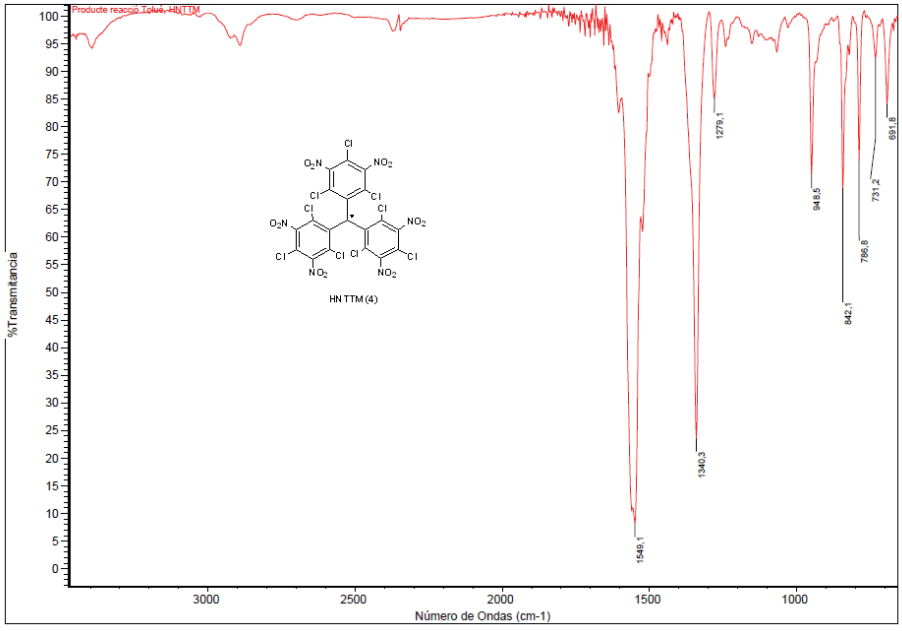

B. IR spectra of the TNPTM product obtained after reflux of **8** in toluene

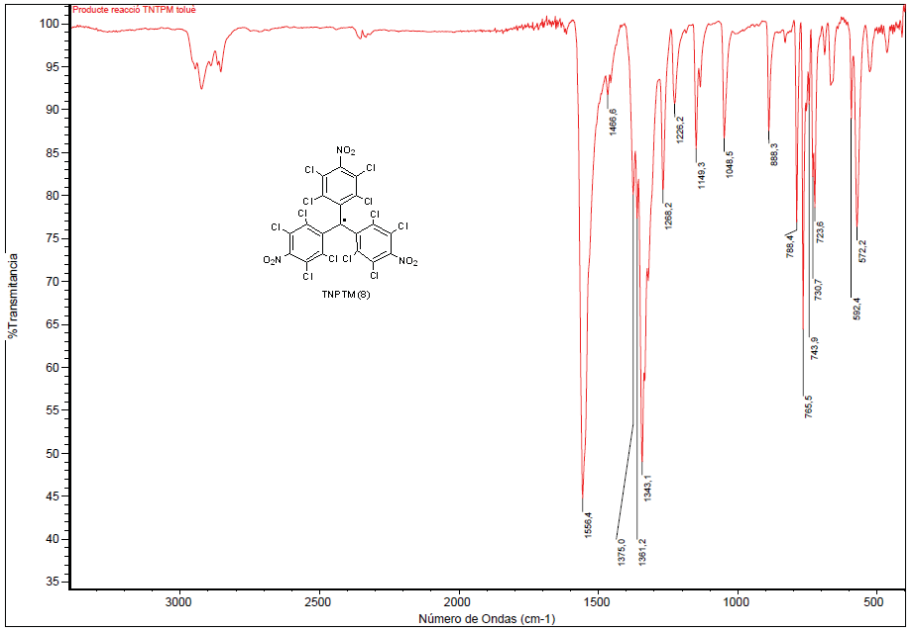

C. IR spectra of the DPPH product obtained after reflux of **9** in toluene.

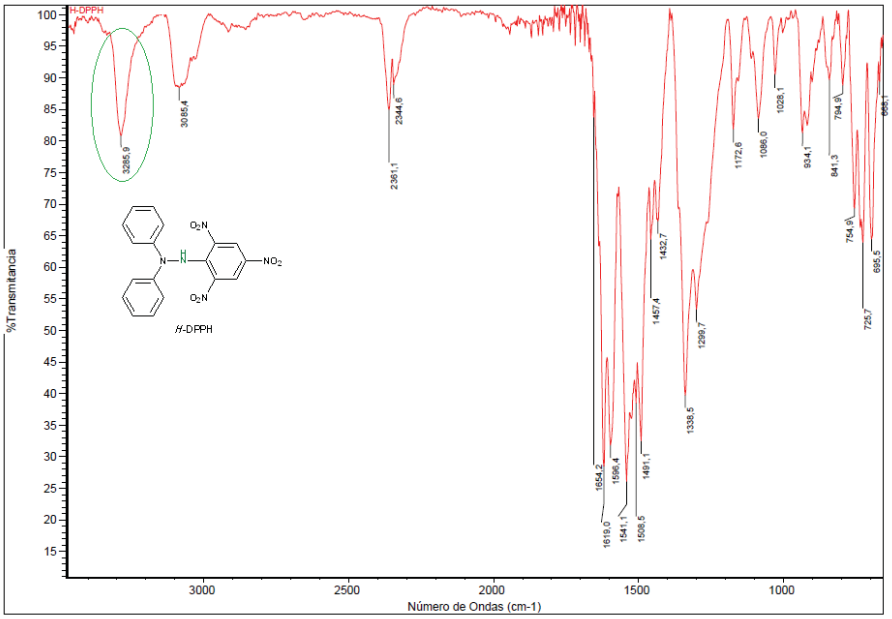

Annex 3. UV-Vis spectra of HNTTM and Bu_4N^+ $^-$HNTTM (salt of 3) in $CHCl_3$

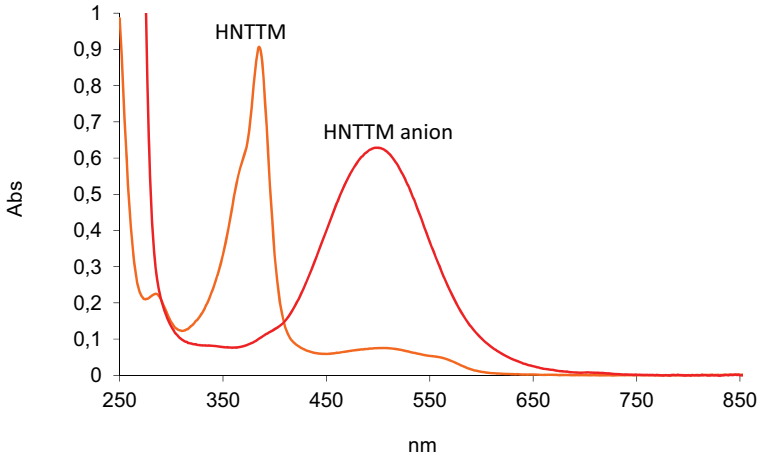

Annex 4. Thermogravimetric (TG) analysis and Differential Scanning Calorimetry (DSC) of Bu_4N^+ $^-$HNTTM (salt of 3)

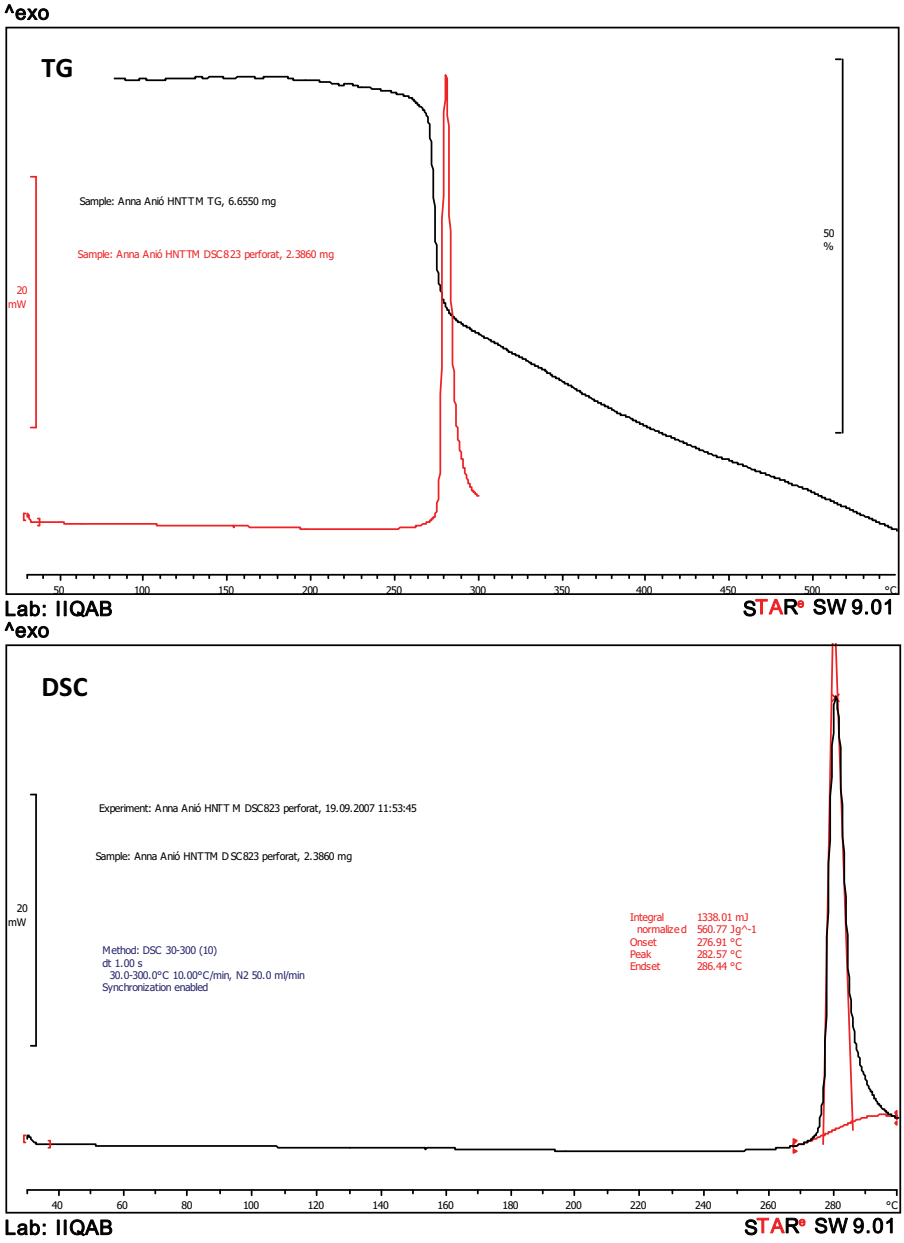

Annex 5. Molecular and crystal structure of Bu_4N^+ $^-$HNTTM (salt of 3)

A. Perspective view of the Bu_4N^+ cation with atom numbering (only non-H atoms).

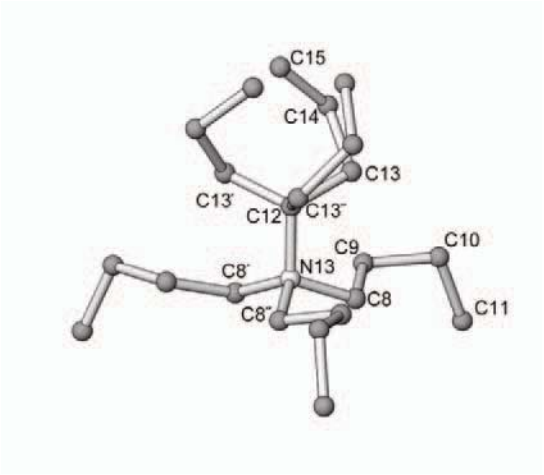

B. Perspective view of the unit cell along *c*. The X anions are on the 6_3 symmetry axis and the Bu_4N^+ cations (space filling style) on the 3 symmetry axes.

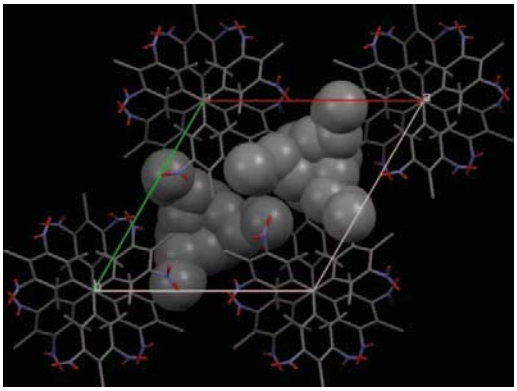

Annex 6. Kinetics of reactions of HNTTM with catechol or pyrogallol in different solvents. Reaction time 5.5 h.

1. Kinetics of catechol (**10**) with HNTTM in $CHCl_3$

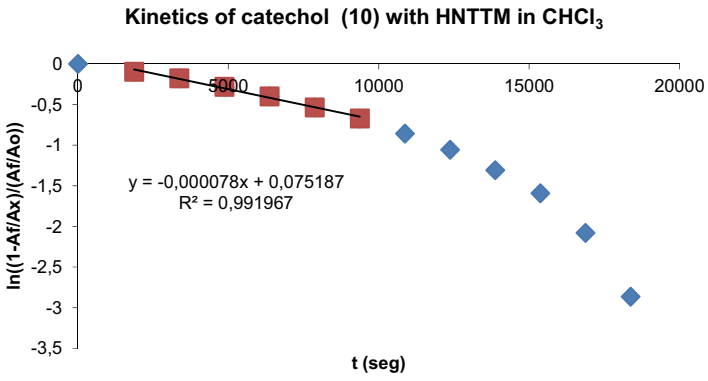

2. Kinetics of catechol (**10**) with HNTTM in benzene

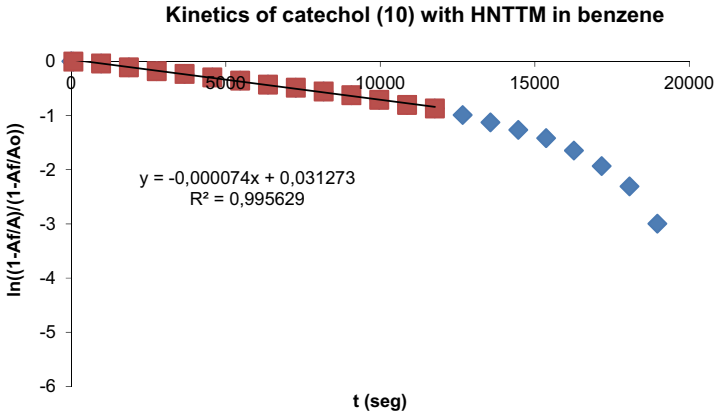

3. Kinetics of catechol (**10**) with HNTTM in $CHCl_3$/MeOH (2:1)

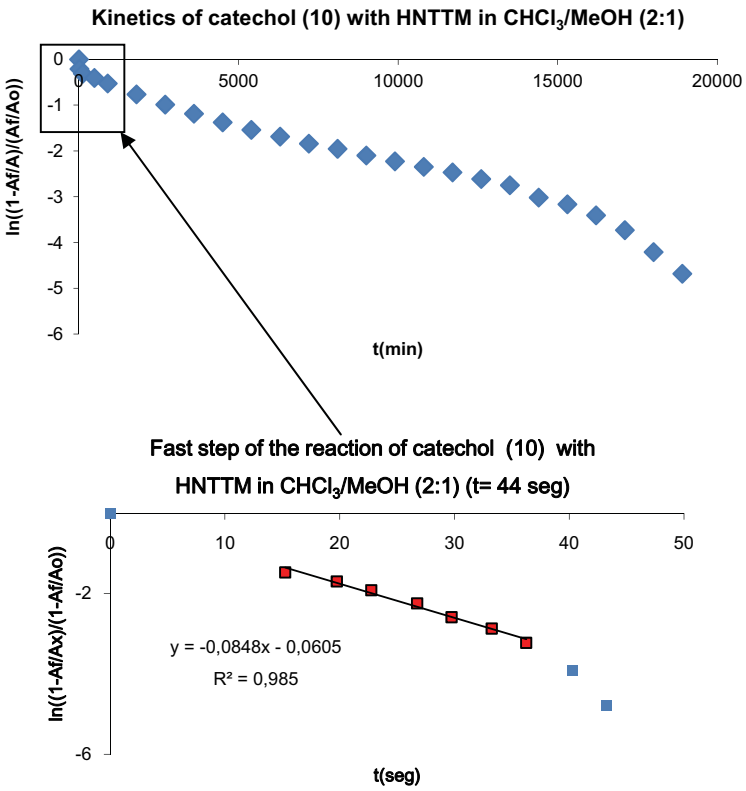

4. Kinetics of pyrogallol (**11**) with HNTTM in $CHCl_3$

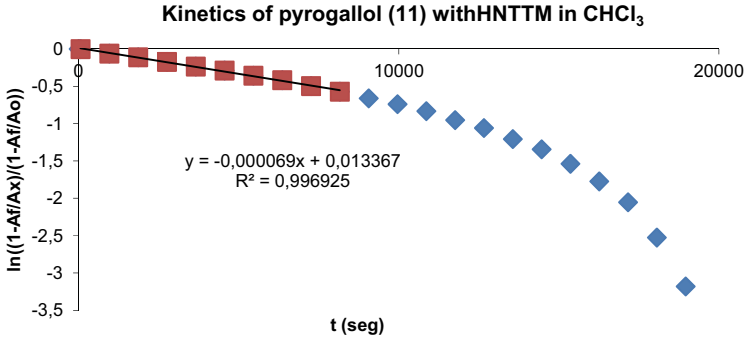

5. Kinetics of pyrogallol (**11**) with HNTTM in benzene

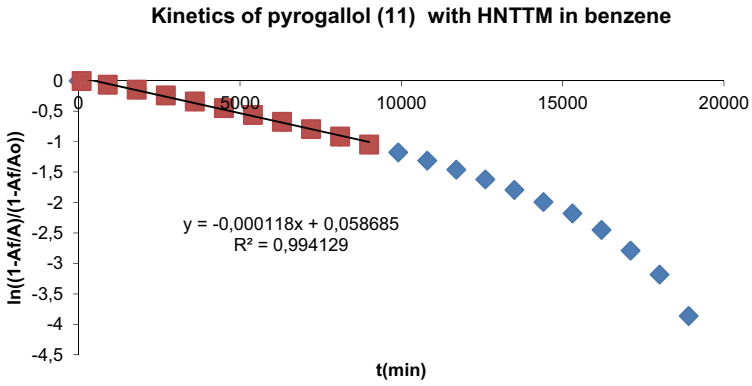

6. Kinetics of pyrogallol (**11**) with HNTTM in $CHCl_3$/MeOH (2:1)

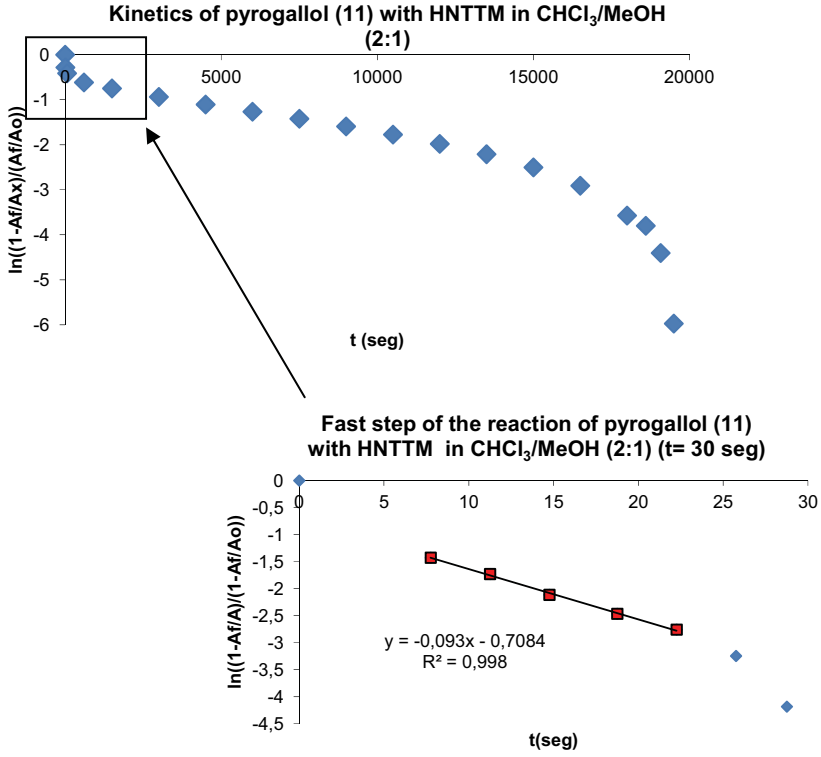

Annex 7. Cyclic voltammetry (CV)

CV of PTM in CH_2Cl_2: Cyclic voltammograms corresponding to the reduction of a 1 mM PTM solution in CH_2Cl_2 with TBAP 0.1 M on Pt at 25 °C.

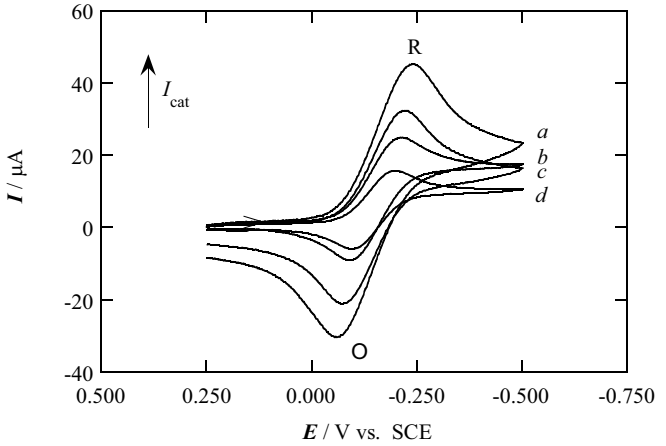

Initial and final potential 0.250 V; reversal potential -0.500 V. Scan rate: (a) 200, (b) 100, (c) 50, (d) 20 mV s^{-1}.

CV of HNTTM (**4**) in $CHCl_3$: Cyclic voltammograms corresponding to the oxidation of a 1mM HNTTM (**4**) solution in $CHCl_3$ with 0.1 M TBAP on Pt at 25 °C.

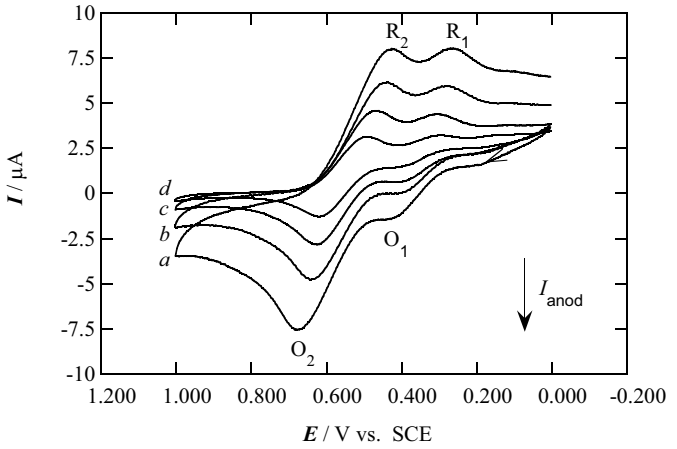

Initial and final potential 0.000 V; reversal potential 1.000 V. Scan rate: (a) 200, (b) 100, (c) 50, (d) 20 mV s^{-1}.

CV of HNTTM (**4**) in benzene: Cyclic voltammograms obtained for the oxidation of a 1mM HNTTM (**4**) solution in benzene with 0.1 M $THAPF_6$ on Pt at 25 °C.

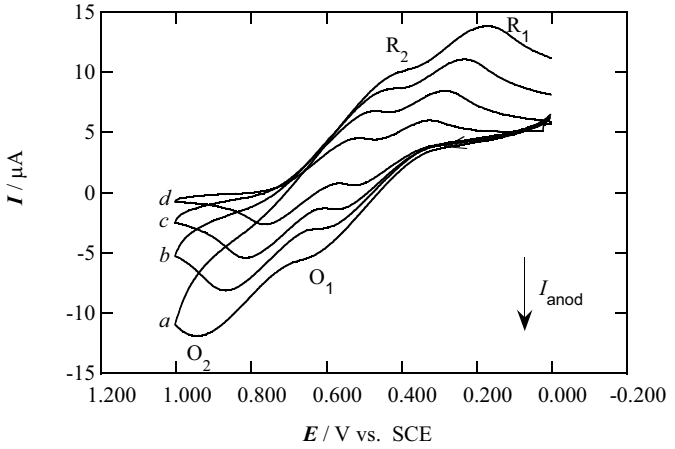

Initial and final potential 0.000 V; reversal potential 1.000 V. Scan rate: (a) 200, (b) 100, (c) 50, (d) 20 mV s^{-1}.

CV of HNTTM (**4**) in $CHCl_3$/MeOH (2:1): Cyclic voltammograms corresponding to the oxidation of a saturated HNTTM (**4**) solution in $CHCl_3$/MeOH (2:1) with TBAP 0.1 M on Pt at 25 °C.

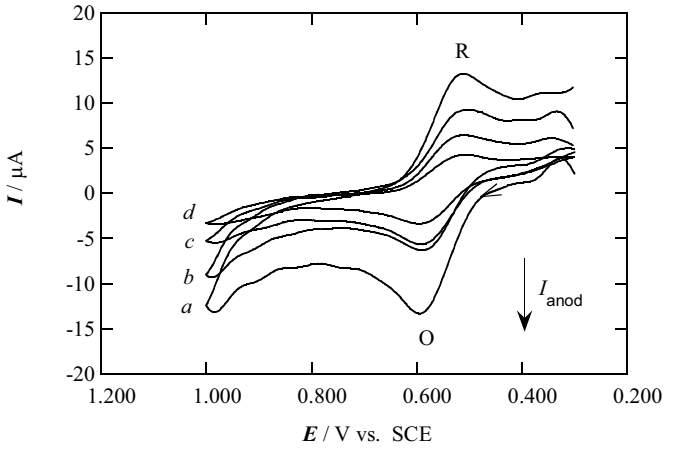

Initial and final potential 0.300 V; reversal potential 1.000 V. Scan rate: (a) 200, (b) 100, (c) 50, (d) 20 mV s^{-1}.

CV of TNPTM in $CHCl_3$/MeOH (2:1): Cyclic voltammograms corresponding to the oxidation of a 1 mM TNPTM solution in $CHCl_3$/MeOH (2:1) with TBAP 0.1 M on Pt at 25 °C.

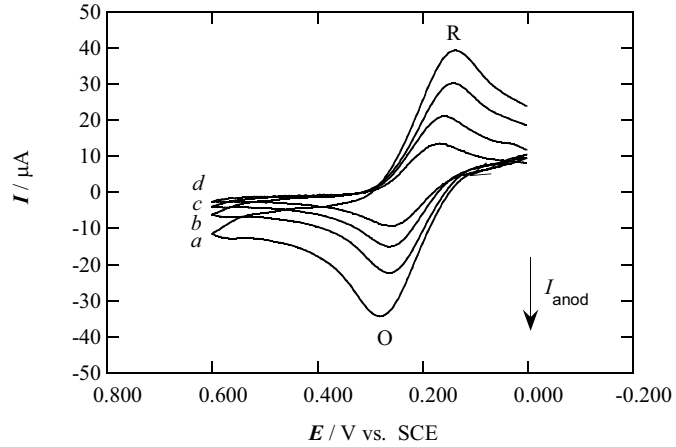

Initial and final potential 0.000 V; reversal potential 0.600 V. Scan rate: (a) 200, (b) 100, (c) 50, (d) 20 mV s^{-1}.

CV of DPPH in $CHCl_3$/MeOH (2:1): Cyclic voltammograms corresponding to the oxidation of a 1 mM DPPH (**9**) solution in $CHCl_3$/MeOH (2:1) with TBAP 0.1 M on Pt at 25 °C

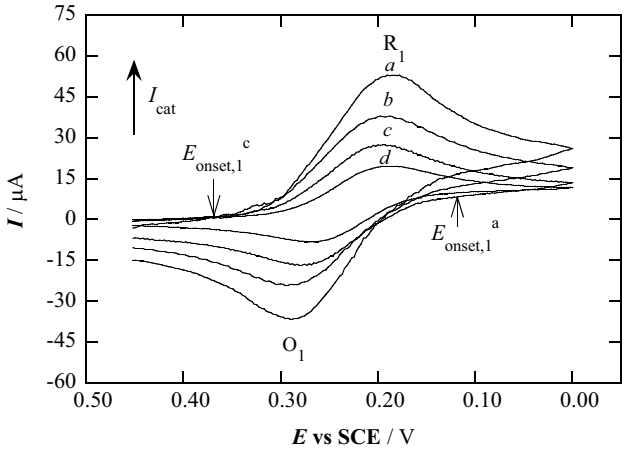

Initial and final potential 0.000 V; reversal potential 0.450 V. Scan rate: (a) 200, (b) 100, (c) 50, (d) 20 mV s^{-1}.

CV of catechol (**10**) in $CHCl_3$: Cyclic voltammograms corresponding to the oxidation of a 1 mM catechol (**10**) solution in $CHCl_3$ with 0.1 M TBAP on Pt at 25 °C.

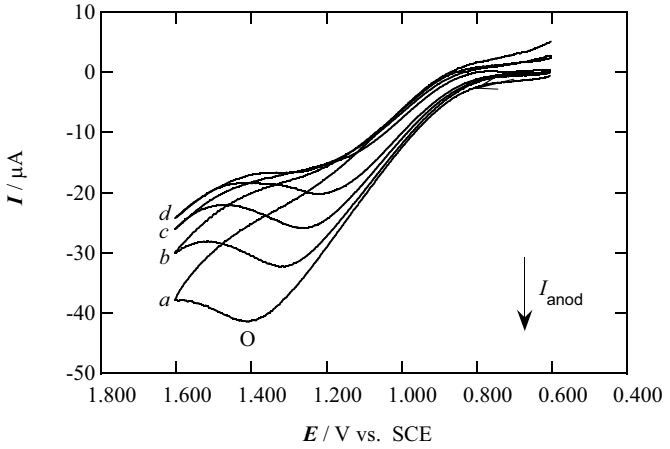

Initial and final potential 0.600 V; reversal potential 1.600 V. Scan rate: (a) 200, (b) 100, (c) 50, (d) 20 mV s^{-1}.

CV of catechol (**10**) in benzene: Cyclic voltammograms for the oxidation of a 1 mM catechol solution in benzene with 0.3 M $THAPF_6$ on Pt at 25 °C.

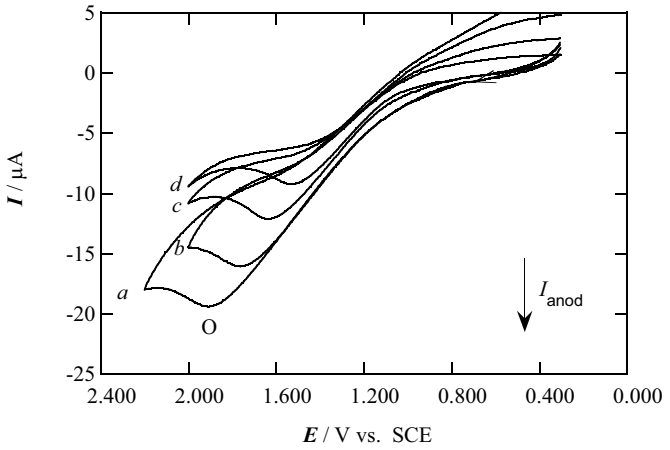

Initial and final potential 0.300 V; reversal potential 2.000 V at scan rate: (b) 100, (c) 50, (d) 20 mV s^{-1}, or 2.200 V at (a) 200 mV s^{-1}.

CV of catechol (**10**) in $CHCl_3$/MeOH (2:1): Cyclic voltammograms corresponding to the oxidation of a 3 mM catechol (**10**) solution in $CHCl_3$/MeOH (2:1) with TBAP 0.1 M on Pt at 25 °C.

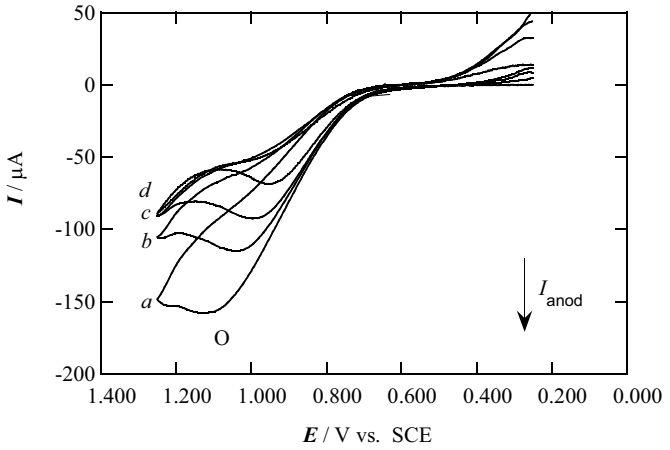

Initial and final potential 0.250 V; reversal potential 1.250 V. Scan rate: (a) 200, (b) 100, (c) 50, (d) 20 mV s^{-1}.

CV of the anion of catechol (**10**): Cyclic voltammograms recorded for the oxidation of a 1 mM catechol (**10**) solution in 2:1 (v/v) $CHCl_3$/MeOH (2:1) with TBAP 0.1 M and 4 mM OH^- as TBAOH on Pt at 25 °C.

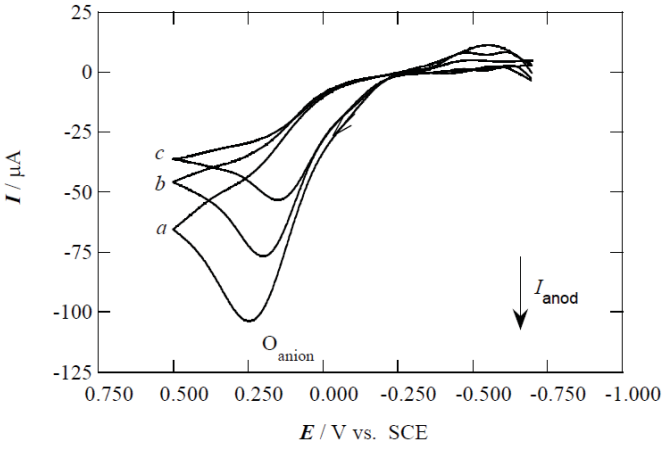

Initial and final potential -0.700 V; reversal potential 0.500 V. Scan rate: (a) 100, (b) 50, (c) 20 mV s^{-1}.

CV of pyrogallol (**11**) in $CHCl_3$: Cyclic voltammograms for the oxidation of a 1 mM pyrogallol (**11**) solution in $CHCl_3$ with 0.1 M TBAP on Pt at 25 °C.

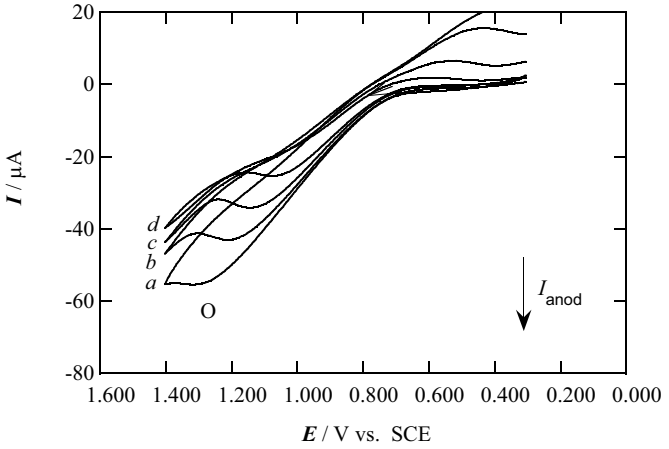

Initial and final potential 0.300 V; reversal potential 1.400 V. Scan rate: (a) 200, (b) 100, (c) 50, (d) 20 mV s^{-1}.

CV of pyrogallol (**11**) in $CHCl_3$/MeOH (2:1): Cyclic voltammograms corresponding to the oxidation of a 1 mM pyrogallol (**11**) solution in $CHCl_3$/MeOH (2:1) with TBAP 0.1 M on Pt at 25 °C.

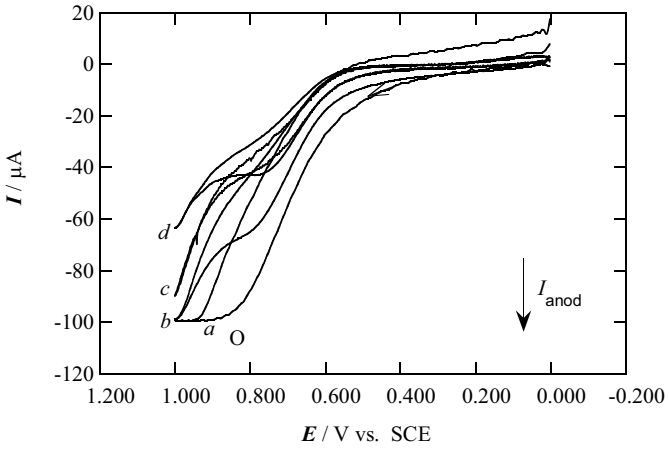

Initial and final potential 0 V; reversal potential 1.000 V. Scan rate: (a) 200, (b) 100, (c) 50, (d) 20 mV s^{-1}.

CV of the anion of pyrogallol: Cyclic voltammograms recorded for the oxidation of a 1 mM pyrogallol (**11**) solution in $CHCl_3$/MeOH (2:1) with TBAP 0.1 M and 3 mM OH^- as TBAOH on Pt at 25 °C.

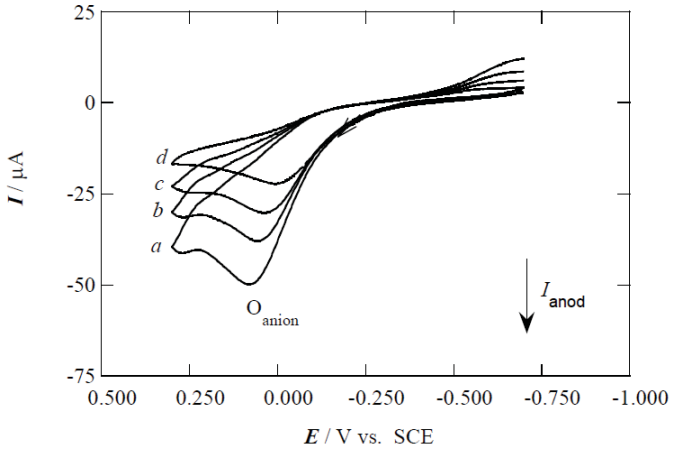

Initial and final potential -0.07 V; reversal potential 0.30 V. Scan rate. (a) 200, (b) 100, (c) 50, (d) 20 mV s^{-1}.

CV of catechol (**10**) in DMF: Cyclic voltammograms recorded for the oxidation of 1.0 mM of catechol (**10**) in DMF with 0.1 M TBAP at 25 °C on a Pt electrode.

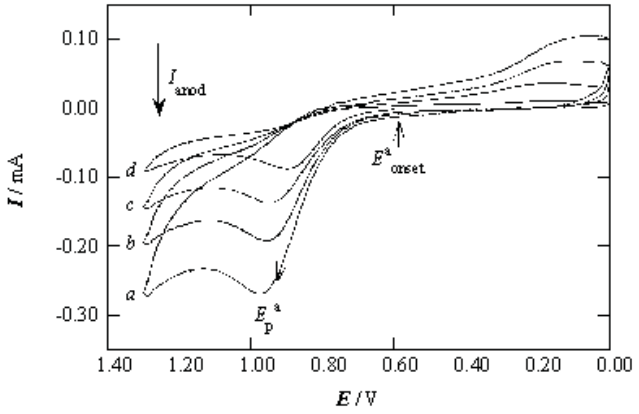

Initial and final potential -0.07 V; reversal potential 1.3 V. Scan rate. (a) 200, (b) 100, (c) 50, (d) 20 mV s^{-1}.

CV of pyrogallol (**11**) in DMF: Cyclic voltammograms recorded for the oxidation of 1.0 mM of pyrogallol (**11**) in DMF with 0.1 M TBAP at 25 °C on a Pt electrode.

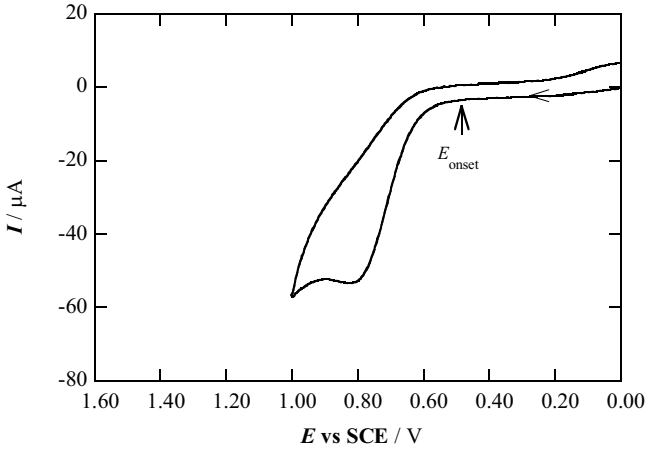

Initial and final potential -0.07 V; reversal potential 1.1 V. Scan rate 50 mV s^{-1}.

CV of methylgallate (**12**) in DMF: Cyclic voltammograms recorded for the oxidation of 1.0 mM of methylgallate (**12**) in DMF with 0.1 M TBAP at 25 °C on a Pt electrode.

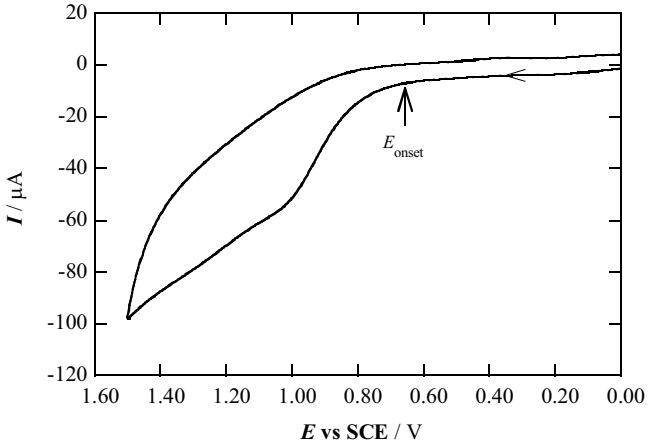

Initial and final potential -0.07 V; reversal potential 1.5 V. Scan rate 50 mV s^{-1}.

CV of DHHDP (**20**) in DMF: Cyclic voltammograms recorded for the oxidation of 1.0 mM of DHHDP (**20**) in DMF with 0.1 M TBAP at 25 °C on a Pt electrode.

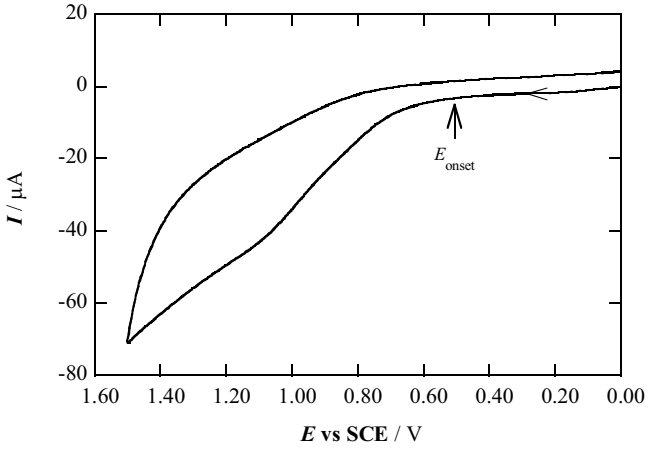

Initial and final potential -0.07 V; reversal potential 1.5 V. Scan rate 50 mV s^{-1}.

CV of EA (**21**) in DMF: Cyclic voltammograms recorded for the oxidation of 1.0 mM of EA (**21**) in DMF with 0.1 M TBAP at 25 °C on a Pt electrode.

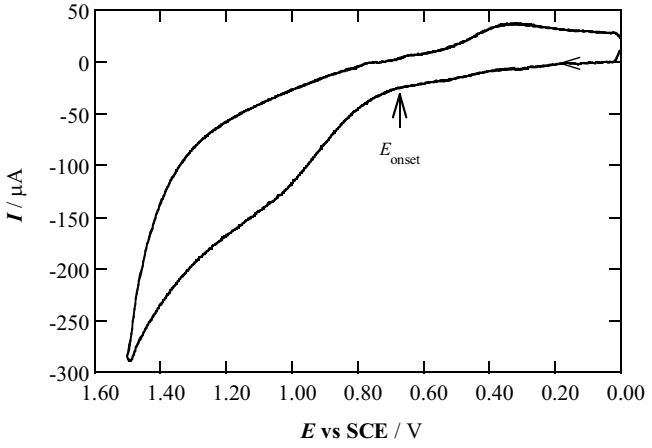

Initial and final potential 0.0 V; reversal potential 1.500 V. Scan rate 50 mV s^{-1}.

Annex 8. NMR spectra of the DHHDP (dimethyl- 4,4',5,5',6,6'-hexahydroxy-2,2'-diphenyl-dicarboxilate).

A. ^{1}H-NMR (400 MHz, CD_3COCD_3): δ= 3.47 (s, 6H, (H_8)), 7.12 (S, 2H (H_6)) ppm.

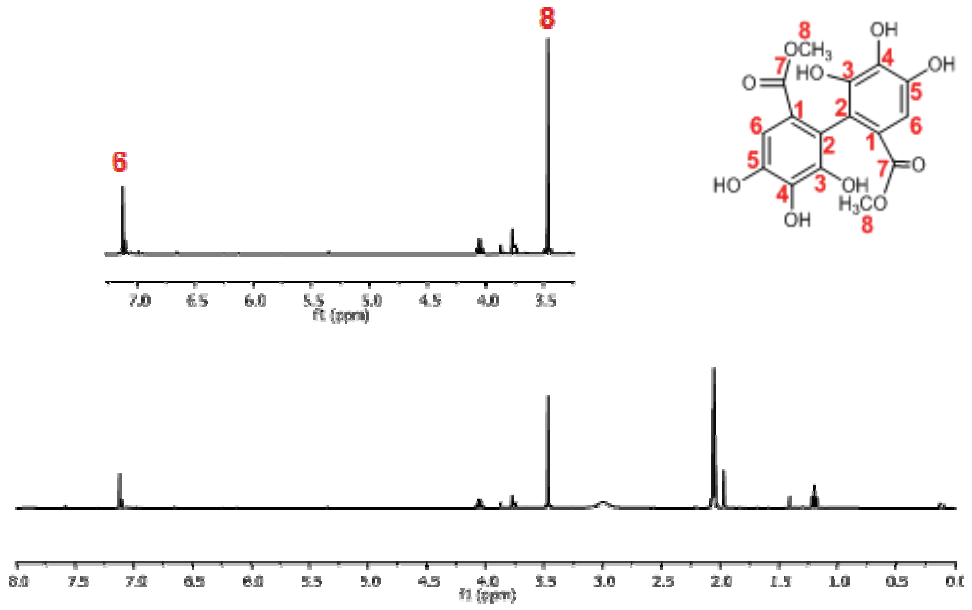

B. ^{13}C-NMR (101 MHz, CD_3COCD_3): δ= 167.53 (C_7), 144.59 (C_3, C_5), 137.44 (C_4), 122.66 (C_1), 118.78, 110.61, 51.45 ppm.

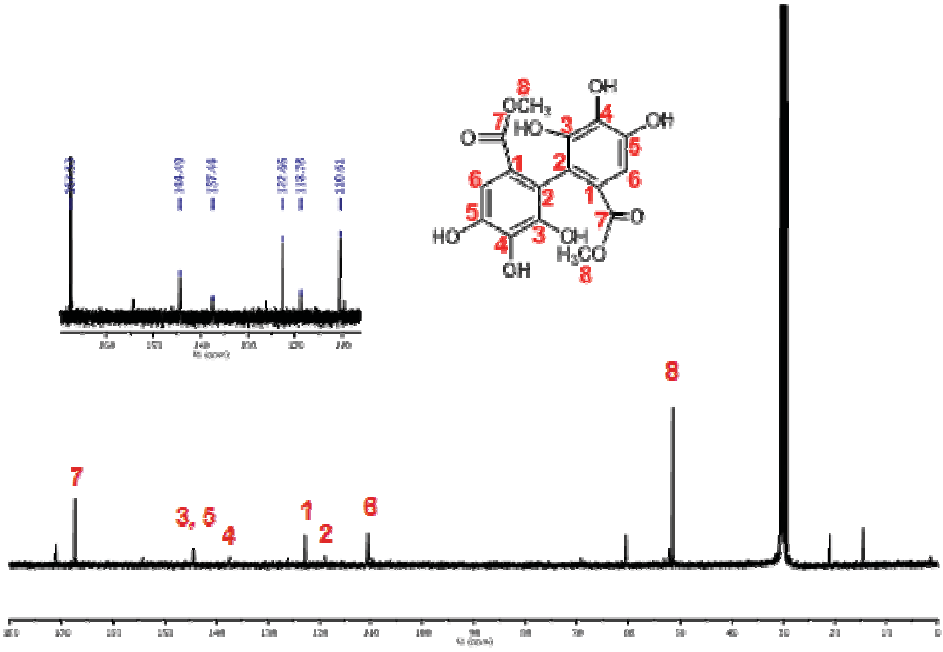

Annex 9. Graphics of the Radical Scavenging Capacity (RSC) of (poly)phenols with HNTTM (4), TNPTM (8) and DPPH (9).

A. Plots of the scavenging percentage versus the amount of (poly)phenols **10** to **21** in µg µmol^{-1} measured with HNTTM (**4**) in $CHCl_3$/MeOH (2:1).

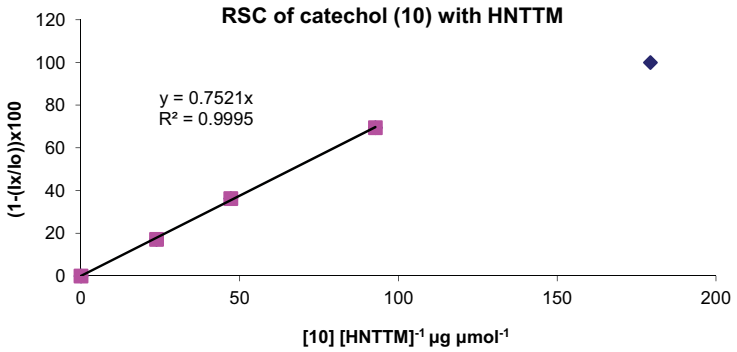

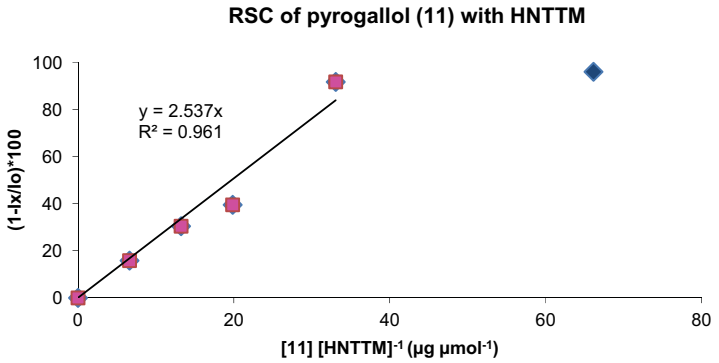

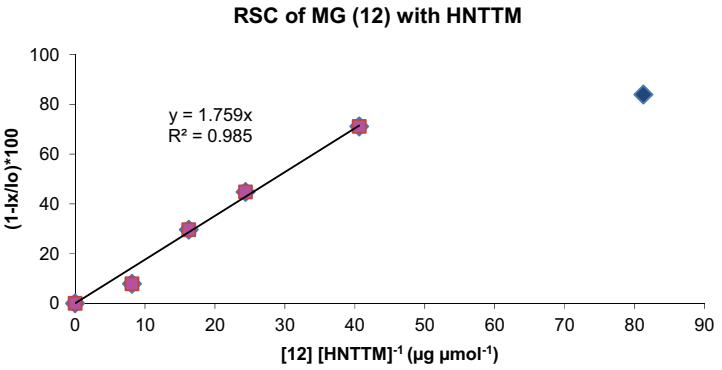

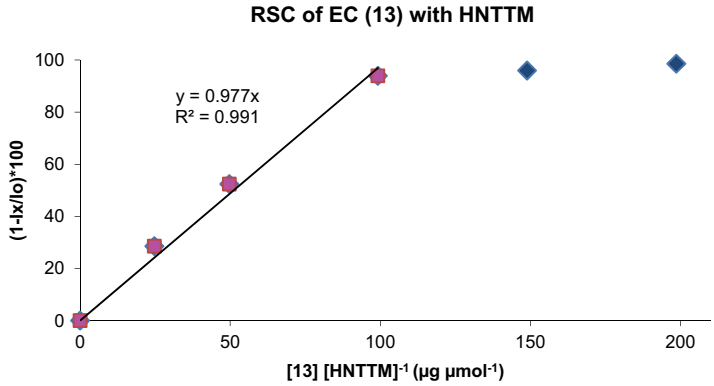
RSC of EC (13) with HNTTM
y = 0.977x
R² = 0.991
(1-Ix/Io)*100
[13] [HNTTM]-1 (µg µmol-1)

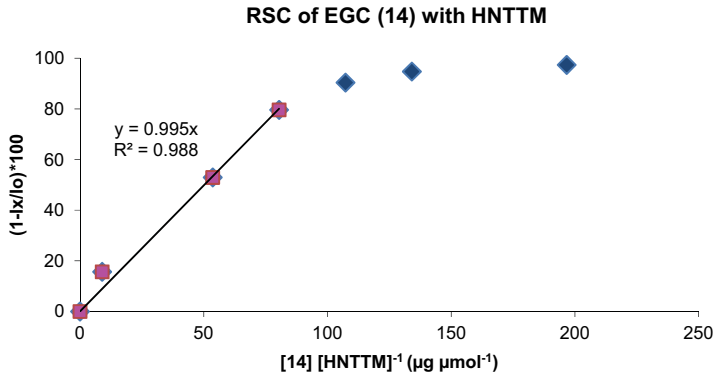
RSC of EGC (14) with HNTTM
y = 0.995x
R² = 0.988
(1-Ix/Io)*100
[14] [HNTTM]-1 (µg µmol-1)

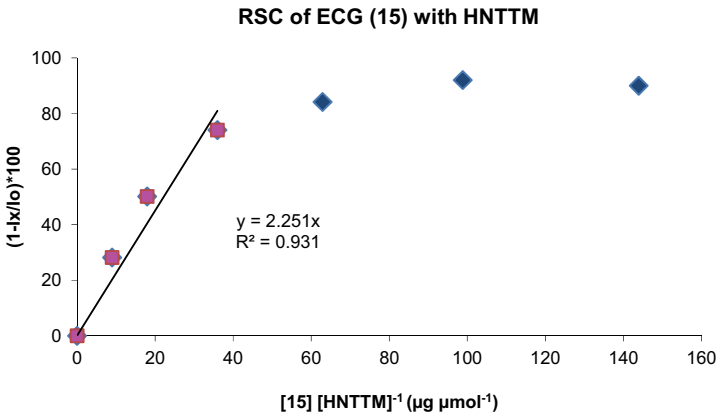
RSC of ECG (15) with HNTTM
y = 2.251x
R² = 0.931
(1-Ix/Io)*100
[15] [HNTTM]-1 (µg µmol-1)

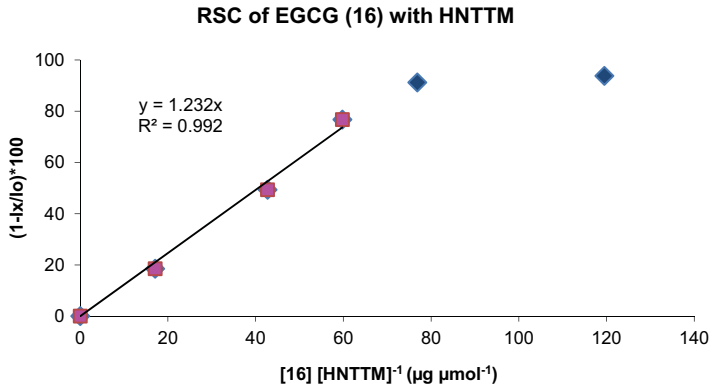
RSC of EGCG (16) with HNTTM
y = 1.232x
R² = 0.992
(1-Ix/Io)*100
[16] [HNTTM]-1 (µg µmol-1)

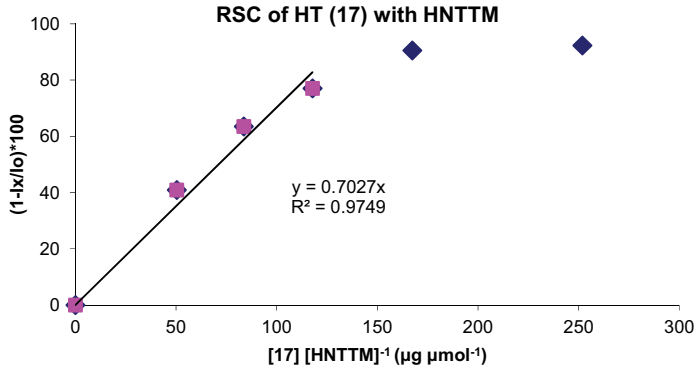
RSC of HT (17) with HNTTM
y = 0.7027x
R² = 0.9749
(1-Ix/Io)*100
[17] [HNTTM]-1 (µg µmol-1)

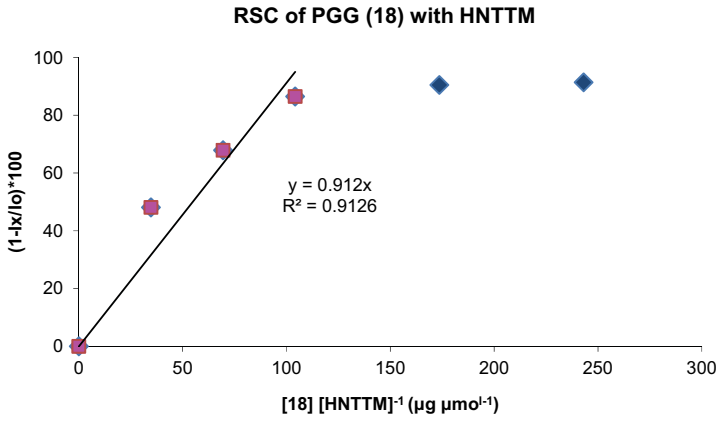
RSC of PGG (18) with HNTTM
y = 0.912x
R² = 0.9126
(1-Ix/Io)*100
[18] [HNTTM]-1 (µg µmol-1)

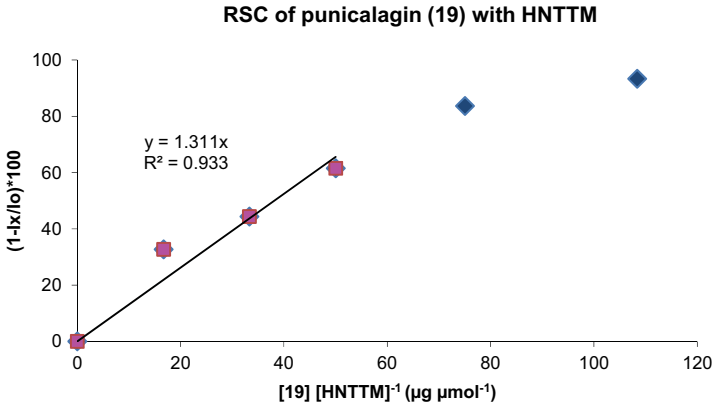
RSC of punicalagin (19) with HNTTM
y = 1.311x
R² = 0.933
(1-Ix/Io)*100
[19] [HNTTM]-1 (µg µmol-1)
0
20
40
60
80
100
120

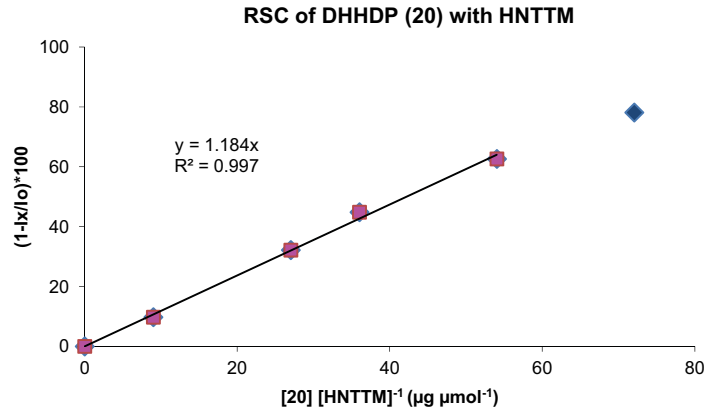
RSC of DHHDP (20) with HNTTM
y = 1.184x
R² = 0.997
(1-Ix/Io)*100
[20] [HNTTM]-1 (µg µmol-1)
0
20
40
60
80
100

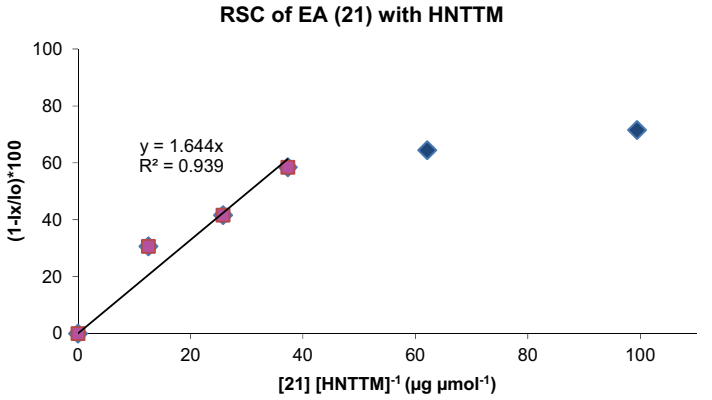
RSC of EA (21) with HNTTM
y = 1.644x
R² = 0.939
(1-Ix/Io)*100
[21] [HNTTM]-1 (µg µmol-1)
0
20
40
60
80
100

B. Plots of the scavenging percentage versus the amount of (poly)phenols **10** to **21** in μmol μmol^{-1} measured with HNTTM (**4**) in $CHCl_3$/MeOH (2:1).

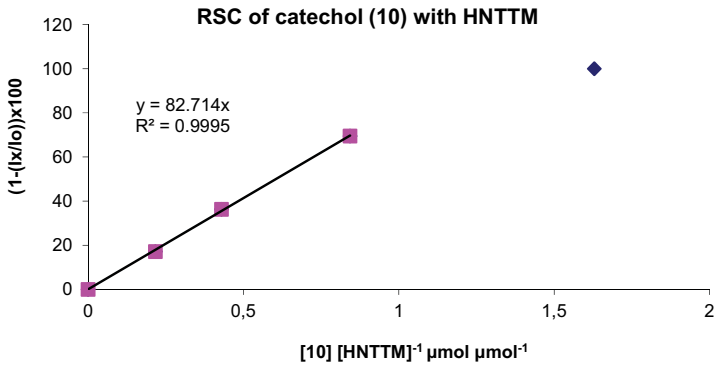

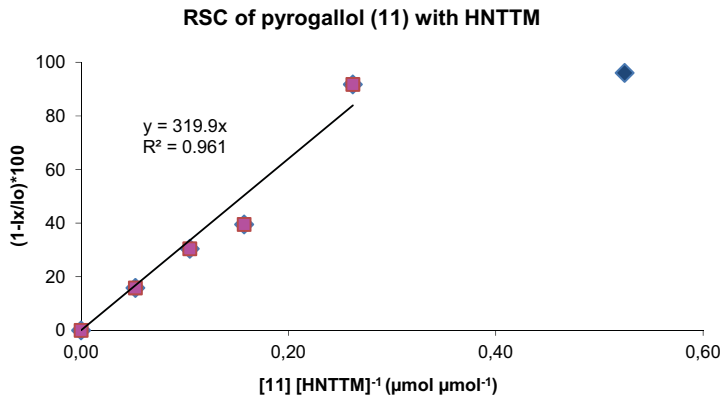

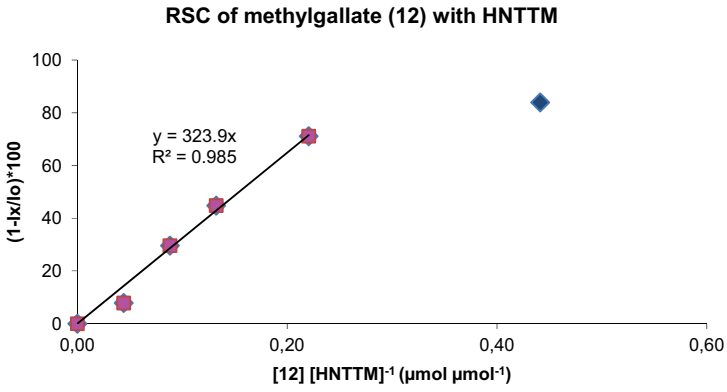

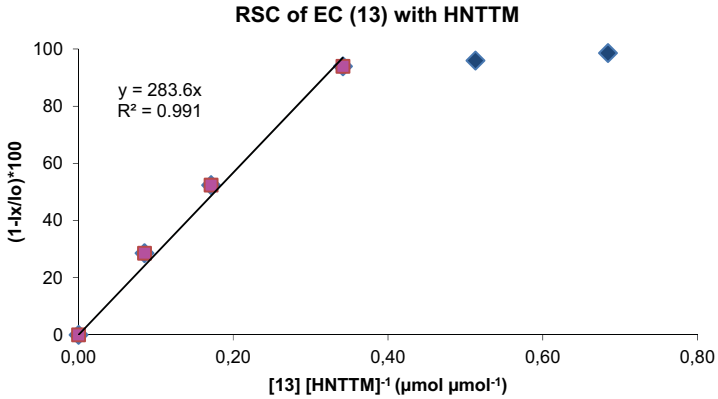
RSC of EC (13) with HNTTM
y = 283.6x
R² = 0.991
(1-Ix/Io)*100
[13] [HNTTM]-1 (µmol µmol-1)
0
20
40
60
80
100
0,00
0,20
0,40
0,60
0,80

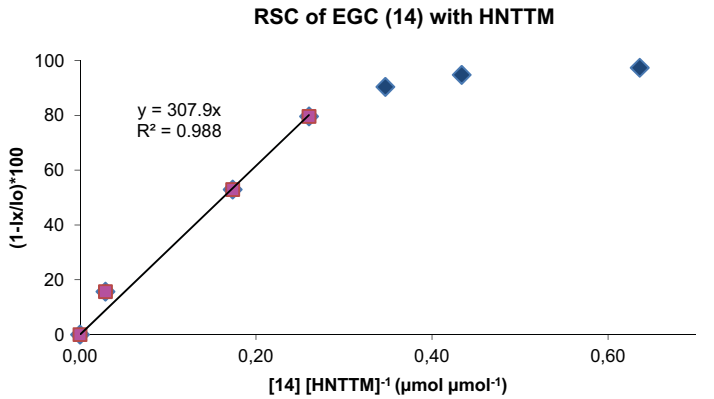
RSC of EGC (14) with HNTTM
y = 307.9x
R² = 0.988
(1-Ix/Io)*100
[14] [HNTTM]-1 (µmol µmol-1)
0
20
40
60
80
100
0,00
0,20
0,40
0,60

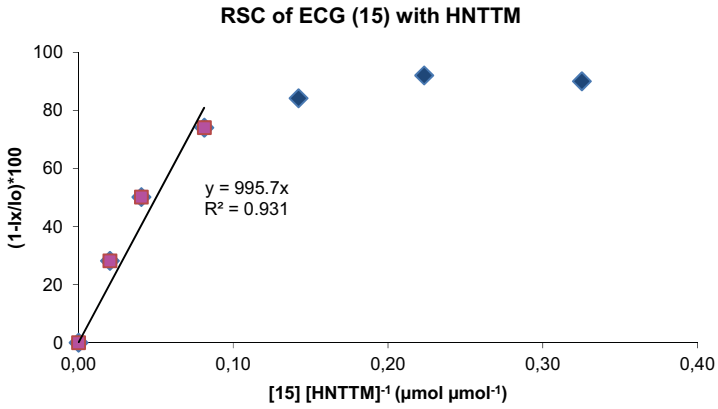
RSC of ECG (15) with HNTTM
y = 995.7x
R² = 0.931
(1-Ix/Io)*100
[15] [HNTTM]-1 (µmol µmol-1)
0
20
40
60
80
100
0,00
0,10
0,20
0,30
0,40

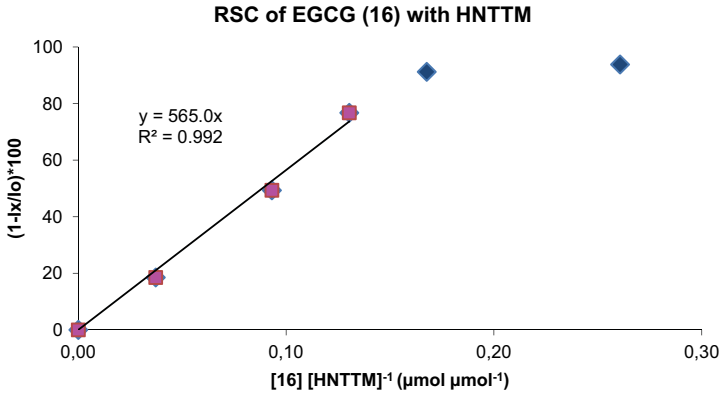
RSC of EGCG (16) with HNTTM
y = 565.0x
R² = 0.992
(1-Ix/Io)*100
[16] [HNTTM]-1 (µmol µmol-1)

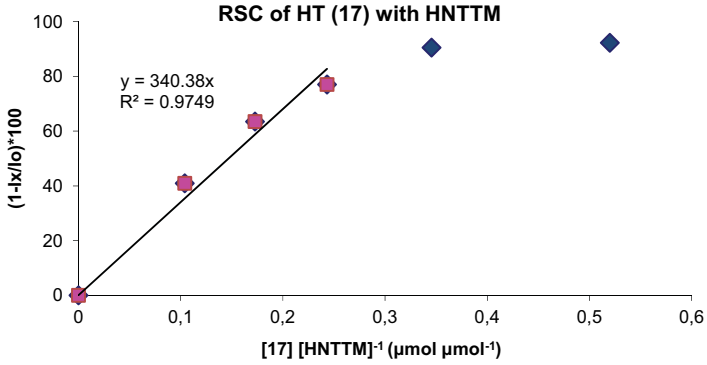
RSC of HT (17) with HNTTM
y = 340.38x
R² = 0.9749
(1-Ix/Io)*100
[17] [HNTTM]-1 (µmol µmol-1)

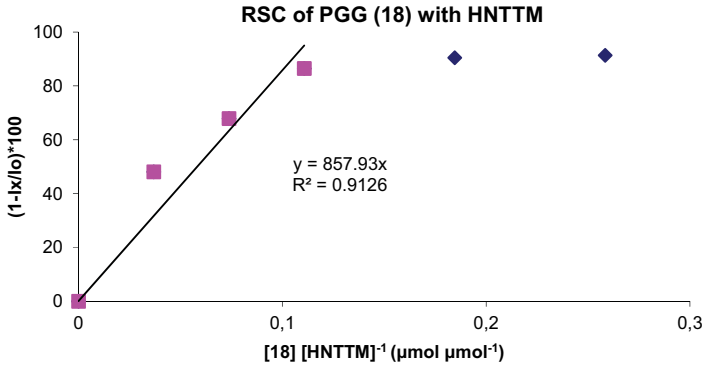
RSC of PGG (18) with HNTTM
y = 857.93x
R² = 0.9126
(1-Ix/Io)*100
[18] [HNTTM]-1 (µmol µmol-1)

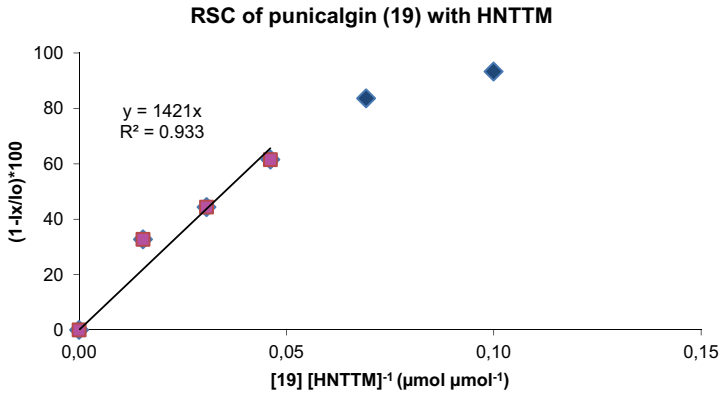
RSC of punicalgin (19) with HNTTM
y = 1421x
R² = 0.933
(1-Ix/Io)*100
[19] [HNTTM]-1 (µmol µmol-1)
0
20
40
60
80
100
0,00
0,05
0,10
0,15

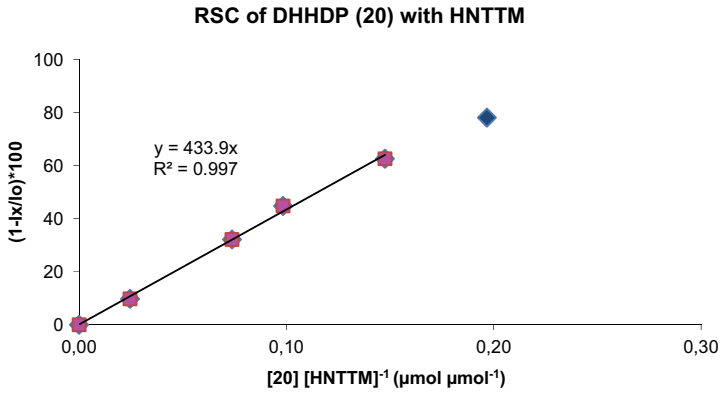
RSC of DHHDP (20) with HNTTM
y = 433.9x
R² = 0.997
(1-Ix/Io)*100
[20] [HNTTM]-1 (µmol µmol-1)
0
20
40
60
80
100
0,00
0,10
0,20
0,30

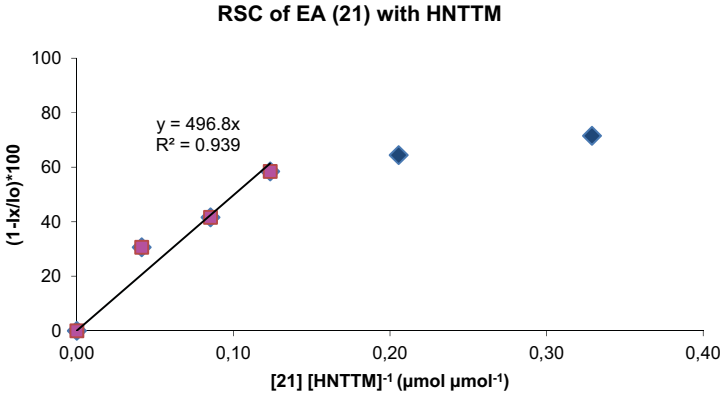
RSC of EA (21) with HNTTM
y = 496.8x
R² = 0.939
(1-Ix/Io)*100
[21] [HNTTM]-1 (µmol µmol-1)
0
20
40
60
80
100
0,00
0,10
0,20
0,30
0,40

C. Plots of the scavenging percentage versus the amount of (poly)phenols **10** to **21** in µg µmol^{-1} measured with TNPTM (**8**) in $CHCl_3$/MeOH (2:1).

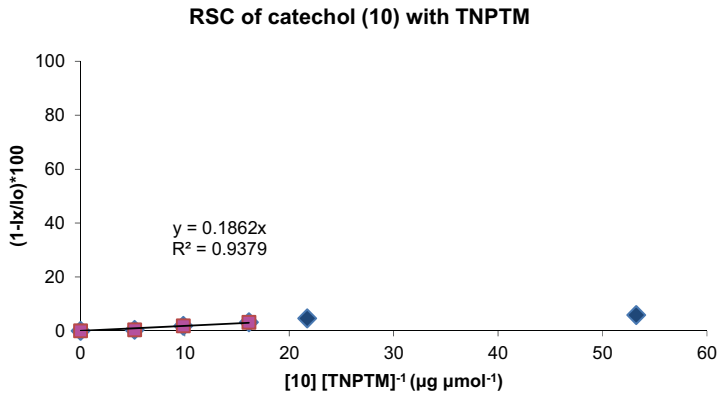

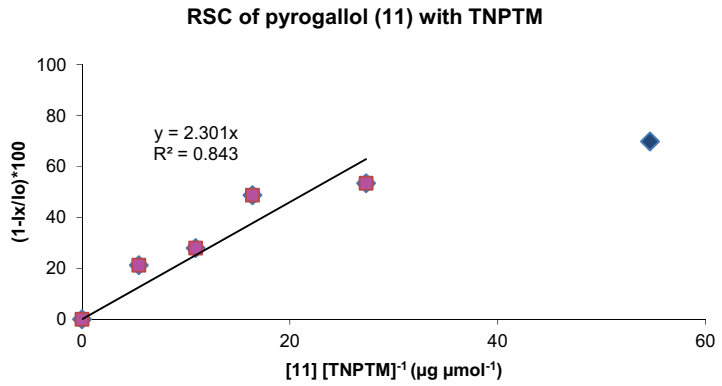

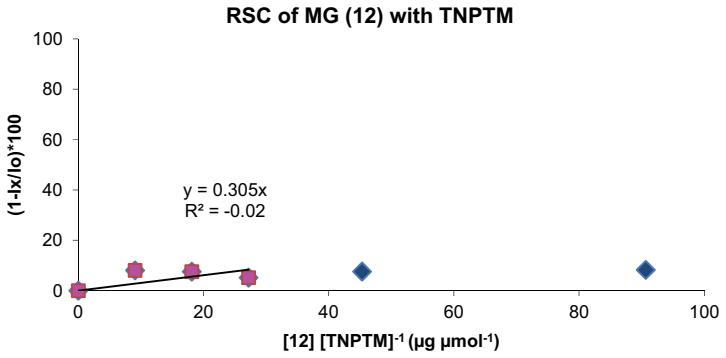

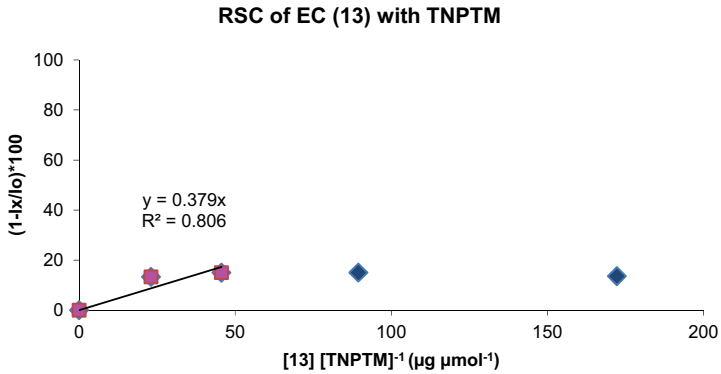
RSC of EC (13) with TNPTM
(1-Ix/Io)*100
y = 0.379x
R² = 0.806
[13] [TNPTM]-1 (µg µmol-1)

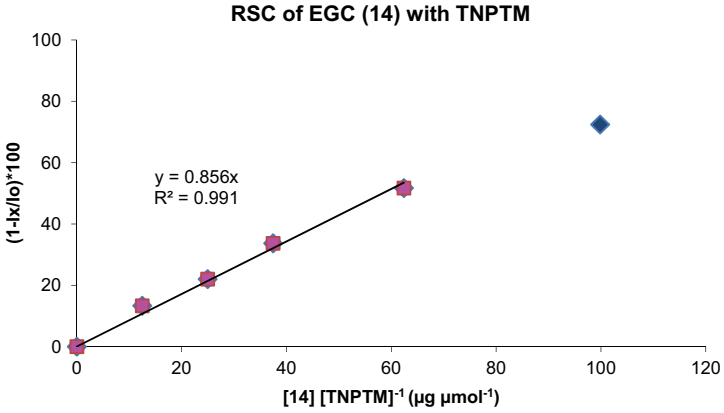
RSC of EGC (14) with TNPTM
(1-Ix/Io)*100
y = 0.856x
R² = 0.991
[14] [TNPTM]-1 (µg µmol-1)

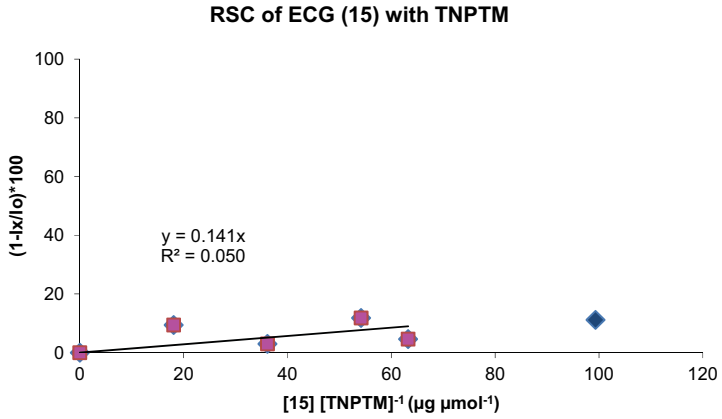
RSC of ECG (15) with TNPTM
(1-Ix/Io)*100
y = 0.141x
R² = 0.050
[15] [TNPTM]-1 (µg µmol-1)

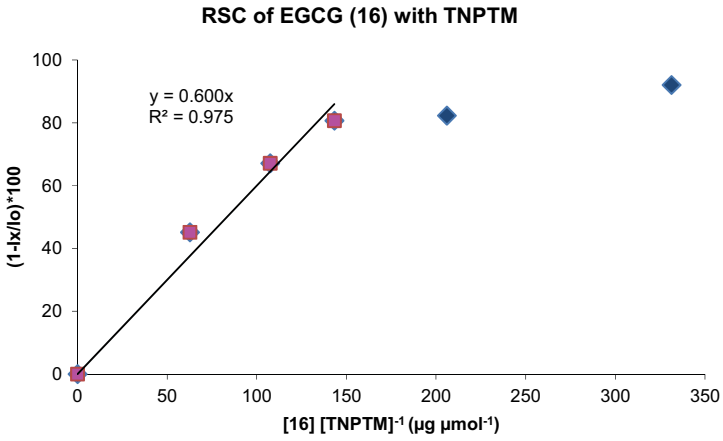
RSC of EGCG (16) with TNPTM
y = 0.600x
R² = 0.975
(1-Ix/Io)*100
[16] [TNPTM]-1 (µg µmol-1)

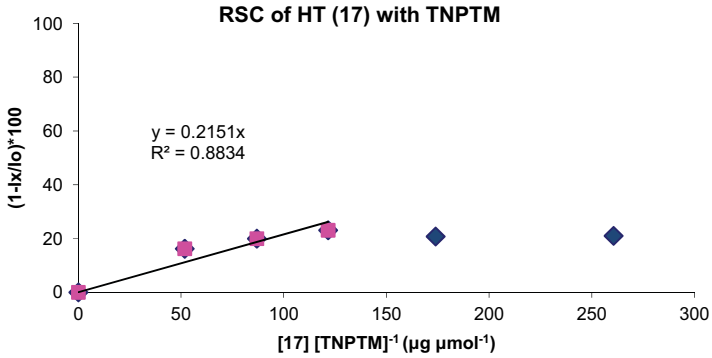
RSC of HT (17) with TNPTM
y = 0.2151x
R² = 0.8834
(1-Ix/Io)*100
[17] [TNPTM]-1 (µg µmol-1)

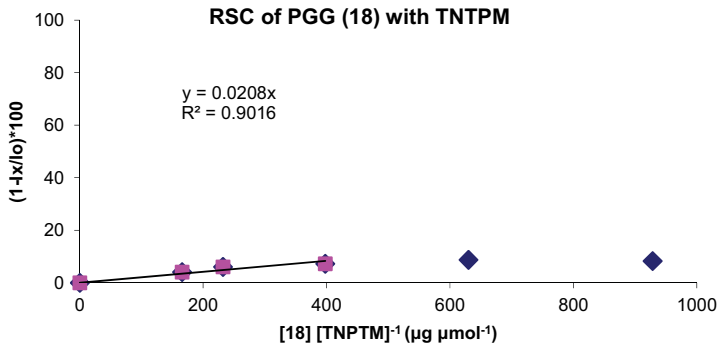
RSC of PGG (18) with TNTPM
y = 0.0208x
R² = 0.9016
(1-Ix/Io)*100
[18] [TNPTM]-1 (µg µmol-1)

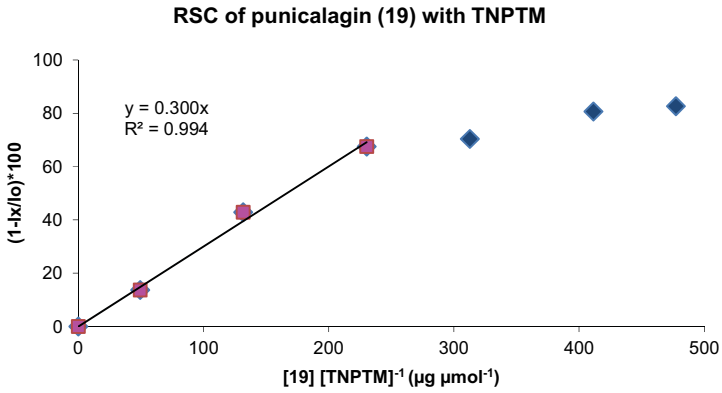
RSC of punicalagin (19) with TNPTM
y = 0.300x
R² = 0.994
(1-Ix/Io)*100
[19] [TNPTM]-1 (µg µmol-1)
0
20
40
60
80
100
0
100
200
300
400
500

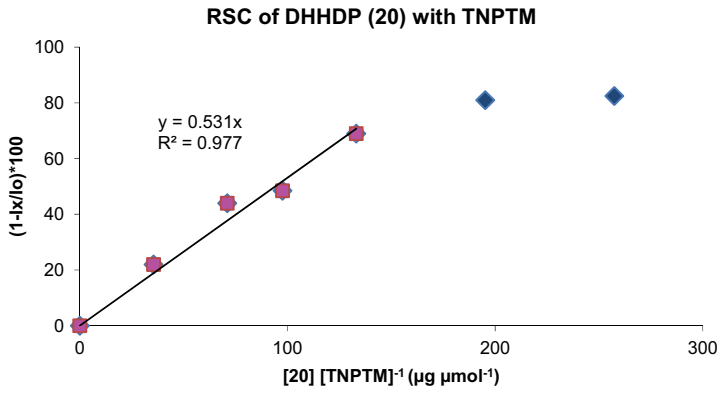
RSC of DHHDP (20) with TNPTM
y = 0.531x
R² = 0.977
(1-Ix/Io)*100
[20] [TNPTM]-1 (µg µmol-1)
0
20
40
60
80
100
0
100
200
300

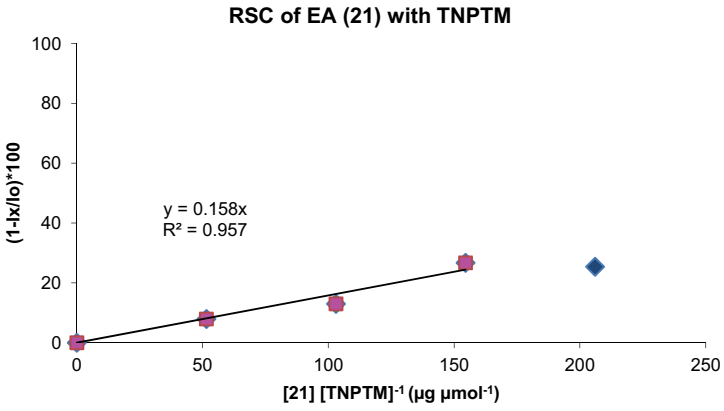
RSC of EA (21) with TNPTM
y = 0.158x
R² = 0.957
(1-Ix/Io)*100
[21] [TNPTM]-1 (µg µmol-1)
0
20
40
60
80
100
0
50
100
150
200
250

D. Plots of the scavenging percentage versus the amount of (poly)phenols **10** to **21** in μmol μmol^{-1} measured with TNPTM (**8**) in $CHCl_3$/MeOH (2:1).

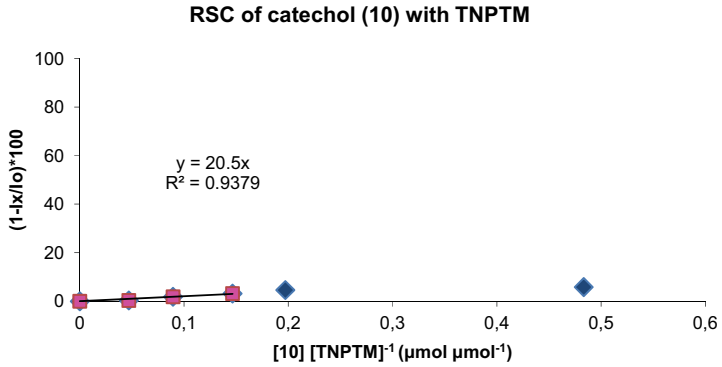

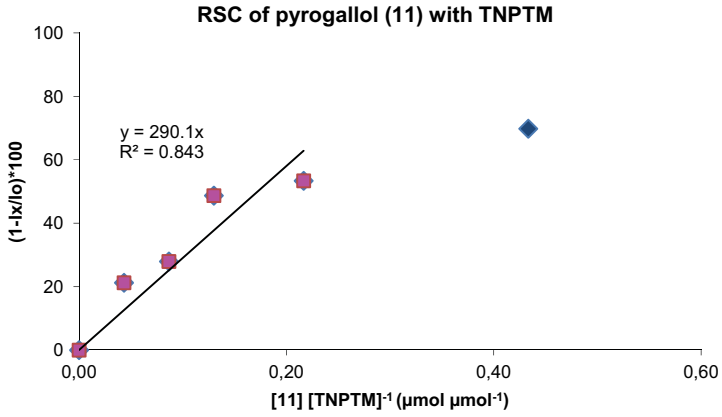

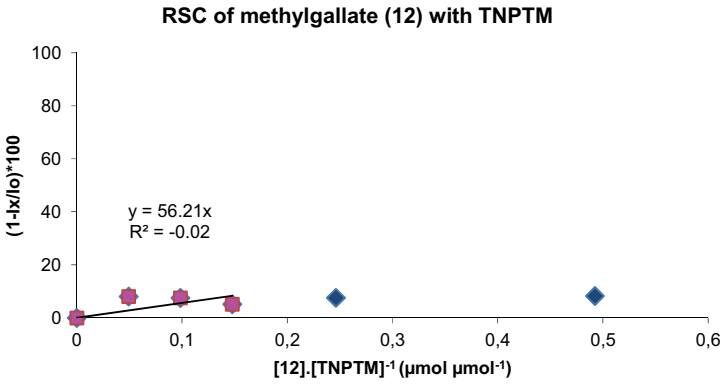

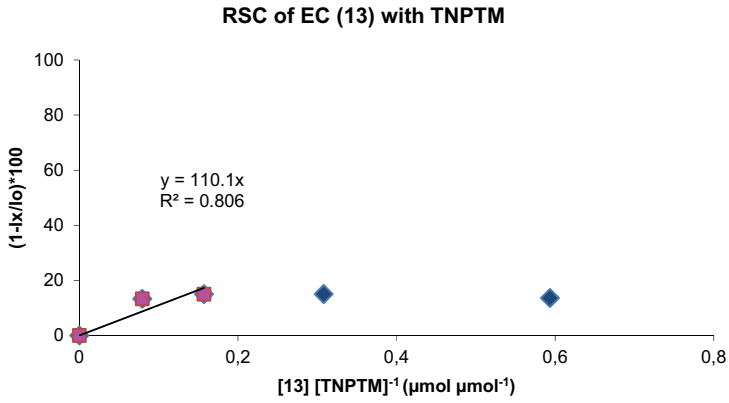
RSC of EC (13) with TNPTM
(1-Ix/Io)*100
y = 110.1x
R² = 0.806
[13] [TNPTM]-1 (µmol µmol-1)

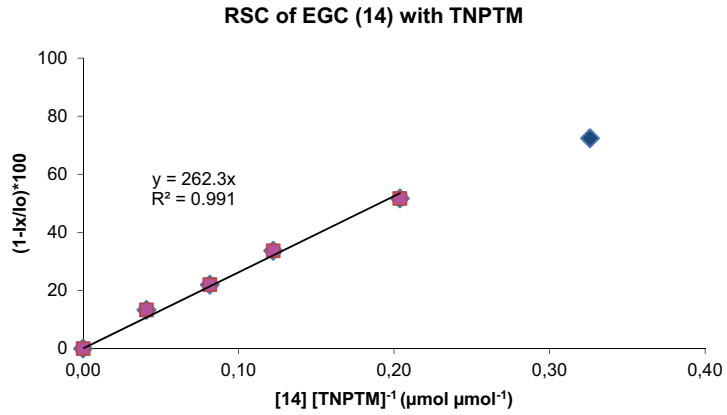
RSC of EGC (14) with TNPTM
(1-Ix/Io)*100
y = 262.3x
R² = 0.991
[14] [TNPTM]-1 (µmol µmol-1)

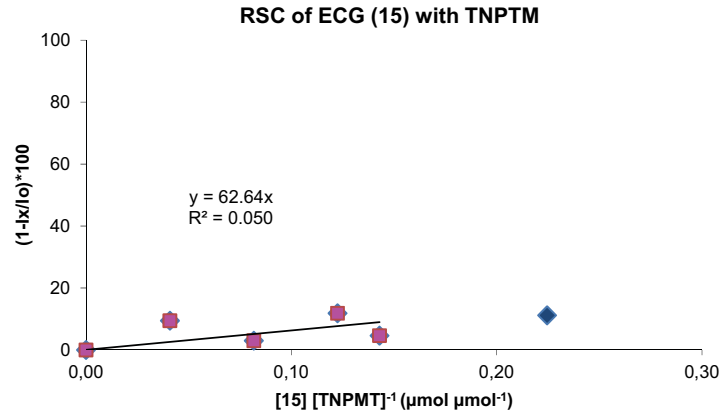
RSC of ECG (15) with TNPTM
(1-Ix/Io)*100
y = 62.64x
R² = 0.050
[15] [TNPMT]-1 (µmol µmol-1)

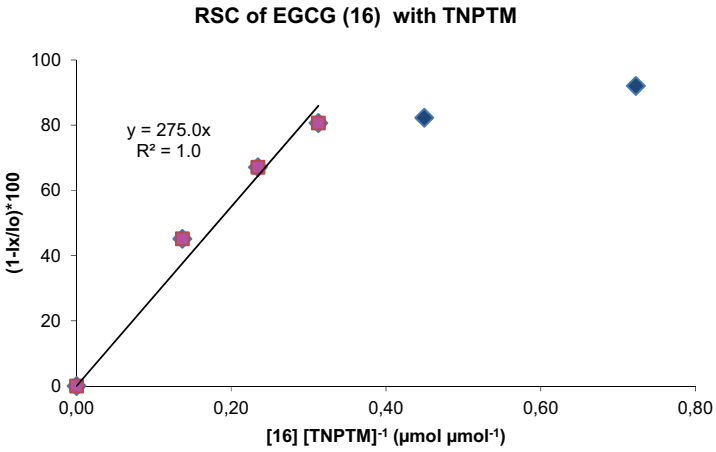
RSC of EGCG (16) with TNPTM
y = 275.0x
R² = 1.0
(1-Ix/Io)*100
[16] [TNPTM]-1 (µmol µmol-1)

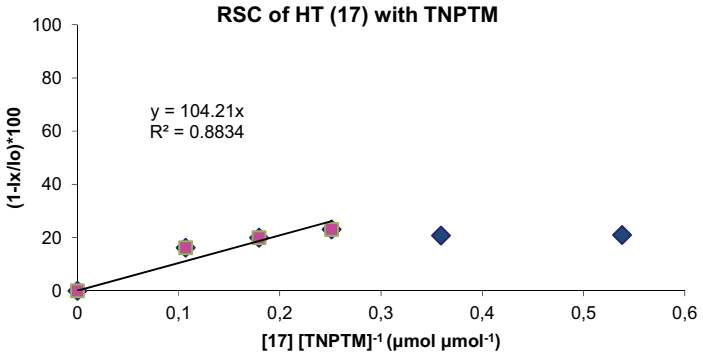
RSC of HT (17) with TNPTM
y = 104.21x
R² = 0.8834
(1-Ix/Io)*100
[17] [TNPTM]-1 (µmol µmol-1)

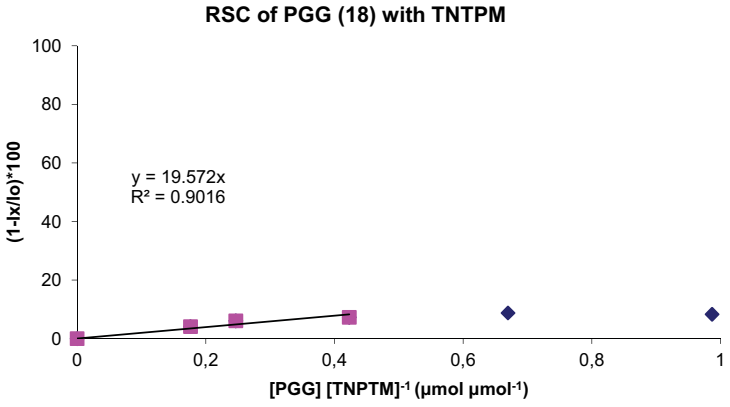
RSC of PGG (18) with TNTPM
y = 19.572x
R² = 0.9016
(1-Ix/Io)*100
[PGG] [TNPTM]-1 (µmol µmol-1)

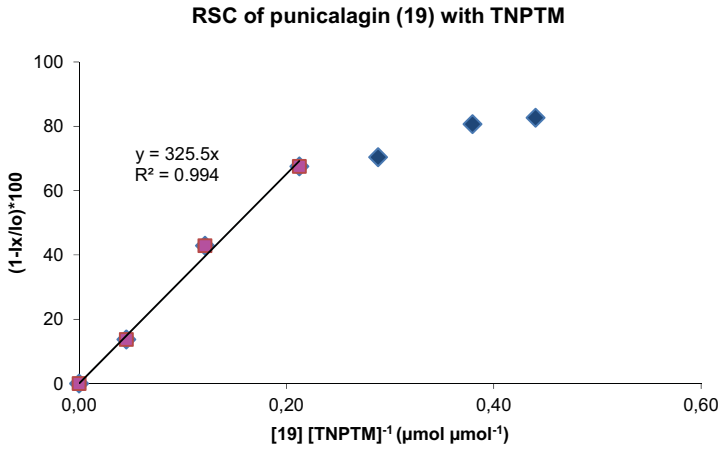
RSC of punicalagin (19) with TNPTM
y = 325.5x
R² = 0.994
(1-Ix/Io)*100
[19] [TNPTM]-1 (µmol µmol-1)
0
20
40
60
80
100
0,00
0,20
0,40
0,60

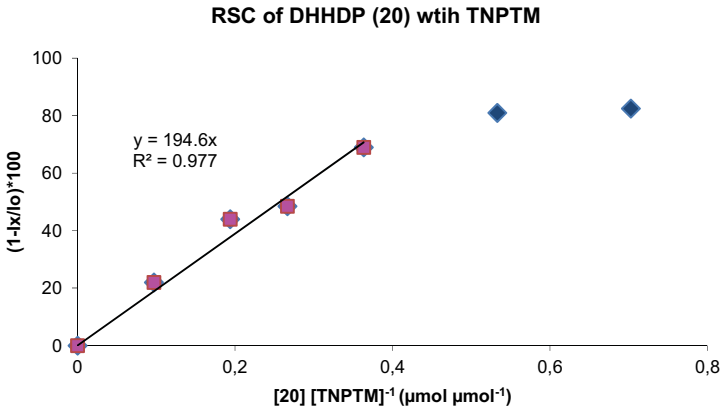
RSC of DHHDP (20) wtih TNPTM
y = 194.6x
R² = 0.977
(1-Ix/Io)*100
[20] [TNPTM]-1 (µmol µmol-1)
0
20
40
60
80
100
0
0,2
0,4
0,6
0,8

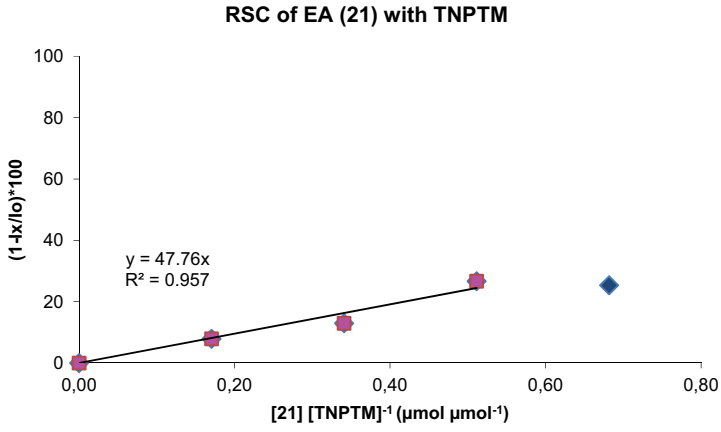
RSC of EA (21) with TNPTM
y = 47.76x
R² = 0.957
(1-Ix/Io)*100
[21] [TNPTM]-1 (µmol µmol-1)
0
20
40
60
80
100
0,00
0,20
0,40
0,60
0,80

E. Plots of the scavenging percentage versus the amount of (poly)phenols **10** to **21** in µg µmol^{-1} measured with DPPH (**9**) in $CHCl_3$/MeOH (2:1).

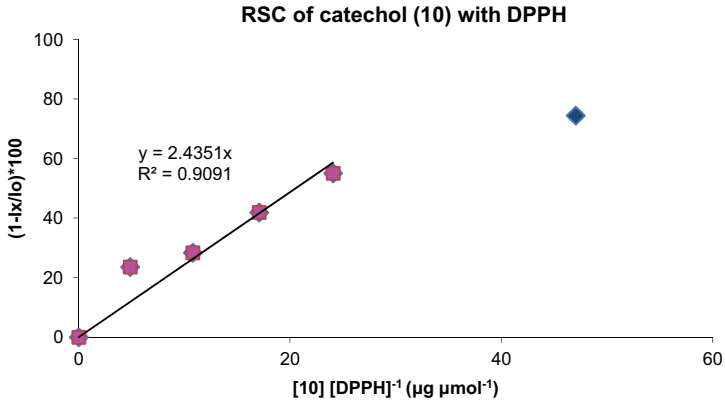

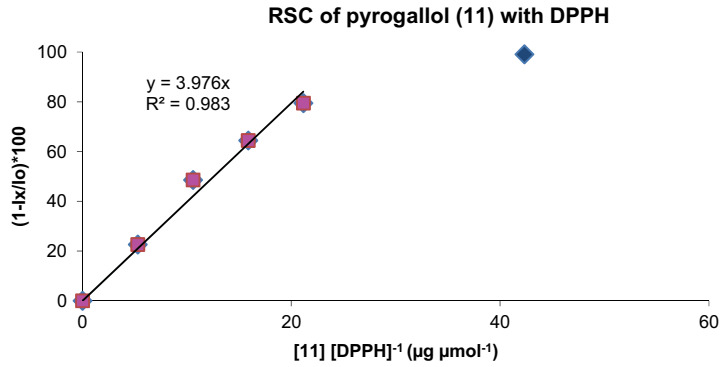

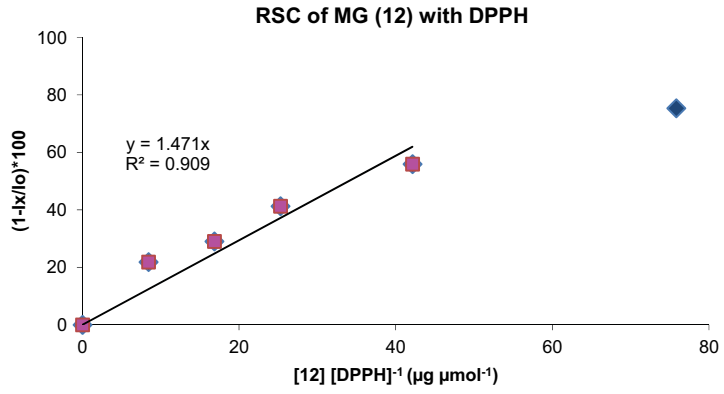

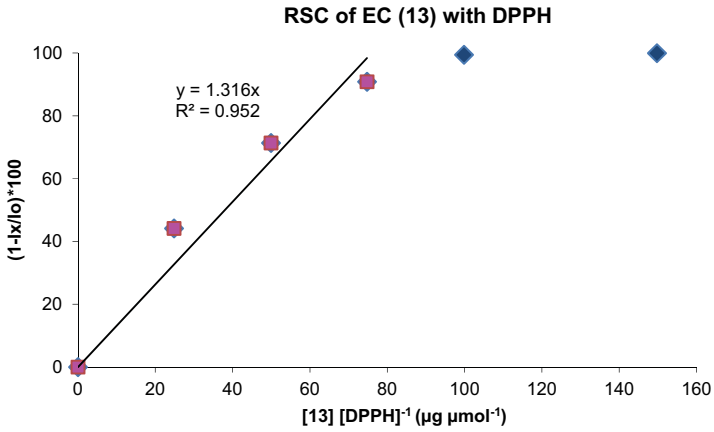
RSC of EC (13) with DPPH
y = 1.316x
R² = 0.952
(1-Ix/Io)*100
[13] [DPPH]-1 (µg µmol-1)

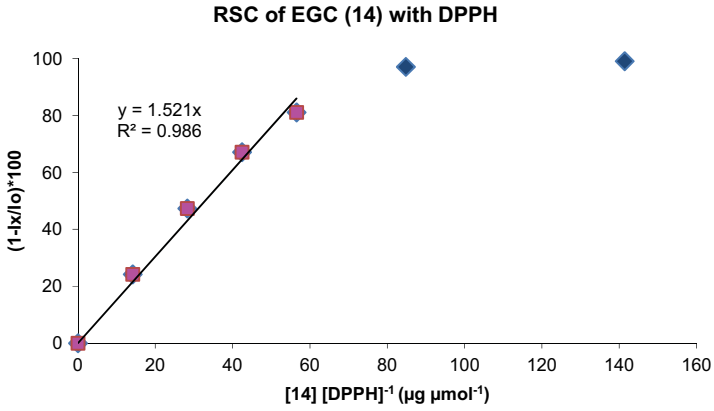
RSC of EGC (14) with DPPH
y = 1.521x
R² = 0.986
(1-Ix/Io)*100
[14] [DPPH]-1 (µg µmol-1)

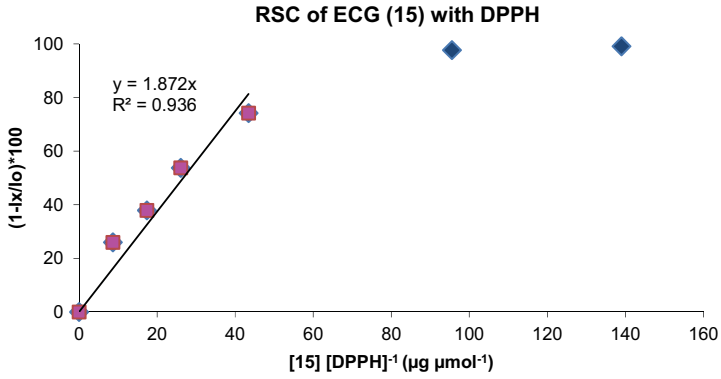
RSC of ECG (15) with DPPH
y = 1.872x
R² = 0.936
(1-Ix/Io)*100
[15] [DPPH]-1 (µg µmol-1)

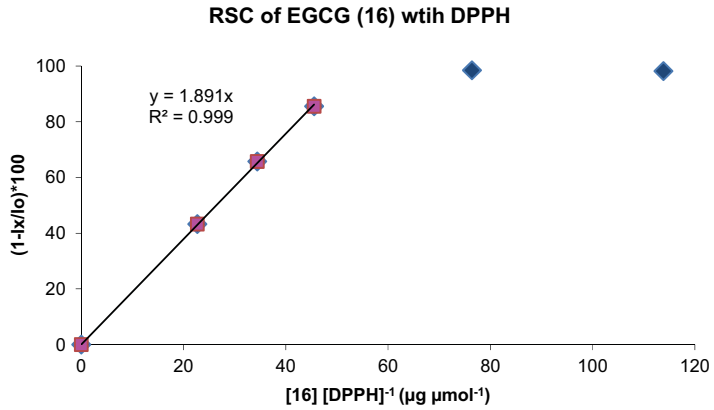
RSC of EGCG (16) wtih DPPH
y = 1.891x
R² = 0.999
(1-Ix/Io)*100
[16] [DPPH]-1 (µg µmol-1)

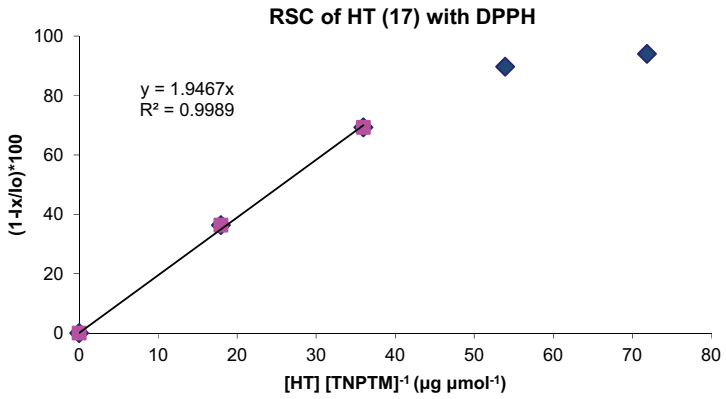
RSC of HT (17) with DPPH
y = 1.9467x
R² = 0.9989
(1-Ix/Io)*100
[HT] [TNPTM]-1 (µg µmol-1)

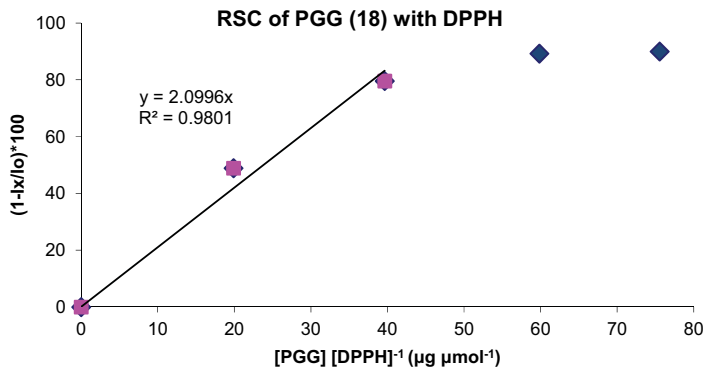
RSC of PGG (18) with DPPH
y = 2.0996x
R² = 0.9801
(1-Ix/Io)*100
[PGG] [DPPH]-1 (µg µmol-1)

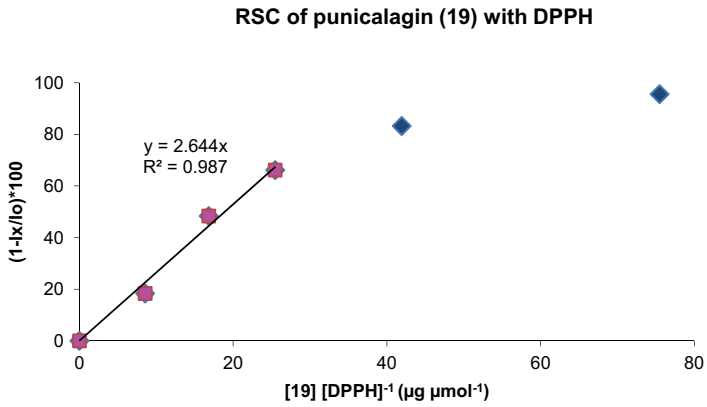
RSC of punicalagin (19) with DPPH
y = 2.644x
R² = 0.987
(1-Ix/Io)*100
[19] [DPPH]-1 (µg µmol-1)

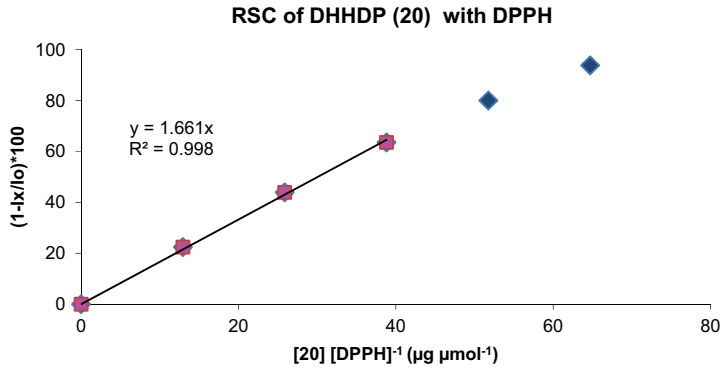
RSC of DHHDP (20) with DPPH
y = 1.661x
R² = 0.998
(1-Ix/Io)*100
[20] [DPPH]-1 (µg µmol-1)

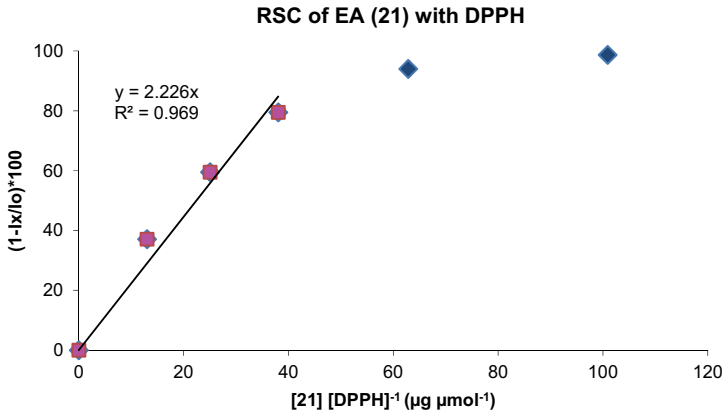
RSC of EA (21) with DPPH
y = 2.226x
R² = 0.969
(1-Ix/Io)*100
[21] [DPPH]-1 (µg µmol-1)

F. Plots of the scavenging percentage versus the amount of (poly)phenols **10** to **21** in μmol μmol^{-1} measured with DPPH (**9**) in $CHCl_3$/MeOH (2:1).

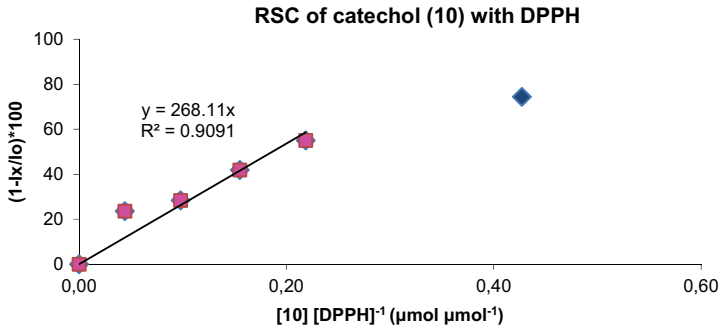

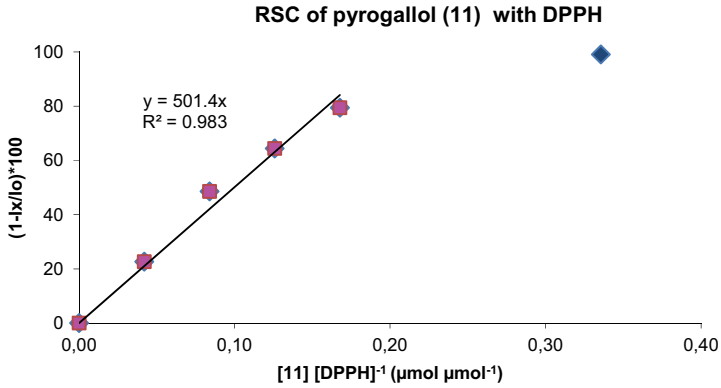

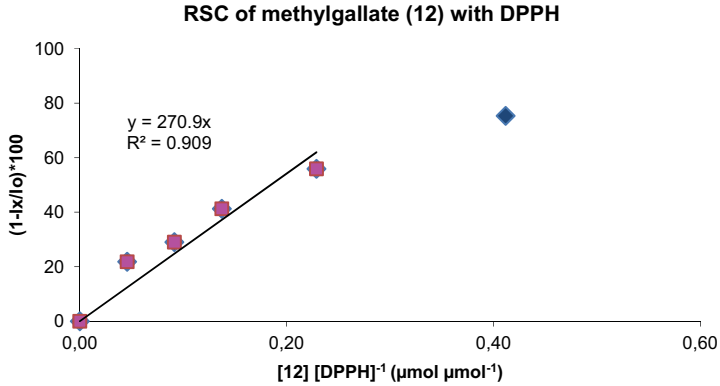

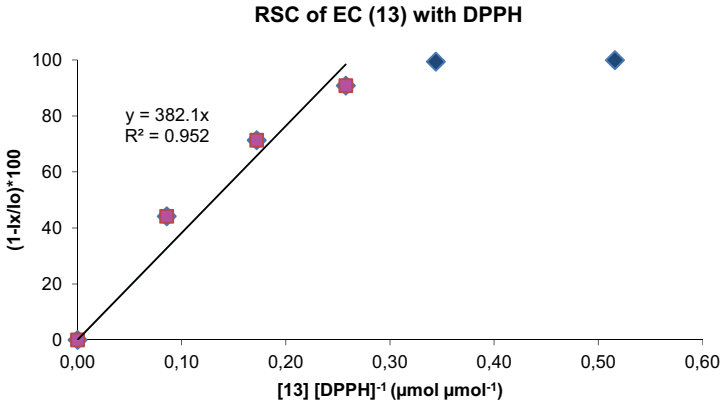
RSC of EC (13) with DPPH
y = 382.1x
R² = 0.952
(1-Ix/Io)*100
[13] [DPPH]-1 (µmol µmol-1)
0
20
40
60
80
100
0,00
0,10
0,20
0,30
0,40
0,50
0,60

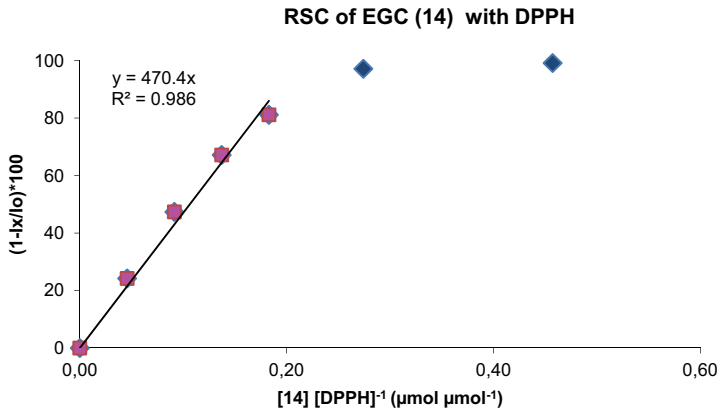
RSC of EGC (14) with DPPH
y = 470.4x
R² = 0.986
(1-Ix/Io)*100
[14] [DPPH]-1 (µmol µmol-1)
0
20
40
60
80
100
0,00
0,20
0,40
0,60

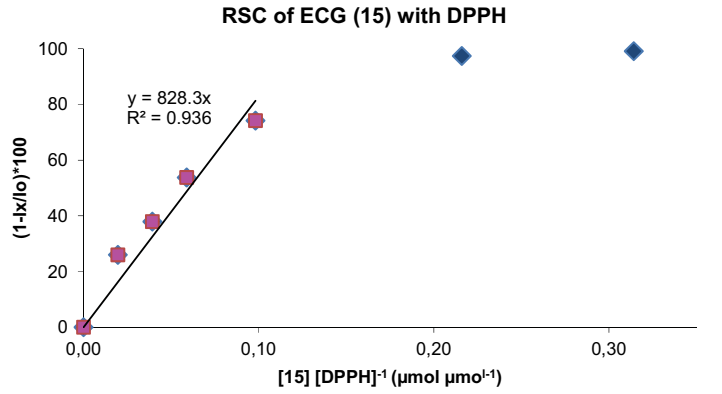
RSC of ECG (15) with DPPH
y = 828.3x
R² = 0.936
(1-Ix/Io)*100
[15] [DPPH]-1 (µmol µmol-1)
0
20
40
60
80
100
0,00
0,10
0,20
0,30

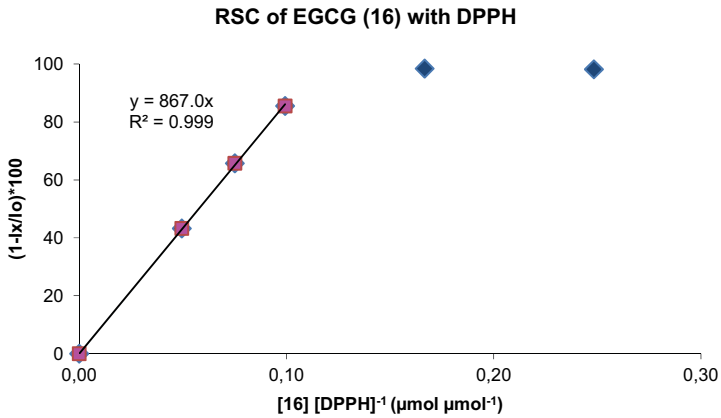
RSC of EGCG (16) with DPPH
y = 867.0x
R² = 0.999
(1-Ix/Io)*100
[16] [DPPH]-1 (µmol µmol-1)
0
20
40
60
80
100
0,00
0,10
0,20
0,30

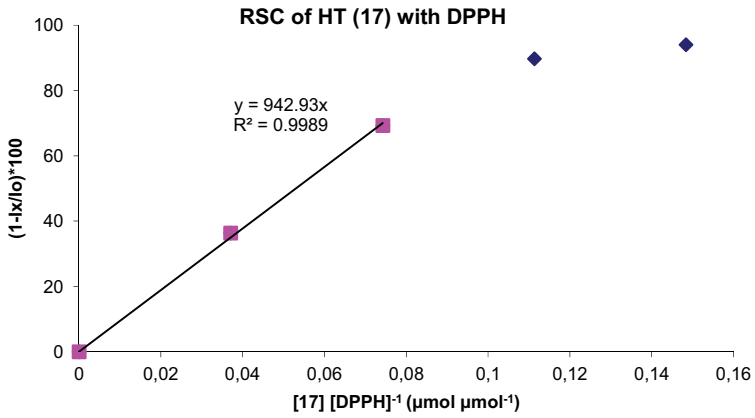
RSC of HT (17) with DPPH
y = 942.93x
R² = 0.9989
(1-Ix/Io)*100
[17] [DPPH]-1 (µmol µmol-1)
0
20
40
60
80
100
0
0,02
0,04
0,06
0,08
0,1
0,12
0,14
0,16

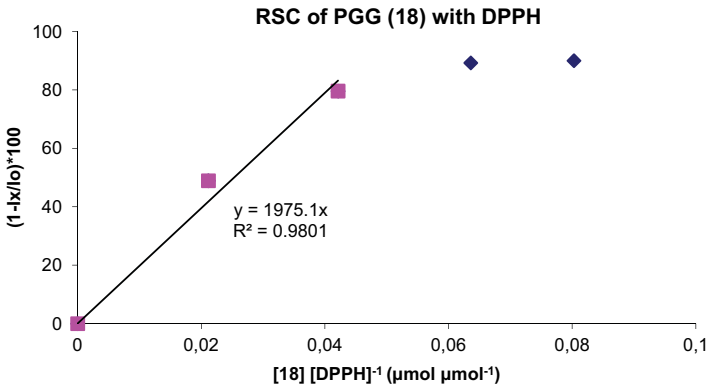
RSC of PGG (18) with DPPH
y = 1975.1x
R² = 0.9801
(1-Ix/Io)*100
[18] [DPPH]-1 (µmol µmol-1)
0
20
40
60
80
100
0
0,02
0,04
0,06
0,08
0,1

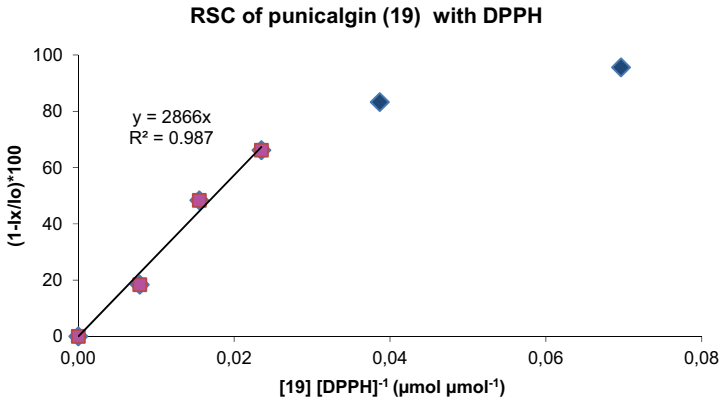
RSC of punicalgin (19) with DPPH
y = 2866x
R² = 0.987
(1-Ix/Io)*100
[19] [DPPH]-1 (µmol µmol-1)
0
20
40
60
80
100
0,00
0,02
0,04
0,06
0,08

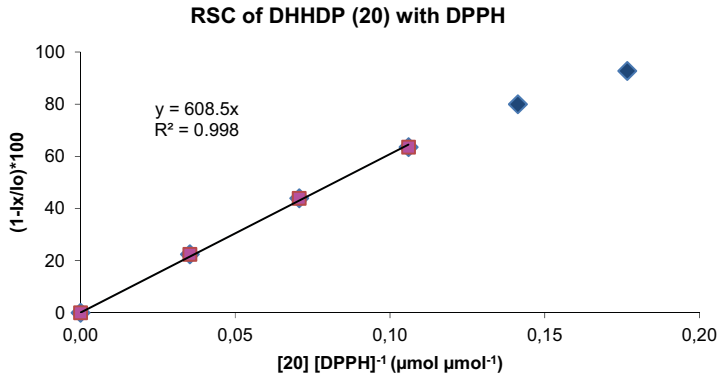
RSC of DHHDP (20) with DPPH
y = 608.5x
R² = 0.998
(1-Ix/Io)*100
[20] [DPPH]-1 (µmol µmol-1)
0
20
40
60
80
100
0,00
0,05
0,10
0,15
0,20

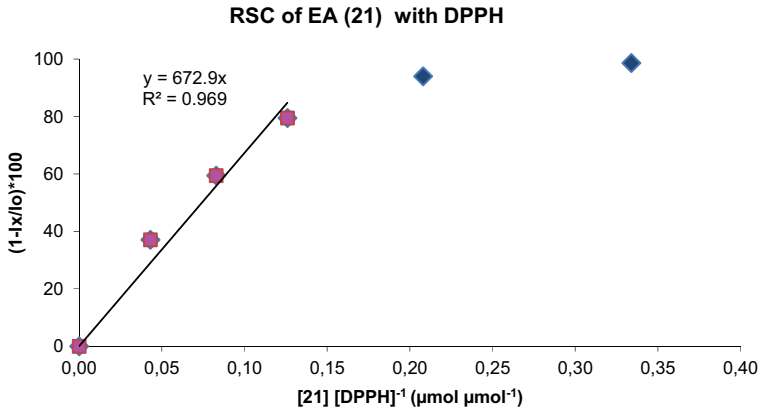
RSC of EA (21) with DPPH
y = 672.9x
R² = 0.969
(1-Ix/Io)*100
[21] [DPPH]-1 (µmol µmol-1)
0
20
40
60
80
100
0,00
0,05
0,10
0,15
0,20
0,25
0,30
0,35
0,40

Annex 10. UV-Vis spectra of TNPTM and its anion 7 in $CHCl_3$/MeOH (2:1)

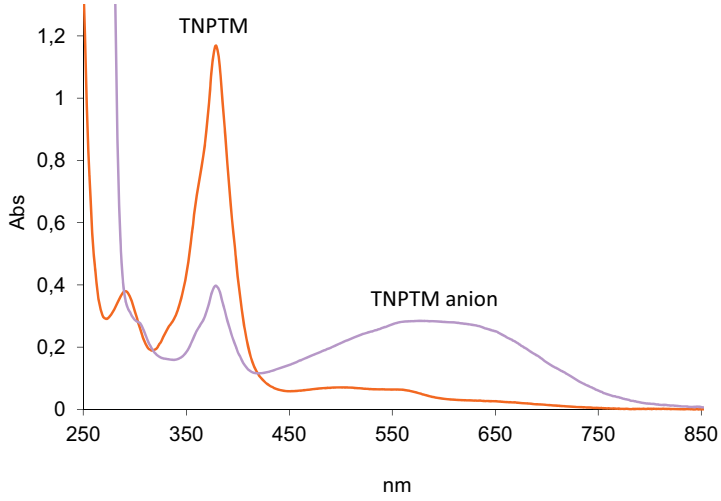

Annex 11. Mass spectra of the reaction between TNPTM and DHHDP

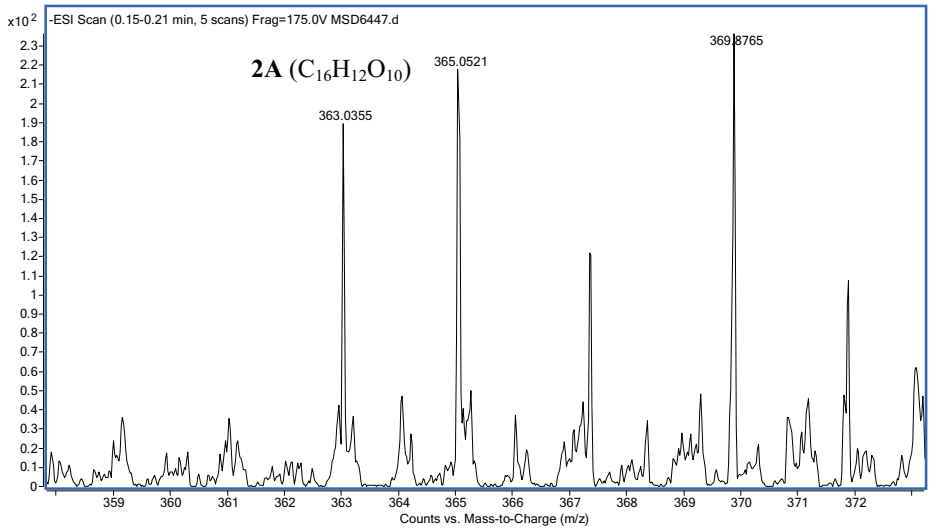

Annex 12. Kinetics of (poly)phenols with TNPTM (t= 48 h)

1. Kinetics of pyrogallol (**11**) with TNPTM in $CHCl_3$/MeOH (2:1)

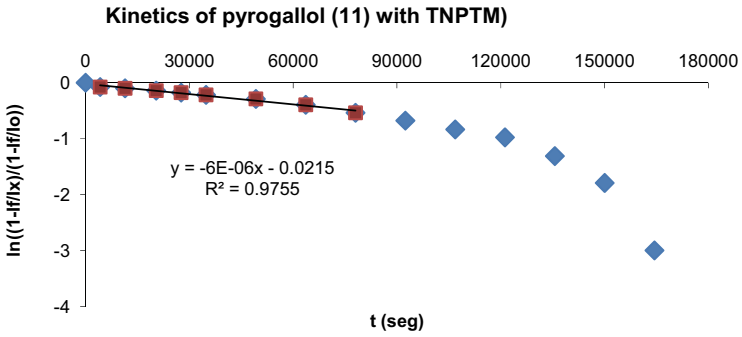

2. Kinetics of EGC (**14**) with TNPTM in $CHCl_3$/MeOH (2:1)

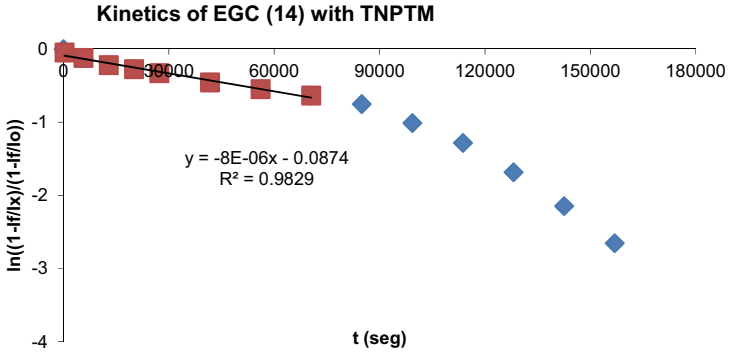

3. Kinetics of EGCG (**14**) with TNPTM in $CHCl_3$/MeOH (2:1)

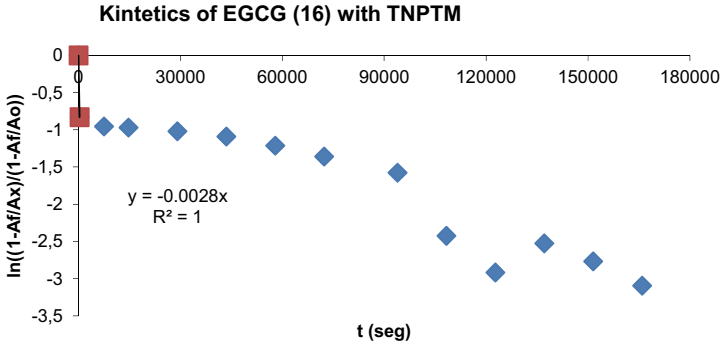

4. Kinetics of HT (**17**) with TNPTM in $CHCl_3$/MeOH (2:1)

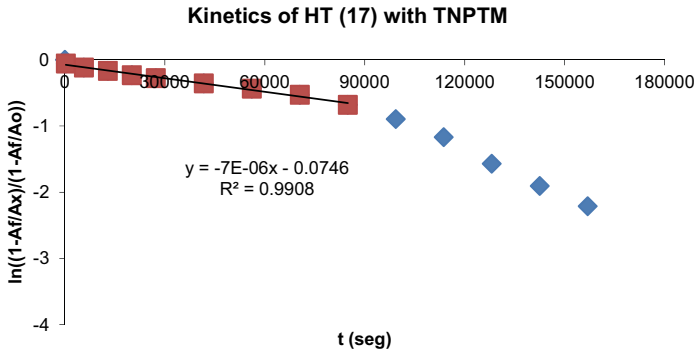

5. Kinetics of punicalagin (**19**) with TNPTM in $CHCl_3$/MeOH (2:1)

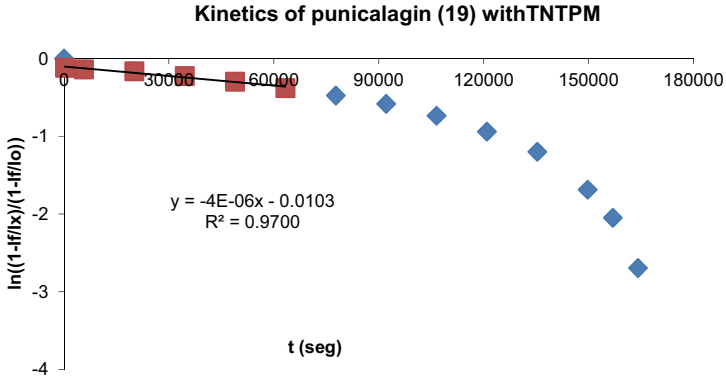

6. Kinetics of DHHDP (**20**) with TNPTM in $CHCl_3$/MeOH (2:1)

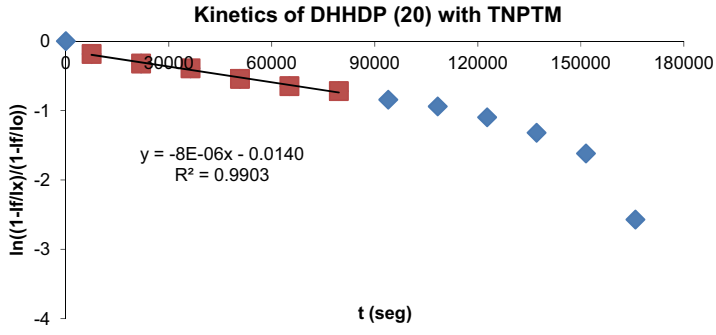

Annex 13. Metal-reducing activity of (poly)phenols measured with the FRAP method

A. Plots of the Reducing Rates of (poly)phenols (**10**-**21**) measured with the FRAP method and represented in μg mL^{-1}.

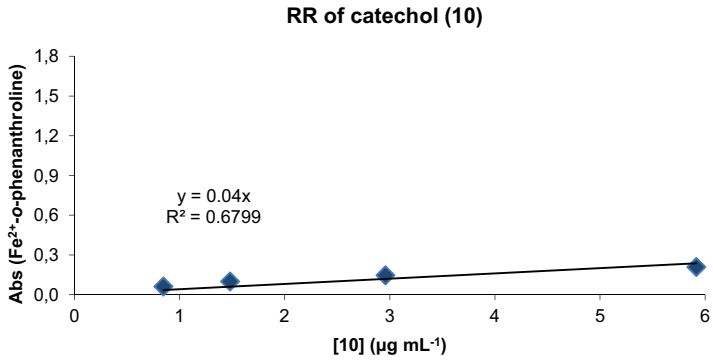

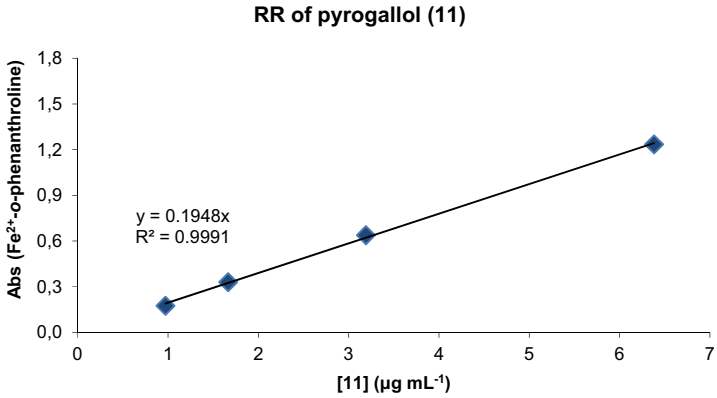

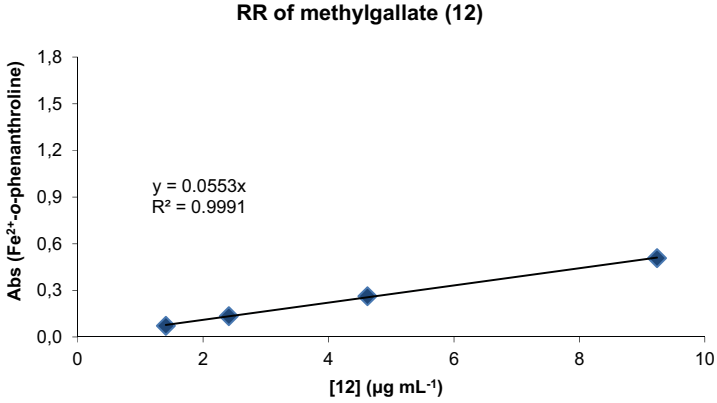

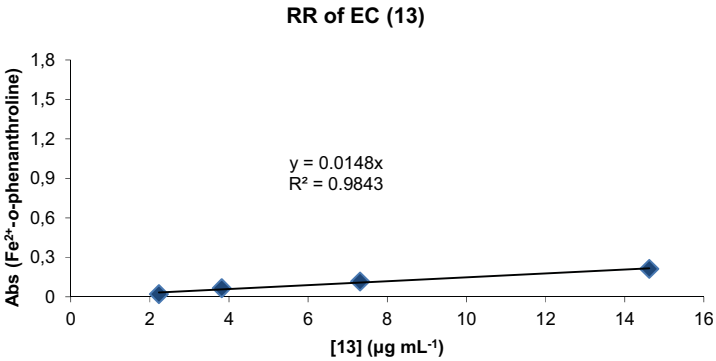
RR of EC (13)
y = 0.0148x
R² = 0.9843
Abs (Fe²⁺-o-phenanthroline)
[13] (µg mL⁻¹)
1,8
1,5
1,2
0,9
0,6
0,3
0
0
2
4
6
8
10
12
14
16

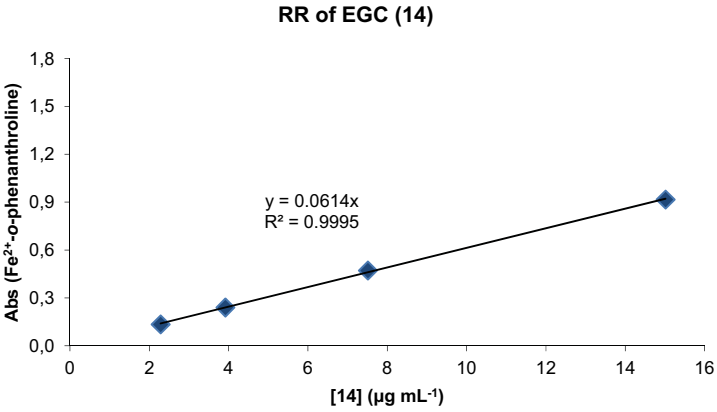
RR of EGC (14)
y = 0.0614x
R² = 0.9995
Abs (Fe²⁺-o-phenanthroline)
[14] (µg mL⁻¹)
1,8
1,5
1,2
0,9
0,6
0,3
0,0
0
2
4
6
8
10
12
14
16

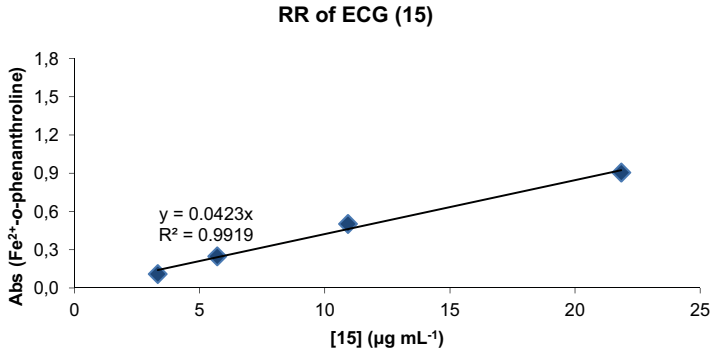
RR of ECG (15)
y = 0.0423x
R² = 0.9919
Abs (Fe²⁺-o-phenanthroline)
[15] (µg mL⁻¹)
1,8
1,5
1,2
0,9
0,6
0,3
0,0
0
5
10
15
20
25

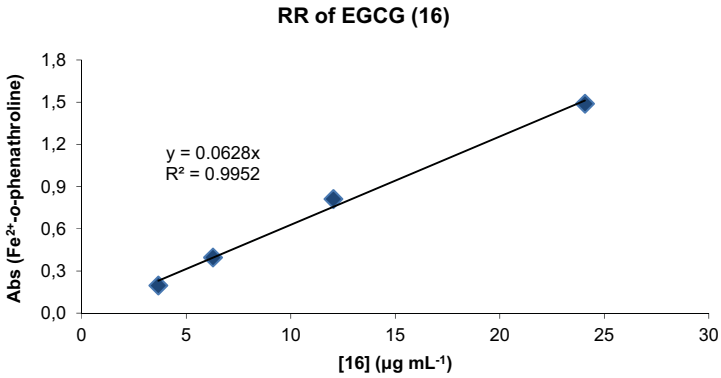
RR of EGCG (16)
Abs (Fe2+-o-phenanthroline)
y = 0.0628x
R² = 0.9952
[16] (µg mL-1)

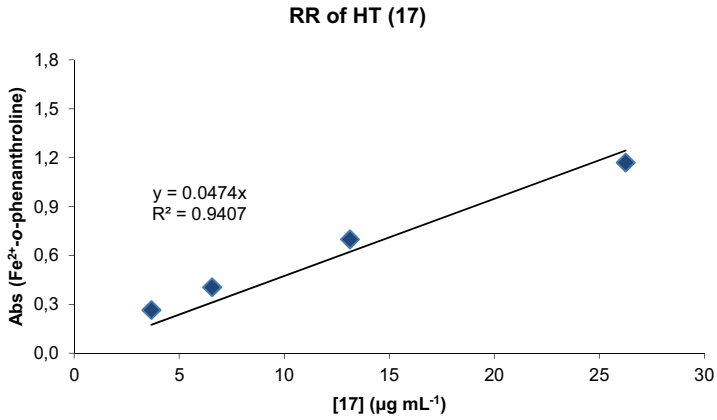
RR of HT (17)
Abs (Fe2+-o-phenanthroline)
y = 0.0474x
R² = 0.9407
[17] (µg mL-1)

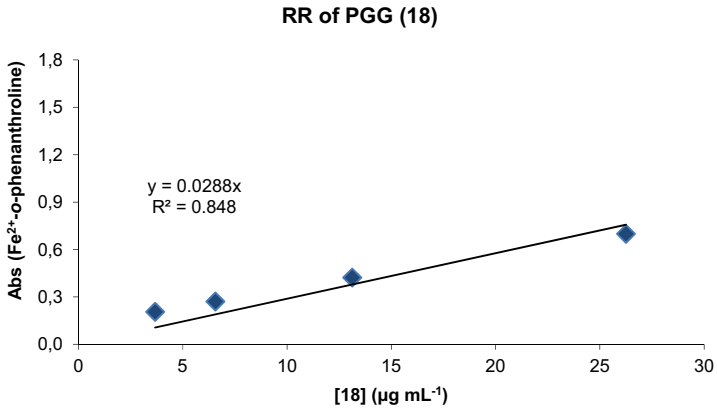
RR of PGG (18)
Abs (Fe2+-o-phenanthroline)
y = 0.0288x
R² = 0.848
[18] (µg mL-1)

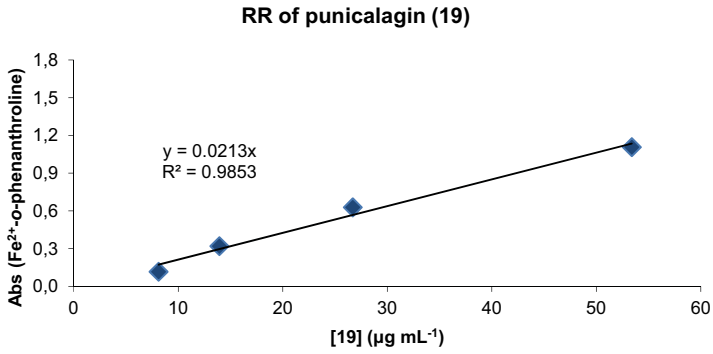
RR of punicalagin (19)
y = 0.0213x
R² = 0.9853
Abs (Fe²⁺-o-phenanthroline)
[19] (µg mL⁻¹)
0,0
0,3
0,6
0,9
1,2
1,5
1,8
0
10
20
30
40
50
60

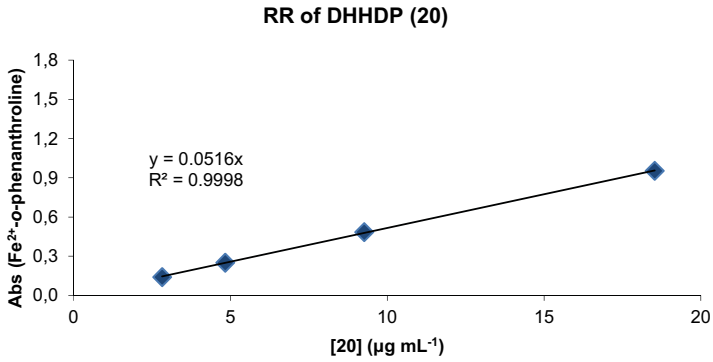
RR of DHHDP (20)
y = 0.0516x
R² = 0.9998
Abs (Fe²⁺-o-phenanthroline)
[20] (µg mL⁻¹)
0,0
0,3
0,6
0,9
1,2
1,5
1,8
0
5
10
15
20

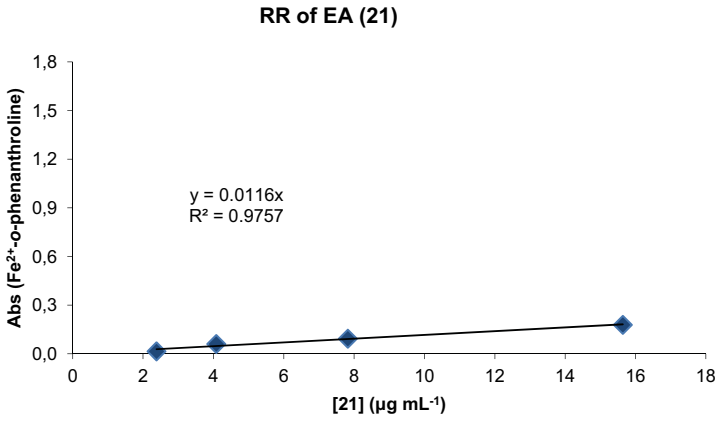
RR of EA (21)
y = 0.0116x
R² = 0.9757
Abs (Fe²⁺-o-phenanthroline)
[21] (µg mL⁻¹)
0,0
0,3
0,6
0,9
1,2
1,5
1,8
0
2
4
6
8
10
12
14
16
18

B. Plots of the Reducing Rates of (poly)phenols (**10**-**21**) measured with the FRAP method and represented in µmol mL^{-1}.

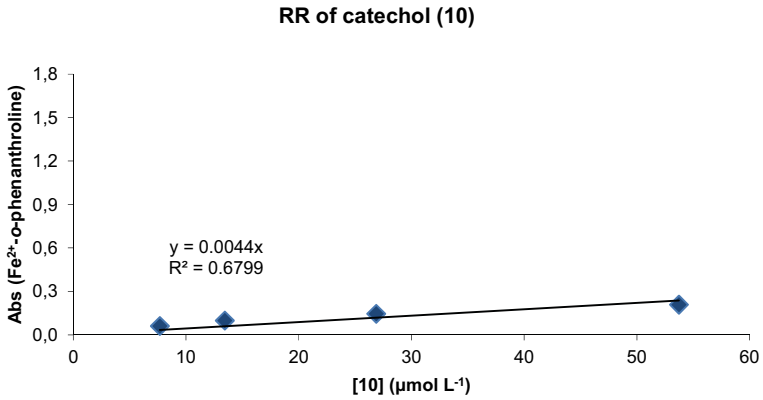

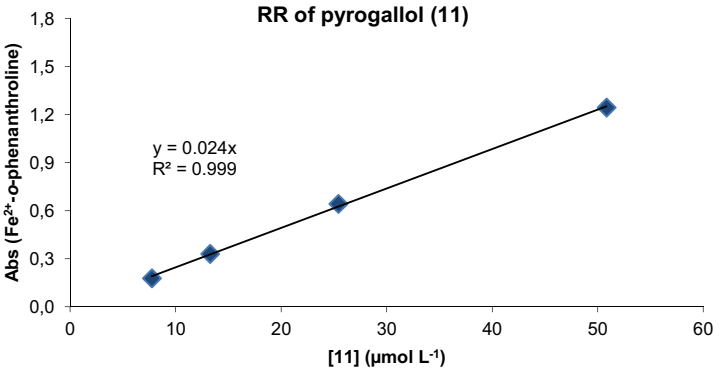

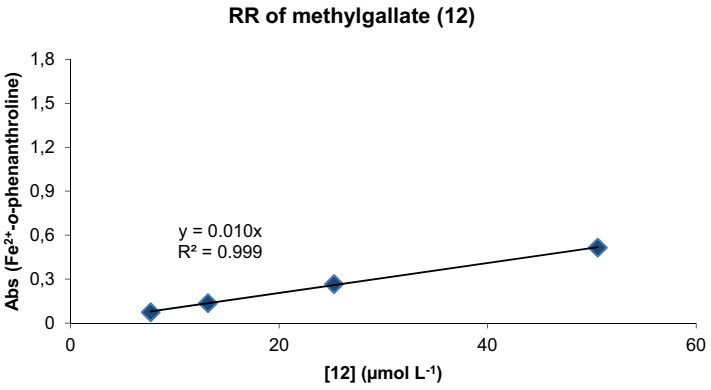

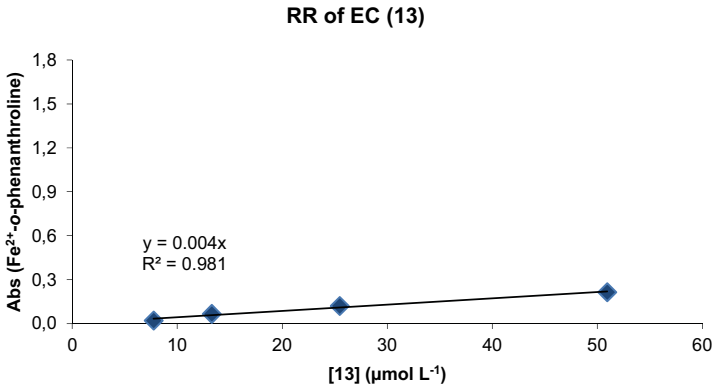
RR of EC (13)
Abs (Fe2+-o-phenanthroline)
y = 0.004x
R² = 0.981
[13] (µmol L-1)

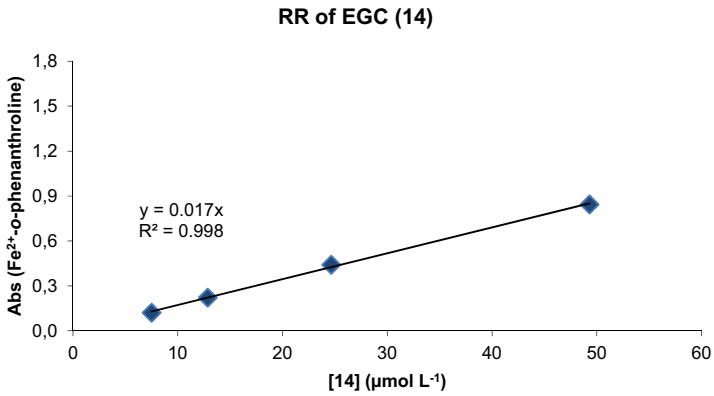
RR of EGC (14)
Abs (Fe2+-o-phenanthroline)
y = 0.017x
R² = 0.998
[14] (µmol L-1)

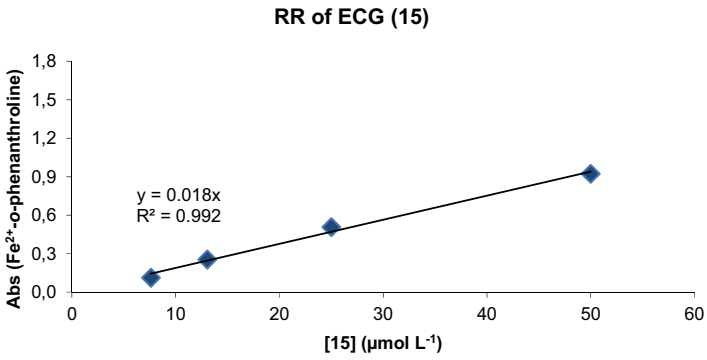
RR of ECG (15)
Abs (Fe2+-o-phenanthroline)
y = 0.018x
R² = 0.992
[15] (µmol L-1)

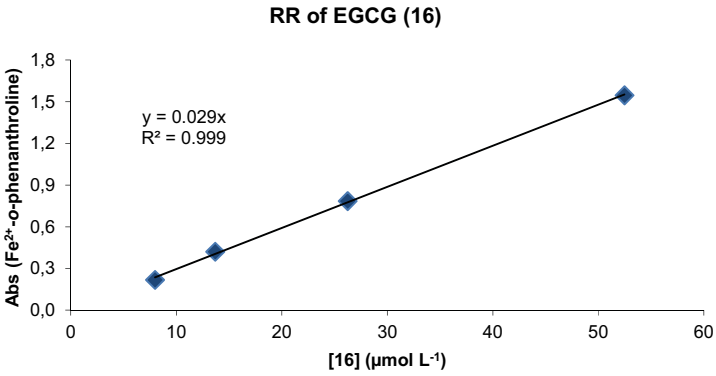
RR of EGCG (16)
y = 0.029x
R² = 0.999
Abs (Fe²⁺-o-phenanthroline)
[16] (µmol L⁻¹)
0,0
0,3
0,6
0,9
1,2
1,5
1,8
0
10
20
30
40
50
60

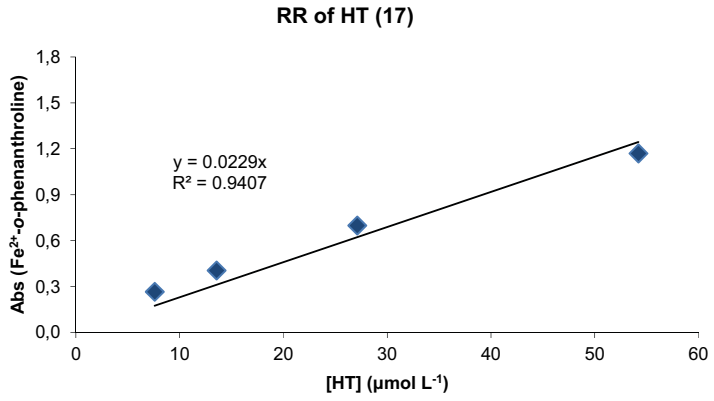
RR of HT (17)
y = 0.0229x
R² = 0.9407
Abs (Fe²⁺-o-phenanthroline)
[HT] (µmol L⁻¹)
0,0
0,3
0,6
0,9
1,2
1,5
1,8
0
10
20
30
40
50
60

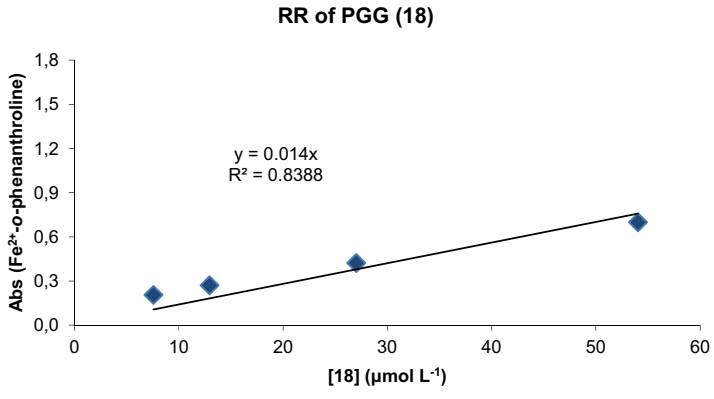
RR of PGG (18)
y = 0.014x
R² = 0.8388
Abs (Fe²⁺-o-phenanthroline)
[18] (µmol L⁻¹)
0,0
0,3
0,6
0,9
1,2
1,5
1,8
0
10
20
30
40
50
60

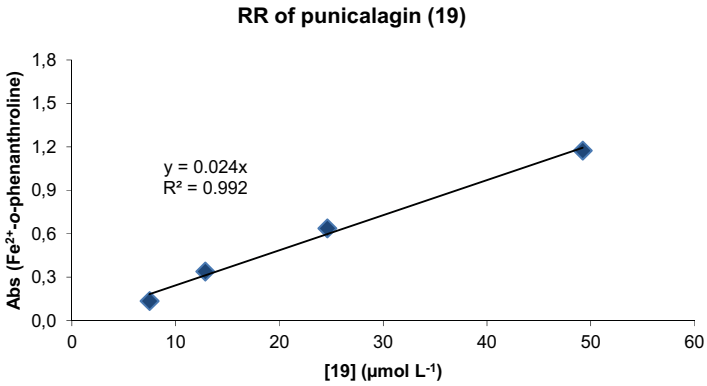
RR of punicalagin (19)
y = 0.024x
R² = 0.992
Abs (Fe²⁺-o-phenanthroline)
[19] (µmol L⁻¹)

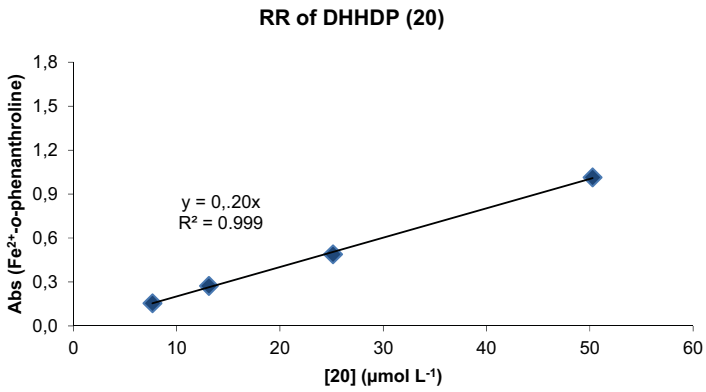
RR of DHHDP (20)
y = 0,.20x
R² = 0.999
Abs (Fe²⁺-o-phenanthroline)
[20] (µmol L⁻¹)

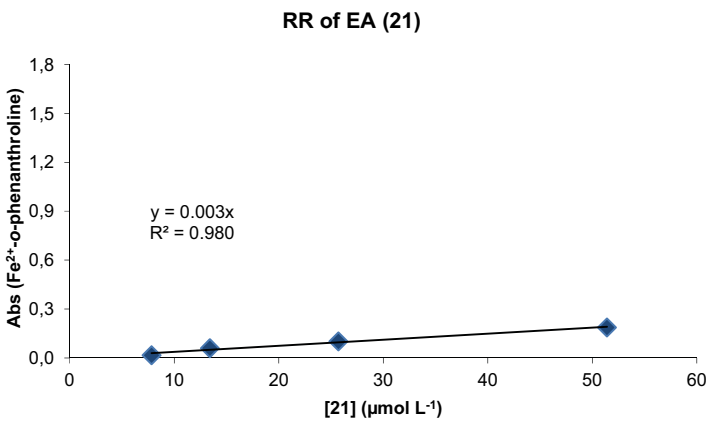
RR of EA (21)
y = 0.003x
R² = 0.980
Abs (Fe²⁺-o-phenanthroline)
[21] (µmol L⁻¹)

C. Plots of the Reducing Capacity of (poly)phenols (**10**-**21**) measured with the FRAP method and represented in μg mL^{-1}.

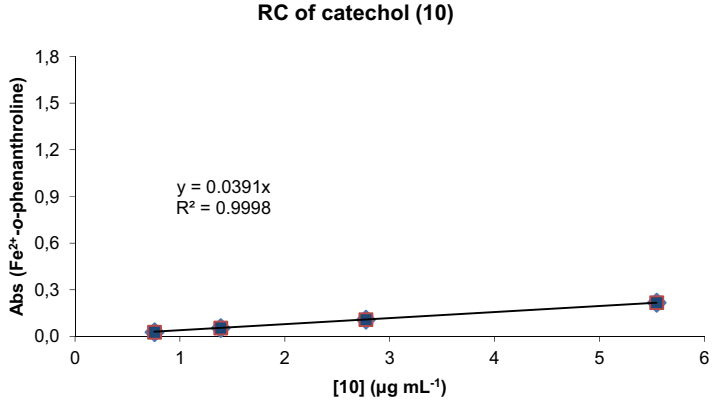

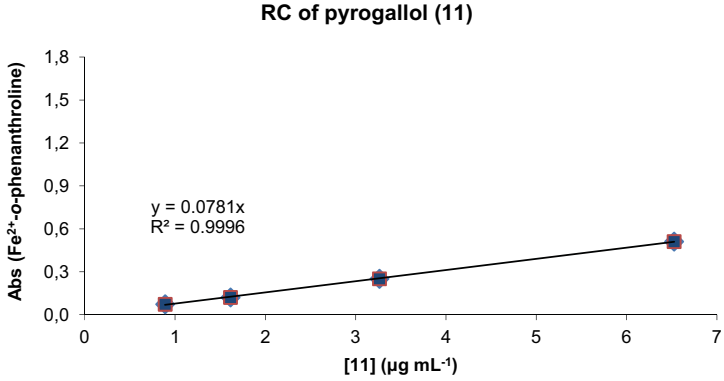

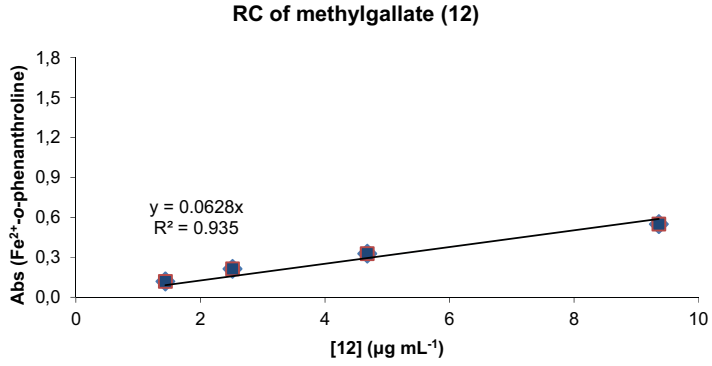

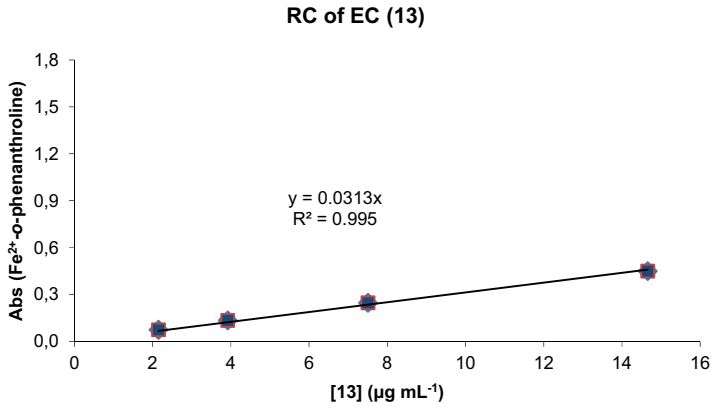
RC of EC (13)
y = 0.0313x
R² = 0.995
Abs (Fe²⁺-o-phenanthroline)
[13] (µg mL⁻¹)
0,0
0,3
0,6
0,9
1,2
1,5
1,8
0
2
4
6
8
10
12
14
16

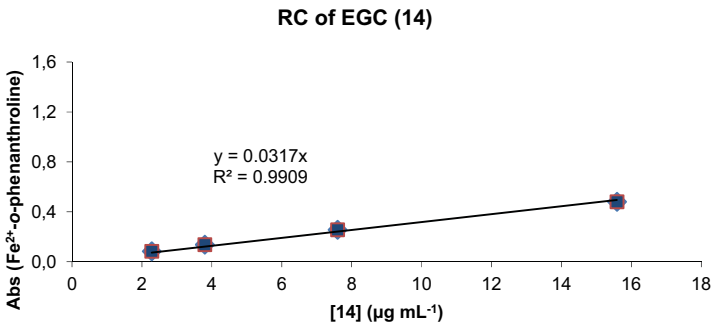
RC of EGC (14)
y = 0.0317x
R² = 0.9909
Abs (Fe²⁺-o-phenanthroline)
[14] (µg mL⁻¹)
0,0
0,4
0,8
1,2
1,6
0
2
4
6
8
10
12
14
16
18

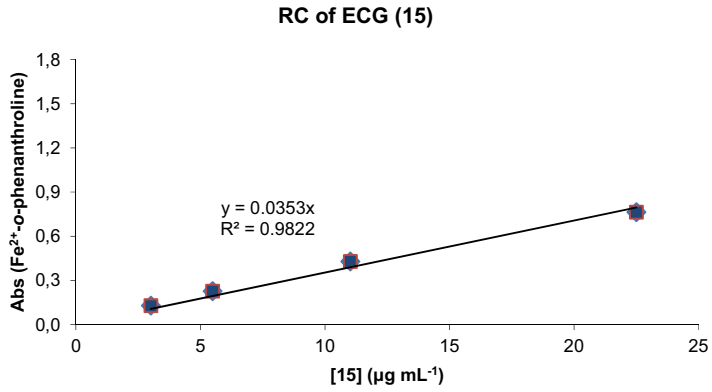
RC of ECG (15)
y = 0.0353x
R² = 0.9822
Abs (Fe²⁺-o-phenanthroline)
[15] (µg mL⁻¹)
0,0
0,3
0,6
0,9
1,2
1,5
1,8
0
5
10
15
20
25

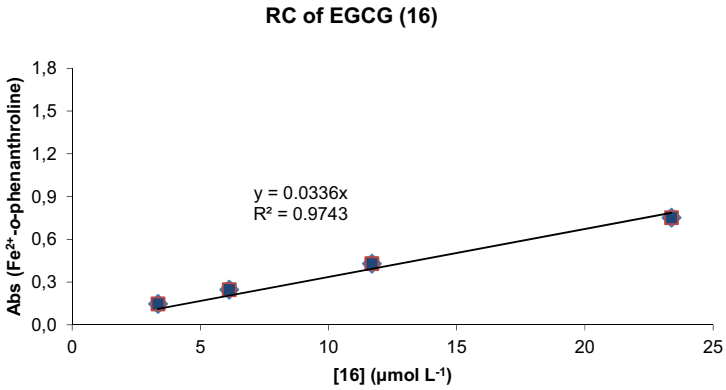
RC of EGCG (16)
Abs (Fe²⁺-o-phenanthroline)
y = 0.0336x
R² = 0.9743
[16] (µmol L⁻¹)

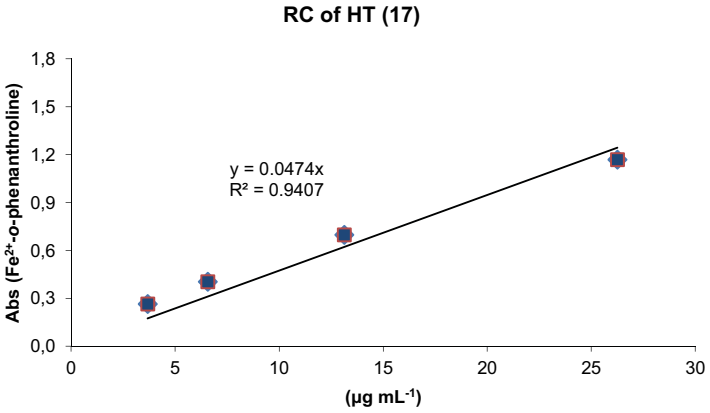
RC of HT (17)
Abs (Fe²⁺-o-phenanthroline)
y = 0.0474x
R² = 0.9407
(µg mL⁻¹)

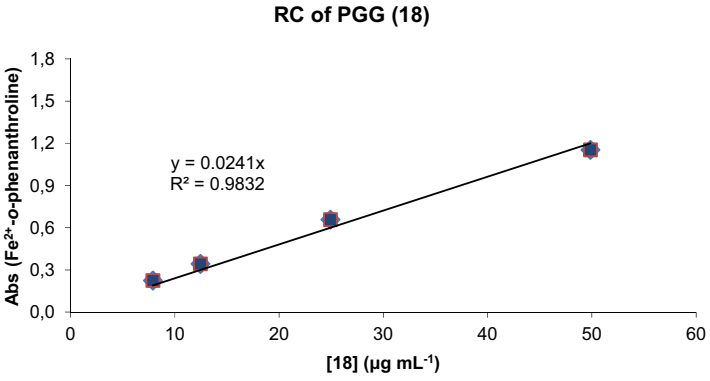
RC of PGG (18)
Abs (Fe²⁺-o-phenanthroline)
y = 0.0241x
R² = 0.9832
[18] (µg mL⁻¹)

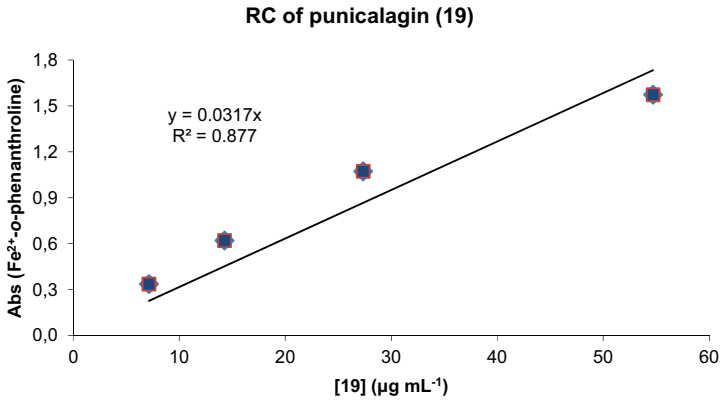
RC of punicalagin (19)
y = 0.0317x
R² = 0.877
Abs (Fe²⁺-o-phenanthroline)
[19] (µg mL⁻¹)
0,0
0,3
0,6
0,9
1,2
1,5
1,8
0
10
20
30
40
50
60

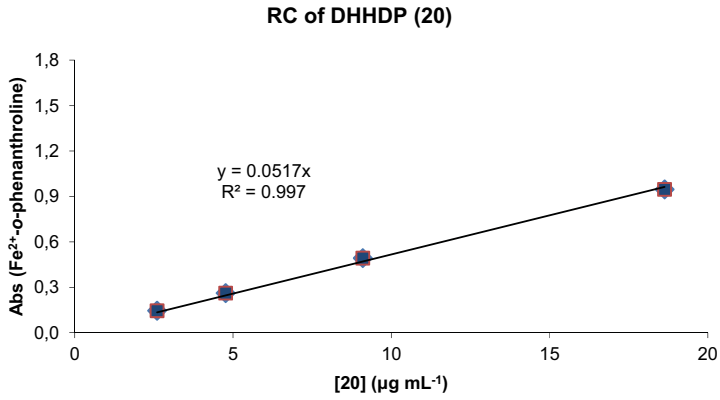
RC of DHHDP (20)
y = 0.0517x
R² = 0.997
Abs (Fe²⁺-o-phenanthroline)
[20] (µg mL⁻¹)
0,0
0,3
0,6
0,9
1,2
1,5
1,8
0
5
10
15
20

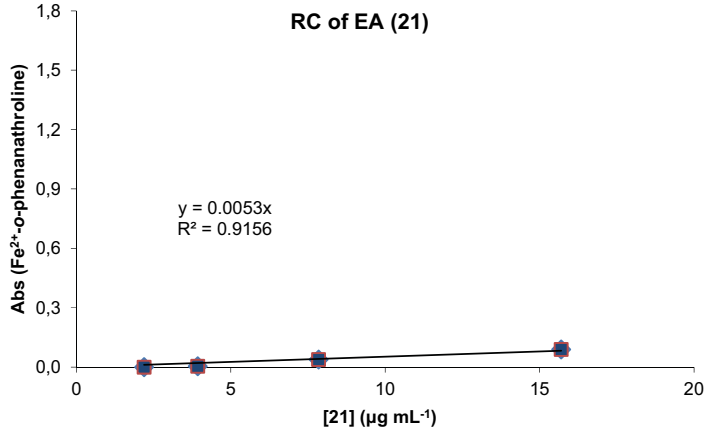
RC of EA (21)
y = 0.0053x
R² = 0.9156
Abs (Fe²⁺-o-phenanthroline)
[21] (µg mL⁻¹)
0,0
0,3
0,6
0,9
1,2
1,5
1,8
0
5
10
15
20

D. Plots of the Reducing Capacity of (poly)phenols (**10**-**21**) measured with the FRAP method and represented in μmol mL^{-1}.

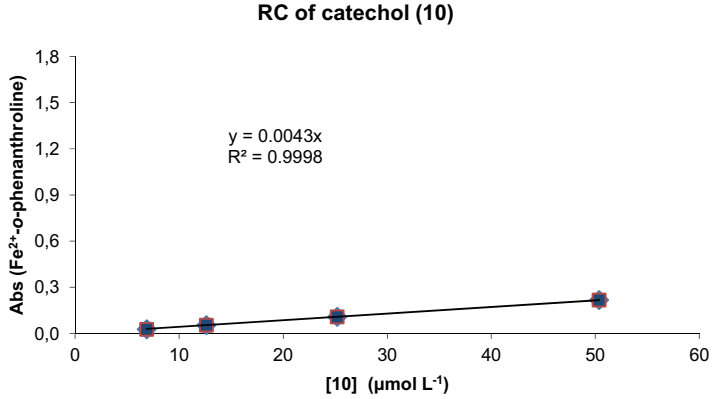

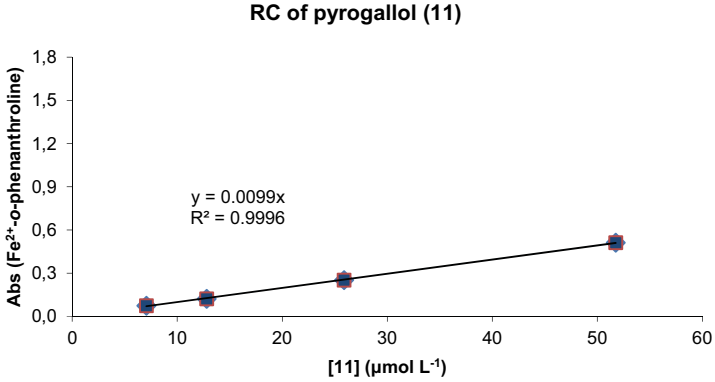

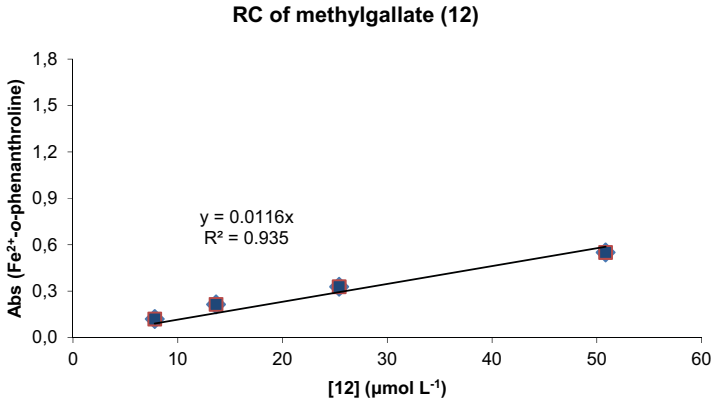

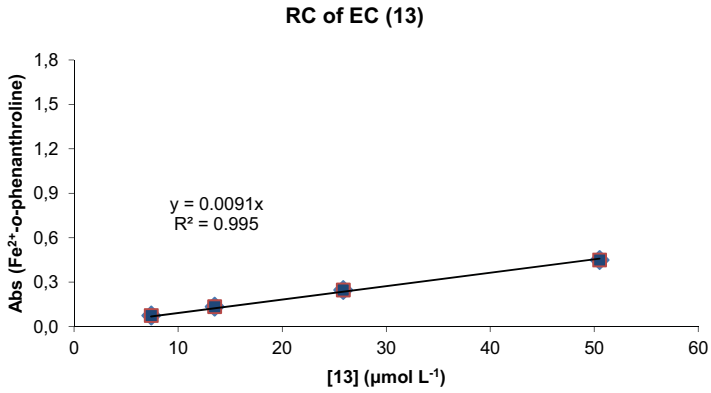
RC of EC (13)
Abs (Fe2+-o-phenanthroline)
y = 0.0091x
R² = 0.995
[13] (µmol L-1)

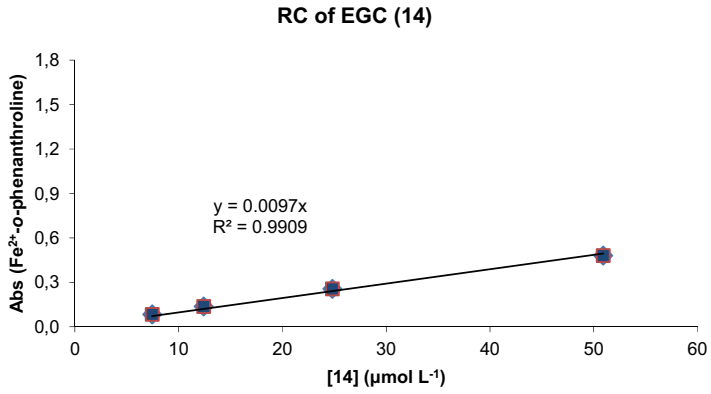
RC of EGC (14)
Abs (Fe2+-o-phenanthroline)
y = 0.0097x
R² = 0.9909
[14] (µmol L-1)

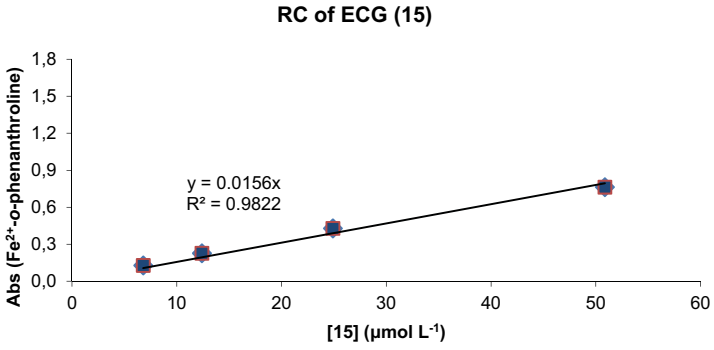
RC of ECG (15)
Abs (Fe2+-o-phenanthroline)
y = 0.0156x
R² = 0.9822
[15] (µmol L-1)

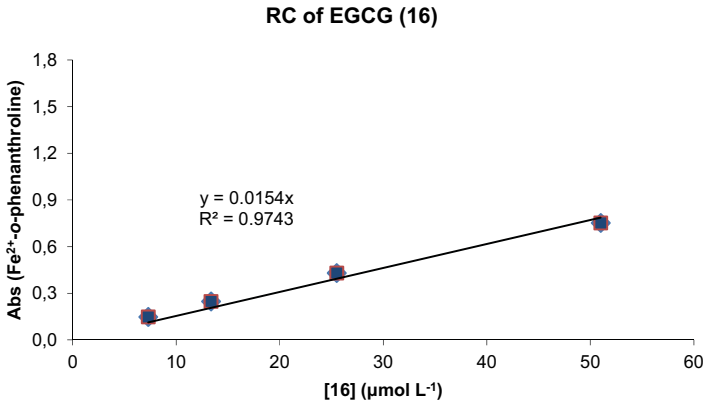
RC of EGCG (16)
y = 0.0154x
R² = 0.9743
Abs (Fe²⁺-o-phenanthroline)
[16] (µmol L⁻¹)
0,0
0,3
0,6
0,9
1,2
1,5
1,8
0
10
20
30
40
50
60

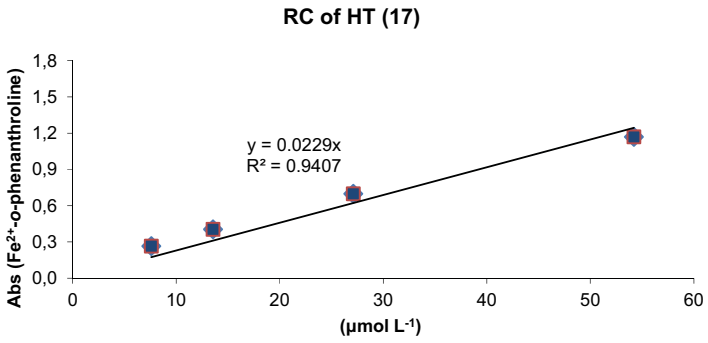
RC of HT (17)
y = 0.0229x
R² = 0.9407
Abs (Fe²⁺-o-phenanthroline)
(µmol L⁻¹)
0,0
0,3
0,6
0,9
1,2
1,5
1,8
0
10
20
30
40
50
60

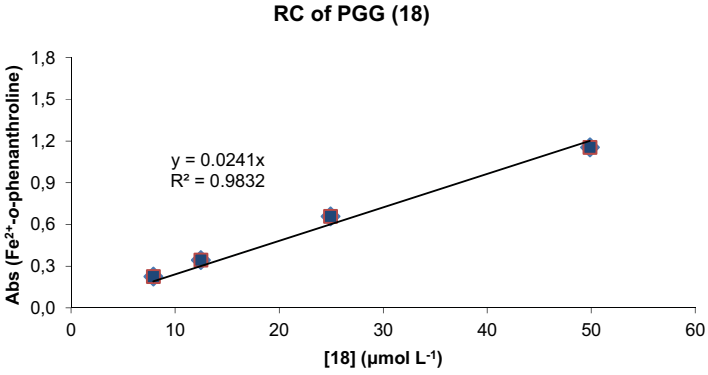
RC of PGG (18)
y = 0.0241x
R² = 0.9832
Abs (Fe²⁺-o-phenanthroline)
[18] (µmol L⁻¹)
0,0
0,3
0,6
0,9
1,2
1,5
1,8
0
10
20
30
40
50
60

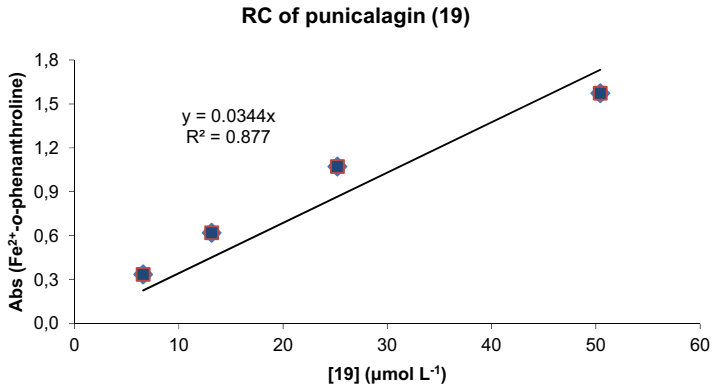
RC of punicalagin (19)
y = 0.0344x
R² = 0.877
Abs (Fe²⁺-o-phenanthroline)
[19] (µmol L⁻¹)
0,0
0,3
0,6
0,9
1,2
1,5
1,8
0
10
20
30
40
50
60

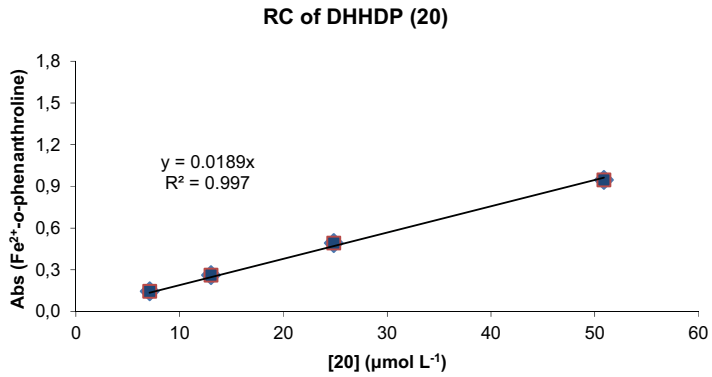
RC of DHHDP (20)
y = 0.0189x
R² = 0.997
Abs (Fe²⁺-o-phenanthroline)
[20] (µmol L⁻¹)
0,0
0,3
0,6
0,9
1,2
1,5
1,8
0
10
20
30
40
50
60

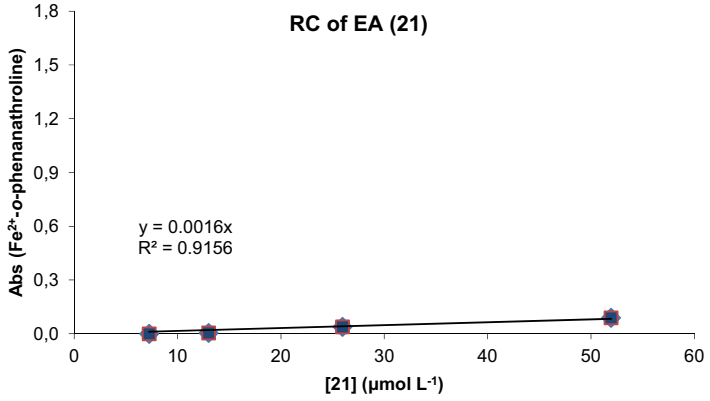
RC of EA (21)
y = 0.0016x
R² = 0.9156
Abs (Fe²⁺-o-phenanathroline)
[21] (µmol L⁻¹)
0,0
0,3
0,6
0,9
1,2
1,5
1,8
0
10
20
30
40
50
60

Annex 14. IC_{50} of (poly)phenols

A. Representation of the proliferation of HT-29 cells treated with thio-flavanols in DMEM for 72 h.

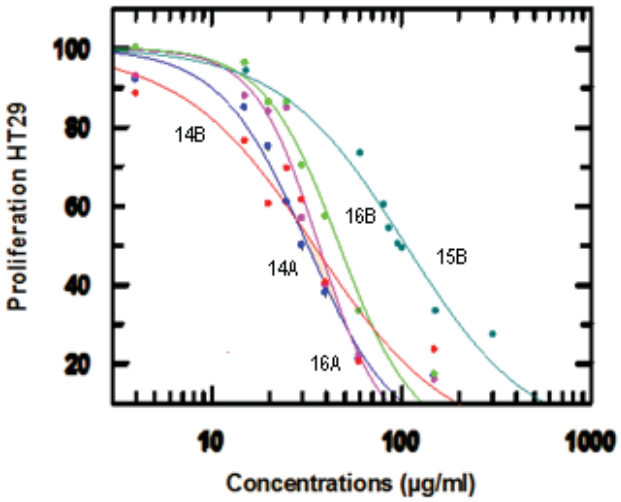

B. Representation of the proliferation of HT-29 cells treated with (poly)phenols **11**-**16** and **19**-**20** in DMEM for 72 h.

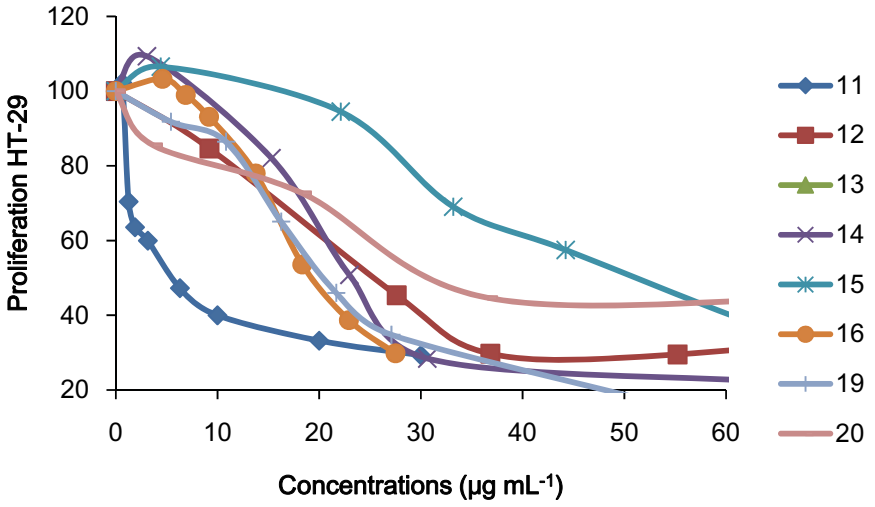

C. Representation of the proliferation of HT-29 cells treated with (poly)phenols **11**-**16** and **19**-**20** in DMEM with catalase for 72 h.

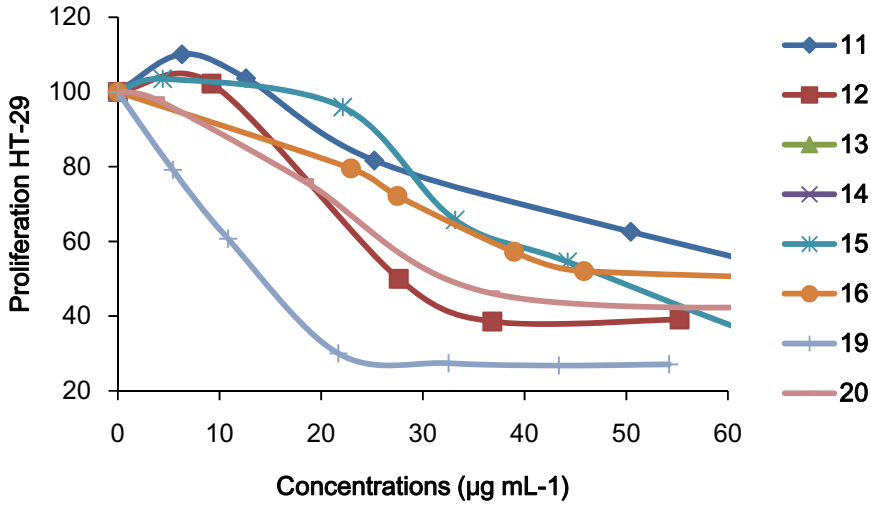

Annex 15. RMN-^{1}H, RMN-^{13}C, HSQC, and HMBC of 16 and A16

EGCG (**16**) ^{1}H NMR (400 MHz, CD_3OD) δ = 6.95 (s, 2H (**H2”**, **H6”**)), 6.51 (s, 2H (**H2’**, **H6’**)), 5.96 (s, 2H (**H6**, **H8**)), 5.53 (s, 1H (**H3**)), 4.97 (s, 1H (**H2**)), 2.98 (dd,1H (**H4β**), 2.84 (dd, 1H (**H4α**)).

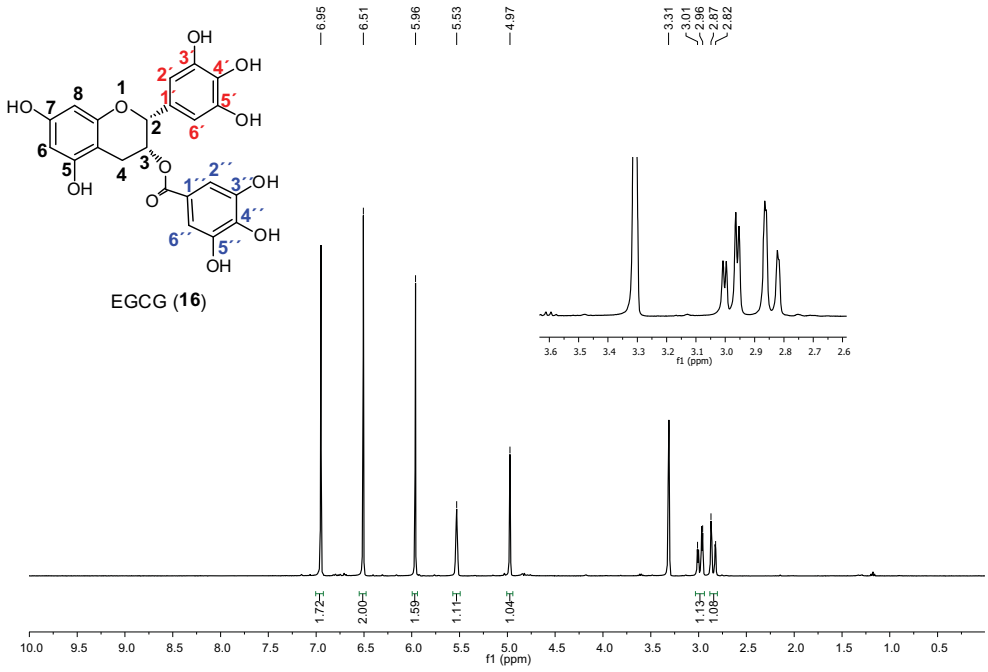

EGCG ^{13}C NMR (101 MHz, CD_3CD) δ 167.64 (C=O), 157.87 (**C9**), 157.81 (**C7**), 157.21 (**C5**), 146.67 (C3", C5"), 146.27 (C3', C5'), 139.77 (C4"), 133.78 (C4'), 130.81 (C1'), 121.53 (C1"), 110.28 (C2", C6"), 106.90 (C2', C6'), 99.44 (**C10**), 96.54 (**C8**), 95.89 (**C6**), 78.61 (**C2**), 69.93 (**C3**), 26.82 (**C4**).

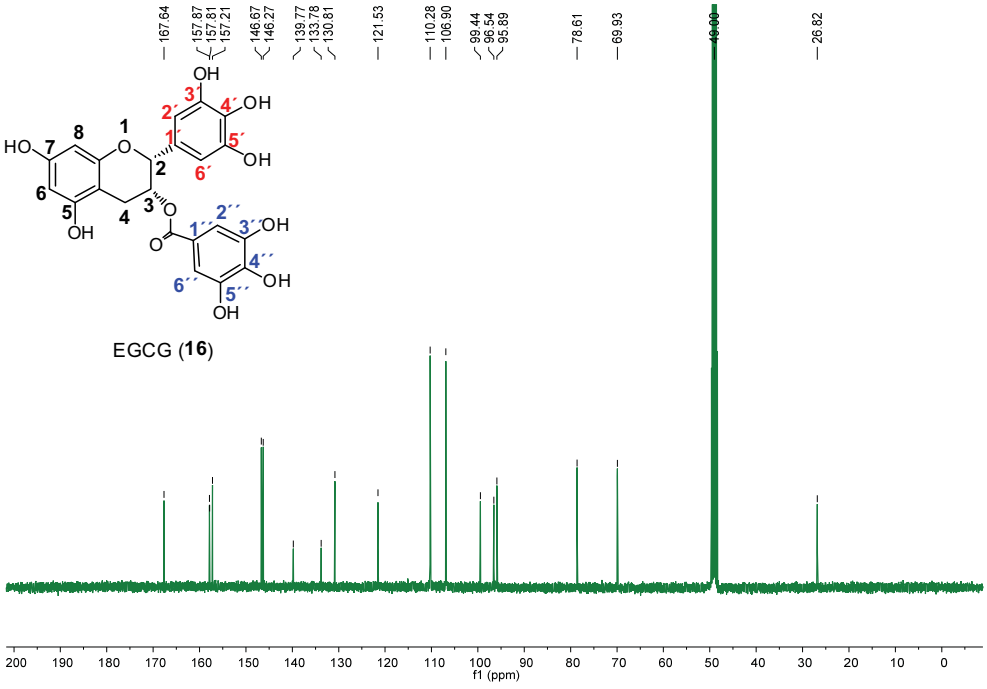

EGCG (**16**) HSQC

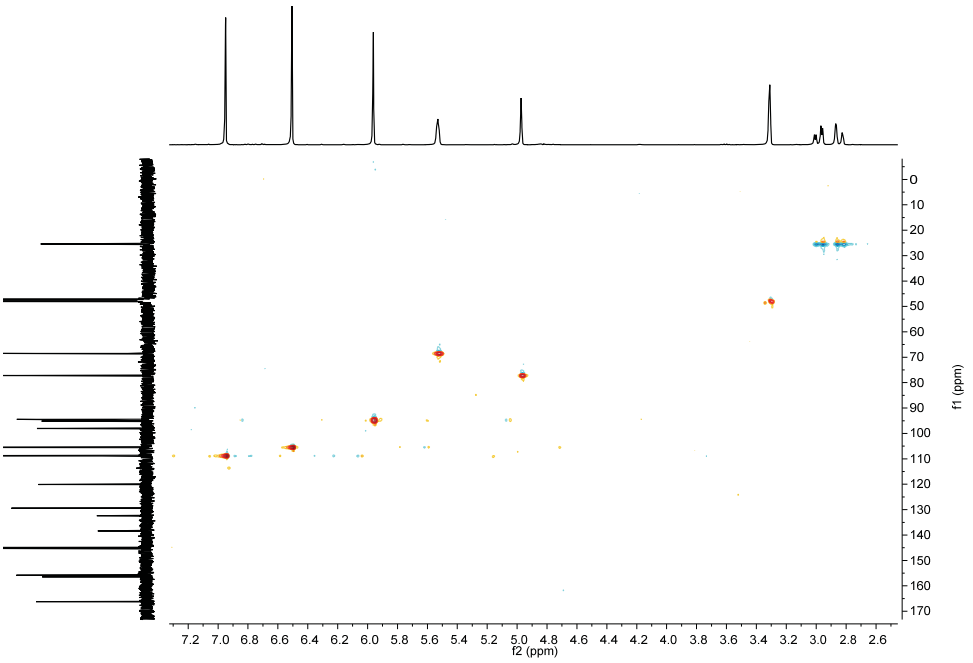
0
10
20
30
40
50
60
70
80
90
100
110
120
130
140
150
160
170
f1 (ppm)
7.2 7.0 6.8 6.6 6.4 6.2 6.0 5.8 5.6 5.4 5.2 5.0 4.8 4.6 4.4 4.2 4.0 3.8 3.6 3.4 3.2 3.0 2.8 2.6
f2 (ppm)

EGCG (**16**) HMBC

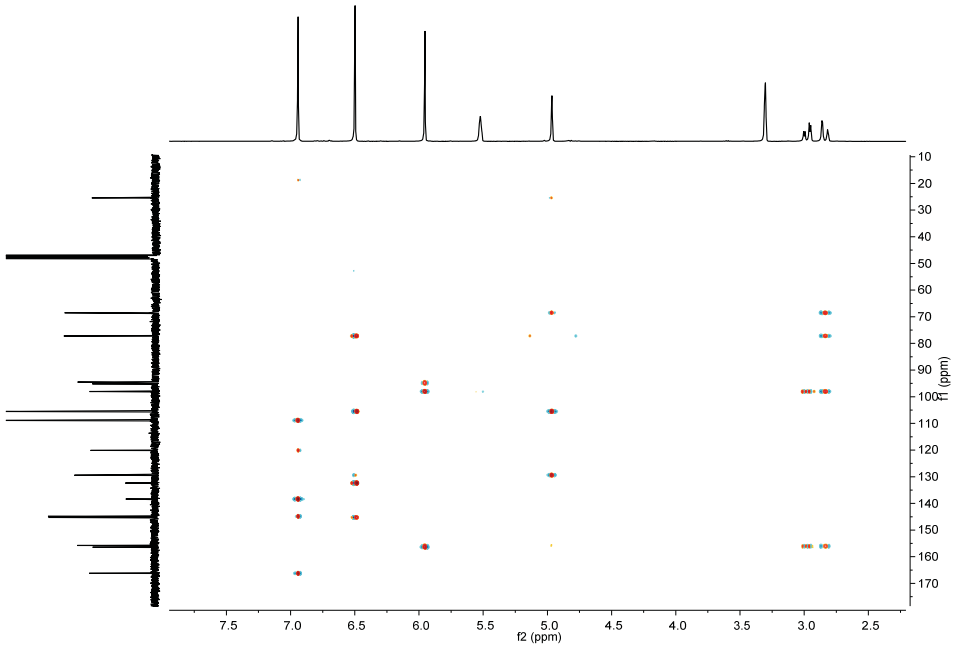
10
20
30
40
50
60
70
80
90
100
110
120
130
140
150
160
170
f1 (ppm)
7.5
7.0
6.5
6.0
5.5
5.0
4.5
4.0
3.5
3.0
2.5
f2 (ppm)

EGCG-4"-*O*-triacetylglucuronide methyl ester (**A16**) ^{1}H NMR (400 MHz, CD_3OD) δ = 6.92 (s, 2H (H2", H6")), 6.49 (s, 2H (H2', H6')), 5.96 (s, 2H (**H6**, **H8**)), 2.98 (dd,1H (**H4β**), 2.87 (dd, 1H (**H4α**)), 3.71 (s, 3H (H10)), 2.00 (s, 9H (H7, H8, H9), 6.50-4.00 (**H2**, **H3**, H1, H2, H3, H4, H5).

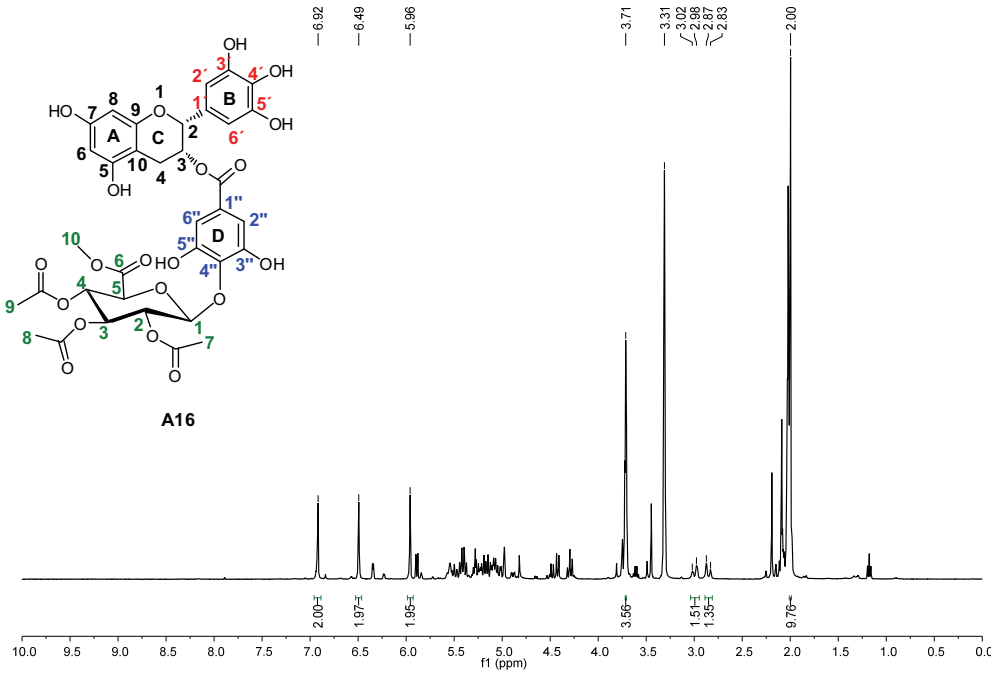

EGCG-4"-*O*-triacetylglucuronide methyl ester (**A16**) ^{13}C NMR (101 MHz, CD_3CD) δ 184.98 (C_6), 166.80 (C=O), 157.93 (C_9), 157.83 (C_7), 157.18 (C_5), 151.88 ($C_{5''}$) 151.57 ($C_{3''}$), 146.72 ($C_{3'}$, $C_{5'}$), 137.26 ($C_{4''}$), 133.78 ($C_{4'}$), 130.73 ($C_{1'}$), 128.29 ($C_{1''}$), 110.22 ($C_{2''}$, $C_{6''}$), 106.81 (C_1), 106.76 ($C_{2'}$, $C_{6'}$), 100.49 (C_{10}), 96.57 (C_8), 95.90 (C_6), 73-79 (C_2, C_3, C_4, C_5), 78.49 (C_2), 70.49 (C_3), 26.78 (C_4), 20,51 (C_7, C_8, C_9, C_{10}).(*1*)

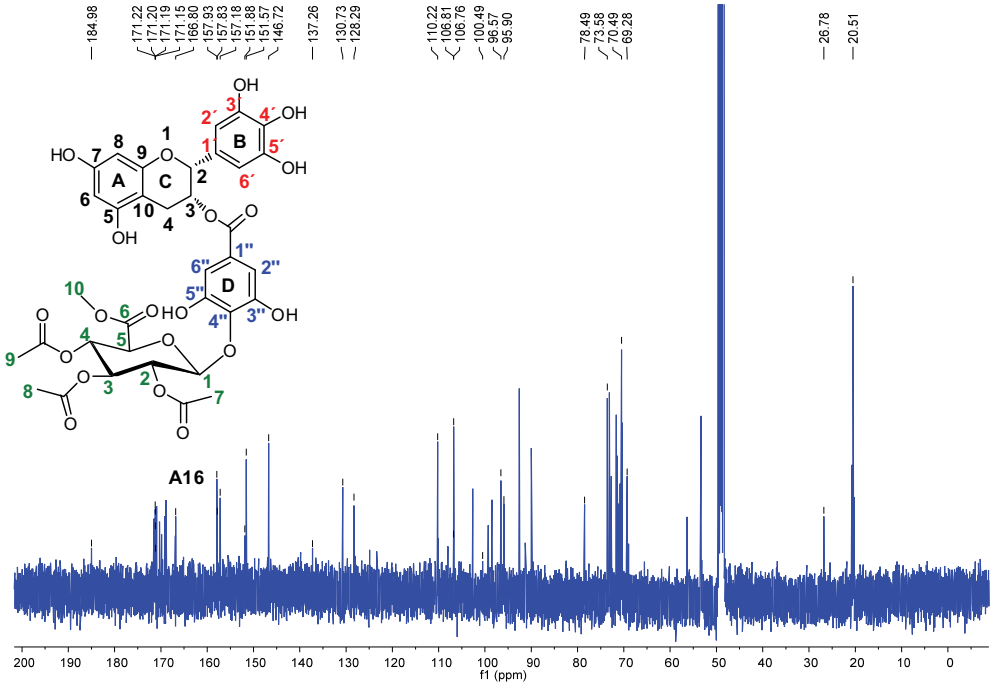

EGCG-4”-*O*-triacetylglucuronide methyl ester (**A16**) HSQC

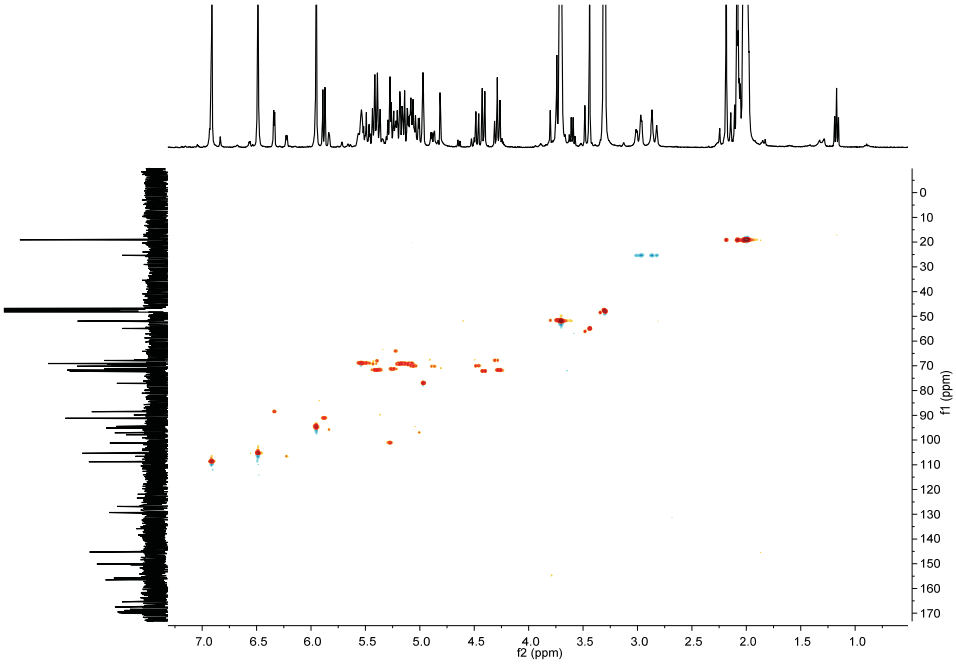

EGCG-4”-*O*-triacetylglucuronide methyl ester (**A16**) HMBC

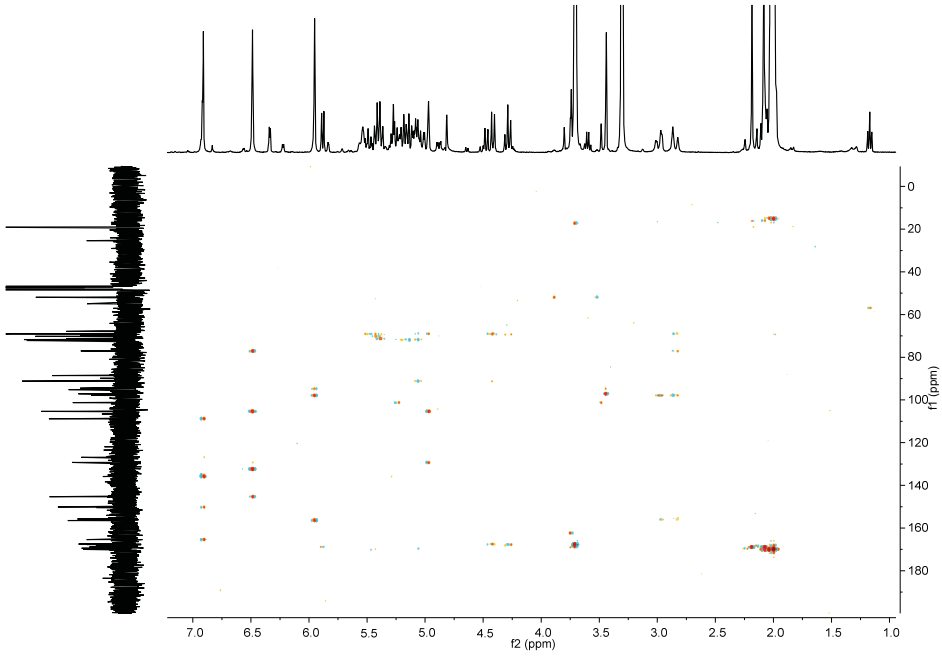

Annex 16. Resum de la tesi en català

1. Introducció

1.1. Organismes aeròbics. Espècies reactives d'oxigen (ROS/RNS) i sistema antioxidant endogen.

Les espècies reactives d'oxigen (ROS/RNS) es produeixen degut al metabolisme aeròbic dels organismes més desenvolupats. Aquestes són espècies radicalàries (p.e. radical superòxid ($O_2^{\bullet -}$), radical hidroxil ($^{\bullet}OH$), radicals peroxil ($ROO^{\bullet}$) i radical òxid nítric ($NO^{\bullet}$)) i no radicalàries (p.e. peròxid d'hidrogen (H_2O_2) i peroxinitrit ($ONOO^-$)) essencials per a la vida en baixes concentracions. En determinades condicions com per exemple, l'exposició al fum del tabac o a la radiació ultraviolada del sol, l'excés d'exercici, i una dieta desequilibrada, es produeix un excés de les ROS/RNS a la cèl·lula produint el que es coneix com a estrés oxidatiu(*2-4*). Aquest desequilibri homeostàtic (desequilibri del procés regulador d'alguna funció cel·lular) està relacionat amb trastorns com el síndrome metabòlic (conjunció de factors de risc que poden provocar en l'individu malalties cardiovasculars o diabetis), càncer o malalties degeneratives.(*5, 6*)

Els organismes vius estan dotats d'un sistema antioxidant endogen (enzims com la catalasa (CAT) i la superòxid dismutasa (SOD)) i petites molècules antioxidants com l'àcid úric, l'ubiquinol-10 i l'àcid lipoic) per tal d'evitar l'excés de ROS/RNS i les seves conseqüències. En determinades ocasions aquest sistema antioxidant endogen no és suficient per a retornar l'equilibri homeostàtic a la cèl·lula degut a que la quantitat de ROS/RNS excedeix la capacitat antioxidant del sistema o per un mal funcionament d'aquest.

Per tal de prevenir o tractar l'estrès oxidatiu, els antioxidants exògens, tals com els (poli)fenols, poden ajudar a eliminar l'excés de ROS/RNS.

1.2. Antioxidants exògens: (Poli)fenols

- *(Poli)fenols de la dieta*

Els (poli)fenols són un conjunt de molècules que comprenen els fenols simples, di-tetrafenols i estructures (poli)fenòliques més complexes. En les últimes dècades, ha augmentat el interès per els (poli)fenols degut a la seva abundància en la dieta (ingestió

diària de 1 g per persona en fruita, vegetals, cereals, oli i xocolata i en begudes com el te, cafè, cervesa i vi) i la seva probable activitat preventiva front diferents malalties relacionades amb l'estrès oxidatiu. La gran diversitat de (poli)fenols de la dieta i la seva complexitat estructural dificulta l'estudi de la relació entra la seva estructura i la seva activitat.

- *Beneficis per a la salut associats a la ingesta de (poli)fenols*

Els beneficis associats amb el consum d'alguns (poli)fenols han sigut corroborat amb estudis amb animals i amb humans en la quemoprevenció del càncer(*7-9*), la hipercolesterolèmia, l'aterosclerosi, les malalties de Parkinson i Alzheimer, i altres desordres associats amb l'edat.(*10*) La quemoprevenció del càncer es refereix a la utilització d'agents per a inhibir, revertir o retardar la tumurogènesi. Evidències epidemiològiques i preclíniques demostren que els (poli)fenols com l'(-)-epigalocatequin-3-*O*-gal·lat (EGCG) (té verd), els flavonoides com la quercetina (ceba) i la genis teïna (soja), la curcumina (curri) i el resveratrol (raïm) aporten una notable eficàcia quemopreventiva en estudis amb models humans preclínics de càncer (p.e. càncer de còlon, de cervell i de pròstata)(*11, 12*).

- *Biodisponibilitat dels (poli)fenols*

Molts estudis *in vitro* s'han focalitzat en l'activitat antioxidant dels (poli)fenols naturals. Els (poli)fenols ingerits són absorbits i metabolitzats com a conjugats (metilats, glucuronats i/o sulfatats) i àcids fenòlics simples(*13, 14*). S'han realitzat pocs estudis per a determinar l'activitat biològica d'aquests metabòlits degut a la poca quantitat d'aquests en mostres fisiològiques (plasma, orina, femta) i a la seva dificultat per a ser sintetitzats en el laboratori en quantitats necessàries per al seu estudi.

1.3. Propietats antioxidants dels (poli)fenols

Les propietats antioxidants dels (poli)fenols estan definides per la seva habilitat per eliminar radicals lliures (transferència d'un àtom d'hidrogen i/o d'un electró al radical lliure), per inhibir enzims productors de radicals lliures (xantina-xantina oxidasa) i per prevenir la formació de radicals lliures (reacció de Fenton).

1.3.1 (Poli)fenols com a captadors de radicals lliures

Els (poli)fenols (POH) eliminen els radicals lliures ($R^{\bullet}$) mitjançant la formació d'un radical més estable i per tant menys reactiu ($PO^{\bullet}$) (**Figura 1** (**1**)). Aquest nou radical

format pot actuar com a terminador de la ruta de propagació d'altres radicals lliures (**Figura 1** (**2**)).

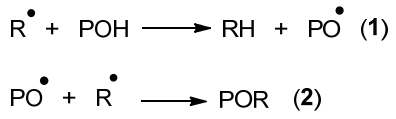

Figura 1. Reaccions d'eliminació de ROS.

1.3.2 Mecanismes de reacció dels (poli)fenols mitjançant la formació d'un radical més estable i menys reactiu.

Els (poli)fenols eliminen radicals lliures mitjançant la transferència d'un àtom d'hidrogen(*15*) (**Figura 2** (**A**)) o d'un electró (transferència electrònica)(*15-18*) (**Figura 2** (**B**), (**C**) i (**D**)).

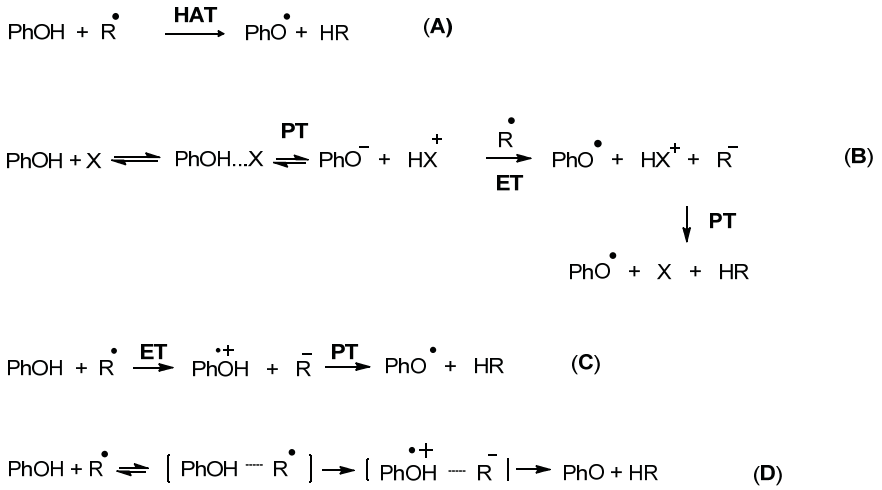

Figura 2. Mecanisme **A** (transferència d'un àtom d'hidrogen, *TAH*), mecanisme **B** (transferència seqüencial de protó i electró, *TSPE*), mecanisme **C** (transferència electrònica seguida per transferència de protó, *TE-TP*), mecanisme **D** (transferència electrònica acoblada a protó, *TEAP*).

1.4. Propietats prooxidants dels (poli)fenols

El mecanisme de transferència electrònica pot estar relacionat amb un efecte prooxidant. Els (poli)fenols amb un potencial d'oxidació suficientment baix, són capaços de transferir un electró a l'oxigen i formar el superòxid radical; font de producció del peròxid d'hidrogen (H_2O_2) generat per l'enzim superòxid dismutasa (SOD) (Figura 3 (**1**)) i del radical hidroxil (•OH) mitjançant la reacció de Fenton (**Figura 3** (**2**)).(*19*) Degut a la propietat quelant dels grups catecol (1,2-dihidroxibenzè), pirogal·lol (1,2,3-trihidroxibenzè) i gal·lat (àcid 3,4,5-trihidroxibenzòic) dels (poli)fenols, el Fe^{3+} i el Cu^{2+} són reduïts a Fe^{2+} i Cu^{+} participant també en la inducció de la reacció de Fenton (**Figura 3** (**2**))(*20, 21*).

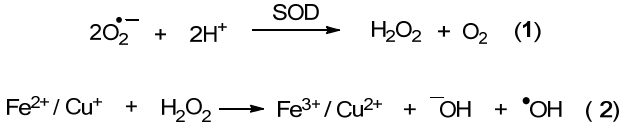

Figura 3. Producció del H_2O_2 per la SOD (**1**), reacció de Fenton (**2**).

1.5. Mètodes per a la determinació de l'activitat antiradicalària dels (poli)fenols

L'eficàcia antiradicalària d'un (poli)fenol o un extracte (poli)fenòlic ve determinada per la seva cinètica i capacitat antiradicalària, és a dir, la velocitat de reacció per a eliminar el radical lliure i el número de molècules de radical lliure que pot reduir una molècula de (poli)fenol. Existeix diferents mètodes per a determinar l'activitat antiradicalària dels (poli)fenols i aquí se'n classificaran alguns d'ells depenent del seu mecanisme de reacció.

1.5.1. Transferència d'àtom d'hidrogen (TAH) i transferència electrònica (TE)

Assaig del radical 1,1-difenil-2-picrilhidrazil (DPPH): És un dels mètodes comercials més utilitzat en l'avaluació de l'activitat antiradicalària de (poli)fenols[7] (**Figura 4**). El DPPH és un radical estable mesurable per espectroscòpia visible i per Ressonància Paramagnètica Electrònica (RPE). El seu mecanisme de reacció depèn del dissolvent utilitzat però es creu que bàsicament reacciona per transferència d'hidrogen.(*15*)

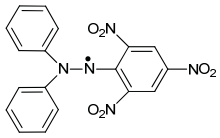

Figura 4. Estructura del radical DPPH.

1.5.2. Transferència d'àtom d'hidrogen (TAH)

Oxygen Radical Absorbance Capacity (ORAC): l'assaig ORAC és un mètode utilitzat per a mesurar l'activitat antiradicalària de (poli)fenols soluble en aigua i mostres biològiques (sang, plasma i teixits). Aquest mètode es basa en la captura per part dels (poli)fenols, de radicals peroxil generats en solució aquosa a partir del hidroclorur de 2,2′-azobis-2-metil-propanimidamida (AAPH). L'activitat es mesura per fluorescència. El (poli)fenol protegeix a la fluoresceïna (λ (emissió)= 521 nm en aigua) i els radicals peroxil la malmeten fent disminuir la seva fluorescència.

Total Oxidant Scavenging Capacity (TOSC): aquest assaig mesura l'activitat antiradicalària de teixits biològics amb (poli)fenols hidrofílics i lipofílics. Amb el dihidroclorur 2,2'-Azobis(2-metil-propionamidina) (ABAP) es produeixen radicals hidroxil que oxiden a l'alfa-keto-gamma-àcid metiolbutiric (KMBA) produint etilè que és quantificat per cromatografia de gasos.

1.5.3. Transferència electrònica (ET)

Trolox Equivalent Antioxidant Capacity (TEAC): aquest mètode és àmpliament utilitzat en assajos amb aliments i mostres biològiques amb (poli)fenols hidrofílics i lipofílics. L'assaig TEAC mesura l'activitat dels (poli)fenols per a eliminar al catió radical $ABTS^{\bullet+}$ generat en medi aquós *in situ* per la oxidació del persulfat $ABTS^{2-}$ (2,2'-azinobis(3-etilbenzotiazolina-6-àcid-sulfònic). La activitat antiradicalària és mesurada per ressonància paramagnètica electrònica (RPE) o per espectroscòpia d'UV-Visible (λ= 734 nm). El radical $ABTS^{\bullet+}$ generat té una vida mitja de 6 min, per tant, no permet determinar la activitat antiradicalària de (poli)fenols lents.

Assaig amb el radical tris(2,4,6-tricloro-3,5-dinitrofenil)metil (HNTTM): Degut a la necessitat de mesurar la capacitat dadora d'electrons dels (poli)fenols es va sintetitzar i caracteritzar el radical lliure estable de la sèrie del 1,3,5-triclorofenilmetil (TTM), el radical tris(2,4,6-tricloro-3,5-dinitrofenil)metil (HNTTM). Aquest radical és estable en

sòlid i en dissolució a la foscor (estabilitat > 99% durant dos dies) en dissolvents orgànics com el $CHCl_3$, mescles $CHCl_3$/MeOH, CH_2Cl_2, benzè, toluè i CH_3CN. L'HNTTM reacciona exclusivament per Transferència-Electrònica (ET) (*22*) en diferents dissolvents orgànics i amb un adequat valor de potencial de reducció ($E°_{HNTTM}$= 0.58 V en CH_2Cl_2) per a oxidar els hidroxils fenòlics dels grups catecol, pirogal·lol i gal·lat. (*23*) L'HNTTM s'ha utilitzat com a quimosensor per a mesurar l'activitat antiradicalària de (poli)fenols naturals i sintètics i d'extractes (poli)fenòlics.(*22-26*)

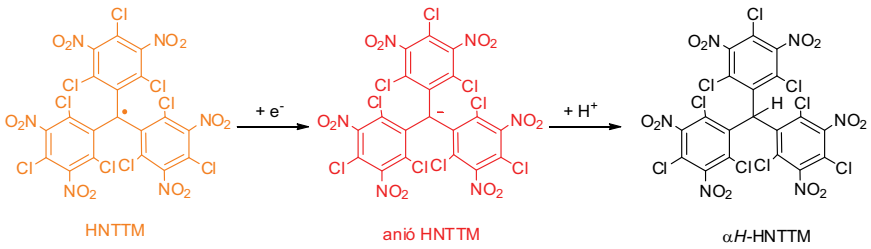

Figura 5. Estructures de l'HNTTM, els seu anió estable i la seva forma protonada α*H*-HNTTM.

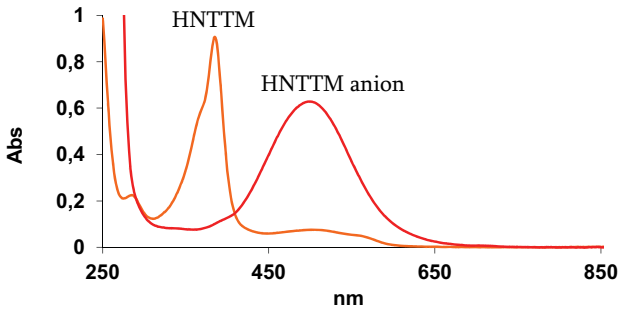

Figura 6. Espectre d'UV-Visible de l'HNTTM i el seu anió en $CHCl_3$/MeOH (2:1). L'espectre de l'anió es va obtenir de la sal de Bu_4N^+ $^-$HNTTM.

1.6. Avaluació de la activitat reductora de metalls dels (poli)fenols

Ferric Reducing Antioxidant Power (FRAP): aquest mètode es basa en la reducció del Fe^{3+} al Fe^{2+}, a baix pH (pH= 3.6), per l'acció dels (poli)fenols. El complexa format amb el Fe^{2+} i la o-fenantrolina produeix una absorbància a 593 nm que és mesurada per espectroscòpia d'UV-Vis.

La transferència d'electrons pot ser un dels mecanismes de reacció dels (poli)fenols relacionat amb la citotoxicitat de cèl·lules i alguns mecanismes d'antiproliferació cel·lular.(*19, 24*) Per aquest motiu, la tesi es basa en la determinació de l'activitat de determinats (poli)fenols per a captar radicals lliures mitjançant el mecanisme de transferència electrònica utilitzant radicals lliures estables com a quimosensors de transferència electrònica, i la determinació de la possible relació entre la activitat per transferència electrònica dels (poli)fenols i la seva activitat en cultius de cèl·lules humanes d'adenocarcinoma de còlon (HT-29). Aquest tipus de cèl·lules canceroses va ser escollit degut a la gran incidència d'aquest càncer i per la accessibilitat dels compostos fenòlics de la dieta en el tracte digestiu.

2. Objectius

El radical lliure estable tris(2,4,6-tricloro-3,5-dinitrofenil)metil (HNTTM), sensible exclusivament a la transferència electrònica, es va sintetitzar en el nostre grup. La química dels radicals lliures estables obre la possibilitat de desenvolupar assajos per a avaluar l'activitat dels (poli)fenols i dels seus metabòlits, per a transferir electrons utilitzant quimosensors selectius amb diferent poder d'oxidació.

Degut a el interès per a la determinació i estudi de la activitat de transferència electrònica de diferents (poli)fenols naturals i dels seus metabòlits, i per a l'estudi de la relació entre la transferència electrònica i la activitat biològica, es van proposar els següents objectius:

1. Estudi de la cinètica, de la capacitat de captació de radicals i dels mecanismes de reacció de (poli)fenols naturals i sintètics amb l'HNTTM com a quimosensor de transferència electrònica.

2. Síntesi d'un radical lliure estable amb un valor de potencial redox més baix (menys oxidant) que el valor de potencial redox de l'HNTTM, el radical tris(2,3,5,6-tetracloro-4-

nitrofenil)metil (TNPTM), radical sensible només a les posicions més reactives dels (poli)fenols.

3. Avaluació del TNPTM com a quimosensor de la transferència electrònica de (poli)fenols naturals i sintètics (cinètiques, capacitat de captació de radicals i mecanismes).

4. Avaluació de la activitat antiproliferativa dels (poli)fenols en cèl·lules HT-29 per a determinar si hi ha relació entre la transferència electrònica i la activitat biològica per part dels (poli)fenols.

5. Síntesi dels principals metabòlits biològicament detectats (glucurònids) del flavanol (–)-epigalocatequin-3-*O*-gal·lat (EGCG) per a futurs estudis de estructura/activitat.

La idea general és construir una col·lecció de radicals selectius sensibles als hidroxils fenòlics d'estructures (poli)fenòliques complexes amb l'objectiu final d'assajar convenientment la possible activitat biològica de mescles naturals complexes i de nous compostos sintètics.

3. Materials i mètodes

3.1 Materials

Espectrofotòmetre d'Ultraviolat-Visible (UV-Vis)

L'obtenció dels espectres d'Ultraviolat-Visible dels radicals orgànics estables es va realitzar amb un espectrofotòmetre Varian model Cary 300 i Cary 50 Bio de Varian (Palo Alto, Canadà), utilitzant mostres dissoltes en $CHCl_3$ (Sigma-Aldrich 99,8% grau espectrofotomètric) i $CHCl_3$/MeOH (2:1) (Metanol anhidre de Sigma-Aldrich 99,8%) en dos parells de cubetes de diferent capacitat, de quars suprasil de 10 i d'1 cm de camí òptic (Hellma, Müllheim, Alemanya).

Espectrofotòmetre d'Infraroig (IR)

L'espectre de IR dels compostos es va realitzar utilitzant pastilles de bromur potàssic (KBr) amb un Nicolette AVATAR 360 FT-IR.

Ressonància Magnètica Nuclear (^{1}H-RMN)

Els espectres de ^{1}H-RMN dels compostos es van obtenir amb un Varian Mercury-500 i amb un Varian Mercury-400 i els espectres de ^{13}C-RMN, HMBC and HSQC es van obtenir amb el Varian Mercury-400.

Ressonància Paramagnètica electrònica (EPR)

Els espectres es van enregistrar amb un espectròmetre Varian model E-109E i amb un Bruker BioSpin EMX-Plus 10/12 treballant a 8.5 GHz (freqüència de banda-X) i equipat amb una cavitat dual (mode V-4532). Es va utilitzar el mateix tub de quars per a fer les mesures de les mostres dissoltes en $CHCl_3$ i $CHCl_3$/MeOH (2:1) en unes condicions determinades de temperatura, potència, modulació i adquisició dependents de l'assaig. La simulació dels espectres es va obtenir amb el programa Winsim.

HPLC-DAD

Per a seguir les reaccions de síntesi dels glucurònids de l'EGCG es va utilitzar un HPLC Elite LaChrome amb detector de Diode Array de VWR.

HPLC semiprepartiu

Per a purificar productes es va utilitzar un HPLC semipreparatiu de Waters LC 4000 amb un detector UV Hitachi L-4000 de Merck.

HPLC-HR-DAD-ESI-TOF-MS

Els anàlisis de masses d'alta resolució es van realitzar amb un LC/MSD-TOF d'Agilent Technologies.

Espectroscòpia d'Ultraviolat-Visible de plaques d'ELISA

Amb un espectrofotòmetre d'UV-Visible (Merck, Sant Cugat del Vallès, Espanya) ELISA System MIOS versió 3.2, es van revelar les plaques de 96 pous en l'assaig de MTT.

3.2 Síntesi de radicals lliures estables

3.2.1. Síntesi del radical tris(2,4,6-tricloro-3,5-dinitrofenil)metil (HNTTM)

*Síntesi del tris(2,4,6-triclorofenil)metà (**1**)*

1,3,5-triclorobenzè (50.8 g; 279.7 mmol), cloroform (2.6 mL; 32.4 mmol) i triclorur d'alumini anhidre (13.0 g; 97.3 mmol) es van afegir en un reactor de vidre hermètic i ben sec. El reactor es va escalfar a 110 °C amb un bany de silicona (5.5 h). La mescla de reacció es va extreure amb una solució diluïda d'aigua-gel-HCl i $CHCl_3$. La fase orgànica es va netejar amb una solució aquosa d'hidrogen carbonat de sodi ($NaHCO_3$) (2 %, 200 mL) i aigua (3 x 100 mL). La fase orgànica es va assecar amb sulfat de magnesi anhidre ($MgSO_4$) i el dissolvent es va eliminar sota pressió reduïda. Es va fer una digestió amb hexà (100 mL) a reflux durant 1 h per a purificar al producte. La fracció insoluble es va separar per filtració i es va obtenir **1** (29.5 g, 57 %) que es va identificar per ^{1}H-RMN. ^{1}H-RMN ($CDCl_3$) δ, 7.29 (d, 3Harom), 7.17 (d, 3Harom), 7.19 (s, 1H) ppm.

*Síntesi del tris(2,4,6-tricloro-3,5-dinitrofenil)metà (**2**)*

A una barreja de tris(2,4,6-triclorofenil)metà (**1**) (2 gr. 3.61 mmol) en àcid nítric fumant (100 ml) s'hi va afegir àcid sulfúric fumant (30 % SO_3) (25 ml) i la mescla resultant es va mantenir en agitació i en calent (80 °C) durant 3 dies. Es va abocar sobre aigua i gel, el precipitat blanc es va separar per filtració i es va assecar a pressió reduïda. Es va obtenir el tris(2,4,6-tricloro-3,5-dinitrofenil)metà (**2**) (2.52 gr. 85 %) identificat per espectroscòpia d'infraroig.

Espectre d'IR (KBr): ν, 2894 (d), 1564 (f), 1244 (d), 1213 (d), 1020 (m), 949 (m), 832 (m), 783 (m), 631 (m) cm^{-1}.

*Síntesi del radical tris(2,4,6-tricloro-3,5-dinitrofenil)metil (HNTTM **4**)*

A una solució de tris(2,4,6-tricloro-3,5-dinitrofenil)metà (**2**) (1 gr. 21 mmol) i acetona (50 ml) s'hi va afegir hidròxid de tetrabutilamoni (1.5 M) (0.93 ml) i es va deixar amb agitació constant durant 20 min per a obtenir l'anió de **2** (**3**). Posteriorment s'hi va afegir òxid de crom (VI) (0.6 gr. 3 mmol) i es va deixar amb agitació constant en la foscor durant 20 h a temperatura ambient i sota atmosfera d'argó. El cru de la reacció es va abocar sobre una solució aquosa diluïda d'àcid clorhídric. La fase orgànica es va extreure amb cloroform (2 x 50) i es va netejar un cop amb aigua, es va assecar amb sulfat de sodi anhidre (Na_2SO_4), es va filtrar i es va evaporar a sequedat. El sòlid obtingut es va cromatografiar en columna (sílica Flaix-gel) utilitzant cloroform com a dissolvent. Es va

obtenir el radical **4** com un sòlid vermell (0.63 gr. 63 %) que es va identificar mitjançant espectroscòpia d'UV-Visible i espectroscòpia d'Infraroig (IR).

Espectre d'UV-Vis ($CHCl_3$): λ (ε), 285 (6345), 385 (21170), 504 (1260), 553 (1080) nm (dm^3mol^{-1} cm^{-1})

Espectre d'IR (KBr): ν, 1549 (f), 1340 (f), 1279 (d), 948 (m), 841 (m), 787 (m), 689 (d), 629 (d) cm^{-1}

3.2.2. Síntesi del radical tris(2,3,5,6-tetracloro-4-nitrofenil)metil (TNPTM)

*Síntesi del tris(2,3,5,6-tetraclorofenil)metà (**5**)*

En un reactor de vidre, hermèticament tancat i prèviament assecat, es va fer reaccionar 1,2,4,5-tetraclorobenzè (28.8 gr. 133.41 mmol), triclorur d'alumini (2.6 gr. 19.5 mmol) i cloroform (1.5 ml) i la barreja es va deixar reaccionar en un bany de silicona a 160 °C de temperatura durant 2 h 15 min (assolint la temperatura de fusió de l'1,2,4,5-tetraclorobenzè, 138-140 °C). Posteriorment es va anar dissolent el producte obtingut amb una mescla d'aigua/gel/àcid clorhídric i cloroform, respectivament. Es va extreure la fase aquosa amb cloroform (3 x 200) i la fase orgànica es va rentar amb una solució d'hidrogencarbonat de sodi ($NaHCO_3$) (2 %, 200 ml) amb aigua (3 x 100) i es va assecar amb sulfat de sodi anhidre (Na_2SO_4). Es va filtrar i es va evaporar a sequedat obtenint-se un precipitat marró clar. Per tal d'eliminar les restes de 1,2,4,5-tetraclorobenzè, el producte es va sotmetre a sublimació a 150 °C durant 30 min i el residu es va cromatografiar en columna (sílica Flaix-gel) utilitzant hexà com a dissolvent. Es va obtenir el tris(2,3,5,6-tetraclorofenil)metà (**5**) com un sòlid blanc (16.4 gr. 56 %) que es va identificar mitjançant ressonància magnètica nuclear (^{1}H-RMN) i espectroscòpia d'infraroig (IR).

Espectre ^{1}H-RMN ($CDCl_3$): δ, 7.65 (s,3H aromàtics), 6.98 (s,1H, CH) ppm

Espectre IR (KBr): ν, 3111(d), 3068(d), 1539(m), 1410(f), 1388(f), 1348(m), 1322(m), 1235(m), 1199(m), 1163(f), 1098(m), 974(m), 865(f), 844(m), 781(m), 646(m), 626(m) cm^{-1}.

*Síntesi del tris(2,3,5,6-tetracloro-4-nitofenil)metà (**6**)*

Es va deixar a reflux durant 21h, una barreja de tris(2,3,5,6-tetraclorofenil)metà (**5**) (5.1 gr. 7.75 mmol) i àcid nítric fumant (50 ml). El cru de reacció es va abocar sobre una barreja d'aigua i gel i el sòlid obtingut es va filtrar i assecar a l'estufa obtenint-se un sòlid

de color blanc. El sòlid obtingut es va purificar mitjançant un reflux amb hexà. Es va obtenir el tris(2,3,5,6-tetracloro-4-nitrofenil)metà (**6**) com un sòlid blanc (4.97 gr, 81 %) que es va identificar mitjançant espectroscòpia d'infraroig (IR).

Espectre IR (KBr): ν, 1557(f), 1377(m), 1344(f), 1301(m), 1134(m), 781(m), 760(m), 733(m), 666(d), 564(d) cm^{-1}.

Síntesi del radical tris(2,3,5,6-tetracloro-4-nitrofenil)metil (TNPTM **8**)

Es va dissoldre tris(2,3,5,6-tetracloro-4-nitrofenil)metà (**2**) (2.51 gr. 3.17 mmol) en THF (100 ml). S'hi va afegir HTBA (2.75 ml) i es va deixar amb agitació constant i atmosfera d'argó durant 4h a 0 °C per a obtenir l'anió de **6** (**7**). La dissolució resultant es va fer reaccionar amb *p*-cloranil (1.1 gr. 4.02 mmol) en les mateixes condicions anteriors durant 2h. El sòlid obtingut es va purificar mitjançant cromatografia en columna (sílica Flaix-gel) utilitzant cloroform com a dissolvent. Es va obtenir el radical TNPTM com un sòlid de color vermell (3.0 gr, 88 %) que es va identificar mitjançant espectroscòpia d'UV-Visible i espectroscòpia d'infraroig (IR):

Espectre UV-Vis ($CHCl_3$): λ (ε), 287 (6320), 378 (17153), 493 (871) nm ($dm^3\ mol^{-1}\ cm^{-1}$).

Espectre de IR(KBr): ν, 1556(f), 1343(f), 1268(d), 1225(d), 1149(d), 1048(d), 888(d), 788(m), 765(m), 723(m), 666(d), 572(m) cm^{-1}.

3.3. Reacció del TNPTM amb toluè

El radical TNPTM (**8**) (31.0 mg; 0.04 mmol) es va dissoldre en toluè desoxigenat (31 mL) amb agitació i a reflux (24 h) en atmosfera inert (Ar). La solució vermella no va canviar de color i el toluè es va eliminar al buit per a donar **8** que es va identificar per IR. El radical **8** es va recuperar quantitativament.

3.4. Mesura de les cinètiques de les reaccions del TNPTM amb els (poli)fenols

Cinètiques de segon ordre: Les cinètiques de reacció entre el TNPTM (**8**) i els (poli)fenols es van determinar a temperatura ambient per ressonància paramagnètica electrònica (RPE). Es van preparar dissolucions de **8** i dels (poli)fenols **10**-**21** en $CHCl_3$/MeOH (2:1) desoxigenat amb una proporció molar **8**/(poli)fenol de 5:1. Les constants de velocitat (k_1 i k) es van determinar amb el model simple i general utilitzat per Dangles et al.*(27)*

$$\ln\frac{1-\frac{I_f}{I_x}}{1-\frac{I_f}{I_o}} = -\frac{k_1.c}{\frac{I_o}{I_f}-1}.t \quad \textbf{(Equació 1)}$$

I_f és la intensitat final, I_x la intensitat a diferents temps, I_o la intensitat inicial, c la concentració inicial de (poli)fenol i t el temps de reacció.

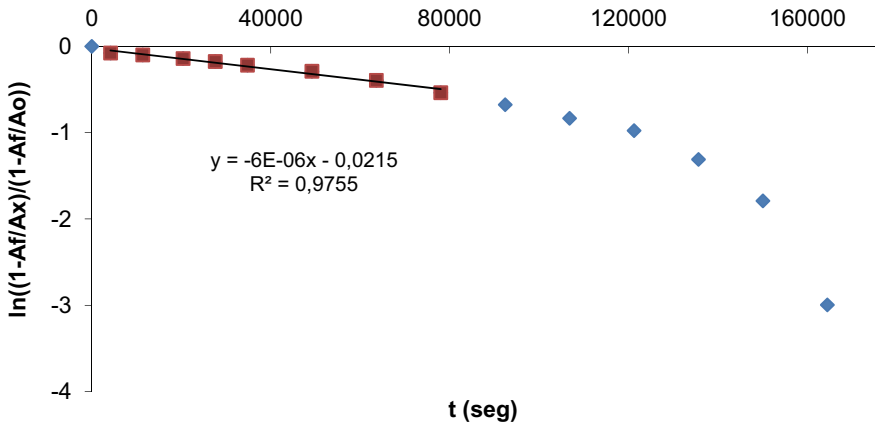

Figure 12. Representació de la cinètica de la reacció entre 11 i el TNPTM *vs* temps (s).

3.5. Determinació de la capacitat antiradicalària dels (poli)fenols

Avaluació de la concentració eficaç al 50 % (EC_{50}). La capacitat antiradicalària dels (poli)fenols es va mesurar per duplicat amb mescles (1:1, v/v) de dissolucions de TNPTM (**8**), HNTTM (**4**) i DPPH (**9**), (120 μM) amb 5 dissolucions de diferents concentracions (1-120 μM) dels (poli)fenols **10**-**21** en $CHCl_3$/MeOH (2:1) desoxigenat a temperatura ambient i a la foscor. El temps final de reacció va ser 30 min per a **9**, 7 h per a **4** i 48 h per a **8**. L'EC (**13**) es va utilitzar com a control i la corba de calibració dels radicals es va utilitzar per a una millor precisió de la concentració del radical.

Les mesures es van obtenir per EPR. El percentatge de radical reaccionat com a funció de la concentració de (poli)fenol per concentració de radical dona la recta que es mostra a la **Figura 13** per a la reacció entre **13** i **4**.

$$\left(1-\frac{I_x}{I_o}\right).100 \quad \textbf{(Equació 2)}$$

I_o i I_x són les intensitat de la senyal de EPR del radical a temps inicial i a un temps determinat de reacció.

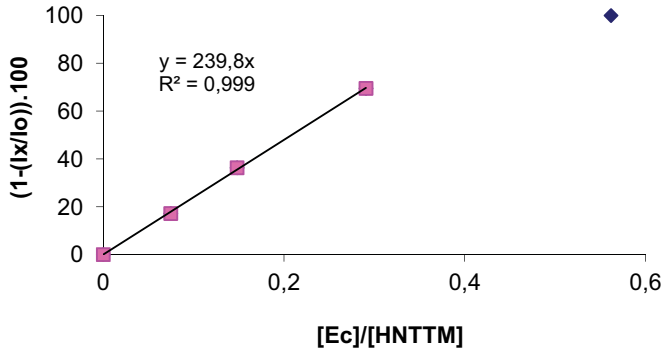

Figura 13. Representació de la línia de calibració obtinguda per a la reacció entre l' EC (**13**) i **4** en µmol µmol^{-1}. Concentracions de **13**, interval 5-40 µM i concentració de **4**, 60 µM.

La capacitat antiradicalària dels (poli)fenols front als radicals TNPTM, HNTTM o DPPH es calculen a partir de la recta que s'obté amb la representació de la **Figura 13**. El valor calculat (EC_{50}, µmol de (poli)fenol/µmol de radical o µg de (poli)fenol/µmol de radical) és la Concentració Eficaç del (poli)fenol per a disminuir la meitat de la concentració inicial de radical dividit pels mols inicials de radical. El Valor Estequiomètric (VE, EC_{50} x 2), el Potencial Antiradicalari (PAR, $1/EC_{50}$) i el número d'electrons o hidrògens transferits per molècula de (poli)fenol ($n_{e/H}$, 1/VE) són els paràmetres obtinguts a partir de la EC_{50} per a cada (poli)fenol.

3.6. Mesura de la Capacitat Reductora (CR) dels (poli)fenols amb el mètode Ferric-Reducing Antioxidant Power (FRAP)

En tampó a pH 3.6 (acetat de sodi) es van preparar quatre concentracions diferents de (poli)fenol (interval 8-50 µM) i se'ls hi va addicionar (1:1, v/v) una solució del mateix tampó amb *o*-fenantrolina (1.2 mg mL^{-1}) i $FeCl_3$ (1 mM). La mescla es va incubar a temperatura ambient a la foscor (1 h) i l'absorbància del complexe Fe(II)-*o*-fenantrolina

format (λ = 510 nm) es va mesurar per UV-Vis. Els resultants es van expressar en relació a la capacitat del flavanol EGCG (**16**).

3.7. Viabilitat cel·lular

L'efecte dels (poli)fenols en la proliferació de cèl·lules HT-29 es va mesurar amb l'assaig MTT (bromur de 3-(4,5-dimetiltiazol-2-yl)-2,5-difenyl tetrazoli). Aquest assaig es basa en la habilitat de les cèl·lules vives per a tallar l'anell tetrazoli produint formazà el qual absorbeix a 570 nm. Les cèl·lules HT-29 cèl·lules (3000 cells/pou) es van fer créixer en una placa de 96 pous durant 24 h. Passat aquest temps es van incubar amb diferents concentracions de (poli)fenols (interval 100-900 μM). Els (poli)fenols més hidrofòbics es van dissoldre en dimetilsulfòxid (DMSO) excepte l'àcid el·làgic (**21**) que es va dissoldre en N-metil-pirrolidona. Passades 72 h es va aspirar el sobrenedant i a cada pou s'hi va afegir 100 μl de solució de MTT amb medi de cultiu (0.5 mg mL^{-1}). La placa es va incubar durant 1 h, es va aspirar el sobrenedant i el precipitat blau (formazan) es va dissoldre amb 100 μL de DMSO. La densitat òptica es va mesurar a 550 nm amb un lector de plaques ELISA. Els experiments es van realitzar també amb catalasa (100 U mL^{-1}). La IC_{50} o concertació de compost capaç de reduir la densitat òptica del colorant en un 50 % relatiu al control, es va estimar amb la recta obtinguda representant la concentració de (poli)fenols i la mesura d'UV-Vis obtinguda.

3.8. Síntesis dels glucurònids de l'EGCG

3.8.1. Reacció de glucuronidació de l'EGCG amb l'àcid acetobrom-α-D-glucurònic metil èster. Reacció de Koenigs-Knorr modificada

La síntesi de l'EGCG (**16**) es va portar a terme seguint les condicions de reacció utilitzades per Gonzalez-Manzano i col·laboradors per a preparar catechin glucurònids.(*28*) L'EGCG (**16**) i l'àcid acetobrom-α-D-glucurònic metil èster (**22**) es van dissoldre en diferents dissolvents desoxigenats, tals com l 'acetona, CH_2Cl_2, DMSO i DMF (0.25 mL). Com a promotor es va utilitzar NaMeO, $Zn(Ac)_2$, *p*-TsOH, Cs_2CO_3, KOH o K_2CO_3. El millor rendiment de reacció es va obtenir amb DMF com a dissolvent i K_2CO_3 com a promotor. L'EGCG (**16**) (5.10 mg; 0.01 mmol) i l'acetobrom-α-D-glucuronic acid metil èster (**22**) (25.2 mg; 0.06 mmol) es van dissoldre en DMF i s'hi va afegir K_2CO_3 (5.20 mg; 0.04 mmol). La mescla es va agitar durant 6 h a temperatura ambient, sota atmosfera

inert (N_2) i a la foscor. Totes les reaccions es van seguir per HPLC-DAD analític i per HPLC-HR-DAD-ESI-TOF-MS.

3.8.2. Desacetilació de l'EGCG-4''-O-triacetilglucurònid metil èster per a obtenir l'EGCG-4''-O-glucurònid metil èster amb diferents disolvents i lipases

Com a dissolvents es va utilitzar el THF, el diisoproil èter amb una resina d'intercanvi iònic o aigua a diferents pH(5.0, 6.1, 6.7 and 8.0). Per a facilitar la solubilitat del glucurònide es van utilitzar dissolvents orgànics com a co-solvents (10% or 20% of MeOH, DMSO or THF). Les lipases utilitzades van ser des de 7.36 a 80.8 mg, la Novozyme-435 (N-435), la lipasa A (LA), la Lypozime IM (LIM), la lipasa pancreàtica de porc (PPL) o la lipasa AS (LAS)). Les reaccions es van portar a terme amb diferents proporcions de EGCG-4''-*O*-triacetilglucurònid metil èster (**A16**):lipasa, (1:15) o (1:30).

El producte l'EGCG-4''-*O*-glucurònid metil èster (**B16**) es va obtenir amb tampó a pH 6.0 amb DMSO com a co-solvent i amb la lipasa AS. **A16** (2.07 mg ± 0.12) es va dissoldre amb tampó de fosfat sòdic pH 6.0 (25 mM; 0.8 mL) i DMSO com a co-solvent (0.2 mL). La Lipasa AS es va immobilitzar per a millorar el rendiment i la seva posterior eliminació, es va afegir LAS immobilitzada a la solució (de 20.1 to 60.4 mg) amb agitació suau a 40 °C de 6 a 22.5 h per a obtenir **B16**. La LAS immobilitzada es va eliminar per filtració amb un paper de filtre. Totes les reaccions es van seguir per HPLC-DAD i HPLC-HR-DAD-ESI-TOF-MS.

3.8.3. Hidròlisi de l'èster metílic de l'EGCG-4''-*O*-glucurònid metil èster per a obtenir l'EGCG-4''-*O*-glucurònid amb la PLE (èsterasa de fetge de porc)

La PLE (4.3 mg) es fa afegir a la solució que conté l'EGCG-4''-*O*-glucurònid metil èster (**B16**) obtinguda en la desacetilació amb la LAS immobilitzada (Secció 4.8.2) La solució es va mantenir amb agitació suau a 40 °C (5.5 h) per a obtenir l'EGCG-4''-*O*-glucurònid (**C16**). La reacció es va seguir per HPLC-DAD.

3.8.4 Mètodes analítics

3.8.4.1. Mètode d'HPLC-DAD utilitzat per a analitzar els productes de la reacció de Koening-Knorr

Les anàlisis d'HPLC-DAD es van realitzar amb una columna C-18 *Mediterranea Sea18* (5µm, 25x0.46) de Teknokroma. Els dissolvents utilitzats pel procediment van ser (A) aigua amb 0.1 % d'àcid acètic i (B) metanol 100 %. El gradient d'elució va ser de 20 a 80 % de B en 34 min utilitzant un flux de 0.8 mL min^{-1} i detecció a 214 and 280 nm.

3.8.4.2 Mètode utilitzat per a analitzar els productes obtinguts en la desacetilació amb les lipases

Les anàlisis d'HPLC-DAD es van realitzar amb una columna C-18 *Mediterranea Sea18* (5µm, 25x0.46) de Teknokroma. Els dissolvents utilitzats pel procediment van ser (A) aigua amb 0.1 % d'àcid acètic i (B) 80 % CH_3CN, 20 % aigua amb 0.095 % àcid acètic. El gradient d'elució va ser de 5 a 80 % de B en 40 min utilitzant un flux de 1 mL min^{-1} i detecció a 214 and 280 nm.

3.8.4.3. Mètode utilitzat per a analitzar els productes obtinguts en la desacetilació amb la Lipasa AS immobilitzada

Els anàlisis d'HPLC-DAD es van realitzar amb una columna C-18 *Mediterranea Sea18* (5µm, 25x0.46) de Teknokroma. Els dissolvents utilitzats pel procediment van ser (A) aigua amb 0.1 % àcid trifluoroacètic (TFA) i (B) 80 % CH_3CN, 20 % aigua amb 0.095 % àcid trifluoroacètic. El gradient d'elució va ser de 10 a 80 % de B en 30 min utilitzant un flux de 1 mL min^{-1} i detecció a 214 and 280 nm.

3.8.4.4 HPLC-HR-DAD-ESI-TOF-MS

Els mètodes utilitzats amb l'HPLC-HR-DAD-ESI-TOF-MS van ser els mateixos que els que es van utilitzar per a l'HPLC-DAD. També es va utilitzar la mateixa columna. El detector de masses va operar en negatiu. Condicions: adquisició *m/z* 100-2000, fragmentador 175 V, flux gas sec 10 L min^{-1}, pressió de nebulització 35 psig, temperatura de gas sec 350 °C, i voltatge de capil·laritat 3500 V. La columna que es va utilitzar per a la analitzar els productes de la reacció amb la lipasa AS immobilitzada va ser una C-18 LiChospher 100 RP-18 (5 µm, 4 x 250 mm) de Merck.

3.8.4.5. Mètode semipreparatiu per a purificar els productes de la reacció de Koenigs-Knorr

La purificació es va realitzar amb una columna C-18 X-Terra (10 μM; 19 x 250 mm) de Waters. Els dissolvents utilitzats van ser els mateixos que els utilitzats en el mètode analític HPLC-DAD amb un gradient d'elució de 5 a 20 % de B en 5 min seguit per un gradient de 20 a 80 % de B en 40 min utilitzant una velocitat de flux de 8 mL min^{-1} i un detector a 214 nm.

4. Resultats i discussió

4.1. Determinació de l'activitat antiradicalària de (poli)fenols amb els radicals TNPTM, HNTTM, DPPH i amb el mètode FRAP, determinació de l'antiproliferació cel·lular en cèl·lules HT-29 d'adenocarcinoma de còlon

Els radicals orgànics de les series del TTM(*29*) (tris(2,4,6-triclofenil)metil) i del PTM(*30*) (perclorotifenilmetil) (**Figura 7**) són espècies molt estables en estat sòlid i en solució en la foscor degut a la presència del (poli)clorofenils, substituents voluminosos que es troben al voltant de l'àtom de carboni trivalent. El potencial redox d'una molècula és una propietat molt important ja que la seva reactivitat front a altres espècies en depèn en gran part. En els nostres radicals, el potencial redox depèn essencialment de la capacitat donadora/acceptora dels grups substituents que es troben en les posicions *meta*- i/o *para*- dels anells aromàtics. Per tant, la síntesi de radicals amb diferents substituents ens permet obtenir una varietat de radicals amb diferents propietats redox. Aquests radicals lliures estables presenten una gran activitat de transferència electrònica, reduint-se a anions amb color, estables en solució i fàcilment caracteritzables per espectroscòpia visible (UV-Vis) i ressonància paramagnètica electrònica (EPR).

4.1.1. Radical tris(2,3,5,6-tetracloro-4-nitrofenil)metil (TNPTM)

Per tal de disposar d'una eina més selectiva que ens permeti determinar el poder antioxidant dels (poli)fenols més reductors, s'ha sintetitzat un nou radical lliure estable de la sèrie del perclorotifenilmetil (PTM) amb un potencial redox més baix que el de l'HNTTM, el radical tris(2,3,5,6-tetracloro-4-nitrofenil)metil (TNPTM) (**Figura 7**). El radical TNPTM només reacciona amb la forma aniònica dels (poli)fenols assajats i el mecanisme de reacció radicalari és l'SPLET (Secció 1.3.2)(*31*).

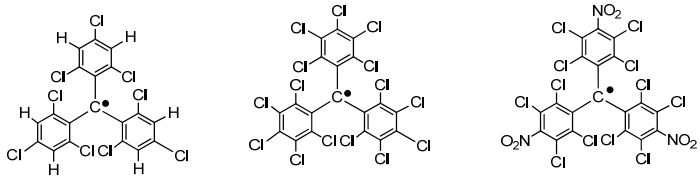

Figura 7. Estructures dels radicals lliures estables i els potencials redox mesurats per voltamperometria cíclica en CH_2Cl_2 amb una concentració de radical de 10^{-3} M i 0.1 M de Bu_4NClO_4 sobre Pt a 100 mV s^{-1}.

4.1.2. Determinació de les capacitats antiradicalàries i de la capacitat reductora dels (poli)fenols

S'han comparat els resultats de l'activitat antiradicalària de diferents (poli)fenols mesurada amb els radicals TNPTM, HNTTM i DPPH (**Taula 1**). Els valors de la capacitat antiradicalària s'han comparat amb els valors de la capacitat de reducció de metalls obtinguts amb el mètode FRAP. S'han estudiat un conjunt de (poli)fenols pertanyents a diferents famílies estructurals: els flavanols EC (**13**), epigalocatequina (EGC, **14**), epicatequin-3-O-gal.lat (ECG, **15**) i l'epigalocatequin-3-O-gal.lat (EGCG, **16**), els **tanins hidrolitzables** (els galotanins hamamelitanin (**17**) i pentagaloilglucosa (**18**) i els elagitanins punicalagin (**19**), dimethyl-hexahidroxidifenil-dicarboxilat (DHHDP, **20**) i l'àcid el.làgic (EA, **21**) així com també els **fenols simples** catecol (**10**), pirogal.lol (**11**) i metilgal.lat (**12**) que es troben formant part estructural dels flavanols, galotanins i elagitanins (**Figura 8**).

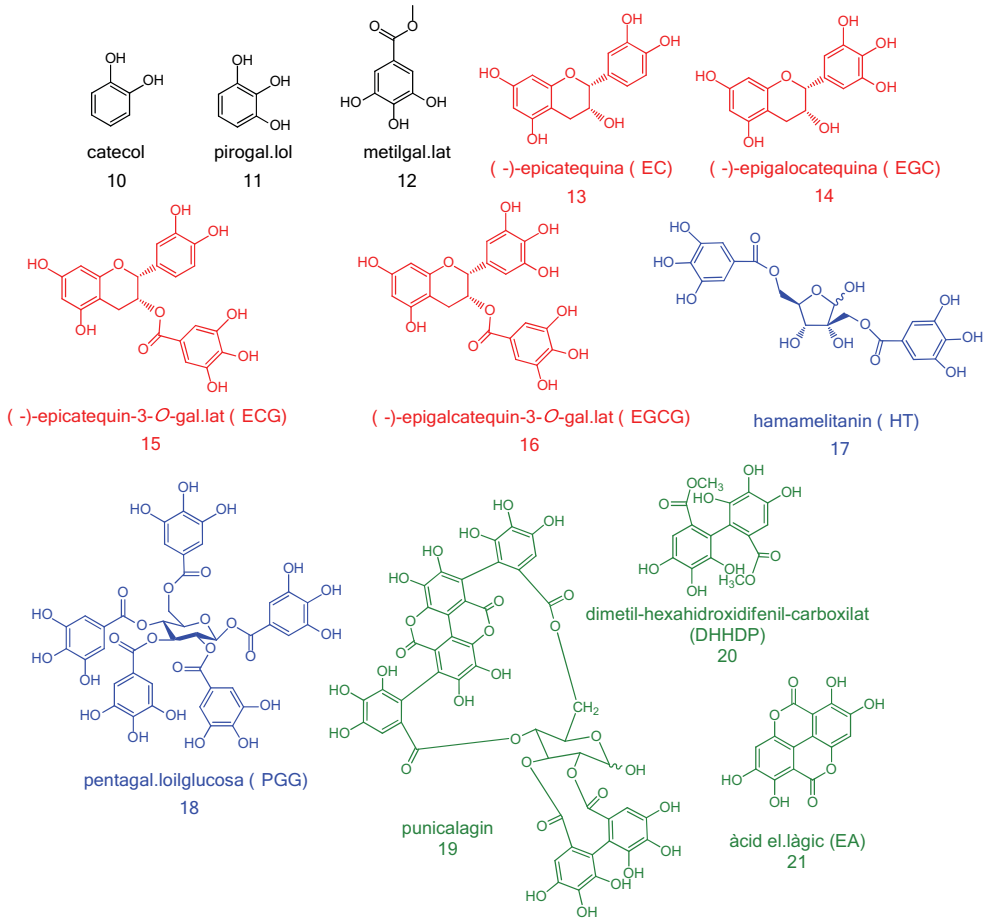

Figura 6. Estructures dels (poli)fenols estudiats.

Taula 1. Activitat reductora de diferents (poli)fenols front als radicals TNPTM, HNTTM i DPPH. Temps de reacció amb el radical TNPTM 48 h, HNTTM 7 h, i DPPH 1 h.

Radical	(poli)fenol	EC_{50}[a]	EC_{50}[b]	PAR	$n_{e/H}$
TNPTM	10	–	–	–	–
	11	21.7	0.17	5.80	2.90
	12	–	–	–	–
	13	–	–	–	–
	14	55.2	0.18	5.55	2.78
	15	-	-	-	-
	16	83.3	0.18	5.50	2.75
	17	232	0.45	4.30	1.04
	18	–	–	–	–
	19	50.3	0.15	6.52	3.30
	20	51.2	0.16	6.22	2.00
	21	–	–	–	–
HNTTM	10	23.1	0.21	43.3	2.3
	11	19.7	0.16	6.40	3.20
	12	28.4	0.15	6.48	3.20
	13	51.2	0.18	5.67	2.84
	14	50.2	0.16	6.16	3.10
	15	22.2	0.05	19.92	9.96
	16	40.6	0.09	11.3	5.70
	17	71.2	0.15	14.0	3.4
	18	54.8	0.06	18.2	8.6
	19	38.1	0.04	28.4	14.2
	20	42.2	0.12	8.68	4.34
	21	30.4	0.10	9.94	5.00
DPPH	10	18.7	0.17	53.4	2.9
	11	12.6	0.10	10.03	5.01
	12	34.0	0.18	5.42	3.18
	13	38.0	0.13	7.64	3.80
	14	32.7	0.11	9.41	4.70
	15	26.7	0.06	16.6	8.32
	16	26.4	0.06	17.34	8.70
	17	27.8	0.06	36.0	8.78
	18	23.8	0.03	42.0	19.8

19	18.9	0.02	57.3	28.7
20	30.1	0.08	12.2	6.10
21	22.5	0.07	13.5	6.73

[a]EC_{50} (μg/μmol), (b) EC_{50} (μmol/μmol)) (Concentració eficaç en el 50 %), PAR (potencial antiradicalari (1/EC_{50}^{b}), $n_{e/H}$ (número d'hidrògens/electrons transferits (1/VE (Valor estequiomètric (2*EC_{50}^{b})). Mesurat per EPR; (—) valors amb n_e < 1.

Els valors de la mesura de la Capacitat Reductora (CR) dels (poli)fenols amb el complex Fe (III)-o-fenantrolina es van expressar en μg de (poli)fenol per mL i en μmol de (poli)fenols per L.

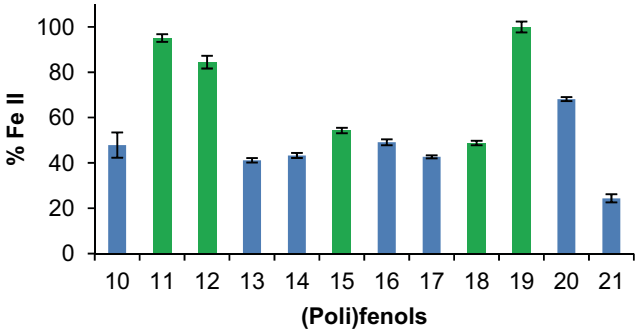

Figura 7. Valors relatius de RC dels (poli)fenols **10**-**21** determinats amb el mètode FRAP utilitzant els mateixos μg per mL de cada (poli)fenol.

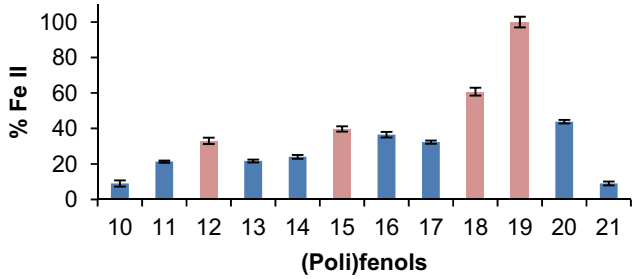

Figura 8. Valors relatius de RC dels (poli)fenols **10**-**21** determinats amb el mètode FRAP utilitzant els mateixos μmol per L de cada (poli)fenol.

La comparació dels valors de la capacitat de transferència electrònica dels (poli)fenols obtinguts amb els quatre mètodes suggereixen importants conclusions: la mesura de la capacitat de transferència electrònica dels (poli)fenols amb els radicals HNTTM i DPPH i amb el mètode FRAP dóna valors relatius (**Taula 2**) similars tot i que els radicals HNTTM i DPPH i el mètode FRAP reaccionen mitjançant diferents mecanismes de reducció i en dissolvents diferents ($CHCl_3$/MeOH (2:1) i aigua). Aquests tres mètodes mostren que els (poli)fenols pirogal·lol (**11**), ECG (**15**), PGG (**18**) i punicalagin (**19**) són els més antiradicalaris i els més reductors de tots els (poli)fenols estudiats. És molt important destacar que, per al grup de (poli)phenols estudiats, només el radical TNPTM és un quimiosensor selectiu ja que reacciona només amb els grups més reactius dels (poli)fenols estudiats. Aquests són el grup pirogal·lol, estructures formades per un enllaç C-C, per exemple entre dos grups gal·lat, com el grup HHDP i entre un gal.lat i l'el.làgic àcid (punicalagin (**19**)) i l'HT (**17**). En conclusió, els radicals HNTTM i TNPTM són dos quimosensors complementaris de transferència electrònica: el radical HNTTM s'utilitza per a avaluar la capacitat antiradicalària dels (poli)fenols i el radical TNPTM detecta selectivament els grups amb més capacitat antiradicalària.

Taula 2. Capacitat antiradicalària i capacitat reductora dels (poli)fenols **10**-**21** mesurada amb l'HNTTM (**4**), TNPTM (**8**), DPPH (**9**) i el mètode FRAP.

	HNTTM		TNPTM		DPPH		FRAP	
	% mmol μg^{-1}	$\mu mol\ \mu mol^{-1}$	% mmol μg^{-1}	$\mu mol\ \mu mol^{-1}$	% mmol μg^{-1}	$mmol\ \mu mol^{-1}$	$\mu g\ mL\text{-}1$	$\mu mol\ L^{-1}$
10	85	76	-	-	67	59	50	42
11	100	100	100	100	100	100	100	100
12	69	107	-	-	37	56	89	155
13	38	64	-	-	33	77	43	102
14	39	100	26	95	39	91	46	113
15	89	320	-	-	47	167	57	186
16	48	178	39	95	48	167	52	171
17	28	107	9	38	45	167	45	152
18	36	267	-	-	53	333	51	285
19	52	400	43	113	67	500	105	469
20	47	133	42	106	42	125	72	206
21	65	160	-	-	56	143	26	42

[a]Valors expresats en % respecta la capacitat antiradicalària representada com a ARP (mmol de radical per µg de (poli)fenol i µmol de radical per µmol de (poli)fenol) o RC (µg per mL de (poli)fenol i µmol per L de (poli)fenol) de pirogal.lol (**11**); [b](-) Valors ≤ 13 (mmol/µg) i 21 (µmol/µmol).

4.1.3. Determinació de les constants de velocitat (k_1 i k)dels (poli)fenols actius front al radical TNPTM

S'han determinat les cinètiques dels (poli)fenols actius front al radical TNPTM (**8**) en $CHCl_3$/MeOH (2:1) (**Taula 2**)

Taula 2. Constants de velocitat de les reaccions dels (poli)fenols actius front al radical 8 en $CHCl_3$/MeOH (2:1).

(Poli)fenol	TNPTM:(poli)fenol proporció molar [b]	k (M^{-1} s^{-1}) k_1(M^{-1} s^{-1})[c]
11	4.6	0.388 ± 0.070
14	4.9	0.266 ± 0.035
16	4.9	71.8 ± 1.02[c]
17	5.0	0.130 ± 0.024
19	5.0	0.125 ± 0.041
20	4.9	0.115 ± 0.010

[a]Temps de reacció 48 h. [b]Concentració inicial del radical **8**, en l'interval 119.2-121.6 μM i dels (poli)fenols, 24.1-25.6 μM (molar ratio, 5:1). Numero de repeticions dels assajos realitzats per a cada (poli)fenol, n= 2.

Els valors de k_1 i k s'han calculat amb el model cinètic i equacions utilitzats per Dangles i col·laboradors (*27*). Els resultats mostren que totes les reaccions són lentes (**Taula 2**) i només en la cinètica del flavanol **16** s'observa un comportament de dues etapes, una ràpida (k_1) amb la transferència de 1.9 electrons i una lenta. La reacció del radical TNPTM amb el pirogal·lol (**11**) és 1.5 cops més ràpida que la del EGC (**14**), flavanol que conté a l'**11** en la seva estructura. Dels elagitanins, el punicalagin (**19**) i la seva subestructura DHHDP (**20**) tenen valors de k similar, així com també el galotanin HT (**17**), tot i que transfereixen diferent número d'electrons (**Taula 1**) (2.9, 2.0 i 1.0, respectivament). Si es compara la constant cinètica de la subestructura activa front al radical TNPTM, dels flavanols, el pirogal·lol (**11**), i dels elagitannins, i el DHHDP (**20**), **11** és aproximadament 3.5 cops més ràpid que el **20**.

4.1.4. Determinació de la relació entre l'estructura i l'activitat química i biològica de diferents (poli)fenols en cèl·lules d'adenocarcinoma de còlon (HT-29)

La relació entre les propietats químiques dels (poli)fenols i la seva activitat biològica es mostra en els resultats obtinguts en assajos *in vitro* amb cèl·lules d'adenocarcinoma de còlon HT-29 (**Taula 3**).

Taula 3. Viabilitat de les cèl·lules HT-29 tractades amb els (poli)fenols **11**-**21**.

Famílies de (poli)fenols	IC_{50}[(a)]	IC_{50}[(b)]
Fenols simples		
11	5.61 ± 0.50	71.4 ± 7.49
12	24.6 ± 8.29	31.6 ± 1.82
Flavanols		
13	≤ 120 ± 18.9	≤ 120 ± 51.2
14	24.1± 2.75	≤ 120 ± 5.28
15	53.7± 11.94	58.9 ± 7.98
16	17.5 ± 3.21	47.9 ± 7.97
Tanins hidrolitzables		
Galotanins		
17	9.69 ± 4.50	6.30 ± 2.22
18	26.3 ± 8.75	31.9 ± 1.13
Elagitanins		
19	21.5 ± 3.53	14.4 ± 0.38
20	32.5 ± 3.88	34.1 ± 0.48
21	≤ 120 ± 27.5	≤ 120 ± 6.32

[(a,b)] IC_{50} en μg per mL, les cèl·lules HT-29 es van tractar amb els compostos durant 72 h, en [(a)]DMEM i [(b)]DMEM amb catalasa. (IC_{50} ± SD (SD= desviació estàndard, número d'experiments repetits per (poli)fenol, n= 2-3).

Els valors d'antiproliferació obtinguts mostres que tots els (poli)fenols estudiats excepte la EC (**13**) i l'àcid el·làgic (**21**) (estructura 1,2-dihidroxifenílica), produeixen antiproliferació en les cèl·lules HT-29. Els resultats mostren que de la família dels flavanols, els que contenen el grup pirogal·lol en la seva estructura, l'EGC (**14**) i l'EGCG (**16**) són els més antiproliferatius. En afegir catalasa la seva activitat (**11, 14** i **16**)

disminueix perquè aquest enzim elimina el peròxid d'hidrogen produït pel grup pirogal·lol (el H_2O_2 és inductor de l'apoptosi). Dels galotanins, l'HT (**17**) i dels elagitanins, el punicalagin (**19**) i el DHHDP (**20**) són els més antiproliferatius (**Taula 3**).

Comparant els resultats de l'antiproliferació cel·lular amb els de capacitat antiradicalària obtinguts amb el radical TNPTM es demostra que, entre els (poli)fenols estudiats, aquells que tenen capacitat reductora front el radical TNPTM són els més antiproliferatius en cèl·lules d'adenocarcinoma de còlon HT-29. Es confirma que els (poli)fenols amb una major capacitat donadora d'electrons produeixen una major antiproliferació cel·lular.

4.2 Síntesi quimoenzimàtica dels glucuronats de l'(-)-epigalocatequin-3-*O*-gal.lat (EGCG) (16).

Els metabòlits dels (poli)fenols poden tenir propietats biològiques diferents dels seus compostos originaris i per tant, és important avaluar la seva activitat. La quantitat de metabòlits que es troben en els fluids biològics no és suficient com per ser aïllada. Per aquest motiu, s'han de buscar vies de síntesi química i/o enzimàtica.

L'(-)-epigalocatequin-3-*O*-galat (EGCG) (**16**) és la catequina a la que s'atribueix més rellevància biològica degut a que és el (poli)fenol més abundant en el te, la segona beguda més consumida mundialment, i per la seva capacitat antioxidant/pro-oxidant.(*19*) Per aquest motiu, l'obtenció dels seu metabòlits com els glucuronats (metabòlits majoritaris), és de gran importància. El metabòlit (-)-EGCG-4''-O-glucurònid va ser sintetitzat per primer cop com a metabòlit majoritari per Lu *et al.,*(*1*) amb microsomes de fetge i intestí prim de ratolí, rata i humà, però l'obtenció preparativa de glucuronats mitjançant la síntesi enzimàtica és molt dificultosa

4.2.1. Síntesi química de l'EGCG-4''-triacetilglucurònid metil èster

En aquesta tesi la síntesi química de derivats glucuronats de l'(-)-epigalocatequin-3-*O*-galat (EGCG, **16**) s'ha basat en la reacció de Koenigs-Knorr (**Figura 9**), on es produeix una substitució nucleòfila entre el carboni anomèric del sucre activat i el/els hidroxils més reactius de la molècula **16**. Es va seguir la reacció de glucuronidació utilitzada per González-Manzano *et al.*(*28*) però amb alguns canvis, com la utilització de DMF en lloc d'acetona com a dissolvent per a una millor solubilitat de **16**.

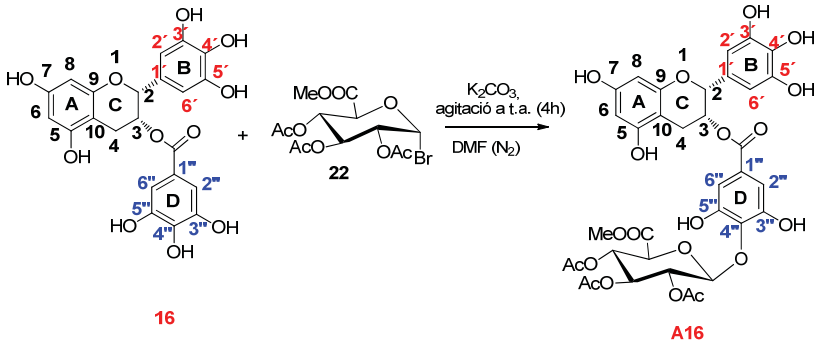

Figura 9. Reacció de glucuronidació de **16**.

La reacció es va seguir per HPLC-DAD i els pics es van caracteritzar per MS-ESI (Masses-ionització amb electroesprai). El producte final es va purificar per HPLC semipreparatiu i es va caracteritzar la fracció escollida per RMN (CD_3OD) (^{1}H-RMN, ^{13}C-RMN, HSQC i HMBC). El producte obtingut va ser l'**A16** (**Figura 9**).

4.2.2. Desacetilació de l'EGCG-4''-traicetilglucurònid metil èster per a obtenir l'EGCG-4''-glucurònid metil èster

La desacetilació de compostos que contenen (poli)fenols és especialment delicada degut a la seva sensibilitat en medi bàsic.(*32*) Es van assajar diferents mètodes de desacetilació: utilització del metòxid sòdic (MeONa) (*33*), una base més suau com el carbonat sòdic (Na_2CO_3)(*34*) , amb acetat de zinc ($Zn(AcO)_2$)(*32*) i amb àcid *para*-toluensulfònic (p-TsOH).(*35*) En no obtenir resultats positius, es va optar per la utilització de les lipases, enzims selectius que trenquen els enllaços èster mantenint intacte la resta de la molècula. L'EGCG (**16**) és un dels (poli)fenols més sensibles al medi bàsic perquè apart de tenir les posicions més sensibles de l'estructura comú dels flavonols, l'anell A i els hidroxils aromàtics, conté un enllaç èster en la posició del C3 molt inestable en condicions bàsiques.

Les lipases utilitzades van ser la Novozyme-435, la PPL (lipasa pancreàtica de porc), la Lypozime, la lipasa A(*36, 37*) i la lipasa AS.(*38*) La lipasa AS immobilitzada en una reïna acrílica (**A16**/LAS 1:17 (w/w)), utilitzant tampó de fosfat sòdic (Na_2HPO_4, 25 mM, pH 6.02) amb DMSO com a co-solvent (20 %) a 40 °C i durant 6 h de reacció, ens va permetre obtenir el producte desitjat **B16**.

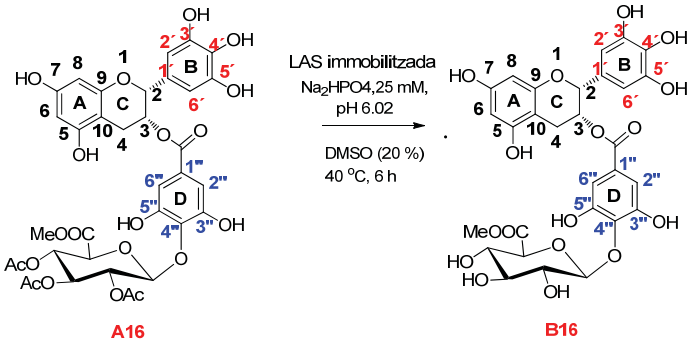

Figura 10. Reacció de desacetilació de l'EGCG-acetilglucurònid metil èster (**B16**).

La reacció es va seguit per HPLC-DAD a 214 nm i per MS-ESI es va poder identificar el pic corresponent a la massa del compost **B16** (**Figura 10**). El producte B16 no s'ha pogut aïllar i per tant no s'ha pogut caracteritzar per RMN.

4.2.3. Hidròlisi de l'èster de metil de l'EGCG-4''-glucurònid metil èster per a obtenir l'EGCG-4''-glucurònid

Finalment, amb PLE (èsterasa de fetge de porc)(*38*) es va obtenir el producte final desitjat **C16** (**Figura 11**) però amb tant poc rendiment que no va poder ser aïllat.

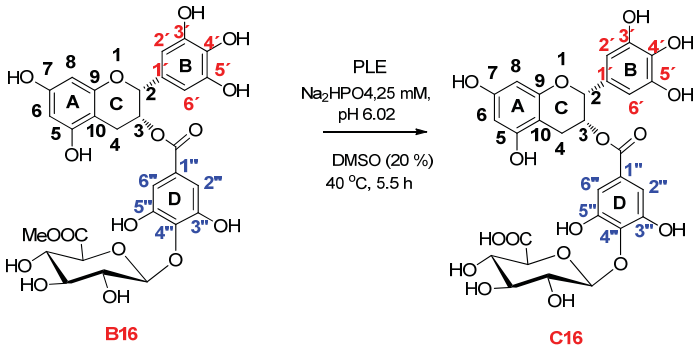

Figura 11. Reacció de desmetilació de l'EGCG-glucurònid metil èster (**C16**).

Conclusions

1. S'ha sintetitzat i caracteritzat el radical tris(2,3,5,6-tetracloro-4-nitrofenil)metil (TNPTM) amb un valor de potencial redox (E°) de 0.20 V en $CHCl_3$/MeOH (2:1).

2. El radical TNPTM reacciona exclusivament amb determinats compostos fenòlics per transferència electrònica com s'ha demostrar amb l'etabilitat del TNPTM en toluè (no s'ha produït transferència d'àtom d'hidrogen), pel seu impediment estèric (raig X), així com també per la detecció de l'anió del TNPTM en la reacció en $CHCl_3$/MeOH (2:1). El radical TNTPM té un potencial redox inferior al del HNTTM.

3. El radical TNPTM i el radical ja descrit HNTTM, s'han utilitzat per a determinar la activitat de captació de radicals (cinètiques i capacitat de captació de radicals) d'una sèrie de (poli)fenols que inclou fenols simples, flavanols i tanins hidrolitzables. Els (poli)fenols estudiats són: els fenols simples catecol (**10**), pirogal·lol (**11**) i metilgal.lat (**12**), els flavanols (–)-epicatequina (EC, **13**), (–)-epigalocatequina (EGC, **14**), (–)-epicatequin-3-*O*-galat (ECG, **15**) i (–)-epigalocatequin-3-*O*-galat (EGCG, **16**), els galotanins hamamelitanin (HT, **17**) i pentagal·loilglucosa (PGG, **18**), l'elagitanin punicalagin i les seves subestructures dimetil-hexahidroxidifenil-dicarboxilat (DHHDP, **20**) i l'àcid el·làgic (EA, **21**).

4. El radical TNPTM reacciona exclusivament amb el pirogal·lol (**11**), EGC (**14**), EGCG (**16**), HT (**17**), punicalagin (**19**) i DHHDP (**20**). El resultants de capacitat obtinguts amb el TNPTM mostren que la subestructura HHDP del punicalagin és una posició particularment reactiva i que l'enllaç C-C de dos grups gal.lats amb el grup àcid ellagic i l'enllaç C-C entre dos gal·lats (HHDP grup) del punicalagin activa un dels grups hidroxil de cada gal·lat.

5. Els valors de capacitat dels (poli)fenols per a captar radicals obtinguts amb l'HNTTM s'han comparat amb els valors obtinguts amb el DPPH (**9**) i el mètode FRAP. Els resultats relatius obtinguts amb els tres mètodes són similars tot i els seus diferents mecanismes de reducció i el diferent dissolvent utilitzat. Els resultats obtinguts amb aquests tres mètodes mostren que de cada grup de (poli)fenols, el pirogal·lol (**11**), l'ECG (**15**), la PGG (**18**) i el punicalagin (**19**) són els mes actius en captar radicals lliures i en reduir metalls. La

capacitat dels (poli)fenols **10**-**21** per a captar radicals lliures determinada amb l'HNTTM coincideix generalment amb el número de grups hidroxils dels (poli)fenols, mentre que amb el DPPH, els valors de capacitat antiradicalària són generalment més elevats que els obtinguts amb l'HNTTM.

6. La introducció del grup cisteïna en la posició 4 de l' EGC (**14**) i de l'EGCG (**16**) no modifica el número d'electrons transferits per molècula de (poli)fenol a l'HNTTM si es compara amb els seus precursors. Per altre banda, la introducció del grup cisteamina en la mateixa posició de l'EGC (**14**), l'ECG (**15**) i l'EGCG (**16**) augmenta en un el número d'electrons transferits per molècula de (poli)fenol.

7. El mecanisme proposat per a les reaccions entre el catecol (**10**) o el pirogal·lol (**11**) amb l'HNTTM en el dissolvent ionitzable $CHCl_3$/MeOH (2:1) és la transferència seqüencial de protó i electró (TSPE). Aquest mecanisme es demostra per anàlisis electroquímics (reacció exergònica només per la forma aniònica dels fenols) i per espectroscòpia d'UV-Vis (l'anió de l'HNTTM és estable i l'intermedi característic de la reacció). Per altre banda, el mecanisme en disolvents no ionitzables com el $CHCl_3$ i el benzè és la transferència electrònica acoblada a protó (TEAP) degut a l'absència de l'anió de l'HNTTM (no detectable per UV-Vis). La reacció del pirogal·lol (**11**) amb l'HNTTM en benzè té lloc a través de la formació d'un complexa entre l'**11** i l'HNTTM, en qual es transfereix l'electró que és detectat per UV-Vis. El radical HNTTM té un potencial d'oxidació suficientment alt com per a oxidar per transferència electrònica als (poli)fenols en la seva forma tant aniònica com molecular.

8. S'ha proposat el mecanisme TSPE per a la reacció entre el pirogal·lol (**11**) o el DHHDP (**20**) amb el radical TNPTM. El TNPTM oxida a aquells (poli)fenols amb un baix potencial de pic aniònic (E_p^a) o amb un baix potencial onset anòdic (E_o^a) (≤ 0.50 V).

9. Les voltamperometries cícliques del TNPTM i del DPPH mostren valors de potencial redox ($E°$) molt similars, 0.20 V and 0.21 V, respectivament en $CHCl_3$/MeOH (2:1). Aquests valors suggereixen que els radicals TNPTM i DPPH reaccionen amb els (poli)fenols en $CHCl_3$/MeOH (2:1) mitjançant mecanismes diferents, transferència electrònica (TE) i transferència d'un àtom d'hidrogen (TAH), respectivament. L'HNTTM reacciona amb els (poli)fenols mitjançant el mateix mecanisme que el TNPTM.

10. Els estudis cinètics realitzat amb el TNPTM mostren que l'EGCG (**16**) és el més ràpid dels (poli)fenols estudiats.

11. Tots els (poli)fenols excepte EC (**13**) i l'EA (**21**) indueixen l'antiproliferació en cèl·lules HT-29. Els (poli)fenols amb més acció antiproliferativa en cèl·lules HT-29 sense catalasa (pirogal·lol (**11**), EGC (**14**) i EGCG (**16**), HT (**17**), punicalagin (**19**) i DHHDP (**20**)) són els que són actius com a captadors del radical TNPTM. Aquesta relació suggereix un possible efecte prooxidant.

12.L'EGCG-4''-*O*-glucurònid (**C16**), metabòlit de l'EGCG més abundant en humans, va ser sintetitzat químicament i caracteritzat en la seva forma acetilada EGCG-4''-*O*-triacetilglucurònid metil èster (**A16**). La transformació de l'**A16** en **C16** es va realitzar utilitzant lipases, però es van obtenir rendiments molt baixos degut a la pobre activitat hidrolítica de l'enzim LAS cap a les posicions acetilades de l'.EGCG-4''-*O*-triacetilglucurònid (**A16-Me**) i per la poca activitat hidrolítica de la esterasa PLE cap a l'èster metílic de l'EGCG-4''-*O*-glucurònid metil èster (**B16**).

6. Bibliografia

1. Lu, H.; Meng, X. F.; Li, C.; Sang, S.; Patten, C.; Sheng, S.; Hong, J.; Bai, N.; Winnik, B.; Ho, C. T.; Yang, C. S. Glucurònides of Tea Catechins: Enzymology of Biosynthesis and Biological Activities. *Drug Metab. Dispos.* **2003**, *31*, 452-461.

2. Heck, D. E.; Vetrano, A. M.; Mariano, T. M.; Laskin, J. D. UVB Light Stimulates Production of Reactive Oxygen Species. *J. Biol. Chem.* **2003**, *278*, 22432-22436.

3. Powers, S. K.; DeRuisseau, K. C.; Quindry, J.; Hamilton, K. L. Dietary antioxidants and exercice. *J. Sports Sci.* **2003**, *22*, 81-94

4. Howard, D. J.; Ota, R. B.; Briggs, L. A.; Hampton, M.; Pritsos, C. A. Environmental tobacco smoke in the workplace induces oxidative stress in employees, including increased production of 8-hydroxy-2'-deoxyguanosine. *Cancer Epidemiol. Biomarkers Prev.* **1998**, *7*, 141-146.

5. Halliwell, B. Oxidative stress and cancer: have we moved forward? *Biochem. J.* **2007**, *401*, 1-11.

6. Ames, B. N.; Shigenaga, M. K.; Hagen, T. M. Oxidants, antioxidants, and the degenerative diseases of aging. *Proc. Natl. Acad. Sci.* **1993**, *90*, 7915-7922.

7. Crespy, V.; Williamson, G. A review of the health effects of green tea catechins in in vivo animal models. *J. Nutr.* **2004**, *134*, 3431S-3440S.

8. Huang, M. T.; Lou, Y. R.; Ma, W.; Newmark, H. L.; Reuhl, K. R.; Conney, A. H. Inhibitory Effects of Dietary Curcumin on Forestomach, Duodenal, and Colon Carcinogenesis in Mice. *Cancer Res.* **1994**, *54*, 5841-5847.

9. Wang, J.; Eltoum, I. E.; Lamartiniere, C. A. Dietary genistein suppresses chemically induced prostate cancer in Lobund-Wistar rats. *Cancer Lett.* **2002**, *186*, 11-18.

10. Zaveri, N. T. Green tea and its polyphenolic catechins: Medicinal uses in cancer and noncancer applications. *Life Sci.* **2006**, *78*, 2073-2080.

11. Bettuzzi, S.; Brausi, M.; Rizzi, F.; Castagnetti, G.; Peracchia, G.; Corti, A. Chemoprevention of Human Prostate Cancer by Oral Administration of Green Tea Catechins in Volunteers with High-Grade Prostate Intraepithelial Neoplasia: A Preliminary Report from a One-Year Proof-of-Principle Study. *Cancer Res.* **2006**, *66*, 1234-1240.

12. Li, N.; Sun, Z.; Han, C.; Chen, J. The Chemopreventive Effects of Tea on Human Oral Precancerous Mucosa Lesions. *Proc. Soc. Exp. Biol. Med.* **1999**, *220*, 218-224.

13. Spencer, J. P. E.; Schroeter, H.; Rechner, A. R.; Rice-Evans, C. Bioavailability of Flavan-3-ols and Procyanidins: Gastrointestinal Tract Influences and Their Relevance to Bioactive Forms In Vivo. *Antiox. Redox Sig.* **2001**, *3*, 1023-1039.

14. Manach, C.; Scalbert, A.; Morand, C.; Rémésy, C.; Jiménez, L. Polyphenols: food sources and bioavailability. *Am. J. Clinic.Nutr.* **2004**, *79*, 727-747.

15. Foti, M. C.; Daquino, C.; Mackie, I. D.; DiLabio, G. A.; Ingold, K. U. Reaction of Phenols with the 2,2-Diphenyl-1-picrylhydrazyl Radical. Kinetics and DFT Calculations Applied To Determine ArO-H Bond Dissociation Enthalpies and Reaction Mechanism. *J. Org. Chem.* **2008**, *73*, 9270-9282.

16. Galian, R. E.; Litwinienko, G.; Pérez-Prieto, J.; Ingold, K. U. Kinetic solvent effects on the reaction of an aromatic ketone pi,pi* triplet with phenol. Rate-retarding and rate-accelerating effects of hydrogen-bond acceptor solvents. *J. Am. Chem. Soc.* **2007**, *129*, 9280-9281.

17. Litwinienko, G.; Ingold, K. U. Abnormal Solvent Effects on Hydrogen Atom Abstraction. 3. Novel Kinetics in Sequential Proton Loss Electron Transfer Chemistry. *J. Org. Chem.* **2005**, *70*, 8982-8990.

18. Sjödin, M.; Irebo, T.; Utas, J. E.; Lind, J.; Merényi, G.; Äkermark, B.; Hammarström, L. Kinetic Effects of Hydrogen Bonds on Proton-Coupled Electron Transfer from Phenols. *J. Am. Chem. Soc.* **2006**, *128*, 13076-13083.

19. Li, G. X.; Chen, Y. K.; Hou, Z.; Xiao, H.; Jin, H.; Lu, G.; Lee, M. J.; Liu, B.; Guan, F.; Yang, Z.; Yu, A.; Yang, C. S. Pro-oxidative activities and dose-response relationship of (-)-epigallocatechin-3-gallate in the inhibition of lung cancer cell growth: a comparative study in vivo and in vitro. *Carcinogenesis* **2010**, *31*, 902-910.

20. Joubert, E.; Winterton, P.; Britz, T. J.; Gelderblom, W. C. A. Antioxidant and Pro-oxidant Activities of Aqueous Extracts and Crude Polyphenolic Fractions of Rooibos (*Aspalathus linearis*). *J. Agric. Food Chem.* **2005**, *53*, 10260-10267.

21. Perron, N. R.; García, C. R.; Pinzón, J. R.; Chaur, M. N.; Brumaghim, J. L. Antioxidant and prooxidant effects of polyphenol compounds on copper-mediated DNA damage. *J. Inorg. Biochem.* **2011**, *105*, 745-753.

22. Torres, J. L.; Varela, B.; Brillas, E.; Juliá, L. Tris(2,4,6-trichloro-3,5-dinitrophenyl)methyl radical: a new stable coloured magnetic species as a chemosensor for natural polyphenols. *Chem. Commun.* **2003**, 74-75.

23. Jiménez, A.; Juliá, L.; Selga, A.; Torres, J. L. Reducing activity of polyphenols with stable radicals of the TTM series. Electron transfer versus H-abstraction reactions in flavan-3-ols. *Org. Lett.* **2004**, *6*, 4583-4586.

24. Lozano, C.; Juliá, L.; Jiménez, A.; Touriño, S.; Centelles, J. J.; Cascante, M.; Torres, J. L. Electron-transfer capacity of catechin derivatives and influence on the cell cycle and apoptosis in HT29 cells. *Febs J.* **2006**, *273*, 2475-2486.

25. Touriño, S.; Selga, A.; Jiménez, A.; Juliá, L.; Lozano, C.; Lizárraga, D. L.; Cascante, M.; Torres, J. L. Procyanidin fractions from pine (Pinus pinaster) bark: Radical scavenging power in solution, antioxidant activity in emulsion, and antiproliferative effect in melanoma cells. *J. Agric. Food Chem.* **2005**, *53*, 4728-4735.

26. Touriño, S.; Lizárraga, D.; Carreras, A.; Lorenzo, S.; Ugartondo, V.; Mitjans, M.; Vinardell, M. P.; Juliá, L.; Cascante, M.; Torres, J. L. Highly galloylated tannin fractions from witch hazel (*Hamamelis virginiana*) bark: Electron transfer capacity, in vitro antioxidant activity, and effects on skin-related cells. *Chem. Res. Toxicol.* **2008**, *21*, 696-704.

27. Goupy, P.; Dufour, C.; Loonis, M.; Dangles, O. Quantitative Kinetic Analysis of Hydrogen Transfer Reactions from Dietary Polyphenols to the DPPH Radical. *J. Agric. Food Chem.* **2002**, *51*, 615-622.

28. González-Manzano, S.; González-Paramás, A.; Santos-Buelga, C.; Dueñas, M. Preparation and Characterization of Catechin Sulfates, Glucuronides, and Methylethers with Metabolic Interest. *J. Agric. Food Chem.* **2009**, *57*, 1231-1238.

29. Armet, O.; Veciana, J.; Rovira, C.; Riera, J.; Castaner, J.; Molins, E.; Rius, J.; Miravitlles, C.; Olivella, S.; Brichfeus, J. Inert carbon free-radicals .8. Polychlorotriphenylmethyl radicals - synthesis, structure, and spin-density distribution. *J. Phys. Chem.* **1987**, *91*, 5608-5616.

30. Ballester, M. Inert free-radicals (IFR)- a unique trivalent carbon species. *Acc. Chem. Res.* **1985**, *18*, 380-387.

31. Torres, J. L.; Carreras, A.; Jiménez, A.; Brillas, E.; Torrelles, X.; Rius, J.; Juliá, L. Reducing power of simple polyphenols by electron-transfer reactions using a new stable radical of the PTM series, tris(2,3,5,6-tetrachloro-4-nitrophenyl)methyl radical. *J. Org. Chem.* **2007**, *72*, 3750-3756.

32. Boumendjel, A.; Blanc, M.; Williamson, G.; Barron, D. Efficient Synthesis of Flavanone Glucurònides. *J. Agric. Food Chem.* **2009**, *57*, 7264-7267.

33. O'Leary, K. A.; Day, A. J.; Needs, P. W.; Sly, W. S.; O'Brien, N. M.; Williamson, G. Flavonoid glucurònides are substrates for human liver beta-glucurònidase. *FEBS Lett.* **2001**, *503*, 103-106.

34. Needs, P. W.; Kroon, P. A. Convenient syntheses of metabolically important quercetin glucurònides and sulfates. *Tetrahedron* **2006**, *62*, 6862-6868.

35. González, A. G.; Brouard, I.; León, F.; Padrón, J. I.; Bermejo, J. A facile chemoselective deacetylation in the presence of benzoyl and *p*-bromobenzoyl groups using *p*-toluenesulfonic acid. *Tetrahedron Lett.* **2001**, *42*, 3187-3188.

36. Prasad, A. K.; Pati, H. N.; Azim, A.; Trikha, S.; Poonam. Lipase-catalysed regio- and enantioselective deacetylation of 2,4-diacetoxyphenyl alkyl ketones. *Biorg. Med. Chem.* **1999**, *7*, 1973-1977.

37. Prasad, A. K.; Kalra, N.; Yadav, Y.; Kumar, R.; Sharma, S. K.; Patkar, S.; Lange, L.; Wengel, J.; Parmar, V. S. Deacylation studies on furanose trièsters using an immobilized lipase: Synthesis of a key precursor for bicyclonucleosides. *Chem. Commun.* **2007,** 2616-2617.

38. Baba, A.; Yoshioka, T. Synthesis of 1-[β]-O-acyl glucurònides of diclofenac, mefenamic acid and (S)-naproxen by the chemo-selective enzymatic removal of

protecting groups from the corresponding methyl acetyl derivatives. *Org. Biomol. Chem.* **2006**, *4*, 3303-3310.

Annex 17. Publications

JOC*Article*

Reducing Power of Simple Polyphenols by Electron-Transfer Reactions Using a New Stable Radical of the PTM Series, Tris(2,3,5,6-tetrachloro-4-nitrophenyl)methyl Radical

Josep Lluís Torres,[†] Anna Carreras,[†] Aurora Jiménez,[†] Enric Brillas,[‡] Xavier Torrelles,[§] Jordi Rius,[§] and Luis Juliá*,[†]

Institut d'Investigacions Químiques i Ambientals—CSIC, Jordi Girona 18-26, 08034 Barcelona, Spain, Departament de Química Física, Universitat de Barcelona, Martí I Franquès 1-11, 08028 Barcelona, Spain, and Institut de Ciència de Materials (CSIC), Campus de la U.A.B., 08193 Bellaterra, Spain

ljbmoh@cid.csic.es

Received December 28, 2006

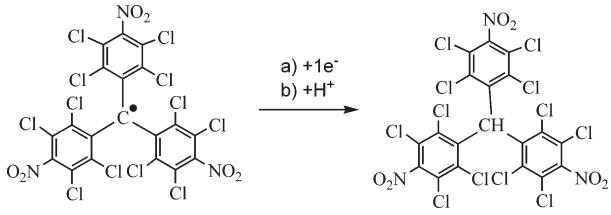

The synthesis and characterization of a new radical and its use for testing the antioxidant activity of polyphenols by electron transfer are reported. This new and stable species of magnetic nature, tris-(2,3,5,6-tetrachloro-4-nitrophenyl)methyl (TNPTM) radical, has been characterized by electron paramagnetic resonance and its molecular structure determined by X-ray analysis. This new radical of the PTM (perchlorotriphenylmethyl) series, unlike 2,2-diphenyl-1-picrylhydrazyl (DPPH) radical, is stable in conditions of hydrogen abstraction reactions. TNPTM radical is able to discriminate between the antioxidant activities of catechol and pyrogallol in hydroxylated solvent mixtures such as chloroform/methanol (2:1). These features determine the antioxidant/pro-oxidant character and the biological activities of natural and synthetic flavonoids.

Introduction

Natural and synthetic polyphenols are a class of organic compounds that show a remarkable ability to act as antioxidants.[1,2] Their protective effects in biological systems are conferred mainly by their scavenging activity against reactive oxygen species (ROS), which cause cellular damage associated with many human degenerative diseases.[3] Among the most known polyphenols, flavanols (catechins) are very active antioxidants extensively found in fruits and vegetables.[4]

Two different chemical mechanisms may be involved in the scavenging effect of polyphenols against harmful oxygen species such as hydroxyl radicals and peroxyl radicals.[5] One of them consists of the hydrogen atom transfer from the phenolic hydroxyl to the neutral oxygen radicals to generate a more stable

[†] Institut d'Investigacions Químiques i Ambientals.
[‡] Universitat de Barcelona.
[§] Institut de Ciència de Materials.

(1) Halliwell, B.; Gutteridge, J. M. C. *Free Radicals in Biology and Medicine*, 2nd ed.; Clarendon Press: Oxford, 1989.

(2) (a) Aruoma, O. I.; Murcia, A. M.; Butler, J.; Halliwell, B. *J. Agric. Food Chem*. **1993**, *41*, 1880−1885. (b) Halliwell, B.; Asechbach, R.; Coliger, J.; Aruoma, O. I. *Food Chem. Toxicol.* **1995**, *33*, 601−617. (c) Rice-Evans, C. A.; Miller, N. J.; Paganga, G. *Free Radical Biol. Med.* **1996**, *20*, 933−956. (d) Yokozawa, T.; Chen, C. P.; Dong, E.; Tanaka, T.; Nonaka, G.-I.; Nishioka, I. *Biochem. Pharmacol*. **1998**, *56*, 213−222.

(3) (a) Harman, D. *J. Gerontol*. **1956**, *2*, 298. (b) Harman, D. *Proc. Natl. Acad. Sci. U.S.A*. **1981**, *78*, 7124−7128. (c) Burton, G. W.; Ingold, K. U. *Acc. Chem. Res*. **1986**, *19*, 194−201. (d) Ozawa, T. *Physiol. Rev*. **1997**, *77*, 425−464. (e) Katiyar, S. K.; Mukhtar, H. J. *Cell. Biochem. Suppl*. **1997**, *27*, 59−67. (f) Beckman, K. B.; Ames, B. N. *Physiol. Rev*. **1998**, *78*, 547−581. (g) Bowry, V. W.; Ingold, K. U. *Acc. Chem. Res*. **1999**, *32*, 27−34. (h) Fremont, L. *Life Sci.* **2000**, *66*, 663−673. (i) Yang, C. S.; Landau, J. M.; Huang, M. T.; Newmark, H. L. *Annu. Rev. Nutr*. **2001**, *21*, 381−406. (j) Murphy, K. J.; Chronopoulos, A. K.; Singh, I.; Francis, M. A.; Moriarty, H.; Pike, M. J.; Turner, A. H.; Mann, N. J.; Sinclair, A. J. *Am. J. Clin. Nutr*. **2003**, *77*, 1466−1473.

10.1021/jo062665a CCC: $37.00
Published on Web 04/17/2007

SCHEME 1

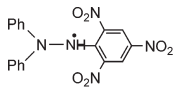

DPPH

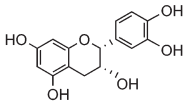

(−)-epicatechin (Ec)

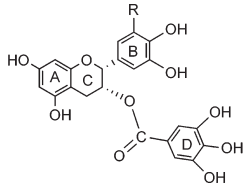

R=H: (−)-epicatechin-3-*O*-gallate (EcG)

R=OH: (−)-epigallocatechin-3-*O*-gallate (EgcG)

phenoxyl radical. The other possible mechanism involves an electron transfer from the polyphenol to the ROS. In general, the ability of polyphenols to donate hydrogen atoms is closely related to their capacity to transfer electrons.[6] This electron-transfer capacity may not be always beneficial since some catechins with low oxidation potentials may end up being pro-oxidant. In what is known as redox cycling, they are able to transfer an electron to oxygen and generate the superoxide radical, a very active radical which is enzymatically converted into hydrogen peroxide.[7,8] Moreover, the super oxide radical appears to mediate apoptosis (programmed cell death).[9] The key structural features determining the chemical reactivity and biological activity of catechins are the catechol or pyrogallol moieties on ring B and the gallate (benzoylic pyrogallol) on ring D (Scheme 1). Pyrogallol appears to be more reactive than catechol,[10] and the gallate moiety may mediate some key cancer related biological events such as inhibition of the proteasome[11] and of other enzymic domains.[12]

One of the most extensively used methods to evaluate the antioxidation activity of polyphenols is the reduction of the stable radical 2,2-diphenyl-1-picrylhydrazyl (DPPH).[13] The mechanism of the reduction depends on the nature of polyphenol and the solvent. These reactions have been largely admitted to occur by hydrogen atom abstraction, although recently some authors have shown that in hydroxylic solvents they can proceed from an electron transfer of the phenolate anion, in equilibrium with its molecular counterpart, to the DPPH radical.[14] Moreover, an electron transfer from the neutral species in polyphenols with very low oxidation potential values cannot be ruled out in some cases.[15]

We have been engaged for some time in the synthesis and evaluation of the antioxidant properties of new derivatives of catechins, particularly flavanols conjugated with thiols.[16] We have measured both H-atom donation and electron-transfer capacities in catechins and found that the electron-transfer capacity may be directly related to the ability of these polyphenols to induce cellular apoptosis.[17] Because the DPPH test is not capable of differentiating hydrogen donation from electron

(4) (a) Harbone, J. B. *The Flavonoids: Advances in Research Since 1986*; Chapman and May: London, 1994. (b) Prieur, C.; Rigaud, J.; Cheynier, V.; Moutounet, M. *Phytochemistry* **1994**, *36*, 781−784. (c) Jovanovic, S. V.; Steenken, S.; Tosic, M.; Marjanovic, B.; Simic, M. G. *J. Am. Chem. Soc*. **1994**, *116*, 4846−4851. (d) Souquet, J.-M.; Cheynier, V.; Brossaud, F.; Moutounet, M. *Phytochemistry* **1996**, *43*, 509−512. (e) Yang, C. S.; Lee, M.-J.; Chen, L.; Yang, G. *Environ. Health Perspect.* **1997**, *105 Suppl 4*, 971−976. (f) Soleas, G. J.; Diamandis, E. P.; Goldberg, D. M. *J. Clin. Lab. Anal.* **1997**, *11*, 287−313. (g) Harbowy, M. E.; Balentine, D. A. *Crit. Rev. Plant Sci.* **1997**, *16*, 415−480. (h) Diplock, A. T.; Charleux, J. L.; Crozier-Willi, G.; Kok, F. J.; Rice-Evans, C.; Roberfroid, M.; Stahl, W.; Viña-Ribes, J. *Br. J. Nutr.* **1998**, *80 Suppl 1*, S77−S112. (i) Bravo, L. *Nutr. Rev.* **1998**, *56*, 317−333. (j) Yang, G. Y.; Liao, J.; Kim, K.; Yurkow, E. J.; Yang, C. S. *Carcinogenesis* **1998**, *19*, 611−616. (k) Ruf, J. C. *Drug Exp. Clin. Res.* **1999**, *25*, 125−131. (l) Packer, L.; Rimbach, G.; Virgili, F. *Free Radical Biol. Med.* **1999**, *27*, 704−724. (m) Cheynier, V.; Souquet, J.-M.; Le Roux, E.; Guyot, S.; Rigaud, J. *Methods Enzymol.* **1999**, *299*, 178−184. (n) Souquet, J. M.; Labarbe, B.; LeGuerneve, C.; Cheynier, V.; Moutounet, M. *J. Agric. Food Chem.* **2000**, *48*, 1076−1080.

(5) (a) Avila, D. V.; Ingold, K. U.; Luszytyk, J.; Green, W. H.; Procopio, D. R. *J. Am. Chem. Soc*. **1995**, *117*, 2929−2930. (b) Banks, J. T.; Ingold, K. U.; Luszytyk, J. *J. Am. Chem. Soc*. **1996**, *118*, 6790−6791. (c) McFaul, P. A.; Ingold, K. U.; Luszytyk, J. *J. Org. Chem*. **1996**, *61*, 1316−1321. (d) Valgimigli, L.; Banks, J. T.; Ingold, K. U.; Luszityk, J. *J. Am. Chem. Soc*. **1995**, *117*, 9966−9971. (e) Valgimigli, L.; Banks, J. T.; Ingold, K. U.; Luszityk, J. *J. Am. Chem. Soc*. **1996**, *118*, 3545−3549. (f) Valgimigli, L.; Banks, J. T.; Luszytyk, J. U.; Ingold, K. U. *J. Org. Chem*. **1999**, *64*, 3381−3383. (g) Snelgrove, D. W.; Luszytyk, J.; Banks, J. T.; Mulder, P.; Ingold, K. U. *J. Am. Chem. Soc*. **2001**, *123*, 469−477. (h) Foti, M. C.; Barclay, L. R. C.; Ingold, K. U. *J. Am. Chem. Soc*. **2002**, *124*, 12881−12888. (i) Foti, M. C.; Ingold, K. U.; Luszytyk, J. *J. Am. Chem. Soc*. **1994**, *116*, 9440−9447. (j) Barclay, L. R. C.; Edwards, C. E.; Vinqvist, M. R. *J. Am. Chem. Soc*. **1999**, *121*, 6226−6231. (k) Foti, M. C.; Ruberto, G. *J. Agric. Food Chem*. **2001**, *49*, 342−348. (l) Jovanovic, S. V.; Jancovic, I.; Josimovic, L. *J. Am. Chem. Soc*. **1992**, *114*, 9018−9021. (m) Nakanishi, I.; Miyazaki, K.; Shimada, T.; Iizuka, Y.; Inami, K.; Mochizuki, M.; Urano, S.; Okuda, H.; Ozawa, T.; Fukuzumi, S.; Ikota, N.; Fukuhara, K. *Org. Biomol. Chem.* **2003**, *1*, 4085−4088.

(6) (a) Burton, G. W.; Doba, T.; Gabe, E. J.; Hughes, L.; Lee, F. L.; Prasad, L.; Ingold, K. U. *J. Am. Chem. Soc*. **1985**, *107*, 7053−7065. (b) Pratt, D. A.; DiLabio, G. A.; Brigati, G.; Pedulli, G. F.; Valgimigli, L. *J. Am. Chem. Soc*. **2001**, *123*, 4625−4626.

(7) Kondo, K.; Kurihara, M.; Miyata, N.; Suzuki, T.; Toyoda, M. *Arch. Biochem. Biophys*. **1999**, *362*, 79−86.

(8) Long, L. H.; Clement, M. V.; Halliwell, B. *Biochem. Biophys. Res. Commun*. **2000**, *273*, 50−53.

(9) (a) Cai, J.; Jones, D. P. *J. Biol. Chem*. **1998**, *273*, 11401−11404. (b) Valko, M.; Leibfritz, D.; Moncol, J.; Cronin, M. T. D.; Mazur, M.; Telser, J. *Int. J. Biochem. Cell Biol.* **2007**, *39*, 44−84.

(10) Kondo, K.; Kurihara, M.; Miyata, N.; Suzuki, T.; Toyoda, M. *Free Radical Biol. Med.* **1999**, *27*, 855−863.

(11) Nam, S.; Smith, D. M.; Dou, Q. P. *J. Biol. Chem*. **2001**, *276*, 13322−13330.

(12) (a) Wang, X.; Song, K.-S.; Guo, Q.-X.; Tian, W.-X. *Biochem. Pharmacol*. **2003**, *66*, 2039−2047. (b) Sah, J. F.; Balasubramanian, S.; Eckert, R. L.; Rorke, E. A. *J. Biol. Chem*. **2004**, *279*, 12755−12762.

(13) (a) Blois, M. S. *Nature* **1958**, *181*, 1199−1200. (b) Brand-Williams, W.; Cuvelier, M. E.; Berset, C. *Lebensm.-Wiss. Technol.* **1995**, *28*, 25. (c) Sanchez-Moreno, C.; Larrauri, J. A.; Saura-Calixto, F. *J. Sci. Food Agric*. **1998**, *76*, 270−276. (d) Goupy, P.; Hugues, M.; Boivin, P.; Amiot, M. J. *J. Sci. Food Agric*. **1999**, *79*, 1625−1634.

(14) (a) Litwinienko, G.; Ingold, K. U. *J. Org. Chem*. **2003**, *68*, 3433−3438. (b) Foti, M. C.; Daquino, C.; Geraci, C. *J. Org. Chem*. **2004**, *69*, 2309−2314. (c) Litwinienko, G.; Ingold, K. U. *J. Org. Chem.* **2004**, *69*, 5888−5896. (d) Musialik, M.; Litwinienko, G. *Org. Lett*. **2005**, *7*, 4951−4954. (e) Litwinienko, G.; Ingold, K. U. *J. Org. Chem*. **2005**, *70*, 8982−8990. (f) Daquino, C.; Foti, M. C. *Tetrahedron* **2006**, *62*, 1536−1547.

(15) Nakanishi, I.; Kawashima, T.; Ohkubo, K.; Kanazawa, H.; Inami, K.; Mochizuki, M.; Fukuhara, K.; Okuda, H.; Ozawa, T.; Itoh, S.; Fukuzumi, S.; Ikota, N. *Org. Biomol. Chem*. **2005**, *3*, 626−629.

(16) (a) Torres, J. L.; Bobet, R. *J. Agric. Food Chem*. **2001**, *49*, 4627−4634. (b) Torres, J. L.; Lozano, C.; Julià, L.; Sánchez-Baeza, F. J.; Anglada, J. M.; Centelles, J. J.; Cascante, M. *Bioorg. Med. Chem*. **2002**, *10*, 2497−2509.

transfer, we introduced the tris(2,4,6-trichloro-3,5-dinitrophenyl)methyl radical (HNTTM) as a chemical sensor of the electron-transfer mechanism.[18]

Organic radicals of the 2,4,6-(trichlorophenyl)methyl (TTM)[19] and perchlorotriphenylmethyl (PTM)[20] series are very stable species, both in the solid state or in solution due to the presence of the very bulky polychlorophenyl substituents around the trivalent carbon atom. However, they are very active in redox processes reacting with electron-donating substrates by electron-transfer reactions. The corresponding reduced species, colored anions, are also very stable in solution, being characterized by the strong absorption in the visible spectrum. The recently reported HNTTM radical is a strong oxidant able to oxidize catechol and natural and synthetic polyphenols incorporating catechol in their structures, such as (−)-epicatechin (Ec). These redox reactions involve electron transfer from polyphenols to the radical. Two reasons support this assertion:[18] (i) the electronic spectra of mixtures of catechol and HNTTM radical display peaks of both the radical and the corresponding negatively charged species, $HNTTM^-$; and (ii) HNTTM radical is quantitatively recovered from a boiling toluene solution after 24 h, while DPPH abstracts hydrogen from toluene.[21] The redox potentials of the radicals of the TTM and PTM series essentially depend on the electron-withdrawing or -donating power of the *meta*- and/or *para*-substituents, so that in such a way a collection of radicals with different redox potentials can be designed and prepared.

None of the currently available methods for testing the radical scavenging activity is able to discriminate between the three kinds of redox-active moieties mentioned (catechol, pyrogallol, and gallate). Stable radicals with lower redox potentials are required. To modulate the oxidant properties of the radicals of the TTM and PTM series, we have decided to reduce the number of the electron-withdrawing nitro groups in the molecule. Now we report on the synthesis of tris(2,3,5,6-tetrachloro-4-nitrophenyl)methyl (TNPTM) radical. The stability of this new radical is similar to that of the radicals of the PTM series, and its molecular structure has been elucidated by X-ray analysis. The redox potential for the reduction of TNPTM has been determined by cyclic voltammetry, and its value has been compared to those of other radicals of the same series. TNPTM radical is reduced by pyrogallol (1,2,3-trihydroxybenzene) in a protic medium and not by catechol. The final goal of this research is to provide new chemical tools to classify the polyphenols as a function of their ability to transfer electrons.

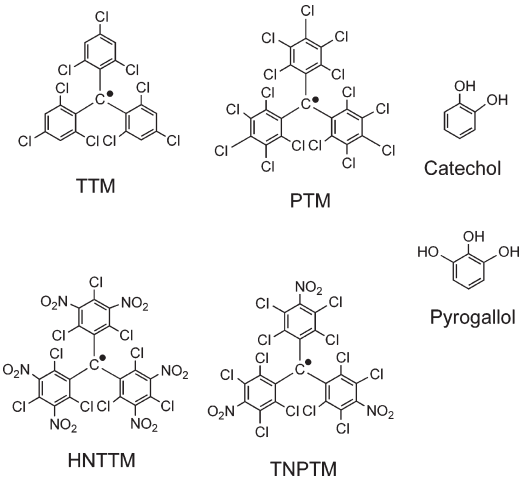

Results and Discussion

Exhaustive nitration of tris(2,3,5,6-tetrachlorophenyl)methane[22] with fuming (100%) nitric acid yielded tris(2,3,5,6-tetrachloro-4-nitrophenyl)methane with good yield. Treatment of this hydrocarbon with a slight excess of an aqueous solution of tetrabutylammonium hydroxide in THF gave a stable blue solution of the carbanion [λ_{max} nm (ϵ, dm mol^{-1} cm^{-1}), 595 (7230) in THF solution] which was oxidized with an excess of 2,3,5,6-tetrachloroquinone to tris(2,3,5,6-tetrachloro-4-nitrophenyl)methyl (TNPTM) radical (Scheme 2).

TNPTM radical, stable in the solid state and in solution in the dark, showed an electronic absorption spectrum in $CHCl_3$ [λ_{max} nm (ϵ, dm mol^{-1} cm^{-1}), 378 (17 000), 493 (870), 549 (630)], characteristic of the radicals of the PTM series.[20] This radical crystallizes in nice dark red crystals from mixtures of $CHCl_3$/hexane. A perspective view of the molecular structure with the atom numbering is shown in Figure 1. The symmetry of the unit cell is *C*2/*c*, and the asymmetric unit contains 22 atoms of the molecule. The straight line defined by N2, C11, C8, and C7 atoms divides the molecule in two equally spaced moieties. This is why the numbering of the atoms is the same in each moiety. All of the distances and angles between the central carbon atom C(7) and the aromatic carbons C(4), C(4), and C(8) are in good agreement with a sp^2 hybridization of the C(7), and therefore, C(7) and bridgehead atoms lie in the same *P*4 plane. Phenyl rings are twisted around this plane with angles shown in Table 1 due to the presence of six chlorine atoms *ortho* to C(7), and the molecule adopts a propeller-like conformation with an approximate 3-fold D_3 symmetry. Conjugation of the aromatic rings with nitro substituents is practically excluded because the presence of vicinal chlorines in an *ortho*-position forces the NO_2 substituents out of the phenyl planes with angles between the planes close to 90° (Table 1).

Cyclic voltammograms of radical TNPTM were obtained in CH_2Cl_2 solution (~10^{-3} M) containing tetra-*n*-butylammonium perchlorate (TBAP) (0.1 M) as supporting electrolyte on platinum wire as the working electrode using a saturated calomel electrode (SCE) as the reference electrode (see Figure S1).

(17) (a) Lozano, C.; Torres, J. L.; Juliá, L.; Jiménez, A.; Centelles, J. J.; Cascante, M. *FEBS Lett.* **2005**, *579*, 4219−4225. (b) Lozano, C.; Juliá, L.; Jiménez, A.; Touriño, S.; Centelles, J. J.; Cascante, M.; Torres, J. L. *FEBS J.* **2006**, *273*, 2475−2486.

(18) (a) Torres, J. L.; Varela, B.; Brillas, E.; Juliá, L. *Chem. Commun.* **2003**, 74−75. (b) Jiménez, A.; Selga, A.; Torres, J. L.; Juliá, L. *Org. Lett.* **2004**, *6*, 4583−4586.

(19) (a) Armet, O.; Veciana, J.; Rovira, C.; Riera, J.; Castañer, J.; Molins, E.; Rius, J.; Miravitlles, C.; Olivella, S.; Brichfeus, J. *J. Phys. Chem.* **1987**, *91*, 5608−5616. (b) Carilla, J.; Fajarí, Ll.; Juliá, L.; Riera, J.; Viadel, Ll. *Tetrahedron Lett.* **1994**, *35*, 6529−6532. (c) Teruel, L.; Viadel, Ll.; Carilla, J.; Fajarí, Ll.; Brillas, E.; Sañé, J.; Rius, J.; Juliá, L. *J. Org. Chem.* **1996**, *61*, 6063−6066. (d) Carilla, J.; Fajarí, Ll.; Juliá, L.; Sañé, J.; Rius, J. *Tetrahedron* **1996**, *52*, 7013−7024. (e) Gamero, V.; Velasco, D.; Brillas, E.; Juliá, L. *Tetrahedron Lett.* **2006**, *47*, 2305−2309.

(20) (a) Ballester, M.; Riera, J.; Castañer, J.; Badía, C.; Monsó, J. M. *J. Am. Chem. Soc.* **1971**, *93*, 2215−2225. (b) Ballester, M. *Acc. Chem. Res.* **1985**, *18*, 380−387 and references cited therein.

(21) Lorimer, J. P.; Kershaw, D.; Mason, T. J. *J. Chem. Soc., Faraday Trans.* **1995**, *91*, 1067−1074.

(22) Ballester, M.; Riera, J.; Castañer, J.; Rovira, C.; Armet, O. *Synthesis* **1986**, 64−66.

SCHEME 2

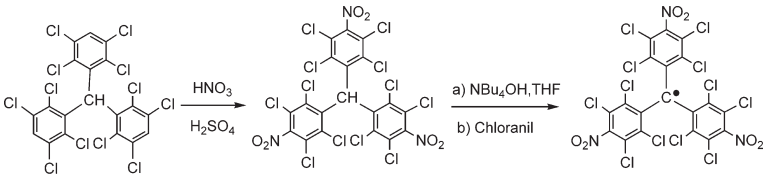

TNPTM

Radical TNPTM exhibits a quasi-reversible reduction process (difference between the anodic and cathodic peak potentials ($E^a_p - E^c_p$) > 60 mV, with $E^a_p = 0.26$ V and $E^c_p = 0.14$ V at 100 mV s^{-1}), attributed to the addition of one electron to the trivalent carbon-centered radical. The value of its standard potential ($E°$) is displayed in Table 2 along with those of radicals TTM, PTM, and HNTTM determined under the same conditions. The $E°$ values for the reduction of these stable radicals increase in following the sequence: TTM < PTM < TNPTM < HNTTM. Although TNPTM radical has a low positive $E°$ value, the highest positive standard potential corresponds to HNTTM radical, a consequence of the strong electron acceptor properties of the phenyl rings. It is also remarkable the significant influence of a *para*-NO_2 group in relation to that of a *para*-chlorine on the $E°$ values of TNPTM and PTM. In spite of the restricted conjugation of NO_2 with the phenyl rings, substitution of chlorine by NO_2 resulted in a positive shift (0.43 V) of $E°$. Results of Table 2 show that the standard potentials for TNPTM and HNTTM radicals are slightly shifted to lower positive values when the solvent is $CHCl_3$/MeOH (2:1).

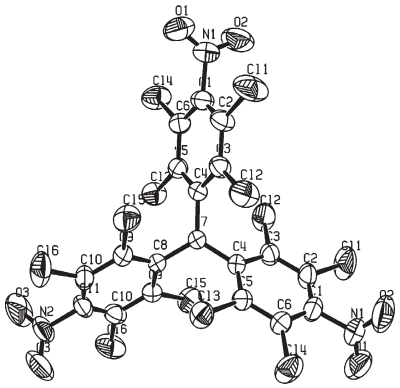

FIGURE 1. A perspective view of the structure of the tris(2,3,5,6-tetrachloro-4-nitrophenyl)methyl radical (TNPTM) with the atom numbering. Angles between planes are given in Table 1.

TABLE 1. Angles between Planes[a] of the Molecular Structure of TNPTM Radical

P1−P5	P2−P6	P1−P4	P3−P4	P2−P4
82.06	83.30	50.41	50.41	54.07

[a] Planes are defined as follows: P1, C1C2C3C4C5C6; P2, C8C9C10C9C8; P3, symmetry-related to P1; P4, C8C7C4C4; P5, N1O1O2; P6, N2O3O3.

TABLE 2. Electrochemical Parameters for the Oxidation of Catechol and Pyrogallol and for the Reduction of Radicals TTM, PTM, TNPTM, and HNTTM in Organic Solution (10^{-3} M) with 0.1 M Bu_4NClO_4 on Pt at a Scan Rate of 100 mV s^{-1}

	E^a_p/V[a] (E^a_p/V, anion)[b]	$E°$/V[c] (E^c_p)[d]	$E°$/V[e] ($E^a_p - E^c_p$/mV)
catechol	1.00 (0.25)		
pyrogallol	0.82 (0.06)		
TTM			−0.66 (100)
PTM			−0.15 (150)
TNPTM		0.20 (0.14)	0.28 (123)
HNTTM		0.55 (0.50)	0.58 (90)

[a] Anodic peak potentials in $CHCl_3$/MeOH (2:1) solution (10^{-3} M) with 0.1 M Bu_4NClO_4 on Pt. [b] Anodic peak potentials of catechol and pyrogallol with an excess of tetrabutylammonium hydroxide of 4 and 3 mM, respectively. [c] Redox potentials in $CHCl_3$/MeOH (2:1). [d] Cathodic peak potentials in $CHCl_3$/MeOH (2:1). [e] Standard redox potentials in CH_2Cl_2 solution.

TABLE 3. Experimental and Calculated Hyperfine Coupling Constants in Gauss for TNPTM Radical

atom	obsd hfc const	calcd hfc const
α-^{13}C	32.25	27.04
bridgehead-^{13}C	12.88	−11.23, −11.45, −11.10
ortho-^{13}C	10.88	9.42, 10.01, 9.62, 10.57, 10.60, 10.19
N	∼0.28	−0.23, −0.23, −0.19

The electron paramagnetic resonance (EPR) spectrum of a degassed and diluted (∼10^{-3} M) solution of radical TNPTM in CH_2Cl_2 at room temperature exhibited a broad and single line (peak to peak line width, $\Delta H_{pp} = 1.63$ G) centered at $g = 2.0026$ (free electron g factor $g_e = 2.0023$; see Figure S12). At higher gain, the isotropic coupling with the ^{13}C nuclear spins (^{13}C atom, natural abundance 1.1%) of the α-carbon, three bridgehead carbons, and six *ortho*-carbons appear as small lines in the sides of the main spectrum, and the values of the hyperfine coupling constants are shown in Table 3. At low temperature (193 K), the main line in the spectrum becomes narrower ($\Delta H_{pp} = 0.23$ G) since the signal amplitude is inversely proportional to the temperature and showed a not very defined septet of lines due to the weak coupling of the free electron with three nitrogens (Table 3 and Figure S13).

The spin density calculations for TNPTM radical were performed by the UB3LYP method with the EPR-II basis set for carbon, nitrogen, and oxygen atoms, and the D95/(d) basis set for chlorine atoms using the geometry determined by X-ray crystallography.[23] The total atomic spin densities are illustrated in Figure 2, and the calculated hyperfine coupling constants for the ^{13}C and nitrogen atoms are compared with the observed ones in Table 3. The calculated values are in good agreement with the observed ones. Figure 2 shows that the spin density resides mainly on the trivalent carbon atom due to the large twisting of the phenyl rings around this carbon atom. Values of the spin density on nitrogens are negligibly small due also to the large twisting (practically 90°) of the NO_2 plane around the phenyl ring.

The reactivity of catechol and pyrogallol with TNPTM radical was measured on the bench from equimolecular solutions of

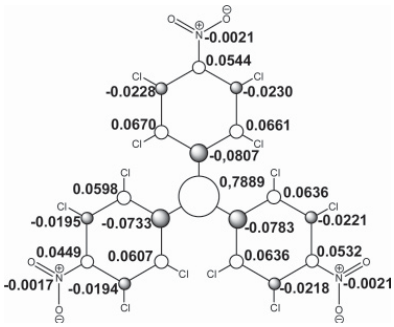

FIGURE 2. Total atomic spin densities of TNPTM radical.

TABLE 4. Reactivity of Catechol and Pyrogallol with TNPTM Radical in $CHCl_3$ and $CHCl_3$/MeOH (2:1) (Equimolecular Solutions)[a]

Catechol		Pyrogallol		
solvent	TNPTM radical (%)[b]	solvent	TNPTM radical (%)[b]	αHTNPTM (%)
$CHCl_3$	96	$CHCl_3$	100	
$CHCl_3$/MeOH	92	$CHCl_3$/MeOH	48	52

[a] Initial concentration of polyphenol and TNPTM radical = 1.26 mM. [b] Recovered radical.

polyphenol and radical in a polar solvent, $CHCl_3$, and in a polar and hydroxylic solvent, $CHCl_3$/MeOH (2:1) (Table 4). The tris-(2,3,5,6-tetrachloro-4-nitrophenyl)methane (αHTNPTM) and the recovered TNPTM radical were identified by infrared and electronic spectra. No other species resulting from any coupling between TNPTM radical and polyphenol were found in the reaction mixture. Three important points come from an analysis of Table 4: (i) TNPTM radical is stable in the presence of catechol and pyrogallol in $CHCl_3$ solution; (ii) TNPTM radical is stable with catechol in $CHCl_3$/MeOH (2:1), but it slowly reacts with pyrogallol; and (iii) the only reaction product with pyrogallol in $CHCl_3$/MeOH (2:1) is αHTNPTM. As a general test of stability established for the radicals of the PTM series,[20] TNPTM radical does not abstract hydrogen from any H-donating solvents since it can be recovered practically in a quantitative yield from a boiling solution in toluene after 24 h. Moreover, the reduction of TNPTM radical with ascorbic acid, similarly to that reported for the PTM radical,[24] proceeds through its anion, detected by visible spectroscopy, as a stable intermediate before being protonated to αHTNPTM. Consequently, TNPTM is only active in electron-transfer processes.

Cyclic voltammograms of catechol and pyrogallol were carried out in $CHCl_3$/MeOH (2:1) solution (10^{-3} M) containing TBAP (0.1 M) as supporting electrolyte on platinum wire as the working electrode using a SCE as the reference electrode to know the electrochemical parameters of both polyphenols (see Figures S2 and S5). The anodic peak potentials of catechol and pyrogallol shown in Table 2 are not positive enough to reduce TNPTM radical in $CHCl_3$/MeOH (2:1); however, in a hydroxylated solvent such as $CHCl_3$/MeOH (2:1), polyphenols are partially ionized to their anionic species according to the equilibrium:

$$\mathrm{Ph(OH)}_n + \mathrm{MeOH} \rightleftharpoons \mathrm{Ph(OH)}_{n-1}\mathrm{O}^{\ominus} + \mathrm{MeOH}_2^{\oplus}$$

Depending on the oxidation potentials of the anionic species, they will be involved or not in the reduction of the TNPTM radical by means of an electron transfer, according to the following process:

$$\mathrm{Ph(OH)}_{n-1}\mathrm{O}^{\ominus} + \mathrm{TNPTM} \rightarrow \mathrm{Ph(OH)}_{n-1}\mathrm{O}^{\bullet} + \mathrm{TNPTM}^{\ominus}$$

In our particular case, the anion of the pyrogallol and not that of the catechol was able to react with TNPTM radical. Cyclic voltammograms of catechol and pyrogallol were then carried out in the presence of an excess of tetrabutylammonium hydroxide to determine the anodic peak potentials of their corresponding phenolate anions (see Figures S3, S4, S6, and S7). These values, depicted in Table 2, show a dramatic shift of 0.75 and 0.76 V for catechol and pyrogallol, respectively, with regard to those of the neutral polyphenols. As it is known, an electrochemical reaction is thermodynamically allowed when the difference between the anodic peak potential (E_p^a) of reductor and cathodic peak potential (E_p^c) of oxidant is a negative value ($E_p^a - E_p^c < 0$). In our particular case, data from Table 2 show that $E_p^a - E_p^c = 0.11$ V for the TNPTM−catechol couple and $E_p^a - E_p^c = -0.08$ V for the TNPTM−pyrogallol one. Consequently, the reaction of TNPTM with catechol at room temperature in $CHCl_3$/MeOH (2:1) is thermodynamically not allowed, whereas the reaction of the same radical with pyrogallol is thermodynamically allowed. This is consistent with the negative free energy change of electron transfer from pyrogallol to TNPTM radical ($\Delta G_{et} = -(E_p^a - E_p^c) \times F = -7719$ J mol^{-1}, where F is the Faraday constant (96 487 C mol^{-1})).

Kinetic measurements of the electron-transfer reaction between pyrogallol and TNPTM radical were performed to determine the rate constant and the stoichiometry of the reaction. The course of the reaction was monitored by electronic spectroscopy by recording the decay of the TNPTM absorbance maximum in the visible ($\lambda_{max} = 378$ nm in $CHCl_3$/MeOH (2:1), molar absorptivity, $\epsilon = 21\,600$ dm^3 mol^{-1} cm^{-1}) as a consequence of the addition of pyrogallol to a TNPTM solution. The experiments were carried out in $CHCl_3$/MeOH (2:1) solutions with two different TNPTM/pyrogallol molar ratios of 10:1 and 5:1 and a long reaction time (48 h) to ensure the complete consumption of pyrogallol (see Figures S8 and S10). The n values of the stoichiometry of the polyphenol were calculated using eq 1:

$$n = \frac{A_0 - A_f}{\Delta\epsilon \cdot c} \quad (1)$$

(23) All DFT calculations were carried out using Gaussian 03Frisch, M. J.; Trucks, G. W.; Schlegel, H. B.; Scuseria, G. E.; Robb, M. A.; Cheeseman, J. R.; Montgomery, J. A., Jr.; Vreven, T.; Kudin, K. N.; Burant, J. C.; Millam, J. M.; Iyengar, S. S.; Tomasi, J.; Barone, V.; Mennucci, B.; Cossi, M.; Scalmani, G.; Rega, N.; Petersson, G. A.; Nakatsuji, H.; Hada, M.; Ehara, M.; Toyota, K.; Fukuda, R.; Hasegawa, J.; Ishida, M.; Nakajima, T.; Honda, Y.; Kitao, O.; Nakai, H.; Klene, M.; Li, X.; Knox, J. E.; Hratchian, H. P.; Cross, J. B.; Adamo, C.; Jaramillo, J.; Gomperts, R.; Stratmann, R. E.; Yazyev, O.; Austin, A. J.; Cammi, R.; Pomelli, C.; Ochterski, J. W.; Ayala, P. Y.; Morokuma, K.; Voth, G. A.; Salvador, P.; Dannenberg, J. J.; Zakrzewski, V. G.; Dapprich, S.; Daniels, A. D.; Strain, M. C.; Farkas, O.; Malick, D. K.; Rabuck, A. D.; Raghavachari, K.; Foresman, J. B.; Ortiz, J. V.; Cui, Q.; Baboul, A. G.; Clifford, S.; Cioslowski, J.; Stefanov, B. B.; Liu, G.; Liashenko, A.; Piskorz, P.; Komaromi, I.; Martin, R. L.; Fox, D. J.; Keith, T.; Al-Laham, M. A.; Peng, C. Y.; Nanayakkara, A.; Challacombe, M.; Gill, P. M. W.; Johnson, B.; Chen, W.; Wong, M. W.; González, C.; Pople, J. A. *Gaussian 03*, revision C.02; Gaussian, Inc.: Wallingford, CT, 2004.

(24) Ballester, M.; Riera, J.; Castañer, J.; Casulleras, M. *Tetrahedron Lett.* **1978**, 643−644.

TABLE 5. Observed Rate Constants and Stoichiometric Factors for the Reaction of TNPTM with Pyrogallol in $CHCl_3$/MeOH (2:1)

TNPTM/pyrogallol molar ratio[a]	k_1 (M^{-1} s^{-1})	n[b]
9.35:1	0.282 ± 0.011	2.6
5.01:1	0.288 ± 0.010	2.6

[a] Initial concentrations = 123.66 and 13.23 μM (molar ratio, 9.35:1), and 129.47 and 25.7 μM (molar ratio, 5.04:1) for TNPTM radical and pyrogallol, respectively. [b] Moles of reduced radical per mole of pyrogallol.

TABLE 6. Reactivity of Pyrogallol with TNPTM Radical[a] in $CHCl_3$/MeOH (2:1)

[pyrogallol] (μM)	9.7	13.5	18.0	27.0
Radical inhibition[b] (%)	13	20	26	35

[a] Initial concentration of TNPTM = 130.99 μM. [b] Results explained in the text.

where A_0 is the initial absorbance, A_f is the final absorbance, c is the initial concentration of the oxidant, and $\Delta\epsilon$ is the difference between the molar absorptivity of the TNPTM radical and that of its reduced α*H*TNPTM. Values of n for the two experiments are depicted in Table 5. A simple kinetic model reported by Dangles et al. was used to estimate the rate constant of the electron transfer from pyrogallol to TNPTM radical.[25] As the stoichiometry of this reaction is $n \sim 2$, 1 mol of pyrogallol is capable of reducing about 2 mol of TNPTM radical. Note that this method assumes that the real concentration of the reductant transferring one electron to TNPTM radical with the same rate constant is, in a rough estimation, twice the concentration of pyrogallol in a second-order kinetics. Therefore, the rate of such reaction is defined as eq 2, and the values of k_1 calculated from the integrated eq 3 are shown in Table 5 (see Figures S9 and S11).

$$-\mathrm{d[TNPTM]}/\mathrm{d}t = k \times 2[\text{pyrogallol}][\text{TNPTM}] = k_1[\text{pyrogallol}][\text{TNPTM}] \quad (2)$$

$$\ln\frac{1 - A_f/A}{1 - A_f/A_0} = -\frac{k_1 c}{A_0/A_f - 1}\,t \quad (3)$$

An alternative method to estimate the stoichiometry of the reaction between pyrogallol and TNPTM radical is based on the determination of the parameter EC_{50}, defined as the amount of polyphenol necessary to decrease the initial concentration of TNPTM radical by 50%. In these experiments, four solutions of polyphenol, at different low concentrations, and a great excess of TNPTM radical in $CHCl_3$/MeOH (2:1) were prepared and left in the dark for 48 h before measuring the absorbance at 378 nm of the unreacted TNPTM radical. The concentrations of the reduced radical with regard to that of the initial TNPTM radical are collected in Table 6. Figure 3 shows that they are linearly dependent on the concentration of the pyrogallol.

The EC_{50} value for pyrogallol is 36.6 μmol. Multiplying EC_{50} by 2 and dividing by the initial number of moles of TNPTM radical, we obtain a stoichiometric value for the reaction of 0.56. The inverse of this value, $n = 1.8$, represents the moles of radical reduced per mole of pyrogallol. This n value agrees with that obtained above from kinetic measurements (see Table 5).

(25) Goupy, P.; Dufour, C.; Loonis, M.; Dangles, O. *J. Agric. Food Chem.* **2003**, *51*, 615−622.

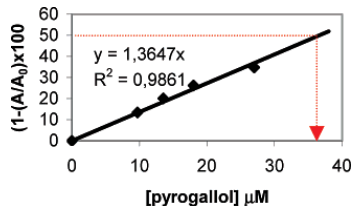

FIGURE 3. Reducing activity of pyrogallol with TNPTM radical in $CHCl_3$/MeOH (2:1) solutions (see Table 5). The x value marked in red is the EC_{50} one (36.6 μM).

Concerning the third point deduced from Table 4 pointed out above, the species derived from the reaction of pyrogallol with TNPTM radical is αHTNPTM. That is, only the compound resulting from the neutralization of the anion generated by electron transfer from pyrogallol is quantitatively obtained:

$$\text{TNPTM} \xrightarrow{1e} \text{TNPTM}^{\ominus} \xrightarrow{H^{\oplus}} \alpha H\text{TNPTM}$$

The mechanistic hypothesis involving any coupling reaction of the intermediate phenoxyl radical, derived from pyrogallol, to TNPTM can be ruled out. The stability of TNPTM radical in processes other than electron-transfer reactions is due to the steric hindrance around the trivalent carbon atom and the poor aromatic ring delocalization of the single electron. The X-ray analysis of the molecular structure of TNPTM radical shows that the phenyl rings are twisted around the plane of the trivalent sp^2 carbon atom with angles large enough to substantially reduce the conjugation. Moreover, the EPR spectrum of the radical (large value of the coupling of the single electron with the α-^{13}C atom) suggests that the spin density is mainly localized at the α-carbon. Consequently, since pyrogallol reacts exclusively by electron transfer with TNPTM radical, the stoichiometric value of 1.8 determined above indicates the total number of electrons transferred per molecule of pyrogallol. A mechanism suggested by the stoichiometry of the overall reaction can be as follows: one molecule of TNPTM reacts with one molecule of pyrogallol by electron transfer in the rate-limiting step of the overall reaction, and then the reaction intermediate, most probably a phenoxyl radical, reacts successively with a second molecule of the TNPTM radical.

In summary, as part of a research effort directed to obtain a collection of organic redox chemosensors of radical nature with the ability to classify polyphenols by their redox properties, we have prepared a new carbon-centered organic radical of the PTM series, the TNPTM radical, by a clean and easy synthetic method with good yield. The stability of this new radical is due to the steric hindrance of three bulky substituents around the trivalent carbon atom. This radical is stable in solution and cannot abstract hydrogens from H-donating reagents. It is only active in electron-transfer reactions, and therefore, it is a good candidate to measure the electron-donating capacity of natural and synthetic polyphenolic antioxidants. As the standard redox potential for the reduction of TNPTM radical to its anion is between those of PTM and HNTTM radicals, and its cathodic peak potential ranges between the anodic peak potentials for the oxidation of the anions of catechol and pyrogallol, TNPTM radical can selectively discriminate between the reducing properties of catechol and pyrogallol in a protic medium. The results presented are of interest because these simple polyphenols, which are part of the structure of more complex molecules,

determine the antioxidant/pro-oxidant character and the biological activities of natural and synthetic flavonoids.

Experimental Section

Tris(2,3,5,6-tetrachloro-4-nitrophenyl)methane. A mixture of tris(2,3,5,6-tetrachlorophenyl)methane[16] (0.503 mg) and fuming nitric acid (100%) (50 mL) was stirred at reflux (18 h) and then poured into an excess of water. The precipitate, separated by filtration and dried under reduced pressure, was chromatographed in silica gel eluting with $CHCl_3$ to give triphenylmethane (0.379 mg, 62%): IR (KBr) 1555 (s), 1345 (s), 1303 (m), 1131 (m), 882 (w), 784 (m), 757 (m), 730 (m), 664 (w), 567 (m) cm^{-1}; ^1H NMR (300 MHz, $CDCl_3$) δ 7.01 (s, 1H) ppm. Anal. Calcd for $C_{19}HCl_{12}N_3O_6$: C, 28.8; H, 0.1; Cl, 53.7; N, 5.3. Found: C, 28.9; H, 0.2; Cl, 53.7; N, 5.1.

Tris(2,3,5,6-tetrachloro-4-nitrophenyl)methyl (TNPTM) Radical. (a) Synthesis. An aqueous solution of tetrabutylammonium hydroxide (40%, 3.71 mL, 5.56 mmol) was added to a solution of tris(2,3,5,6-tetrachloro-4-nitrophenyl)methane (3.389 g, 4.28 mmol) in THF (50 mL) and stirred at 0 °C (2 h). Tetrachloro-*p*-quinone (1.473 g, 5.99 mmol) was added, and the mixture was stirred at 0 °C in an inert atmosphere and in the dark (30 min). The mixture was dried and purified by chromatography in silica gel eluting with hexane/$CHCl_3$ (3:1) to give radical TNPTM (1.638 g, 48%): IR (KBr) 1556 (s), 1344 (s), 1268 (w), 1225 (w), 1149 (w), 1134 (w), 1049 (w), 888 (w), 788 (m), 765 (m), 731 (m), 666 (w), 570 (m) cm^{-1}. Anal. Calcd for $C_{19}Cl_{12}N_3O_6$: C, 28.8; Cl, 53.7; N, 5.3. Found: C, 28.8; Cl, 54.0; N, 5.1.

(b) X-ray Analysis. Crystal and Intensity Data: $C_{19}Cl_{12}N_3O_6$, MW = 791.59, monoclinic, space group *C*2/*c*, a = 16.581(1) Å, b = 20.907(2) Å, c = 9.078(7)) Å, β = 95.87(3)°, V = 3130.47(23) Å^3, D_{calcd} = 1.748 g/cm^3, Mo Kα radiation, μ = 1.108 mm^{-1}, $F(000)$ = 1612. Crystal size: 0.38 × 0.24 × 0.15 mm^3; θ range for data collection, 1.60 to 30.00°. Index ranges $-23 < h < 23$, $0 < k < 29$, $-12 < l < 0$. Scan width is 0.80 + 0.50 tan(θ) and maximum final scan time is 90 s. Reflections collected, 4944; independent reflections, 4563. The cell parameters were determined from refinement of nine reflections using the CAD4 Express software.[26] Three standard reflections were measured every 3600 s to check for the intensity variation, and three more standards were measured every 55 reflections to check the crystal orientation. No intensity decay was recorded. Data reduction was completed with WINGX32.[27] **Solution and Refinement:** The structure was solved by direct methods using the origin-free modules sum function[28] and was refined by full-matrix least-squares on F^2 for all reflections using the SHELXL-93 program.[29] Data/restraints/parameters = 4563/0/191. Goodness-of-fit on F^2, 1.191. Final R indices = [$I > 2\sigma(I)$], $R1$ = 0.0776, $wR2$ = 0.2720. R indices (all data) = $R1$ = 0.0924, $wR2$ = 0.2720. The definition of the R values is $R1 = \sum||F_o| - |F_c||/\sum|F_o|$; $wR2 = [\sum w(F_o^2 - F_c^2)^2/\sum w(F_o^2)^2]^{1/2}$; $w = 1/[\sum\sigma(F_o^2)^2 + (0.0706P)^2 + 0.00P]$; $P = [\max(F_o^2,0) + 2F_c^2]/3$; GOF = $[(\sum w(F_o^2 - F_c^2))/(n - p)]^{1/2}$; n = number of reflections; p = number of parameters. Final shifts/esd were less than 0.01 in the last cycle (with convergence to zero), and the maximum and minimal residual electron densities in the final Fourier difference were 1.21 and −0.86 e/Å^3. The plot showing the perspective view of the molecule with thermal vibration ellipsoids was carried out with ORTEP32.[30]

Acknowledgment. Financial support for this research from the MEC (Spain) through Grant Nos. PB96-0836 and AGL2006-12210-C03-02, from the Catalonian DURSI through Grant No. 2005SGR00111, and from an associated contract with Greenlane Biodevelopments SL is gratefully acknowledged. We also thank the EPR service of the Institut d'Investigacions Químiques i Ambientals de Barcelona (CSIC) for recording the EPR spectra. The calculations carried out in this work have been done at the Centre de Supercomputació de Catalunya (CESCA), whose services are gratefully acknowledged.

Supporting Information Available: General methods of the Experimental Section, cyclic voltammograms for the reduction of TNPTM radical, and oxidation of catechol and pyrogallol in neat and basicified solvents (Figures S1−S7). Graphics for kinetics of TNPTM and pyrogallol (Figures S8−S11). Electron paramagnetic resonance spectra for TNPTM radical in CH_2Cl_2 at room temperature and 193 K (Figures S12 and S13). X-ray crystallographic data of molecular structure of tris(2,3,5,6-tetrachloro-4-nitrophenyl)-methyl (TNPTM) radical. This material is available free of charge via the Internet at http://pubs.acs.org.

JO062665A

(26) *CAD4-Express* operating Software, V. 5.1 Enraf-Nonius, Delft Instruments X-Ray Diffraction: Delft, The Netherlands, 1992.

(27) Farrugia, L. J. *J. Appl. Crystallogr.* **1999**, *32*, 837−838.

(28) Rius, J. *Acta Crystallogr.* **1993**, *A49*, 406−409.

(29) Sheldrick, J. *SHELXL-93*, a fortran-77 program for refinement of crystal structures from diffraction data; Institut für Anorg. Chemie: Göttingen, Germany 1993.

(30) Farrugia, L. J. *J. Appl. Crystallogr.* **1997**, *32*, 565.

JOC Article

Oxidant Activity of Tris(2,4,6-trichloro-3,5-dinitrophenyl)methyl Radical with Catechol and Pyrogallol. Mechanistic Considerations

Anna Carreras,[†] Isaac Esparbé,[‡] Enric Brillas,[‡] Jordi Rius,[§] Josep Lluís Torres,[†] and Luis Julià*,[†]

Departament de Química Biològica i Modelització Molecular, Institut de Química Avançada de Catalunya (CSIC), Jordi Girona 18-26, 08034 Barcelona, Spain, Departament de Química Física, Universitat de Barcelona, Martí Franquès 1-11, 08028 Barcelona, Spain, abd Institut de Ciència de Materials (CSIC), Campus de la U.A.B., 08193 Bellaterra, Spain

ljbmoh@cid.csic.es

Received November 18, 2008

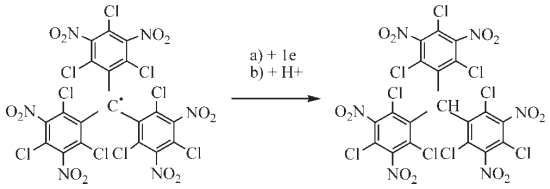

The reducing activity of simple polyphenols (PhOH), catechol and pyrogallol, is tested in different solvents in front of tris(2,4,6-trichloro-3,5-dinitrophenyl)methyl (HNTTM) radical, a stable organic free radical of the TTM series. HNTTM radical is very active in electron-transfer reactions to give a very stable anion. The standard potential for the reduction of HNTTM radical by cyclic voltammetry in different solvents is $E^\circ = 0.60 \pm 5$ V vs SCE. In hydroxylic solvents, the electron transfer is a very rapid process and the electron-donating species is the ionized PhO^-, whereas in nonpolar solvents, it is suggested that the electron transfer is facilitated by the formation of an intermediate complex between HNTTM and PhOH.

Introduction

Polyphenols show a remarkable ability to be involved in many oxidation−reduction reactions in chemistry and biology. Many of them are constituents of natural antioxidant extracts whose significant role is associated with the ability to scavenge reactive oxygen species. Among the different methods designed to measure the activity of the antioxidants,[1] stable radicals leading to color changes upon reaction with them have received great attention. The hydrazyl radical DPPH is a commercially available stable radical that has been widely used to test the antioxidant properties of natural and synthetic polyphenols.[1,2] In nonpolar and aprotic solvents, it is extensively accepted that the activity of DPPH is evaluated by its capacity to abstract hydrogen atoms of the antioxidants, and the ability of these compounds to release hydrogen atoms depends mainly on the stability of the generated radicals.[3] This is a free-radical reaction in which a hydrogen atom is transferred from the hydroxyl group, in the case of polyphenols as antioxidants, to the nitrogen of DPPH (reaction 1). Sometimes, the number of reduced DPPH molecules per polyphenol molecule corresponds to the number of available hydroxyl groups. However, for the majority of polyphenols tested, the mechanism is more complex.[4]

$$\mathrm{ROH} + \mathrm{DPPH} \rightarrow \mathrm{RO}^{\bullet} + \mathrm{DPPH\text{-}H} \qquad (1)$$

More recently, a new mechanism associated with a proton-coupled electron transfer (PCET) process has been proposed for the reduction of free radicals with phenols.[5,6] This mecha-

[†] Institut de Química Avançada de Catalunya.
[‡] Universitat de Barcelona.
[§] Institut de Ciència de Materials.

(1) Huang, D.; Ou, B.; Prior, R. L. *J. Agric. Food Chem.* **2005**, *53*, 1841–1856, and references therein.

(2) Blois, M. S. *Nature* **1958**, *181*, 1199–1200. Brand-Williams, W.; Cuvelier, M. E.; Berset, C. *Lebensm.-Wiss.-Technol.* **1995**, *28*, 25. Sanchez-Moreno, C.; Larrauri, J. A.; Saura-Calixto, F *J. Sci. Food Agric.* **1998**, *76*, 270–276. Goupy, P.; Hugues, M.; Boivin, P.; Amiot, M. J. *J. Sci. Food Agric.* **1999**, *79*, 1625–1634.

(3) A clear example of the hydrogen atom donating ability of antioxidants in front of alkyl, alkoxyl, and peroxyl radicals is: Lucarini, M.; Pedrielli, P.; Pedulli, G. F.; Valginigli, L.; Gigmes, D.; Tordo, P. *J. Am. Chem. Soc.* **1999**, *121*, 11546–11553.

(4) Dangles, O.; Fargeix, G.; Dufour, C. *J. Chem. Soc., Perkin Trans. 2* **1999**, 1387–1395. (a) Dangles, O.; Fargeix, G.; Dufour, C. J. *Chem. Soc., Perkin Trans. 2* **2000**, 1653–1663.

10.1021/jo802559x CCC: $40.75
Published on Web 02/20/2009

nism involves an intermediate hydrogen-bonding complex either between the phenol and the radical (an oxygen-centered radical) (reaction 2) or between the phenol and the solvent (a hydrogen bond accepting solvent) (reaction 3) that gives phenoxyl radical by electron-transfer reaction followed by or concerted with proton transfer.

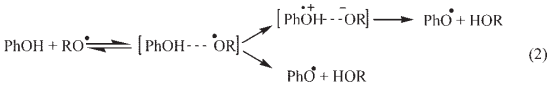

(2)

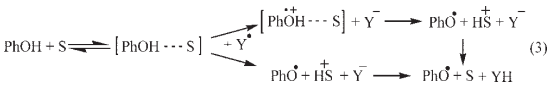

(3)

However, polyphenols are partially ionized losing a proton to give the corresponding anions in ionizable solvents, i.e., solvents able to accept protons such as methanol. In these cases, it has been suggested that the reaction of polyphenols with radicals consists of a fast electron-transfer process from the phenoxide anion to radical (reaction 4).[7]

$$\begin{aligned} \mathrm{PhOH + MeOH} \rightleftharpoons \mathrm{Me\overset{+}{O}H_2 + PhO^-} \xrightarrow{+\mathrm{Y}^\bullet} \\ \mathrm{Me\overset{+}{O}H_2 + PhO^\bullet + Y^-} \\ \mathrm{Me\overset{+}{O}H_2 + Y^-} \rightarrow \mathrm{MeOH + HY} \end{aligned} \quad (4)$$

The studies to measure the antioxidant activity of polyphenols using DPPH as a persistent free-radical sensor do not provide clear information of the mechanism involved, and both mechanisms, hydrogen abstraction and electron transfer, have been proposed as alternative reduction paths. We have been engaged for a long time with stable organic radicals of the tris(2,4,6-trichlorophenyl)methyl (TTM)[8] and perchlorotriphenylmethyl (PTM)[9] series. These free radicals are very persistent species, both in solid or in solution, due to the presence of the very bulky polychlorophenyl substituents around the trivalent carbon atom. As a general rule, they cannot abstract hydrogen atoms from H-donating compounds because the reactant species have a great steric hindrance to yield effective molecular collisions. However, they are very active species in electron-transfer processes reacting with electron-donating and/or electron-accepting substrates to give stable anions and/or cations, respectively. In fact, many of them behave as electrochemical amphoteric species, being reduced in the cathode and oxidized in the anode in quasireversible processes. These characteristic physicochemical properties of the free radicals of the TTM and PTM series provide a supporting base to use them to test the antioxidant power of polyphenols by electron-transfer reactions. In this context, we have reported the synthesis of tris(2,4,6-trichloro-3,5-dinitrophenyl)methyl (HNTTM) radical with strong electron-acceptor properties (standard potential $E^\circ = 0.55$ V vs NaCl-saturated calomel electrode (SCE) in $CHCl_3$/MeOH (2:1), by cyclic voltammetry) and the study of the reducing activity of some flavan-3-ols with HNTTM.[10] More recently, we have reported the synthesis of a new radical of the PTM series, tris(2,3,5,6-tetrachloro-4-nitrophenyl)methyl (TNPTM) radical ($E^\circ = 0.20$ V vs SCE in $CHCl_3$/MeOH (2:1), by cyclic voltammetry) as a new sensor to distinguish selectively the antioxidant power of catechol (1,2-dihydroxybenzene) and pyrogallol (1,2,3-trihydroxybenzene). This stable radical is able to accept an electron from pyrogallol and not from catechol.[11]

The strong oxidant power of HNTTM radical presumably involves a reduced species of a great stability. Now we report the chemical generation and characterization of this species, the corresponding triphenylcarbanion $HNTTM^-$, isolated as the tetrabutylammonium salt, and the oxidant activity of HNTTM radical in front of two simple polyphenols, catechol and pyrogallol, as essential components of the molecular structure of many natural antioxidants such as flavonoids. From the results obtained in these last experiments, we suggest some mechanistic considerations about the species responsible of the electron transfers involved in these reactions.

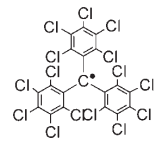

PTM

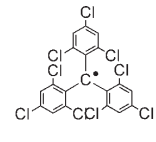

TTM

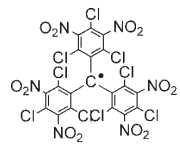

HNTTM (1•)

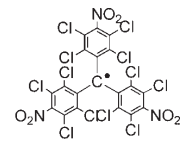

TNPTM

Results and Discussion

The reaction of HNTTM radical with an aqueous solution of tetrabutylammonium hydroxide (TBAH) in THF yielded a strong blue solution of the salt **2**.

$$\mathrm{HNTTM + Bu_4NOH} \xrightarrow[\mathrm{THF}]{} \mathrm{Bu_4N^+ \bullet HNTTM^-} \quad (5)$$

The one-electron reducing power of the hydroxide ion in polar solvents other than water, such as DMSO, HMPT, and THF

(5) Mayer, J. M.; Hrovat, D. A.; Thomas, J. L.; Borden, W. T. *J. Am. Chem. Soc.* **2002**, *124*, 11142–11147. Mayer, J. M. *Annu. Rev. Phys. Chem.* **2004**, *55*, 363–390.

(6) Galian, R. E.; Litwinienko, G.; Pérz-Prieto, J.; Ingold, K. U. *J. Am. Chem. Soc.* **2007**, *129*, 9280–9281. Litwinienko, G.; Ingold, K. U. *Acc. Chem. Res.* **2007**, *40*, 222–230.

(7) (a) Litwinienko, G.; Ingold, K. U. *J. Org. Chem.* **2003**, *68*, 3433–3438. (b) Foti, M. C.; Daquino, C.; Geraci, C. *J. Org. Chem.* **2004**, *69*, 2309–2314. (c) Litwinienko, G.; Ingold, K. U. *J. Org. Chem.* **2004**, *69*, 5888–5896. (d) Foti, M. C.; Daquino, C.; Geraci, C. *J. Org. Chem.* **2004**, *69*, 2309–2314. (e) Musialik, M.; Litwinienko, G. *Org. Lett.* **2005**, *7*, 4951–4954. (f) Litwinienko, G.; Ingold, K. U. *J. Org. Chem.* **2005**, *70*, 8982–8990. (g) Daquino, C.; Foti, M. C. *Tetrahedron* **2006**, *62*, 1536–1547.

(8) Armet, O.; Veciana, J.; Rovira, C.; Riera, J.; Castañer, J.; Molins, E.; Rius, J.; Miravitlles, C.; Olivella, S.; Brichfeus, J. *J. Phys. Chem.* **1987**, *91*, 5608–5616. (b) Carilla, J.; Fajarí, Ll.; Juliá, L.; Riera, J.; Viadel, Ll. *Tetrahedron Lett.* **1994**, *35*, 6529–6532. (c) Teruel, L.; Viadel, Ll.; Carilla, J.; Fajarí, Ll.; Brillas, E.; Sañé, J.; Rius, J.; Juliá, L. *J. Org. Chem.* **1996**, *61*, 6063–6066. (d) Carilla, J.; Fajarí, Ll.; Juliá, L.; Sañé, J.; Rius, J. *Tetrahedron* **1996**, *52*, 7013–7024. (e) Gamero, V.; Velasco, D.; Brillas, E.; Juliá, L. *Tetrahedron Lett.* **2006**, *47*, 2305–2309.

(9) Ballester, M.; Riera, J.; Castañer, J.; Badia, C.; Monsó, J. M. *J. Am. Chem. Soc.* **1971**, *93*, 2215–2225. (b) Ballester, M. *Acc. Chem. Res.* **1985**, *18*, 380–387, and references cited therein.

(10) (a) Torres, J. L.; Varela, B.; Brillas, E.; Juliá, L. *Chem. Commun.* **2003**, *74*, 75. (b) Jiménez, A.; Selga, A.; Torres, J. L.; Juliá, L. *Org. Lett.* **2004**, *6*, 4583–4586.

(11) Torres, J. L.; Carreras, A.; Jiménez, A.; Brillas, E.; Torrelles, X.; Rius, J.; Juliá, L. *J. Org. Chem.* **2007**, *72*, 3750–3756.

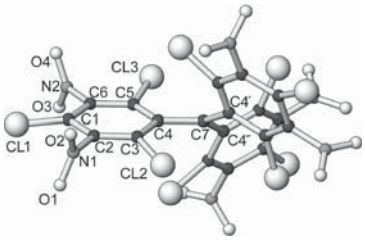

FIGURE 1. Perspective view of the anion of the salt **2** with atom numbering. To indicate the presence of a 3-fold symmetry axis in the molecule, the symmetry-related atoms of C4 have been labeled as C4′ and C4″.

has been reported in the literature.[12,13] This one-electron donation character of the hydroxide anion is assisted by the presence of powerful electron-acceptor substrates. Some perchlorinated aromatic substrates, such as perchlorinated triphenylmethyl radicals with enhanced electron affinity, have been very suitable substrates for this kind of electron-transfer reactions. Salt **2** is very stable in solid and in solution at room temperature, and it has been fully characterized. The absorption spectrum in chloroform solution shows a typical and broadband at $\lambda(\varepsilon) = 499$ nm (26700 $dm^3\ mol^{-1}\ cm^{-1}$). The thermal stability has been measured by thermogravimetric (TG) and differential scanning calorimetry (DSC) analysis, and it is stable at temperatures up to 273 °C. Salt **2** yields small dark violet needles by slow evaporation of a saturated solution in methanol. The molecular and crystal structure of **2** was solved from an X-ray powder diffraction pattern measured on a conventional laboratory equipment (Cu $K\alpha_{1,2}$ radiation) (see the Supporting Information for experimental, structure solution and refinement, and Figures S1−S4). The perspective view of the anion of salt **2** with the atom numbering is shown in Figure 1.

Due to the limited resolution of the powder data (minimum *d* spacing ≅1.43 Å), final bond distances are largely influenced by the target values introduced in the restraints. Consequently, the most reliable and useful information supplied by the refinement are the torsion angles and the dihedral angles between mean planes describing the overall geometry of the molecule (Table 1 as well as the crystal packing of the compound. Twist angles of phenyl rings around the plane defined by the sp^2 C7 and C4, C4′, C4″ (51°) are very similar to the corresponding angles in the molecular structure of TNPTM radical.[11] Similarly, NO_2 planes are forced out of the phenyl planes (80°) due to the presence of *o*-chlorine atoms.

The stability of the reduced species, carbanions, derived from radicals of the TTM series is determined by the reversible reduction potential of the corresponding radical. At the same time, the reduction potential is predominantly related to the effects of the substituents in the phenyl rings, although the extent of localization of the charge density in the phenyl rings is partially inhibited by the twist angles around the central carbon atom. HNTTM radical exhibits a quasireversible reduction process in cyclic voltammetry with a standard potential (E° = 0.58 V vs SCE) in CH_2Cl_2 solution, attributed to the addition of one electron to the trivalent carbon atom.[10a] This positive and large value, compared with that of the TTM radical (E° = −0.66 V vs SCE) is a consequence of the strong electron acceptor properties of the six *m*-nitro groups in the phenyl rings. The nitro group has traditionally been considered as a strong electron-withdrawing group, with a mode of action both inductive and through resonance. In the particular case of HNTTM radical, the nitro groups act by inductive effect. In fact, the E° value for the HNTTM radical is the highest value found into the radicals of the TTM series.)

TABLE 1. Angles (deg) between Planes[a] of the Molecular Structure of HNTTM Radical

A−D	A−B	A−C	A−A′	A−A″
51(1)	79(1)	80(1)	76.5(10)	67.4(10)

[a] Planes are defined as follows: A (C1 to C7, N1 N2), B (C2, N1, O2, O3), C (C6, N2, O3, O4), D (C4, C4′, C4″, C7), A′ (C1′ to C7′, N1′ N2′) and A″ (C1″ to C7″, N1″ N2″).

The reactivity of simple polyphenols such as catechol (1,2-dihydroxybenzene) and pyrogallol (1,2,3-trihydroxybenzene) with stable radical **1**• was measured on the bench from equimolecular solutions of both reactants in solvents of different polarity such as benzene and $CHCl_3$ and in a polar solvent with hydroxylic hydrogen atoms such as a mixture of $CHCl_3$/MeOH (2:1). The experiments with concentrations of the reactants (∼0.1 M) much higher than those of the analytical tests were made during short (4 h) and long (47 h) times to assess and characterize all the HNTTM-containing products of the reaction in each trial. To measure reaction rates and stoichiometric factors of these redox processes, obviously any coupling reaction between HNTTM radical and any radical species derived from the decomposition of polyphenols must be discarded. These experiments were carried out as shown in the Supporting Information, and the reactivity results obtained are collected in Table 2. All of them were very clean and simple processes yielding the diamagnetic species **1** as the result of the reduction of **1**•. In some of the tested experiments, the compounds reacted very slowly or did not react at all, being recovered part of the species **1**•.

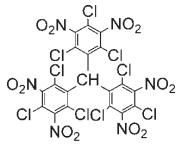

1

From an analysis of Table 2, it follows that **1**• reacts very slowly with catechol in benzene and $CHCl_3$ but gently in $CHCl_3$/MeOH (2:1). On the other hand, **1**• reacts smoothly with pyrogallol in benzene and $CHCl_3$, although the reaction proceeds very fast in $CHCl_3$/MeOH (2:1). The different results obtained in these experiments depended both on the electron-donating strength of the polyphenols and on the nature of the solvent employed. Thus, the reaction rates of **1**•with catechol and with pyrogallol either in benzene, $CHCl_3$ or in $CHCl_3$/MeOH (2:1) are in accordance with their different anodic peak potentials in

(12) Pearson, R. G. *J. Am. Chem. Soc.* **1986**, *108*, 6109–6114.
(13) Ballester, M. *Pure Appl. Chem.* **1967**, *15*, 123–151. Ballester, M.; Riera, J.; Castañer, J.; Badia, C.; Monso, J. M. *J. Am. Chem. Soc.* **1971**, *93*, 2215–2225. Ballester, M.; Castañar, J.; Riera, J.; Ibáñez, A.; Pujadas, J. *J. Org. Chem.* **1982**, *47*, 259–264. Ballester, M.; Riera, J.; Castañer, J.; Rodríguez, A.; Rovira, C.; Veciana, J. J. *Org. Chem* **1982**, *47*, 4498–4505. Ballester, M.; Castañer, J.; Riera, J.; Pujadas, J. *J. Org. Chem.* **1984**, *49*, 2884–2887. Ballester, M.; Castañar, J.; Riera, J.; Pujadas, J.; Armet, O.; Onrubia, C.; Rio, J. A. *J. Org. Chem.* **1984**, *49*, 770–778. Roberts, J. L.; Sugimoto, H., Jr.; Barrette, W. C.; Sawyer, D. T., Jr. *J. Am. Chem. Soc.* **1985**, *107*, 4556–4557. Ballester, M.; Pascual, I. *J. Org. Chem.* **1991**, *56*, 841–844. Lu, Y.; Liu, J.; Diffee, G.; Liu, D.; Liu, B. *Tetrahedron Lett.* **2006**, *47*, 4597–4599.

TABLE 2. Reactivity of Catechol and Pyrogallol with 1• in Benzene, $CHCl_3$, and $CHCl_3$/MeOH (2:1) (Equimolecular Solutions)[a]

		reagent			
solvent	time (h)	Catechol **1**• (%)[b] **1** (%)		Pyrogallol **1**• (%)[b] **1** (%)	
benzene	4	92	8	76	24
	47	71	29	51	49
$CHCl_3$	4	96	4	75	25
	47	73	27	50	50
$CHCl_3$/MeOH (2:1)	4	34	66	<5	>95
	47	11	89	0	100

[a] Initial concentration of polyphenol and HNTTM radical, 0.12 M. [b] Recovered radical.

TABLE 3. Cyclic Voltammetry Parameters for the Oxidation of Catechol and Pyrogallol and for the Reduction of Radical 1•

solvent	catechol E_p^a/V[a]	pyrogallol E_p^a/V[a]	radical **1**• $E°$/V[a] (E^c_p/V)[a]
benzene	1.64	—[b]	0.65 (0.48)
$CHCl_3$	1.27	1.15	0.58 (0.50)
$CHCl_3$/MeOH (2:1)	1.00	0.82	0.55 (0.46)

[a] Anodic peak potential (E_p^a), standard potential ($E°$) and cathodic peak potential (E_p^a) for the substrate (10^{-3} M) with 0.4 M tetrahexylammonium hexafluorophosphate in benzene and 0.1 M tetrabutylammonium perchlorate in $CHCl_3$ or $CHCl_3$/MeOH (2:1), on Pt at scan rates of 50 mV s^{-1} and 25.0 °C. [b] Not determined by partial adsorption of the substrate on Pt.

cyclic voltammetry[14] (E_p^a[pyrogallol] < E_p^a[catechol]) (Table 3; Figures S5−S7, Supporting Information). So, the reactivity of **1**• with pyrogallol is greater than with catechol and it follows the order $CHCl_3$/MeOH (2:1) ≫ $CHCl_3$ ∼ benzene. The dramatic increase in $CHCl_3$/MeOH (2:1) may be due to the partial ionization of the phenol to phenolate ion in hydroxylic solvents, as it has been accepted by other authors.[7] In this case, the anodic peak potential of the phenolate ion is much lower than that of phenol.[11]

All these reactions lead to the stable charged species $\mathbf{1}^-$ by electron transfer from the polyphenol and, finally, to the diamagnetic triphenylmethane **1** by abstraction of a hydrogen ion. The presence of the charged species $\mathbf{1}^-$ has been confirmed by electronic spectroscopy. Thus, electronic spectra of the products present in the course of the reaction between **1**• and pyrogallol in $CHCl_3$/MeOH (2:1) and in benzene are shown in Figures 2 and 3, respectively. In Figures 2 and 3 (right), the lowest-energy band intensities for the products resulting after a few minutes of mixturing of both reactants, **1**• and pyrogallol, are displayed together with a simulation of the spectra of single species **1**• and $\mathbf{1}^-$ in the same solvents. The simulated spectra were obtained by a linear combination of the spectra of **1**• and $\mathbf{1}^-$ showing that both species are present in solution in ∼19% and ∼81% in $CHCl_3$/MeOH and in ∼99% and ∼1% in benzene, respectively. Figure 3 (left) displays the evolution of the absorption band of a more concentrated solution of **1**• and pyrogallol, clearly observing the presence of the small absorption band of $\mathbf{1}^-$ immersed into the very large band of **1**•.

To determine the kinetic parameters of the reactions of catechol and pyrogallol with radical **1**•, these processes were

(14) Cyclic voltammograms for the oxidation of catechol and pyrogallol solutions (1 mM) in $CHCl_3$ and $CHCl_3$/MeOH 2:1 (v/v) with tetrabutylammonium perchlorate (0.1 M) on Pt at 25 °C and in benzene with tetrahexylammonium hexafluorophosphate (0.3 M) on Pt at 25 °C were recorded. It was not possible to assign an anodic peak potential for the oxidation of pyrogallol in benzene due to the strong adsorption of the oxidized species in the electrode.

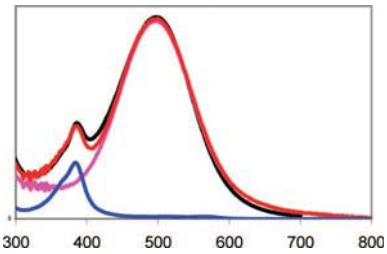

FIGURE 2. Absorption spectra of **1**• (blue), $\mathbf{1}^-$ (purple) ($\lambda = 494$ nm), and **1**• + pyrogallol in $CHCl_3$/MeOH (2:1) after a few minutes of reaction (black) and a simulation of the black spectrum by a combination of **1**• and $\mathbf{1}^-$ (red).

carried out in $CHCl_3$/MeOH (2:1) and benzene as solvents and monitored by electronic spectroscopy, recording the decay of the maximum absorbance of **1**• (λ_{max} = 384 and 387 nm in benzene and $CHCl_3$/ MeOH (2:1), respectively) as a consequence of the electron addition to give anion $\mathbf{1}^-$. The experiments were effected with a **1**•/polyphenol molar ratio of ∼5:1 and an initial concentration of **1**• of 54 μM. The reactions were completed when the absortivities in the electronic spectra remained practically constants. The n-values of the stoichiometry of polyphenols were calculated using eq 6

$$n = \frac{A_0 - A_f}{\varepsilon \cdot c} \tag{6}$$

where A_0 and A_f are the initial and final absorbances of the radical **1**•, respectively, *c*is the initial concentration of the antioxidant, and ε is the molar absortivity of the radical.

The *n* values for the reactions of **1**• with catechol and pyrogallol in $CHCl_3$/MeOH (2:1) and **1**• with pyrogallol in benzene are given in Table 4. While catechol reduces two molecules of radical per molecule, pyrogallol reduces up to three molecules of radical per molecule. Two steps of the decay of the absorbance of radical **1**•, one fast and one slow, with the antioxidant, catechol, or pyrogallol, in $CHCl_3$/MeOH and only one slow decay step with pyrogallol in benzene can be distinguished in the course of the reducing processes. Calculated second-order rate constants (k_1) for the first fast step of the reactions in $CHCl_3$/MeOH and for the only slow step in benzene are shown in Table 4.

Reactions of catechol and pyrogallol with radical **1**• in $CHCl_3$/MeOH (2:1) and pyrogallol with **1**• in benzene could be evaluated after a moderate time (5.5 h) because they are practically completed and the number of electrons transferred per molecule of polyphenol were approximately 3 for pyrogallol and 2 for catechol. The rate constant values were estimated by using a simple kinetic model reported by Dangles et al.[15] and are shown in Table 4 (Graphics of the kinetics of the reactions are displayed in the Supporting Information; see Figures S8−S10).

Experiments of catechol with radical **1**• in benzene were also distinguished by only one very slow step. The number of electrons transferred from catechol to **1**• after a long reaction time (13 h) corresponds to approximately one electron per

(15) Goupy, P.; Dufour, C.; Loonis, M.; Dangles, O. *J. Agric. Food Chem.* **2003**, *51*, 615–622.

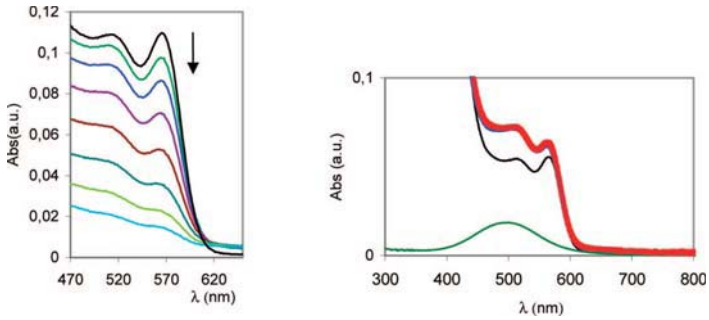

FIGURE 3. Left: Evolution of the lowest energy band intensity of a solution of **1**• (120.2 μM) and pyrogallol (1.63 mM) in dry benzene at different times (first band in black, **1**• in benzene; intervals of 10 min). Right: Lowest energy band in the absorption spectra of **1**• (black), $\mathbf{1}^-$ (green) (λ, 499 nm), theoretical combination: **1**• + $\mathbf{1}^-$ (red), and **1**• (54.0 μM) + pyrogallol (10.6 μM) in dry benzene after 3 min of reaction (blue).

TABLE 4. Observed Rate Constants and Stoichiometric Factors for the Reactions[a] of Radical 1• with Catechol and Pyrogallol in $CHCl_3$/MeOH (2:1) and with Pyrogallol in Dry Benzene

	solvent	**1**•:polyphenol molar ratio[b]	k_1 (M^{-1} s^{-1})	n^c
catechol	$CHCl_3$/MeOH (2:1)	5.1	1123 ± 95	1.9
pyrogallol	$CHCl_3$/MeOH (2:1)	4.6	5115 ± 82	3.1
pyrogallol	benzene	5.1	14.5 ± 0.4	3.0

[a] Time of reaction, 5.5 h. [b] Initial concentrations of radical **1**•, 54 ± 2 μM. [c] Number of electrons transferred per molecule of polyphenol.

SCHEME 1

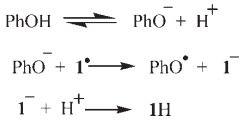

molecule of catechol, and values of the rate constant in the initial steps of these processes as low as $k_1 = 0.6$ M^{-1} s^{-1} were estimated.[16]

The rather fast reactions of catechol and pyrogallol with radical **1**• in $CHCl_3$/MeOH (2:1) are due, as mentioned above, to the fact that polyphenols are partially ionized to charged species PhO^- in this medium and these species can be more easily oxidized ($E_p^a = 0.25$ V vs SCE for catechol and $E_p^a = 0.06$ V vs SCE for pyrogallol in $CHCl_3$/MeOH (2:1) in the presence of an excess of tetrabutylammonium hydroxide)[11] than the corresponding molecular species PhOH (see Table 3). Judging from the anodic peak potentials of catechol and pyrogallol, and the cathodic peak potential of **1**• (see Table 3), both reactions should be exoergonic. The electron-deficient radical **1**• reacts very fast by electron transfer reaction with the generally low concentration of PhO^- present in equilibrium with PhOH. Thus, the sequential proton loss−electron transfer (SPLET) mechanism, first reported by Litwinienko[7a] and Foti,[7b] occurs in these processes as described in Scheme 1.

The reaction of radical **1**• with pyrogallol in benzene deserves especial mention. Benzene is a nonionizable solvent with a very low dielectric constant and it shows weak interactions with charged and polar species. However, the reaction of pyrogallol with radical **1**•, although slow as shown by the low value of the rate constant (Table 4), takes place through the generation of

(16) Values of k_1 were estimated proceeding with the Dangles' kinetic model. Now, the A_f value in eq 8 corresponds to the visible absorbance ($\lambda = 384$ nm) of the radical **1**• after 13 h when the reaction is not finished.

SCHEME 2

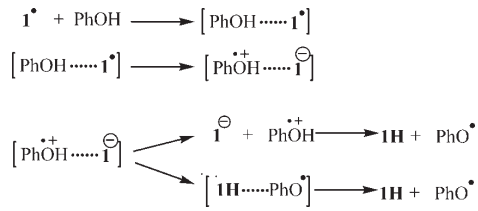

the corresponding $\mathbf{1}^-$ (see Figure 3). Now, if we pay attention to the onset potential values for pyrogallol and radical **1**• in benzene from their corresponding cyclic voltammograms, i.e., when the electron transfer on Pt begins to take place, we obtain $E_{onset}^a \sim 1.1$ V for the oxidation of the former and $E_{onset}^c \sim 0.75$ V for the reduction of the latter, the electron-transfer reaction between pyrogallol and **1**• should be endoergonic. To overcome this difficulty, it is reasonable to envisage the formation of a complex intermediate between both species. The strength of interactions between the phenol and the radical **1**• can seriously affect the electrochemistry of both reactants providing an efficient intermolecular electron transfer from the pyrogallol. This intermediate may be constituted by hydrogen-bonding between the nitro oxygen atoms of the radical and the hydroxyl hydrogen atoms of the polyphenol, increasing the electron density on the phenolic oxygen and making it easier to be oxidized (Scheme 2).

This sequence of steps explains favorably the detection of the reduced species $\mathbf{1}^-$ by electronic spectroscopy. Thus, once the electron is transferred into the complex, this rapidly dissociates leading to the free ions. Anion $\mathbf{1}^-$ has been clearly detected by spectroscopy before the protonation of $\mathbf{1}^{--}$ takes place. However, it is not discounted at all that the protonation of $\mathbf{1}^-$ might take place in part into the complex as the acidity of the phenol significantly increases after one-electron oxidation to the radical cation.

In conclusion, the reactions between radical **1**• and pyrogallol (PhOH) in different solvents occur by electron-transfer reaction to the SOMO of **1**• to give the charged $\mathbf{1}^-$, which is consecutively protonated to **1H**. In hydroxylic solvents, the electron transfer is a very rapid process and the electron-donating species is the ionized PhO^-, whereas in nonpolar and nonhydroxylic solvents, the electron transfer is facilitated by assuming an intermediate complex between **1**• and PhOH. An additional experimental proof against the hydrogen atom abstraction mechanism of this last process is that TTM radical does not

react at all with pyrogallol in benzene, although TTM and HNTTM have similar stability due to the steric hindrance provided by the six chlorine atoms around the trivalent carbon. The difference between both radicals resides in their electrochemical properties, HNTTM radical being much more oxidant ($E° = 0.58$ V vs SCE) than TTM radical ($E° = -0.66$ V vs SCE).[11]

Experimental Section

Synthesis of Tetrabutylammonium Tris(2,4,6-trichloro-3,5-dinitrophenyl)methide (2). To a stirred solution of tris(2,4,6-trichloro-3,5-dinitrophenyl)methane (**1**) (269 mg; 0.3 mmol) in THF (15 mL) at rt was added an aqueous solution of tetrabutylammonium hydroxide (TBAH) (1.5 M) (26 μL; 0.4 mmol), and the mixture was left in argon for a period of time (6 h). The precipitate (253 mg) was filtrated off, washed with water, and dried under reduced pressure to give salt **2** (253 mg; 73%): IR (KBr) 2973 (w), 2929 (w), 2871 (w), 1553 (s), 1465 (w), 1358 (m), 1222 (w), 945 (w), 833 (w), 784 (w), 735 (w), 677 (w), 638 (w) cm. Anal. Calcd for $C_{35}H_{36}Cl_9N_7O_{12}$: C, 39.4; H, 3.4; N, 9.2; Cl, 29.9. Found: C, 39.7; H, 3.6; N, 8.8; Cl, 29.2.

Reactions of Radical 1$^\bullet$ with Polyphenols. Equimolecular solutions of tris(2,4,6-trichloro-3,5-dinitrophenyl)methyl (**1**$^\bullet$) radical (50 mg) and catechol (6.7 mg) or pyrogallol (7.6 mg) in three different solvents (50 mL), $CHCl_3$, $CHCl_3$/MeOH (2:1), and dry C_6H_6, were stirred (47 h) at rt in the dark and in an inert atmosphere (Ar). The solutions were treated with water, and the organic fractions, dried over sodium sulfate, were evaporated off to yield a solid identified as a mixture of radical **1**$^\bullet$ and methane **1** by IR and UV−visible spectra. The course of the reactions was monitored by UV−vis spectroscopy after 4 and 47 h of reaction.

Kinetic Measurements. An estimation of the kinetics of reactions of radical **1**$^\bullet$ with catechol and pyrogallol in $CHCl_3$/MeOH (2:1) and dry C_6H_6 at rt were performed. Procedure: To 3 mL of a freshly prepared solution (60 μM) of **1**$^\bullet$ in the solvent, placed in the spectrometer cell, was added a freshly prepared solution (90.8 μM) (390 μL) of the polyphenol in the same solvent. The UV−vis spectra were recorded at different time intervals.

All of the procedures were carried out with an excess of radical. The rate constant of the electron transfer from phenol to HNTTM radical was estimated with a simple and general kinetic model reported by Dangles et al.[15] making no hypothesis about the mechanism of polyphenol degradation, and only the fast steps of the reactions in $CHCl_3$/MeOH were subjected to a kinetic analysis. Hence, in eqs 7 and 8, the digit 3 represents the number of moles of HNTTM radical that 1 mol of pyrogallol is capable to reduce, A_0 is the initial absorbance of the radical **1**$^\bullet$ in the UV−visible spectra, A_f is the absorbance at the end of the fast step in the reactions in $CHCl_3$/MeOH and at the end of the single step in the reaction in benzene, and c is the initial concentration of pyrogallol.

$$-\mathrm{d[TNPTM]}/\mathrm{d}t = k \cdot 3 \cdot \mathrm{[pyrogallol][TNPTM]}$$

$$= k_1\mathrm{[pyrogallol][TNPTM]} \qquad (7)$$

$$\ln \frac{1 - A_f/A}{1 - A_f/A_0} = -\frac{k_1 c}{A_0/A_f - 1} t \qquad (8)$$

Acknowledgment. Financial support for this research from the MCT (Spain) through project AGL2006-12210-C03-02/ALI is gratefully acknowledged.

Supporting Information Available: Synthesis and X-ray powder diffraction study (experimental, structure solution, and refinement) of salt **2**; final atomic coordinates and observed and calculated X-ray diffraction patterns. Graphics for kinetics of HNTTM with pyrogallol and catechol. Cyclic voltammograms. This material is available free of charge via the Internet at http://pubs.acs.org.

JO802559X

JOURNAL OF AGRICULTURAL AND FOOD CHEMISTRY

Article

pubs.acs.org/JAFC

Punicalagin and Catechins Contain Polyphenolic Substructures That Influence Cell Viability and Can Be Monitored by Radical Chemosensors Sensitive to Electron Transfer

Anna Carreras,[†] María Luisa Mateos-Martín,[†] Amado Velázquez-Palenzuela,[§] Enric Brillas,[§] Marta Cascante,[⊗] Luis Juliá,[†] and Josep Lluís Torres*[,†]

[†]Department of Biological Chemistry and Molecular Modelling, Institute for Advanced Chemistry of Catalonia, IQAC-CSIC, Jordi Girona 18-26, 08034 Barcelona, Spain

[§]Department of Physical Chemistry, University of Barcelona, Martí i Franquès 1-11, 08028 Barcelona, Spain

[⊗]Department of Biochemistry and Molecular Biology, Unit Associated with CSIC, University of Barcelona, Avinguda Diagonal 645, 08028 Barcelona, Spain

Supporting Information

ABSTRACT: Plant polyphenols may be free radical scavengers or generators, depending on their nature and concentration. This dual effect, mediated by electron transfer reactions, may contribute to their influence on cell viability. This study used two stable radicals (tris(2,3,5,6-tetrachloro-4-nitrophenyl)methyl (TNPTM) and tris(2,4,6-trichloro-3,5-dinitrophenyl)methyl (HNTTM)) sensitive only to electron transfer reduction reactions to monitor the redox properties of polyphenols (punicalagin and catechins) that contain phenolic hydroxyls with different reducing capacities. The use of the two radicals reveals that punicalagin's substructures consisting of gallate esters linked together by carbon−carbon (C−C) bonds are more reactive than simple gallates and less reactive than the pyrogallol moiety of green tea catechins. The most reactive hydroxyls, detected by TNPTM, are present in the compounds that affect HT-29 cell viability the most. TNPTM reacts with C−C-linked gallates and pyrogallol and provides a convenient way to detect potentially beneficial polyphenols from natural sources.

KEYWORDS: *punicalagin, catechins, pyrogallol, TNPTM chemosensor, cell viability*

INTRODUCTION

The question of whether natural polyphenols provide benefits in terms of human health is a controversial one among scientists. Ever since Harman published his paper on free radicals and aging,[1] it has been assumed that polyphenols prevent disease and delay aging because they scavenge toxic free radicals, which progressively damage biomolecules in live tissues mainly by oxidation.[2] Because they scavenge potentially oxidizing free radicals, polyphenols are referred to as antioxidants. Nevertheless, although it is true that polyphenols scavenge radicals in solution, their intracellular effectiveness is less obvious, and many authors consider them to be virtually inactive in vivo after oral intake.[3] The reason is that the live organism prevents polyphenols from greatly altering the redox homeostasis by rapidly metabolizing and excreting them, as well as by activating regulatory enzymatic systems. Polyphenols are conjugated into glucuronides, methyl esters, and sulfates mainly in the intestine and liver.[4,5] Most of these conjugates are no longer free radical scavengers, and the very small amounts of remaining intact polyphenolic moieties are very unlikely to modify the redox homeostasis significantly.[3] The skin and intestinal tract may be exceptions to this because local concentrations of intact phenolics may be present in significant amounts in these tissues.[6] Moreover, not only may polyphenols be effective free radical scavengers, they may actually generate free radicals depending on the nature and concentration of the specific polyphenols.[3] This so-called pro-oxidant activity may be behind the moderate toxicity of green tea extracts at very high concentrations[7] and the reason why polyphenols are rapidly transformed and excreted after ingestion. Interestingly, at concentrations that are not so high, this mild pro-oxidant activity may result in an overall antioxidant effect via a mechanism known as hormesis, which can be defined as a low-dose stimulation of defense systems with a subsequent beneficial effect.[8] In the case of foodstuffs in which the redox regulation systems progressively lose their efficiency during the shelf life of the product (e.g., fish rich in PUFA), polyphenols have proven to effectively prevent lipid oxidation.[9] Whatever the case, if polyphenols exert an influence over the redox status of any system, whether it is antioxidant, toxic pro-oxidant, or hormetic pro-oxidant, it is somehow related to the reactivity of the constitutive hydroxyl groups in the polyphenols, the functional groups that first react with oxidants.

Different chemical mechanisms may be involved in the free radical-scavenging and/or free radical-generating effects of polyphenols. To better characterize the scavenging activity of polyphenols, several assays focused on different possible mechanisms of their overall action should be considered.[10] The mechanisms that have been proposed are hydrogen atom transfer (HAT), proton-coupled electron transfer (PCET), and sequential proton loss electron transfer (SPLET), with the generation of a

Received: March 1, 2011
Revised: January 5, 2012
Accepted: January 27, 2012

   dx.doi.org/10.1021/jf204059x | J. Agric. Food Chem. XXXX, XXX, XXX−XXX

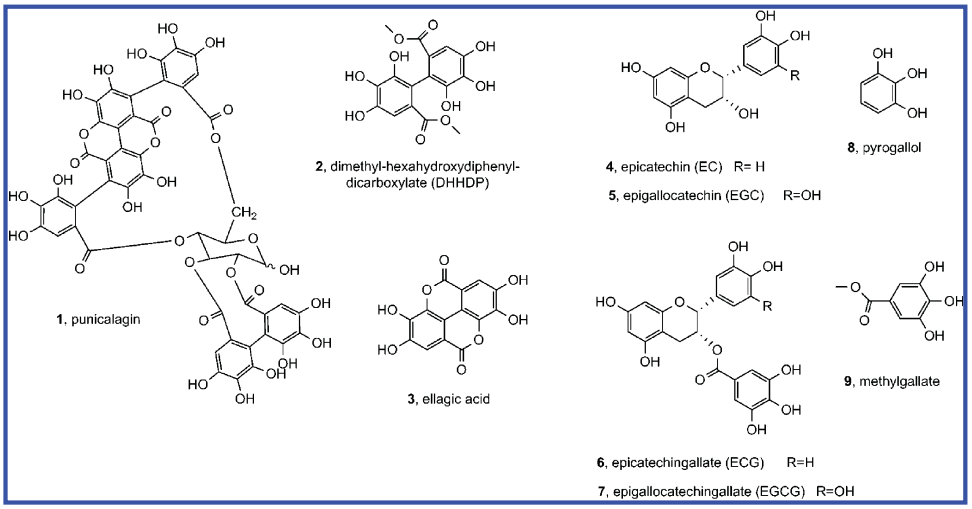

Figure 1. Structures of punicalagin (**1**), related compounds (**2** and **3**), green tea catechins (**4**–**7**), and simple phenols (**8** and **9**).

more stable phenoxyl radical.[11−13] Electron transfer to oxygen generates the superoxide radical $O_2^{\bullet-}$, which is enzymatically converted into hydrogen peroxide[14,15] and ultimately into the deleterious hydroxyl radical in the presence of transition metal cations (e.g., Fe^{2+}).[16] Moreover, the superoxide radical seems to mediate apoptosis.[17,18] Electron transfer appears to be most relevant in the redox cascades involving polyphenols, whether they scavenge or generate reactive radicals. To evaluate the electron transfer capacity of polyphenols, we developed stable radicals of the (2,4,6-trichlorophenyl)methyl (TTM) and perchlorotriphenylmethyl (PTM) series, which react exclusively by electron transfer.[13,19,20] We and others have used these radicals to evaluate the electron transfer capacity of natural and synthetic phenolic scavengers.[21,22] As the activity of the stable radicals of the TTM and PTM series essentially depends on the electron-withdrawing or electron-donating character of the meta- and/or para- substituents introduced into the phenyl rings, radicals with different redox potentials can be designed. The advantage of devising assays using this combination of radicals is that they can discriminate between oxidizing agents by their oxidizing ability, in contrast to the ferric ion reduction method that also operates exclusively by electron transfer processes but measures only the reducing ability based upon the redox potential of the ferric ion. Moreover, the outcome of the ferric ion method is also influenced by binding of the polyphenol to the ion.

Polyphenols may contain more than one reactive polyphenolic substructure. Punicalagin (**1**) (Figure 1), the most abundant polyphenol in pomegranate (*Punica granatum* L.),[23] is a hydrolyzable tannin of the ellagitannin kind because it contains an ellagic acid substructure (**3**). Punicalagin (**1**) releases ellagic acid (**3**) in the small intestine via spontaneous lactonization with later conversion into urolithin A by the gut microbiota.[24] Punicalagin (**1**) also contains in its structure gallate (three geminal phenolic hydroxyls and a carboxylate function) esters linked by carbon−carbon (C−C) bonds either to themselves (hexahydroxy-2,2′-diphenyl, HHDP moiety) or to the ellagic acid substructure. This ensemble of substructures and their metabolites contributes to the bioactivity of the whole molecule. The C−C bond structures constitutive of ellagitannins appear to be important for their activity. Pedunculagin, another hydrolyzable tannin that contains the HHDP moiety, shows higher cytotoxic activity than pentagalloylglucose, a hydrolyzable tannin that contains only simple gallate esters in its structure.[25] Catechins (flavanols of the flavan-3-ol type) are another family of polyphenols that display different polyphenolic substructures and are relevant to dietary considerations. Green tea is a common source of catechins, mainly, in order of abundance, (−)-epigallocatechin gallate (EGCG) (**7**), (−)-epigallocatechin (EGC) (**5**), (−)-epicatechin (EC) (**4**), and (−)-epicatechin gallate (ECG) (**6**) (Figure 1).[26] Tea flavanols scavenge reactive oxygen and nitrogen species, interfere with pro-oxidant processes, or inhibit pro-oxidant enzymes.[27] Polyphenols appear to exert their biological activity through different mechanisms involving redox reactions and protein−ligand interactions. Because the present paper focuses on the redox reactivity of different phenolic moieties and its possible relationship to cell viability in vitro, we selected pomegranate punicalagin (**1**) and green tea flavanols **4**–**7** for our study; together they contain a broad range of polyphenolic substructures. Here, we examine the electron transfer capacity (reducing power) of punicalagin (**1**), and its metabolite ellagic acid (**3**), its related substructure **2**, and green tea flavanols **4**–**7** bearing the catechol, pyrogallol, and gallate moieties, and we evaluate the effect of all these molecules on the viability of colon carcinoma HT-29 cells.

MATERIALS AND METHODS

Tris(2,3,5,6-tetrachloro-4-nitrophenyl)methyl (TNPTM) and tris-(2,4,6-trichloro-3,5-dinitrophenyl)methyl (HNTTM) were synthesized in our laboratory as described previously.[19,20] 1,1-Diphenyl-2-picrylhydrazyl (DPPH) was purchased from Sigma-Aldrich (St. Louis, MO). Punicalagin (**1**) (≥98% (HPLC)) was obtained from Biopurify (Sichuan, China), ellagic acid (**3**) and the catechins **4**–**7** were from from Sigma-Aldrich, and dimethyl-hexahydroxydiphenyl dicarboxylate (DHHDP, **2**) was synthesized in our laboratory following procedures described elsewhere[28] (see the Supporting Information).

Radical-Scavenging Capacity. The scavenging capacity was determined from mixtures (1:1, v/v) of fresh solutions of stable radicals (TNPTM, HNTTM, DPPH; 120 μM) and fresh solutions of polyphenols **1**–**9** in $CHCl_3$/MeOH (2:1) at different concentrations (1−120 μM) at room temperature. All of the solutions were prepared

dx.doi.org/10.1021/jf204059x | J. Agric. Food Chem. XXXX, XXX, XXX−XXX

and deoxygenated in the darkness. The reactions were monitored by electron paramagnetic resonance (EPR) on an EMX-Plus 10/12 (Bruker BioSpin, Rheinstetten, Germany) after 48 h (TNPTM), 7 h (HNTTM), and 30 min (DPPH). Operating conditions were as follows: center field, 3615 G; scan range, 250 G; microwave power, 5.2 mW; microwave frequency, 9.86 GHz; modulation frequency, 100 kHz; receiver gain, 6×10^3; and time constant, 4.1 s. The scavenging capacity of polyphenols is given as EC_{50}, which corresponds to the amount (micrograms or micromoles) of polyphenol able to consume half the amount of free radical divided by micromoles of initial radical. The results in micrograms per micromole convey the idea of the scavenging capacity of a given amount of polyphenol, and the results in micromoles per micromole provide information about the number of equivalents per molecule. To facilitate the comparison between structures, the results were also expressed as antiradical capacity (ARC), which is the inverse of EC_{50} in micrograms per micromole and hydrogen atoms donated or electrons transferred per molecule of polyphenol (H/e), which is the inverse of $2 \times EC_{50}$ in micromoles per micromole.

Kinetic Measurements. The rate constants of the reactions between TNPTM and polyphenols **2** and **8** were estimated by EPR. Freshly prepared solutions of TNPTM in CH_3Cl/MeOH (2:1) (240 μM) and the polyphenol (48 μM in the same solvent) were mixed (1:1, v/v, molar ratio 5:1), and the decay of the TNTPM band was followed at room temperature. Operating conditions were as follows: center field, 3450 G; scan range, 250 G; microwave power, 1.0 mW; microwave frequency, 9.86 GHz; modulation frequency, 100 kHz; receiver gain, 8.9×10^3; and time constant, 40.96 s. The rate constants and the total number of electrons transferred per polyphenol (n_e) were estimated with a simple and general kinetic model reported by Dangles et al.[29] defined by eq 1. The values for the rate constant, k were calculated from the integrated eq 2.

$$-\mathrm{d}[\mathrm{TNPTM}]/\mathrm{d}t = k \times n[(\mathrm{poly})\mathrm{phenol}][\mathrm{TNPTM}] = k_1[(\mathrm{poly})\mathrm{phenol}][\mathrm{TNPTM}] \quad (1)$$

$$\ln \frac{1 - I_f/I_x}{1 - I_f/I_0} = -\frac{k_1 c}{I_0/I_f - 1} t \quad (2)$$

In eqs 1 and 2, n represents the number of reduced moles of TNPTM per mole of polyphenol; I_0 is the initial intensity of the TNPTM signal in the EPR spectra; I_f is the final visible intensity; and c is the initial concentration of polyphenol. The n_e values of the stoichiometry of the polyphenol were calculated using eq 3; ε is the molar absorptivity characteristic of the stable free radical.

$$n_e = \frac{I_0 - I_f}{\epsilon \times C} \quad (3)$$

Cyclic Voltammetry. Cyclic voltammetries were carried out in a standard thermostated cylindrical, one-compartment, three-electrode cell. A platinum (Pt) disk of 0.093 cm^2 area was used as the working electrode and a Pt wire as the counter electrode. The reference electrode was a saturated calomel electrode (SCE), submerged in a salt bridge of the same electrolyte, which was separated from the test solution by a Vycor membrane. Solutions of polyphenols ($\sim 10^{-3}$ M) in DMF containing tetrabutylammonium perchlorate (0.1 M) as the background electrolyte were studied. The volume of all test solutions was 50 mL. Electrochemical measurements were performed under an argon atmosphere at 25 °C using an Eco Chemie Autolab PGSTA-T100 potentiostat-galvanostat (Autolab, Utrecht, The Netherlands) controlled by a computer with Nova 1.5 software (Autolab). Cyclic voltammograms of all the solutions were recorded at scan rates ranging from 20 to 200 mV s^{-1}.

Cell Culture and Viability Assay. HT-29 human colon adenocarcinoma cells were obtained from the American Type Culture Collection. HT-29 cells were cultured in Dulbeco Modified Eagle's Medium (DMEM with 4500 mg L^{-1} glucose, L-glutamine, and sodium bicarbonate, without sodium pyruvate; Sigma-Aldrich), supplemented with 10% fetal bovine serum (PAA Laboratories, Pasching, Austria) and antibiotics, 100 U mL^{-1} penicillin and 100 mg L^{-1} streptomycin (Invitrogen, Paisley, U.K.), at 37 °C in a humidified atmosphere of CO_2 (5%). The effect of treatment with different polyphenols upon proliferation of HT-29 colon cancer cells was measured by the 3-(4,5-dimethylthiazol-2-yl)-2,5-diphenyl tetrazolium bromide (MTT) (Sigma-Aldrich) assay, which is based on the ability of live cells to cleave the tetrazolium ring, thus producing formazan, which absorbs at 570 nm. HT-29 cells (3000 cells/well) were grown on a 96-well plate for 24 h and then incubated with the different polyphenols at different concentrations (10−300 μM) in dimethyl sulfoxide (DMSO) (Sigma-Aldrich), except ellagic acid (**3**), which was dissolved in *N*-methylpyrrolidone because of its poor solubility in DMSO. After 72 h, 100 μL of MTT solution (0.5 mg mL^{-1}) was added to each well. After 1 h of incubation, the formazan salt was resuspended in 100 μL of DMSO. Cell viability was measured by absorbance at 550 nm on an ELISA plate reader (Tecan Sunrise MR20-301, TECAN, Austria). The experiments were also run in the presence of catalase (Sigma-Aldrich), 100 U mL^{-1} in DMEM.[30] The results were expressed as IC_{50}.

RESULTS

Radical-Scavenging Capacity of Polyphenols Measured by TNPTM, HNTTM, and DPPH. The scavenging capacity of punicalagin (**1**) and related compounds **2** and **3**, flavanols **4**−**7**, pyrogallol (**8**), and methylgallate (**9**) was measured by making them react with the stable radicals TNPTM, HNTTM, and DPPH in a mixture that includes a polar hydroxylated solvent ($CHCl_3$/MeOH (2:1) (v/v)) and monitoring the decrease of the EPR radical signal. TNPTM and HNTTM are reduced exclusively by accepting electrons, in contrast to DPPH, which reacts by HAT and/or ET depending on the solvent. Table 1 summarizes the results of the scavenging capacity of **1**−**9** against the three radicals.

Punicalagin (**1**), ECG (**6**), and EGCG (**7**) were the most active polyphenols against HNTTM and DPPH. The number of electrons transferred to HNTTM roughly corresponded to the number of putative reactive positions (geminal hydroxyls) of the flavanols except for ECG (**6**), which consumed a larger amount of radical. Surprisingly, DHHDP (**2**) transferred 4.3 electrons instead of 6, and punicalagin (**1**) transferred 14.2 electrons instead of 16. The scavenging capacities of the polyphenols against TNPTM radical were lower than those obtained with HNTTM and DPPH because TNPTM reacts only with the most reactive hydroxyls. One molecule each of EGC (**5**), EGCG (**7**), and pyrogallol (**8**) reacted with 3 molecules of TNPTM (roughly 1 electron transferred from each of the three geminal hydroxyls); 1 molecule of punicalagin (**1**) and its substructure DHHDP (**2**) reacted with 3.3 and 2 molecules of TNPTM, respectively (roughly 1 electron transferred from each C−C linked gallate). In contrast, ellagic acid (**3**), EC (**4**), ECG (**6**), and methylgallate (**9**) did not react at all with TNPTM. Figure 2 shows graphically the selective reactivity of characteristic phenolic moieties with TNPTM, monitored by the decrease of the TNPTM radical EPR signal upon reaction with DHHDP (**2**), pyrogallol (**8**), and methylgallate (**9**).

Kinetic Measurements. To further characterize the scavenging activity of the hexahydroxydiphenyl moiety within punicalagin (**1**) and pyrogallol (**8**), which are the only simple structures that react with TNTPM, we made kinetic measurements of the reactions of DHHDP (**2**) and pyrogallol (**8**) with TNPTM. The course of the reaction was monitored using EPR by recording the decay of the TNPTM signal as a result of the addition of the polyphenol in $CHCl_3$/MeOH (2:1) at a molar ratio TNPTM/polyphenol of 5:1. To calculate the stoichiometric factor, the reaction was monitored to completion over a period of 48 h.

dx.doi.org/10.1021/jf204059x | J. Agric. Food Chem. XXXX, XXX, XXX−XXX

Table 1. Scavenging Capacity of Ellagitannins and Flavanols against Stable Radicals[a]

radical	polyphenol	EC_{50} $\mu g\ \mu mol^{-1}$	EC_{50} $\mu mol\ \mu mol^{-1}$	ARP[b]	e/H[c]
TNPTM	ellagitannins				
	1	50.3 (2.6)	0.15 (0.01)	6.5 (0.3)	3.3 (0.2)
	2	51.2 (0.0)	0.26 (0.00)	3.9 (0.1)	1.9 (0.0)
	3	–[d]	–	–	–
	flavanols				
	4	–	–	–	–
	5	55.2 (6.5)	0.18 (0.02)	5.6 (0.6)	2.8 (0.3)
	6	–	–	–	–
	7	83.3 (5.9)	0.18 (0.01)	5.5 (0.3)	2.7 (0.1)
	simple phenols				
	8	21.7 (1.6)	0.17 (0.01)	5.8 (0.4)	2.9 (0.2)
	9	–	–	–	–
HNTTM	ellagitannins				
	1	38.1 (3.9)	0.04 (0.00)	28.4 (2.7)	14.2 (1.4)
	2	42.2 (5.0)	0.12 (0.02)	8.7 (1.1)	4.3 (0.5)
	3	30.4 (1.1)	0.10 (0.00)	9.9 (0.3)	5.0 (0.1)
	flavanols				
	4	54.0 (4.0)	0.19 (0.02)	5.3 (0.5)	2.7 (0.2)
	5	50.2 (2.2)	0.16 (0.01)	6.2 (0.0)	3.1 (0.1)
	6	24.0 (2.6)	0.05 (0.01)	18.5 (2.0)	9.3 (1.0)
	7	38.3 (3.2)	0.08 (0.01)	11.9 (0.9)	5.9 (0.4)
	simple phenols				
	8	19.7 (1.2)	0.16 (0.01)	6.4 (0.4)	3.2 (0.2)
	9	30.2 (2.5)	0.15 (0.01)	6.5 (0.5)	3.2 (0.3)
DPPH	ellagitannins				
	1	20.0 (1.6)	0.02 (0.00)	55.0 (3.3)	27.5 (1.7)
	2	31.2 (1.6)	0.08 (0.00)	12.2 (0.4)	6.1 (0.2)
	3	22.1 (0.2)	0.07 (0.00)	13.7 (0.3)	6.8 (0.1)
	flavanols				
	4	36.8 (1.6)	0.13 (0.01)	7.9 (0.3)	3.9 (0.2)
	5	31.5 (1.8)	0.11 (0.00)	9.1 (0.3)	4.6 (0.1)
	6	28.9 (3.1)	0.07 (0.01)	15.4 (1.6)	7.8 (0.8)
	7	31.4 (6.1)	0.06 (0.02)	17.3 (3.4)	8.7 (1.7)
	simple phenols				
	8	12.6 (1.2)	0.10 (0.01)	10.0 (0.8)	5.0 (0.4)
	9	31.7 (3.2)	0.17 (0.02)	5.8 (0.6)	2.9 (0.3)

[a]Values are means (standard deviation), $n = 3$. [b]Antiradical power ($1/EC_{50}$ ($\mu g\ \mu mol^{-1}$)). [c]Moles of reduced radical per mole of polyphenol ($1/(2 \times EC_{50})$) corresponding to the number of electrons or hydrogen atoms transferred per molecule of polyphenol. [d]EC_{50} ($\mu g\ \mu mol^{-1}$) $\geq$ 132).

The rate constants and stoichiometric factors for these reactions are given in Table 2. The reaction with pyrogallol (**8**) was faster than that with DHHDP (**2**), and the stoichiometric factors were consistent with those estimated from the concentration/activity curve and shown in Table 1, roughly corresponding to 2 and 3 electrons from DHHDP (**2**) and pyrogallol (**8**), respectively. As commented before, methylgallate (**9**) did not reduce the TNPTM.

Anodic Onset Potentials. To explain why most of the phenolic hydroxyls reacted with HNTTM and only some of them with TNPTM, the anodic onset potentials for the oxidation of DHHDP (**2**), ellagic acid (**3**), pyrogallol (**8**), and methylgallate (**9**) were measured by cyclic voltammetry in DMF solutions. The comparative results obtained at 100 mV s^{-1} are summarized in Table 3. The lower the anodic onset potential, the more reactive the phenolic hydroxyl is. Results in Table 3 show that the compounds reactive against TNPTM (**2** and **8**) possess the lowest anodic onset potentials.

Cell Viability of HT-29 Colon Adenocarcinoma Cells. The influence of polyphenols **1**–**9** on the viability of HT-29 colon cells was measured in regular DMEM and also in the presence of catalase[30] to account for artifactual results due to the formation of H_2O_2 from the superoxide radical generated in the medium by electron transfer to oxygen.[3] The results are presented in Table 4.

The active compounds were those that contained pyrogallol, hexahydroxydiphenyl, or gallate moieties (ellagitannins **1** and **2**; flavanols **5** and **7**; and simple pyrogallol **8**). Polyphenols bearing only two geminal hydroxyls (compounds **3** and **4**) were inactive. The effect on cell viability recorded for pyrogallol and structures containing pyrogallol (compounds **5** and **7**) was, at least in part, artifactual because catalase diminished or eliminated the activity. In contrast, catalase did not influence the activity of ellagitannins **1** and **3**, as well as the related compound **2**, which means that this activity was not due to extracellular hydrogen peroxide.[31]

dx.doi.org/10.1021/jf204059x | J. Agric. Food Chem. XXXX, XXX, XXX–XXX

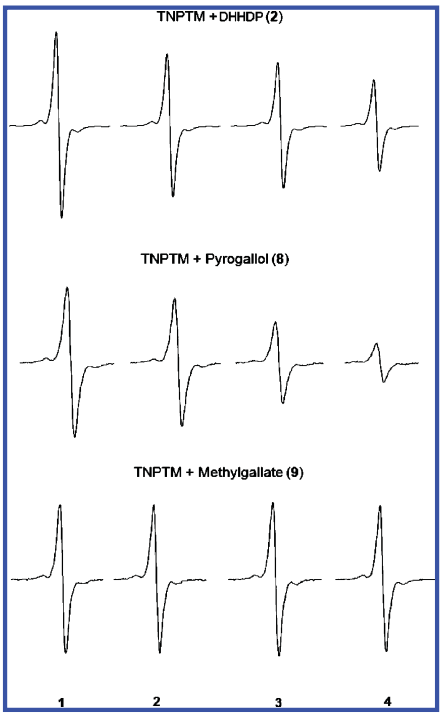

Figure 2. EPR spectra of TNPTM, initial concentration ~120 μM, upon reaction with DHHDP (**2**), pyrogallol (**8**), and methylgallate (**9**) at different initial concentrations: 0 μM (1), 5.7 μM (2), 18.1 μM (3), and 55.1 μM (4) for 48 h. Lande's factor for the TNPTM, g = 2.0026.

Table 2. Rate Constants and Stoichiometric Factors for the Reaction of TNPTM with DHHBD (2), Pyrogallol (8), and Methylgallate (9) in $CHCl_3$/MeOH (2:1)

polyphenol	TNPTM/polyphenol molar ratio[a]	k[b] (M^{-1} s^{-1})	n[c]
2	4.9–4.9	0.115 (0.010)	1.9
8	4.6–4.6	0.338 (0.070)	3.6
9	4.3–4.0	–	–

[a]Range of ratios for a number of experiments between 2 and 5. Initial concentrations around 120 and 24 μM (molar ratio, 5:1) for TNPTM and polyphenol, respectively. [b]Values are means (standard deviation), n = 2–5. [c]Moles of reduced radical per mole of polyphenol corresponding to the number of electrons transferred per molecule of polyphenol.

DISCUSSION

The biological relevance of polyphenols is still a matter of debate, even after decades of intense research. Particularly, the significant structural features behind polyphenol activities have not been satisfactorily established, probably because they interact with live systems in complex ways at different levels including redox reactions and protein–ligand interactions. Polyphenols may modify redox homeostasis by scavenging reactive radicals, by generating reactive radicals, or by a combination of the two. The electron transfer capacity of different phenolic hydroxyl groups determines the kind of effect elicited, if any. Pyrogallol (**8**) (three geminal hydroxyls) and polyphenols such as EGC (**5**) and EGCG (**7**) (gallocatechins), which contain this substructure, may be both scavengers and generators of free radicals and are among the most biologically active polyphenols. The gallate moiety (pyrogallol with an esterified carboxylate function) is another important structural feature. It has been widely reported that polyphenols that contain pyrogallols and/or gallates lower cell viability either by disrupting the cell cycle and triggering apoptosis or by other effects that involve redox reactions and/or protein–ligand interactions.[32−34] We focus our attention here on the redox reactions of polyphenols by using chemosensors that are able to discriminate between different phenolic hydroxyls according to their redox potentials. The results are compared with the influence on cell viability in vitro. Polyphenols **1**–**9** reacted with HNTTM, whereas only some of them (**1**, **2**, **5**, **7**, **8**) were able to reduce the TNPTM radical. This was expected for the structures containing pyrogallol (**5**, **7**, **8**)[20] and not for the ellagitanin punicalagin (**1**) because ellagic acid (**3**) was inactive against TNPTM. As expected, TNPTM did not react with catechols (two geminal hydroxyls) (**4**) or gallates (**6**, **9**). Punicalagin (**1**) contains an ellagic acid conjugated substructure and other substructures composed of gallate moieties linked by C–C bonds to each other (hexahydroxydiphenyl) or to an ellagic acid moiety. The stable radical TNPTM is reactive against these C–C-linked gallates as proven by the redox behavior of synthetic DHHDP (**2**). This dimeric gallate transferred two electrons to TNPTM, whereas methylgallate (**9**) was unreactive (Tables 1 and 2, last columns). The C–C bond appears to have activated two hydroxyl positions. Inspection of the structure of punicalagin (**1**) and the number of electrons (3.3) transferred to TNPTM (Table 1, last column) leads us to hypothesize that the C–C bond between the gallate moiety and the ellagic acid moiety produces the same hydroxyl activation that we detected for the

Table 3. Anodic Onset Potential (AOP) of Polyphenolic Moieties

polyphenol	AOP[a] (V vs SCE)
DHHDP (**2**)	0.50
ellagic acid (**3**)	0.64
pyrogallol (**8**)	0.45
methylgallate (**9**)	0.65

[a]10^{-3} M in DMF solutions with 0.1 M Bu_4NClO_4 on Pt at 100 mV s^{-1} and 25 °C.

Table 4. Viability of HT-29 Cells in the Presence of Polyphenols

	IC_{50}[a]	
polyphenol	μg mL^{-1} in DMEM	μg mL^{-1} in DMEM with catalase
ellagitannins and related compounds		
1	21.5 (3.5)	14.4 (0.4)
2	32.5 (3.9)	34.1 (0.5)
3	≥100	≥100
flavanols		
4	≥100	≥100
5	24.1 (2.7)	≥100
6	53.7 (12.0)	58.9 (8.0)
7	17.5 (3.2)	47.9 (8.0)
simple phenols		
8	5.6 (0.5)	71.4 (7.5)
9	24.6 (8.3)	31.6 (1.8)

[a]Cells were treated with the compounds for 72 h, and viability was monitored with MTT. Values are means (standard deviation), n = 2–3

dx.doi.org/10.1021/jf204059x | J. Agric. Food Chem. XXXX, XXX, XXX–XXX

hexahydroxydiphenyl substructure. The formation of hydrogen bonds between hydroxyls ortho to the C−C bond may be behind the reactivity of these diphenyl structures.[35] This result was corroborated by measuring the anionic onset potential (AOP) of the gallate conjugates **2**, **3**, and **9** and pyrogallol **8**. The reactivity of polyphenols given by the AOP followed the order **8** > **2** > **3** = **9** (Table 3). These results are also in agreement with the kinetic measurements (Table 2).

The outcome of the cell viability assay cannot be related to the redox behavior of the polyphenolic structures in a straightforward way because polyphenols influence cell functions by more than one mechanism. Whatever the case, our results (Table 3) corroborate that pyrogallols and gallates are active against colon adenocarcinoma cells and suggest that the hydroxydiphenyl substructure of punicalagin may play a role involving a particularly reactive redox position. As some of the effects ascribed to pyrogallols in vitro may be due to the artifactual generation of H_2O_2 in the culture medium,[3,15] we ran the in vitro experiments in the presence of catalase. This resulted in a significant decrease in the activity of the polyphenols that contained pyrogallols in their structure. This does not alter the fact that pyrogallols are the most reactive species, because they must be able to generate the superoxide radical as the first step in the formation of H_2O_2; it just shows that the experimental setup does not adequately mimic the situation in vivo, where the extracellular oxygen concentration is much lower.[3] Punicalagin (**1**) affected cell viability as effectively as gallocatechins. In this case, the effect was not artifactual because it was not affected by the addition of catalase to the medium, which suggests that punicalagin (**1**) did not generate the superoxide radical extracellularly, at least not to a sufficient extent to affect cell viability.

By combining the outcome of HNTTM and TNPTM assays, we may generate a picture of both the total electron transfer capacity of polyphenols and the presence of highly reactive hydroxyls. TNPTM detects the most redox reactive phenolics (e.g., pyrogallols and C−C-linked gallates) and may anticipate their influence on cell viability. Independent of whether these highly reactive positions directly scavenge radicals or trigger antioxidant defense responses, TNPTM is a useful chemical probe that easily detects the presence of some of the most biologically significant phenolic structures. This will be useful when the antioxidant potential of extracts and functional foods as well as new synthetic polyphenolic molecules is examined.

In conclusion, we show here that substructures of punicalagin that contain gallate moieties, linked either to each other (hexahydroxydiphenyl moieties) or to the ellagic acid moiety by C−C bonds, present phenolic hydroxyls that are more redox reactive than those in simple gallates and that these structures can be detected by the stable radical TNPTM. The most reactive polyphenolic structures are also those that have the greatest effect on cell viability in vitro. The chemosensor TNPTM may be a useful tool for detecting other potentially beneficial highly reactive polyphenols from natural sources.

■ ASSOCIATED CONTENT

Supporting Information

IR spectrum of TNPTM; plots of scavenging activity against TNPTM, HNTTM and DPPH; kinetics of the reaction between TNPTM and HDDP/pyrogallol; plots of cell viability on HT-29 cells. This material is available free of charge via the Internet at http://pubs.acs.org.

■ AUTHOR INFORMATION

Corresponding Author

*Phone: +34 93 400 61 12. Fax: +34 93 204 59 04. E-mail: josepluis.torres@iqac.csic.es.

Funding

This work was supported by the Spanish Ministry of Education and Science (research grants AGL2006-12210-C03-02/ALI; SAF2008-00164; AGL2009-12374-C03-03/ALI), the Instituto de Salud Carlos III and European Regional Development Fund (ISCIII-RTICC, RD06/0020/0046), the Generalitat de Catalunya (2009SGR1308, 2009CTP 00026, and Icrea Academia award 2010 granted to M.C.), and the European Commission (Etherpaths Project KBBE-Grant Agreement 222639).

■ ACKNOWLEDGMENTS

We are grateful to the EPR facility at the Institut de Química Avançada de Catalunya (CSIC) for recording the EPR spectra. We appreciate language revision by Christopher Evans.

■ ABBREVIATIONS USED

DMEM, Dulbecco Modified Eagle's Medium; EGCG, epigallocatechin gallate; EGC, epigallocatechin; EC, epicatechin; ECG, epicatechin gallate; DHHDP, dimethylhexahydroxydiphenyl dicarboxylate; HHDP, hexahydroxy-2,2′-diphenyl; HNTTM, tris(2,4,6-trichloro-3,5-dinitrophenyl)methyl; TNPTM, tris(2,3,5,6-tetrachloro-4-nitrophenyl)methyl; DPPH, 1,1-diphenyl-2-picrylhydrazyl.

■ REFERENCES

(1) Harman, D. Aging: a theory based on free radical and radiation chemistry. *J. Gerontol.* **1956**, *11*, 298−300.

(2) Harman, D. The aging process. *Proc. Natl. Acad. Sci. U.S.A.* **1981**, *78*, 7124−7128.

(3) Halliwell, B. Are polyphenols antioxidants or pro-oxidants? What do we learn from cell culture and in vivo studies? *Arch. Biochem. Biophys.* **2008**, *476*, 107−112.

(4) Kuhnle, G.; Spencer, J. P. E; Schroeter, H.; Shenoy, B.; Debnam, E. S.; Srai, S. K. S.; Rice-Evans, C.; Hahn, U. Epicatechin and catechin are *O*-methylated and glucuronidated in the small intestine. *Biochem. Biophys. Res. Commun.* **2000**, *277*, 507−512.

(5) Gonthier, M. P.; Donovan, J. L.; Texier, O.; Felgines, C.; Rémésy, C.; Scalbert, A. Metabolism of dietary procyanidins in rats. *Free Radical Biol. Med.* **2003**, *35*, 837−844.

(6) Halliwell, B.; Zhao, K. C.; Whiteman, M. The gastrointestinal tract: a major site of antioxidant action? *Free Radical Res.* **2000**, *33*, 819−830.

(7) Lambert, J. D.; Sang, S. M.; Yang, C. S. Possible controversy over dietary polyphenols: benefits vs risks. *Chem. Res. Toxicol.* **2007**, *20*, 583−585.

(8) Mattson, M. P. Hormesis defined. *Ageing Res. Rev.* **2008**, *7*, 1−7.

(9) Pazos, M.; Gallardo, J. M.; Torres, J. L.; Medina, I. Activity of grape polyphenols as inhibitors of the oxidation of fish lipids and frozen fish muscle. *Food Chem.* **2005**, *92*, 547−557.

(10) Liu, Z.-Q. Chemical methods to evaluate antioxidant ability. *Chem. Rev.* **2010**, *110*, 5675−5691.

(11) Foti, M.; Ingold, K. U.; Lusztyk, J. The surprisingly high reactivity of phenoxyl radicals. *J. Am. Chem. Soc.* **1994**, *116*, 9440−9447.

(12) Foti, M.; Ruberto, G. Kinetic solvent effects on phenolic antioxidants determined by spectrophotometric measurements. *J. Agric. Food Chem.* **2000**, *49*, 342−348.

(13) Carreras, A.; Esparbé, I.; Brillas, E.; Rius, J.; Torres, J. L.; Juliá, L. Oxidant activity of tris(2,4,6-trichloro-3,5-dinitrophenyl)methyl radical with catechol and pyrogallol. Mechanistic considerations. *J. Org. Chem.* **2009**, *74*, 2368−2373.

(14) Kondo, K.; Kurihara, M.; Miyata, N.; Suzuki, T.; Toyoda, M. Scavenging mechanisms of (−)-epigallocatechin gallate and (−)-epicatechin gallate on peroxyl radicals and formation of superoxide during the inhibitory action. *Free Radical Biol. Med.* **1999**, *27*, 855−863.
(15) Long, L. H.; Clement, M. V.; Halliwell, B. Artifacts in cell culture: rapid generation of hydrogen peroxide on addition of (−)-epigallocatechin, (−)-epigallocatechin gallate, (+)-catechin, and quercetin to commonly used cell culture media. *Biochem. Biophys. Res. Commun.* **2000**, *273*, 50−53.
(16) Azam, S.; Hadi, N.; Khan, N. U.; Hadi, S. M. Prooxidant property of green tea polyphenols epicatechin and epigallocatechin-3-gallate: implications for anticancer properties. *Toxicol. in Vitro* **2004**, *18*, 555−561.
(17) Alanko, J.; Riutta, A.; Holm, P.; Mucha, I.; Vapaatalo, H.; Metsä-Ketelä, T. Modulation of arachidonic acid metabolism by phenols: relation to their structure and antioxidant/prooxidant properties. *Free Radical Biol. Med.* **1999**, *26*, 193−201.
(18) Afanas'ev, I. Signaling functions of free radicals superoxide and nitric oxide under physiological and pathological conditions. *Mol. Biotechnol.* **2007**, *37*, 2−4.
(19) Jiménez, A.; Selga, A.; Torres, J. L.; Juliá, L. Reducing activity of polyphenols with stable radicals of the TTM series. Electron transfer versus H-abstraction reactions in flavan-3-ols. *Org. Lett.* **2004**, *6*, 4583−4586.
(20) Torres, J. L.; Carreras, A.; Jiménez, A.; Brillas, E.; Torrelles, X.; Rius, J.; Juliá, L. Reducing power of simple polyphenols by electron-transfer reactions using a new stable radical of the PTM series, tris(2,3,5,6-tetrachloro-4-nitrophenyl)methyl radical. *J. Org. Chem.* **2007**, *72*, 3750−3756.
(21) Touriño, S.; Lizárraga, D.; Carreras, A.; Lorenzo, S.; Ugartondo, V.; Mitjans, M.; Vinardell, M. P.; Juliá, L.; Cascante, M.; Torres, J. L. Highly galloylated tannin fractions from witch hazel (*Hamamelis virginiana*) bark: electron transfer capacity, in vitro antioxidant activity, and effects on skin-related cells. *Chem. Res. Toxicol.* **2008**, *21*, 696−704.
(22) Yang, J.; Liu, G.-Y.; Lu, D.-L.; Dai, F.; Qian, Y.-P.; Jin, X.-L.; Zhou, B. Hybrid-increased radical-scavenging activity of resveratrol derivatives by incorporating a chroman moiety of vitamin E. *Chem.—Eur. J.* **2010**, *16*, 12808−12813.
(23) Gil, M. I.; Tomás-Barberán, F. A.; Hess-Pierce, B.; Holcroft, D. M.; Kader, A. A. Antioxidant activity of pomegranate juice and its relationship with phenolic composition and processing. *J. Agric. Food Chem.* **2000**, *48*, 4581−4589.
(24) Cerdá, B.; Tomás-Barberán, F. A.; Espín, J. C. Metabolism of antioxidant and chemopreventive ellagitannins from strawberries, raspberries, walnuts, and oak-aged wine in humans: Identification of biomarkers and individual variability. *J. Agric. Food Chem.* **2005**, *53*, 227−235.
(25) Fernandes, A.; Fernandes, I.; Cruz, L.; Mateus, N.; Cabral, M.; de Freitas, V. Antioxidant and biological properties of bioactive phenolic compounds from *Quercus suber* L. *J. Agric. Food Chem.* **2009**, *57*, 11154−11160.
(26) Wang, H. F.; Helliwell, K.; You, X. Q. Isocratic elution system for the determination of catechins, caffeine and gallic acid in green tea using HPLC. *Food Chem.* **2000**, *68*, 115−121.
(27) Aron, P. M.; Kennedy, J. A. Flavan-3-ols: nature, occurrence and biological activity. *Mol. Nutr. Food Res.* **2008**, *52*, 79−104.
(28) Quideau, S.; Feldman, K. S. Ellagitannin chemistry. The first synthesis of dehydrohexahydroxydiphenoate esters from oxidative coupling of unetherified methyl gallate. *J. Org. Chem.* **1997**, *62*, 8809−8813.
(29) Goupy, P.; Dufour, C.; Loonis, M.; Dangles, O. Quantitative kinetic analysis of hydrogen transfer reactions from dietary polyphenols to the DPPH radical. *J. Agric. Food Chem.* **2003**, *51*, 615−622.
(30) Bellion, P.; Hofmann, T.; Pool-Zobel, B. L.; Will, F.; Dietrich, H.; Knaup, B.; Richling, E.; Baum, M.; Eisenbrand, G.; Janzowski, C. Antioxidant effectiveness of phenolic apple juice extracts and their gut fermentation products in the human colon carcinoma cell line Caco-2. *J. Agric. Food Chem.* **2008**, *56*, 6310−6317.
(31) Sakagami, H.; Jiang, Y.; Kusama, K.; Atsumi, T.; Ueha, T.; Toguchi, M.; Iwakura, I.; Satoh, K.; Ito, H.; Hatano, T.; Yoshida, T. Cytotoxic activity of hydrolyzable tannins against human oral tumor cell lines − a possible mechanism. *Phytomedicine* **2000**, *7*, 39−47.
(32) Lizárraga, D.; Lozano, C.; Briedé, J. J.; van Delft, J. H.; Touriño, S.; Centelles, J. J.; Torres, J. L.; Cascante, M. The importance of polymerization and galloylation for the antiproliferative properties of procyanidin-rich natural extracts. *FEBS J.* **2007**, *274*, 4802−4811.
(33) Galati, G.; Lin, A.; Sultan, A. M.; O'Brien, P. J. Cellular and in vivo hepatotoxicity caused by green tea phenolic acids and catechins. *Free Radical Biol. Med.* **2006**, *40*, 570−580.
(34) Fernandes, I.; Faria, A.; Azevedo, J.; Soares, S.; Calhau, C. A.; De Freitas, V.; Mateus, N. Influence of anthocyanins, derivative pigments and other catechol and pyrogallol-type phenolics on breast cancer cell proliferation. *J. Agric. Food Chem.* **2010**, *58*, 3785−3792.
(35) Amorati, R.; Lucarini, M.; Mugnaini, V.; Pedulli, G. F. Antioxidant activity of o-bisphenols: the role of intramolecular hydrogen bonding. *J. Org. Chem.* **2003**, *68*, 5198−5204.

Highly Galloylated Tannin Fractions from Witch Hazel (*Hamamelis virginiana*) Bark: Electron Transfer Capacity, In Vitro Antioxidant Activity, and Effects on Skin-Related Cells

Sonia Touriño,[†] Daneida Lizárraga,[‡] Anna Carreras,[†] Sonia Lorenzo,[†] Vanessa Ugartondo,[§] Montserrat Mitjans,[§] María Pilar Vinardell,[§] Luis Juliá,[†] Marta Cascante,[‡] and Josep Lluís Torres*[,†]

Institute for Chemical and Environmental Research (IIQAB-CSIC), Jordi Girona 18-26, 08034 Barcelona, Department of Biochemistry and Molecular Biology, Associated Unit to CSIC, Universitat de Barcelona, Avinguda Diagonal 645, 08028 Barcelona, and Departament de Fisiologia, Associated Unit to CSIC, Facultat de Farmàcia, Universitat de Barcelona, Av. Joan XXIII s/n, 08028 Barcelona, Spain

Received December 5, 2007

Witch hazel (*Hammamelis virginiana*) bark is a rich source of both condensed and hydrolizable oligomeric tannins. From a polyphenolic extract soluble in both ethyl acetate and water, we have generated fractions rich in pyrogallol-containing polyphenols (proanthocyanidins, gallotannins, and gallates). The mixtures were highly active as free radical scavengers against ABTS, DPPH (hydrogen donation and electron transfer), and HNTTM (electron transfer). They were also able to reduce the newly introduced TNPTM radical, meaning that they included some highly reactive components. Witch hazel phenolics protected red blood cells from free radical-induced hemolysis and were mildly cytotoxic to 3T3 fibroblasts and HaCat keratinocytes. They also inhibited the proliferation of tumoral SK-Mel 28 melanoma cells at lower concentrations than grape and pine procyanidins. The high content in pyrogallol moieties may be behind the effect of witch hazel phenolics on skin cells. Because the most cytotoxic and antiproliferative mixtures were also the most efficient as electron transfer agents, we hypothesize that the final putative antioxidant effect of polyphenols may be in part attributed to the stimulation of defense systems by mild prooxidant challenges provided by reactive oxygen species generated through redox cycling.

Introduction

Phenolics from plants are appreciated for their putative health-promoting properties (*1, 2*). The antioxidant activity, taken in a broad sense, is believed to be responsible for the preventative properties of flavonoids. The main mechanisms behind this antioxidant activity are direct free radical scavenging (*3, 4*), transition metal chelation (*5, 6*), and maintenance of endogenous antioxidants such as the glutathione and superoxide dismutase systems (*7*). Interestingly, polyphenols may be antioxidant and prooxidant at the same time (*8, 9*). While all phenolics are scavengers of reactive oxygen species (ROS), strongly reducing species such as pyrogallol (three adjacent phenol groups) containing (−)-epigallocatechin (EGC)[1] and (−)-epigallocatechingallate (EGCG) are able to form the superoxide radical from molecular oxygen (*10, 11*) (Figure 1). Moreover, the *ortho*-quinones formed by the loss of two electrons from pyrogallol and catechol moieties may participate in enzymatic redox cycling with the formation of superoxide and other ROS (*12, 13*). Apart from their participation in redox-related events, tannins may modify cell functions by substrate−receptor interactions (e.g., kinase inhibition), which may or may not involve redox reactions (*14*). This ensemble of activities influence cell proliferation, cell cycle regulation, and apoptosis, and the pyrogallol moieties, both on ring B and as gallate ester at C-3, appear to play a pivotal role (*15, 16*).

Whether all of these effects detected in vitro have any significance in vivo is controversial. Because polyphenols are extensively metabolized into less reactive species (*17*) and the cell redox system is too carefully regulated to be influenced by low concentrations of scavengers, it has been argued that polyphenols may not exert any significant effect on the cell redox status of complex organisms (*18, 19*). However, it can also be argued that polyphenols, particularly the less metabolized oligomeric species, may still have a significant influence on organs such as the skin and the intestinal tract (*20, 21*). In any case, flavonoid-containing nutritional supplements and over the counter drugs have become so popular and available that people risk overdosing. This is why it is important to examine the action of these plant actives from different angles and to evaluate their putative benefits and risks. Most of the information available in the literature about the antioxidant/prooxidant activities and substrate−receptor interactions of phenolics relates to monomeric EGCG and quercetin (*13, 14, 22*). Because the redox and binding properties of phenolics are affected by polymerization

* To whom correspondence should be addressed. Tel: 34 93 400 61 12. Fax: 34 93 204 59 04. E-mail: jltqbp@iiqab.csic.es.

[†] CSIC.

[‡] Department of Biochemistry and Molecular Biology, Universitat de Barcelona.

[§] Departament de Fisiologia, Universitat de Barcelona.

[1] Abbreviations: AAPH, 2,2′-azobis(amidinopropane)dihydrochloride; ARC, antiradical capacity; C, catechin; Cya, cysteamine; EC, epicatechin; ECG, epicatechin-gallate; EGC, epigallocatechin; EGCG, epigallocatechin-gallate; GC, gallocatechin; DMEM, Dulbecco's modified Eagle's medium; DPPH, 1,1-diphenyl-2-picrylhydrazyl free radical; FCS, fetal calf serum; HNTTM, Tris(2,3,6-trichloro-3,5-dinitrophenyl)methyl; HPLC-DAD, high-performance liquid chromatography with diode array detection; MTT, 3-[4,5-dimethylthiazol-2yl]-2,5-diphenyltetrazolium bromide; NRU, neutral red uptake; RP-HPLC, reversed-phase high-performance liquid chromatography; RCBs, red blood cells; TFA, trifluoroacetic acid; Trolox, 2,5,7,8-tetramethylchroman-2-carboxylic acid; TNPTM, tris(2,3,5,6-tetrachloro-4-nitrophenyl)-methyl.

10.1021/tx700425n CCC: $40.75
Published on Web 03/01/2008

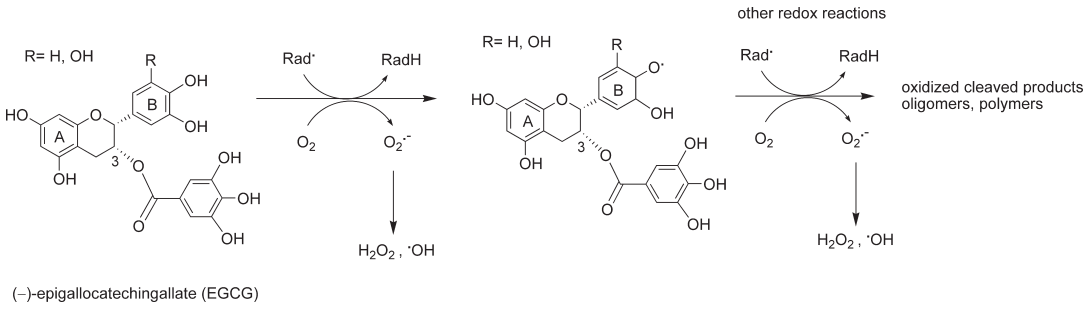

Figure 1. Scavenging of ROS and superoxide formation by catechins.

(*23, 24*), it is of great interest to evaluate the activity of the oligomers (e.g., proanthocyanidins) on cells. We have previously reported the extraction and fractionation of phenolics from grape pomace and pine bark and the evaluation of their free radical scavenging capacity, antioxidant activity in vitro, cytotoxicity on nontumoral 3T3 fibroblasts and keratinocites, and antiproliferative activity on melanoma cells (*25–27*). Polyphenols from grape and pine were essentially procyanidins (oligomeric catechins with only two hydroxyls on ring B, catechol moiety) with low gallate content or no galloylation at all, respectively. The fractions were effective free radical scavenger antiproliferative agents against skin and colon tumoral cells and weakly cytotoxic. To test the behavior of phenolics with high pyrogallol content, we have now prepared and evaluated a homologous series of fractions from witch hazel (*Hamamelis virginiana*) bark, which contains gallocatechins and prodelphinidins (monomeric and oligomeric catechins with three hydroxyls on ring B) with a high proportion of gallates. The gallates come from both condensed and hydrolyzable tannins. As compared to grape and pine, phenolics from hamamelis showed higher electron transfer capacity, cytotoxicity, and antiproliferative activity against skin-related cell lines.

Experimental Procedures

The starting material was witch hazel (*H. virginiana*) chopped stems provided by Martin Bauer GMBH (Alveslohe, Germany). The sample was stored in the dark at room temperature.

Solvents and Reagents. For extraction, deionized water, bulk EtOH (Momplet y Esteban, Barcelona, Spain), bulk acetone (Quimivita, Sant Adrià del Besòs, Spain), and bulk hexane (Quimivita) were used for polyphenol extraction. For purification, deionized water, analytical grade MeOH (Panreac, Montcada i Reixac, Spain), and analytical grade acetone (Carlo Erba, Milano, Italy) and preparative grade CH_3CN (E. Merck, Darmstadt, Germany) were used for semipreparative and preparative chromatography; milli-Q water and HPLC grade CH_3CN (E. Merck) were used for analytical reversed-phase high-performance liquid chromatography (RP-HPLC). Analytical grade MeOH (Panreac) was used for thioacidolysis and free radical scavenging assays, and analytical grade CH_3Cl (Panreac) was used for the electron transfer assays. Trifluoroacetic acid (TFA, Fluorochem, Derbyshire, United Kingdom) biotech grade was distilled in-house. Cysteamine hydrochloride was from Sigma-Aldrich Chemical (Steinheim, Germany), and 37% HCl and acetic acid were from E. Merck. Triethylamine (E. Merck) was of buffer grade. Deuterated solvents for nuclear magnetic resonance (NMR) were from SDS (Peypin, France). 1,1-Diphenyl-2-picrylhydrazyl free radical (DPPH) (95%) was from Aldrich (Gillingham-Dorset, United Kingdom), 6-hydroxy-2,5,7,8-tetramethyl-chroman-2-carboxylic acid (Trolox) (97%) was from Aldrich (Milwaukee, WI), and standards of (−)-epicatechin, (+)-catechin, (+)-gallocatechin (−)-epigallocatechin, (−)-epigallocatechin 3-*O*-gallate, gallic acid, methyl gallate, and hamamelitannin were purchased from Sigma Chemical (St. Louis, MO). 4-β-(2-Aminoethylthio)catechin, 4-β-(2-aminoethylthio)epicatechin, β-(2-aminoethylthio)epicatechin-3-*O*-gallate, 4-β-(2-aminoethylthio)epigallocatechin, and β-(2-aminoethylthio)epigallocatechin-3-*O*-gallate were synthesized and purified from grape and witch hazel extracts essentially as described (*28*). 2,2′-Azinobis-(3-ethylbenzothiazoline-6-sulfonic acid) (ABTS) crystallized diammonium salt, horseradish peroxidase type IV (RZ A403/A275 <3) and 2,2′-azobis(amidinopropane)dihydrochloride (AAPH) were obtained from Sigma Chemical. Hydrogen peroxide (3% v/v) was from Sigma Chemical. Tris-(2,4,6-trichloro-3,5-dinitrophenyl)-methyl (HNTTM) and tris(2,3,5,6-tetrachloro-4-nitrophenyl)methyl (TNPTM) radicals were synthesized as described (*29, 30*). Dulbecco's modified Eagle's medium (DMEM) and Dulbecco's phosphate buffer saline were from Gibco-BRL (Eggenstein, Germany), fetal calf serum (FCS) was from Invitrogen (Carlsbad, CA), and trypsin EDTA solution C (0.05% trypsin–0.02% EDTA) was from Biological Industries (Kibbutz Beit Haemet, Israel). 3-[4,5-Dimethylthiazol-2yl]-2,5-diphenyltetrazolium bromide (MTT) was from Sigma Chemical.

Extraction and Solvent Fractionation. The preparation of the crude extract was performed using already described methodology (*25, 31, 32*). Brief, witch hazel chopped stems (3 kg) were incubated with an acetone–water mixture (7:3, 10.5 L) for a period of 24 h at room temperature, with occasional shaking. The solid was filtered off, and the acetone was evaporated at reduced pressure. The remaining solution was defatted with *n*-hexane (3 × 300 mL), and the oligomeric fraction was extracted with ethyl acetate (3 × 600 mL). This organic phase was dried under vacuum, the pellet was dissolved in deionized water, and the solution was filtered through a porous plate. The dry fraction OWH (28.5 g), soluble in both ethyl acetate and water, was obtained by lyophilization.

Chromatographic Fractionation. Fractions IH (hydrophilic) and IIH (hydrophobic) were obtained by preparative RP-HPLC essentially as described before (*26, 33*). The rest of the fractions were generated from these two or directly from OWH by semipreparative chromatography on Toyopearl TSK HW-40F (TosoHass, Tokyo, Japan) following a protocol previously described by the authors (*25, 26*) (Scheme 1). The phenolics were eluted with MeOH and water/acetone 1:1, evaporated almost to dryness, redissolved in 100 mL of Milli-Q water, and freeze-dried; from OWH, 315 mg of IIIH and 573 mg of IVH; from fraction IH, 235 mg of VH and 336 mg of VIH; and from fraction IIH, 126 mg of VIIH and 468 mg of VIIIH. The fractions were analyzed by high-performance liquid chromatography with diode array detection (HPLC-DAD) using a Hitachi (San Jose, CA) Lachrom Elite HPLC system equipped with a quaternary pump, autosampler, in-line degassing unit, temperature control unit, photodiode array UV detector, and fitted with an analytical column Kromasil C18 (Teknokroma, Barcelona, Spain) (25 cm × 0.4 cm i.d., 100 Å, 5 μm particle size). Acquisitions were made using EZChrom Elite 3.1.3 from Scientific Software Inc. (Pleasanton, CA). Load, 40 μL, 10 μg; elution, (A) 0.1% (v/v) aqueous TFA and (B) 0.08% (v/v) TFA in water/CH_3CN 1:4,

Scheme 1

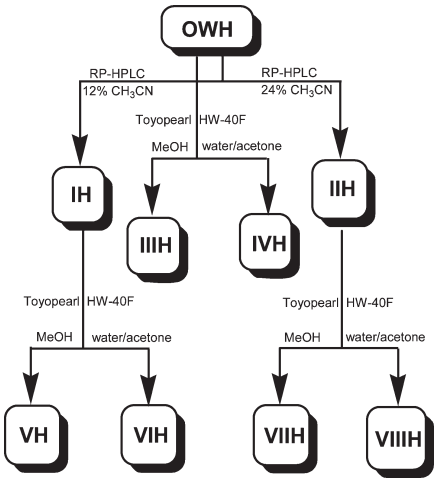

gradient 12−30% B over 30 min at a flow rate of 1 mL/min. DAD detection was performed from 210 to 380 nm. Data were acquired in triplicate.

Characterization by Thiolysis with Cysteamine and RP-HPLC. The size and composition of the proanthocyanidins within the fractions were estimated from the HPLC analysis of acid-catalyzed degradation of proanthocyanidins in the presence of cysteamine, followed by RP-HPLC as described (*34*). Briefly, the terminal flavan-3-ols units were released as such by acid cleavage in the presence of cysteamine whereas the extension moieties were released as the cysteamine derivatives on the fourth position of the flavanoid system. The resulting mixtures were submitted to analytical RP-HPLC using the same conditions described above for the intact samples, and the molar amount (nanomoles) of all of the released moieties was calculated from the peak areas and calibration curves obtained with pure samples. Terminal units: (+)-gallocatechin (GC), (−)-EGC, (+)-C, (−)-epicatechin (EC), (−)-EGCG, and (−)-ECG; extension units: cysteamine (Cya)-C, Cya-EC, Cya-EGC, Cya-EGCG, and Cya-ECG. Mean degree of polymerization (mDP) = total nmol/nmol terminal units.

Characterization by Chromatography Coupled to Mass Spectrometry. Liquid chromatography–mass spectrometry (LC-MS-MS) was used for the identification of gallotannins and gallates within the fractions. The analyses were carried out on an Agilent 1100 (Waldrom, Germany) coupled to an API 3000 triple quadrupole mass spectrometer (Perkin-Elmer Sciex, Concord, ON, Canada) at the Parc Cientific de la Universitat de Barcelona. Mass scan (MS) and daughter (MS/MS) spectra were measured from *m*/*z* 100 to 1500. Mass spectrometry data were acquired in the negative ionization mode.

ABTS Radical Cation Decolorization Assay. The method is based on the capacity of a sample to scavenge the ABTS radical cation ($ABTS^{\bullet+}$) as compared to a standard antioxidant (Trolox). $ABTS^{\bullet+}$was generated from ABTS as described (*35*) with some modifications (*26*). To prepare the initial $ABTS^{\bullet+}$ solution, 3‰ H_2O_2 (45μL) was added to a reaction mixture containing ABTS (54.9 mg, 1 mM) and horseradish peroxidase (HRP, 1.1 mg, 0.25 μM) in 50 mM gly HCl buffer, pH 4.5 (100 mL). The reaction mixture was left to stand at room temperature for 15 min in the dark. Then, the polyphenolic solutions (50 μL) at concentrations of 0.3, 0.2, 0.15, 0.10, and 0.05 mg/mL in MeOH were added to the $ABTS^{\bullet+}$ solution (1950 μL). The total time needed to carry out each assay was 20 min, including ABTS radical generation, addition of antioxidant, and acquisition of final absorbance value. The decrease of absorbance at 734 nm with respect to the 1 mM solution of $ABTS^{\bullet+}$ was recorded on a UV spectrophotometer Cary 300-Bio (Varian, Palo Alto, CA). The assay was performed in triplicate. The dose–response curves obtained with the antioxidant mixtures and Trolox were plotted as the percentage of absorbance decrease against the amount of antioxidants expressed as μg/mL. The total antioxidant activity (TAA) of the fractions was expressed in mmol Trolox equiv/g of OWH.

DPPH Assay. The antiradical efficiency of the fractions was evaluated by the DPPH stable radical method (*36, 37*). The samples (0.1 mL) were added to aliquots (3.9 mL) of a solution made up with DPPH (4.8 mg) in MeOH (200 mL), and the mixture was incubated for 1 h at room temperature in the dark. The initial concentration of DPPH, approximately 60 μM, was calculated for every experiment from a calibration curve made by measuring the absorbance at 517 nm of standard samples of DPPH at different concentrations. The equation of the curve was $Abs_{517nm} = 11345 \times C_{DPPH}$ as determined by linear regression. The results were plotted as the percentage of absorbance disappearance at 517 nm $[(1 - A/A_0) \times 100]$ against the amount of sample divided by the initial concentration of DPPH. Each point was acquired in triplicate. A dose–response curve was obtained for every fraction. ED_{50} corresponds to micrograms of fraction able to consume half the amount of free radical divided by micromoles of initial DPPH. The results were expressed as antiradical capacity (ARC), which is the inverse of ED_{50}. UV measurements were made on a UV spectrophotometer Cary 300-Bio (Varian).

Electron Transfer Capacity against HNTTM and TNPTM. The fractions were dissolved in CH_3Cl/MeOH (2:1) at different concentrations. Aliquots (1 mL) were added to a solution (1 mL) of HNTTM [120 μM in CH_3Cl/MeOH (2:1)] (*29*), and the mixture was incubated for 7 h. The exact initial concentration of radical, around 60 μM, was calculated for every experiment from calibration curves made by measuring the absorbance (A_0) at 385 nm of standard samples of the radical at different concentrations. The equations of the curve was $A_0 = 21170 \times C_{radical}$. The results were plotted as the percentage of absorbance disappearance $[(1 - A/A_0) \times 100]$ against the amount of sample divided by the initial micromoles of the radical as described for DPPH. Each point was acquired in triplicate. A dose–response curve was obtained for every fraction. The results were expressed as the efficient dose ED_{50} given as micromoles of fraction able to consume half the amount of free radical divided by micromoles of initial HNTTM.

The working conditions with TNPTM were essentially those described for HNTTM with some differences. The incubation time was 48 h, and the absorbance was measured at 378 nm. The equation for the calibration curve was $A_0 = 17153 \times C_{radical}$. The results were plotted as described for HNTTM. UV measurements were made on a UV spectrophotometer Cary 300-Bio (Varian). A solution of pyrogallol [60 μM in CH_3Cl/MeOH (2:1)] was stable for 48 h as ascertained by RP-HPLC under the elution conditions described before for the analysis of the fractions.

Antioxidant Activity on Red Blood Cells by the AAPH Assay. Blood samples were obtained from healthy donors by venipuncture (Blood Bank of Hospital Vall d'Ebron, Barcelona, Spain) following the ethical guidelines of the hospital and collected in citrated tubes. Red blood cells (RBCs) were separated from plasma and buffy coat by centrifugation at 1000*g* for 10 min. The erythrocyte layer was washed three times in phosphate buffer isotonic saline (PBS) containing 22.2 mM Na_2HPO_4, 5.6 mM KH_2PO_4, 123.3 mM NaCl, and 10.0 mM glucose in distilled water (pH 7.4). The cells were then suspended in isotonic saline solution at a density of 8×10^9 cells/mL. We measured the hemolysis of RBCs mediated by AAPH using a modification of the method described previously (*38*). The addition of AAPH (a peroxyl radical initiator) to the suspension of RBCs induces the oxidation of cell membrane lipids and proteins, thereby resulting in hemolysis. The erythrocyte suspension (250 μL) was incubated in the presence of AAPH at a final concentration of 100 mM for 150 min at 37 °C to achieve 100% hemolysis. Hemolysis was assessed by measuring the absorbance of the supernatant fraction, that is, the hemoglobin release, at 540 nm in a Shimadzu spectrophotometer (Shimadzu, Japan). The antihemolytic activity of the fractions was studied by adding the compounds at several concentrations (10−150 μg/mL)

to the RBCs suspension in the presence of 100 mM AAPH at 37 °C for 2.5 h. The IC_{50} (sample concentration causing 50% protection) of the hemolysis induced by AAPH was determined for each compound.

Cytotoxicity on Keratinocytes and Fibroblasts. To evaluate the cytotoxicity on nontumoral cells, we used the spontaneously immortalized human keratinocyte cell line HaCaT and the mouse fibroblast cell line 3T3. Cells were grown in DMEM (4.5 g/L glucose) supplemented with 10% fetal bovine serum, 2 mM L-glutamine, 10 mM Hepes buffer, and 1% penicillin (10000 U/mL) streptomycin (10000 μg/mL) maintained in a humidified atmosphere with 5% CO_2 at 37 °C. When 75 cm^2 culture flasks were approximately 80% confluent, the cells were seeded into the central 60 wells of 96-well plates as described previously (*39*) at a density of 5.5×10^4 cells/mL for HaCaT and 1.5×10^4 cells/mL for 3T3 (*40*). Plates were incubated at 37 °C and 5% CO_2 for 24 h. Triplicate runs were undertaken with different passage cells. After 1 day of incubation, the growth medium was removed and replaced with exposure medium (DMEM medium supplemented with 5% FBS, 2 mM L-glutamine, 10 mM Hepes buffer, and 1% antibiotic mixture), with or without the polyphenolic mixtures, which were previously sterilized by filtration. Controls, containing culture medium only, were included in each plate. Cells were then incubated at 37 °C and 5% CO_2 for 72 h.

The cell viability was assessed by the neutral red uptake (NRU) assay and performed as described (*41*) and modified to avoid the use of formaldehyde (*42*). After the treatments, medium was aspired and replaced with 100 μL/well of NR solution (50 μg/mL in RPMI medium without phenol red and serum). After 3 h of incubation at 37 °C and 5% CO_2, the medium was aspirated, the cells were washed twice with PBS, and a solution containing 50% ethanol absolute and 1% acetic acid in distilled water was added (100 μL/well) to release the dye incorporated into the viable cells into the supernatant. After 10 min on a microtiter plate shaker, the absorbance of the neutral red was measured at a wavelength of 550 nm in a Bio-Rad 550 microplate reader (Bio-Rad Laboratories, Hercules, CA).

The cytotoxicity of each fraction was expressed as a percentage of viability as compared to control wells (the mean optical density of untreated cells was set to 100% viability) in terms of its IC_{50} (concentration of product that causes 50% inhibition of growth or death of the cell population), calculated from the dose–response curves by linear regression analysis. NRU assay results were expressed as the percentage of uptake of neutral red dye by the lysosomes. Each experiment was performed at least three times using three replicates for each concentration assayed. The results were expressed as means ± SEM. Statistical significance was determined by Student's *t* test and one-way analysis of variance (ANOVA) using the SPSS software (SPSS Inc., Chicago, IL). Statistical significance was considered at $P < 0.05$.

Antiproliferative Activity on SK-Mel-28 Human Melanoma Cells. SK-MEL-28 adherent cells (ATCC #HTB-72) were grown in DMEM supplemented with 10% (v/v) heat-inactivated FCS in the presence of 0.1% (v/v) antibiotics (10000 U/mL penicillin and 10000 μg/mL streptomycin) at 37 °C in a humidified environment with 5% CO_2. The cells were split (ratio 1:2 to 1:5) by mild trypsinization every 4–5 days, and the medium was changed every 2–3 days. The cell culture used in this study was free of mycoplasm infection as shown by the EZ-PCR Mycoplasm test kit (Biological Industries) prior to the treatment with the samples. The cell viability was determined using the Mosmann assay (*43*) with some modifications. Cells were seeded into 96-well plates at 1×10^4 cells/mL density, 200 μL/well, and incubated for 24 h in the culture medium prior to addition of the samples dissolved in DMEM. Control wells were treated with equal volumes of DMEM as the test cultures. After 72 h of culture, the supernatant was aspirated and 100 μL of sterile-filtered MTT (0.5 mg/mL in DMEM) was added to each well. The plates were incubated at 37 °C and 5% CO_2 for 1 h. The supernatant was removed, the blue MTT formazan that precipitated was dissolved in DMSO (100 μL), and the optical density (OD) was measured at 550 nm on a multiwell reader (Merck ELISA System MIOS).

The inhibitory effect of the fractions at each concentration was expressed as a percentage [(mean OD treated cells after 72 h of incubation with the product/mean OD of control cells after 72 h of incubation with extra medium instead of product) × 100]. The IC_{50} or sample concentration causing a 50% reduction in the mean OD value relative to the control at 72 h of incubation was estimated using GraFit 3.00 (Data Analysis and Graphics Program, Erithacus Software Ltd. Microsoft Corp., Surrey, United Kingdom) curve option: IC_{50} curve − start at 0.

Results and Discussion

Fractionation of Witch Hazel Oligomeric Tannins. Following a combination of already described methods (*25, 28, 44*), a polyphenolic mixture of monomeric and oligomeric tannins soluble in both ethyl acetate and water (OWH) was obtained from witch hazel bark. First, a sugar free mixture was obtained by extraction with water/acetone (3:7). After the acetone was evaporated, the lipid soluble material was eliminated with hexane, and the resulting aqueous phase was extracted with ethyl acetate. The organic solvent was eliminated to yield a crude polyphenolic mixture (28.5 g from 3 kg of dry stems, ca. 1% yield). Witch hazel contained more small and medium-sized phenolics (OWH) than grape pomace (OWG, yield ca. 0.1%) (*28*) or pine bark (OWP, yield >0.1%) (*26*). This crude mixture was fractionated (Scheme 1) into eight fractions by a combination of two chromatographic techniques, namely, reversed-phase and size discrimination using the same strategy applied to grape and pine extracts (*25, 26*). RP-HPLC retains solutes by hydrophobicity while Toyopearl HW-40 has been shown to separate flavonoids in order of increasing sizes (*45*). In this way, we generated a collection of mixtures containing hydrolyzable tannins and oligomeric pronthocyanidins of different mean degrees of polymerization, galloylation, and prodelphinidin contents.

Characterization of the Fractions. The structures of significant compounds found in OWH and its fractions are depicted in Figure 2. In accordance with the literature (*44, 46*), the mixtures contained flavanol (catechin) monomers, proanthocyanidins, and hydrolyzable tannins such as hamamelitannin. Some of the mixtures also contained methyl gallate and pentagalloyl glucose. Tables 1 and 2 summarize the results obtained from the HPLC analysis after thioacidolysis (condensed tannins) and direct HPLC-DAD analysis (hamamelitannin, gallic acid, methyl gallate, and pentagalloylglucose). The mean degree of polymerization and composition in constituent monomers of the condensed tannin portion (monomers + proanthocyanidins) were estimated by thioacidolysis in the presence of cysteamine as described in the Experimental Procedures. This procedure, which uses cysteamine hydrochloride as an alternative reagent to thiol-α-toluene, was originally applied to procyanidins (catechol-containing condensed tannins). Now, we have extended the method to prodelphinidins. The appropriate pyrogallol containing new standards, namely, 4-β(2-aminoethylthio) epigallocatechin (Cya-EGC) and 4-β(2-aminoethylthio) epigallocatechin 3-*O*-gallate (Cya-EGCG), have been obtained from the polymeric fraction insoluble in ethyl acetate following essentially the procedures described before (*28*). All of the fractions contained condensed tannins, both monomers and oligomers. Interestingly, the more retained mixture on reversed-phase HPLC (IIH) contained less condensed tannins (34.7%) than IH (79.1%). Small condensed tannins from witch hazel are markedly hydrophilic as compared to phenolics from pine and grape. This is due to the presence of the pyrogallol moiety on ring B,

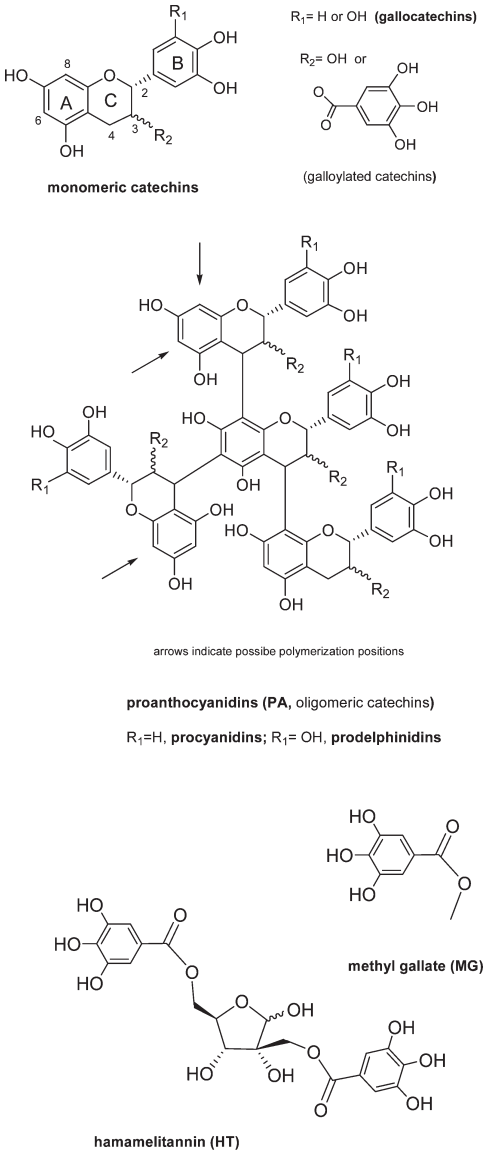

Figure 2. Structures of polyphenolics in *H. virginiana* bark extract.

which is absent in pine and very sparse in grape. Data from Table 2 show that the hydrophobic fractions IIH, VIIH, and VIIIH were low in gallocatechins, which were mainly found in IH, VIH, and IVH. The higher amounts of gallocatechins in the more retained fractions on Toyopearl indicate that they are mainly included in oligomeric structures (prodelphinidins) in contrast with tea gallocatechins, which are monomeric (*47*). This is in agreement with the composition of fraction VH, which was mainly monomeric and low in gallocatechins. The extract and fractions also contained the so-called galloylhamameloses, hydrolyzable tannins that were identified by liquid chromatography coupled to tandem mass spectrometry (LC-MS/MS). Di- and trigalloyl hamamelofuranoses have been described before (*46, 48*). We have identified hamamelitannin (2′,5′ di-*O*-galloyl hamamelose HT *m/z* [M − H]$^-$483, Figure 2) and a pentagalloyl glucose (PGG, *m/z* [M − H]$^-$ 939) as the two main galloyltannins in OWH and derived fractions. Gallic acid (GA) and methyl gallate (MG *m/z* [M − H]$^-$ 183) were detected in some of the fractions. The pentagalloyl glucose content was particularly high in fractions IIH and VIIIH.

Table 1. Polyphenolic Composition of Fractions from Witch Hazel Bark[a]

fraction	% M + PA[b]	mDP[c] M + PA	% HT[d]	% GA[d]	% MG[d]	% PGG[e]
OWH	62.7	1.2	7.9	21.9		7.4
IH	79.1	1.1	10.9	4.1		5.8
IIH	34.7	1.7	2.5	14.7		48.2
IIIH	62.3	1.0	2.1	35.4		0.6
IVH	62.7	1.6	15.0	2.3		19.9
VH	78.8	1.1	2.0	12.1	7.0	
VIH	41.9	2.6	16.1	1.8	18.2	21.7
VIIH	7.9	1.0	0.6	43.3	30.4	17.8
VIIIH	4.3	1.1	0.5	2.4	31.8	61.0

[a] Molar percentages in the total measured phenolics. [b] M + PA, monomeric catechins and proanthocyanidins estimated from the thioacidolysis experiment. [c] mDP, mean degree of polymerization. Mean of three independent thioacidolysis experiments with three RP-HPLC replicate injections. [d] HT, hamamelitannin; GA, gallic acid; and MG, methyl gallate, estimated by HPLC and standards. [e] PGG, pentagalloylglucose, expressed as HT equivalents.

Table 2. Composition of the Condensed Tannins in Polyphenolic Fractions from Witch Hazel Bark[a]

fraction	% GC	% EGC	% C	% EC	% EGCG	% ECG
OWH	14.1	2.0	67.4	5.8	3.6	7.1
IH	11.4	1.5	73.3	7.0	1.6	5.2
IIH	2.8	0.6	70.7	6.2	2.7	16.9
IIIH	4.6	0.4	86.5	6.2	0.3	1.9
IVH	24.9	4.3	38.4	9.3	5.7	17.4
VH	2.1	0.3	89.4	6.5	0.4	1.3
VIH	29.2	4.1	32.9	10.9	4.4	18.4
VIIH	0.0	0.9	75.7	5.7	1.4	16.3
VIIIH	1.5	2.4	44.1	14.1	4.5	3.4

[a] Molar percentage. Mean of three independent thioacidolysis experiments with three RP-HPLC replicate injections.

Briefly, all of the mixtures derived from witch hazel bark presented high amounts of galloylated species pertaining to both condensed and hydrolyzable types of tannins. Some of the fractions, particularly IVH and VIH, also contained the pyrogallol moiety on ring B of their condensed tannins (gallocatechins and prodelphinidins). Because all of the fractions were rich in heavily hydroxylated phenolic molecules, we expected to obtain high free radical-scavenging activities.

Total Antioxidant Activity TAA. The total antioxidant activity of the polyphenolic mixture OWH and its fractions was measured by the ABTS cation radical method, which is a widely used assay for the evaluation of natural antioxidant mixtures such as extracts, juices, and wine (*49, 50*). OWH contained 6 mmol of Trolox equiv/g. In general agreement with the number of hydroxyls per molecule, the OWH extract showed a total antioxidant activity 70% higher than OWP (homologous extract from pine). TAA for the fractions generated from OWH are summarized in Figure 3. As compared to pine bark (*26*), hamamelis was a richer source of free radical-scavenging phenolics. The fractions retained on Toyopearl (IVH, VIH, and VIIIH), which contain bulky galloylated species, concentrated most of the activity, followed by fraction VH. To obtain information on the scavenging efficiency of the phenolics in every fraction, we then turned to the use of stable radicals.

Free Radical Scavenging and Electron Transfer Capacity. The extract and fractions were evaluated as free radical scavengers using different stable radicals, namely, DPPH and the newly introduced HNTTM and TNPTM. DPPH reacts with

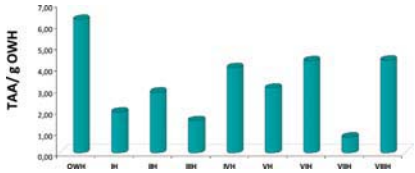

Figure 3. Total antioxidant activity (TAA) of the fractions by the ABTS cation radical method. TAA expressed as mmol Trolox equiv obtained per g of OWH.

Table 3. Hydrogen Donation and Electron Transfer Capacity of Polyphenolic Fractions from Witch Hazel Bark

	DPPH		HNTTM		TNPTM	
fractions	ED_{50}[a]	ARC[b]	ED_{50}	ARC[b]	ED_{50}[a]	ARC[b]
OWH	42.4	23.6	49.8	20.1	1225.5	0.8
IH	44.6	22.4	38.2	26.2	922.5	1.1
IIH	26.1	38.3	60.3	16.6	1592.4	0.6
IIIH	57.9	17.3	86.2	11.6	1059.3	0.9
IVH	28.6	35.0	57.2	17.5	956.0	1.0
VH	58.8	17.0	69.4	14.4	605.3	1.6
VIH	29.5	33.9	45.5	22.0	1488.1	0.7
VIIH	52.8	18.9	77.5	12.9	534.2	1.9
VIIIH	26.4	37.9	49.1	20.4	1265.8	0.8
			control			
Ec	49.3	20.3	60.9	16.4	NR	NR

[a] ED_{50} μg of fraction/μmol of radical, mean of three experiments. [b] ARC, $(1/ED_{50}) \times 10^3$; NR, no reaction.

polyphenols by mechanisms that may include both hydrogen donation and electron transfer (*37, 51*), while the new radicals are only sensitive to electron transfer (*30, 52*). Interestingly, HNTTM reacts with both catechol and pyrogallol moieties, while TNPTM will react only with the most reducing positions, namely, the pyrogallol group on ring B of condensed tannins, while being inactive against cathecols and gallates (*30*). By comparing the results generated with the three radicals, we gained information about the combined hydrogen donation and electron transfer capacity (DPPH), global electron transfer capacity (HNTTM), and the presence of highly reactive electron transfer positions (Figure 1). The results with HNTTM and particularly TNPTM may provide valuable information about the ability of some components to engage in putatively prooxidant/toxic effects involving electron transfer to oxygen. Table 3 summarizes the results obtained with the three radicals. As expected, witch hazel fractions were more potent (1.5−3-fold) scavengers than the homologous pine bark fractions. Again, fractions VIH and VIIIH, rich in bulky galloylated phenolics, were particularly efficient hydrogen donors and electron transfer agents (DPPH and HNTTM assays). Interestingly, fractions IVH (mainly condensed tannins) and VIIIH (mainly hydrolyzable tannins) were equally effective. Because the common structural feature of both fractions is the pyrogallol/gallate group, our results underscore the relevance of the trihydroxybenzene moiety for the scavenging activity of tannins. All of the fractions were active against the TNPTM radical, meaning that they contained highly reactive species. Because the ARCs were low, these reactive species are probably present as minor components. Interestingly, the most effective mixtures (VH and VIIH) were not those with the highest global electron transfer capacity. Both fractions, excluded from the Toyopearl column, were low in proanthocyanidins. Fraction VH contained monomeric catechin as the major component, and both included gallic acid and methyl gallate. None of these single molecules reacted with TNPTM when tested alone. This suggests that the mixtures might contain other reactive species. Alternatively, because all of the fractions were reactive to some extent, it may be that under the test conditions, highly reactive species are formed from otherwise inert precursors. These hypotheses are currently being tested in our laboratory.

Antioxidant Protection of Red Blood Cells. To evaluate the antioxidant protective effect of hamamelis fractions on cells submitted to oxidative stress, we used red blood cells (RBCs). Because of their susceptibility to peroxidation, RBCs have been used as a model to investigate oxidative damage in biomembranes. We investigated the oxidation of RBCs induced by AAPH, a well-known peroxyl radical initiator that causes hemolysis by means of membrane lipid and protein oxidation. Dose–response curves were analyzed, and IC_{50}(concentration triggering 50% inhibition of APPH induced hemolysis) values were obtained for some significant fractions. All of the fractions tested showed an inhibition of the in vitro AAPH-induced RBC hemolysis in a dose-dependent manner (data not shown). The IC_{50} values were 21.5 ± 1.6 (OWH), 22.6 ± 1.7 (IVH), and 24.5 ± 0.8 μg/mL (VIIIH), and all of them were more effective than the homologous fractions from grape and pine (*27*).

Cytotoxicity on Keratinocytes and Fibroblasts. To gain preliminary information about the cytotoxicity of the fractions as compared to their pine and grape homologues, the mixtures were tested on nontumoral HaCat keratinocytes and 3T3 fibroblasts. We selected the 3T3 neutral red uptake assay because this test is recommended by the U.S. National Institute of Environmental Health Science (NIEHS) Interagency Coordinating Committee on the Validation of Alternative Methods (ICCVAM). Nontumorigenic HaCat, a spontaneously immortalized keratinocyte cell line, provides an almost unlimited supply of identical cells, ensuring high intra- and interlaboratory reproducibility. Selected fractions showed some capacity to inhibit the proliferation of nontumoral skin cells with IC_{50} values of 41 ± 2 (OWH), 38 ± 3 (IVH), and 68 ± 10 μg/mL (VIIIH) on HaCat keratinocytes; and 51 ± 3 (OWH), 51 ± 1 (IVH), and 33 ± 3 μg/mL (VIIIH) on 3T3 fibroblasts. The cytotoxicity of the mixtures was relatively low. To visualize how safe the mixtures were for skin cells at their antioxidant active concentration, we calculated the relationship between the cytotoxicity index (IC_{50}) at 72 h in 3T3 and the antioxidant potential. We found that antioxidant concentrations were approximately 1.4−2.4-fold lower than the cytotoxic concentrations. We can conclude that an effective antioxidant activity of the fractions can be obtained at a concentration range not toxic for the nontumoral cell lines studied.

Antiproliferation of SK-Mel 28 Human Melanoma Cells. We and others have shown that plant phenolics influence the viability of eukaryotic cells by arresting the cell cycle and inducing cell death by apoptosis or necrosis (*53–55*). These effects appear to relate to the number and position of phenolic hydroxyls and, consequently, to the free radical scavenging and electron transfer capacity of the active species (*8, 55, 56*). To test the effect of the hamamelis phenolics on skin cancer cells, selected fractions (OWH, IVH, VH, VIH, and VIIIH) homologous to those from grape pomace and pine bark tested before (*25, 26*) were assayed for their influence on the proliferation of SK-Mel 28 human melanoma cells. All of the fractions showed some activity at relatively high concentrations. The IC_{50} values obtained were 26 ± 2 (OWH), 29 ± 2 (IVH), 32 ± 2 (VH), 28 ± 2 (VIH), and 39 ± 2 μg/mL (VIIIH). Interestingly again, the phenolics from witch hazel bark fractions were more efficient antiproliferative agents than those from grape and pine on this tumoral cell line. Particularly, hamamelis phenolics were between 4- and 6-fold more potent than pine bark procyanidins.

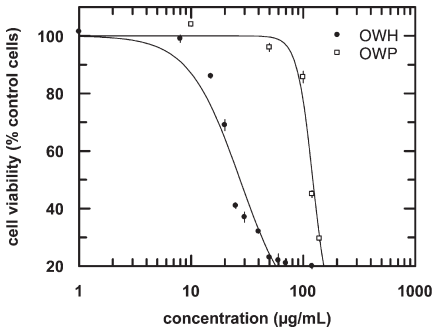

Figure 4. Percentage of proliferation of SK-Mel 28 human melanoma cells as a function of polyphenolic mixture concentration. Samples shown are the crude mixtures soluble in both ethyl acetate and water OWH (□) and OWP (●). Cells were incubated for 72 h with medium alone (control) or containing the polyphenols. $IC_{50} = 26 \pm 2$ μg/mL (OWH) and 122 ± 5 μg/mL (OWP). Data are given as the mean value ± SEM; experiments were performed in triplicate.

Figure 4 depicts the dose–response curve corresponding to the crude extract OWH as compared to the homologous mixture from pine bark (OWP). In agreement with the results on scavenging capacity, fractions IVH and VIIIH, which differed in percentage of condensed and hydrolyzable tannins but had in common a high content in trihydroxybenzene moieties (pyrogallol/gallates), were equally effective against cell proliferation.

In general agreement with the literature (*8, 27, 53, 55*), our comparative results show that the most efficient scavengers (hamamelis phenolics as compared to pine and grape components) as measured with both DPPH and HNTTM stable radicals were also the most cytotoxic/antiproliferative agents. This could be due to the so-called pro-oxidant effect of polyphenols. The generation of the superoxide radical and other ROS by EGCG, quercetin, and other phenolics in a variety of experimental setups have been reported before (*11–13, 22*) and might be behind the mild effect of phenolics on cell growth and apoptotic/necrotic death. The common structural feature mainly responsible for the high activity of witch hazel fractions appears to be the pyrogallol group both on ring B of gallocatechins/prodelphinidins and on galloyl moieties (gallates). Interestingly, fraction VH showed lower global electron transfer capacity than VIH or VIIIH as measured with HNTTM but higher electron transfer capacity as measured by TNPTM. The fact that all three fractions were equally antiproliferative against melanoma cells is in agreement with the presence in VH of the highly reactive species suggested above. The new radical TNPTM may have picked up on some relevant information by detecting the presence of putative cytotoxic species through a simple chemical test. Alternatively or complementarily, the gallate group may be interacting with relevant domains for cell replication (e.g., kinase domains of phosphorylating factors).

Concluding Remarks

Natural plant polyphenols appear to exert their action on living organisms by a combination of redox reactions and receptor–ligand interactions (*14*). They are considered antioxidants and perceived popularly as beneficial agents for the prevention of many diseases. However, what do we really mean by antioxidants? The concept is usually linked to free radical scavenging since it has been accepted that the underlying cause of cell damage is the production of ROS by mitochondrial metabolism and that ROS are essentially harmful and should be eliminated. However, ROS may not be always harmful. First, ROS as well as reactive nitrogen species (RNS) are key agents in the regulation of cell functions by acting as secondary messengers in intracellular signaling cascades (*8, 57*). Second, moderate generation of ROS may end up producing an antioxidant effect by fostering the endogenous defenses. It is becoming evident that mild prooxidant challenges such as physical exercise trigger mild transient oxidative stress with subsequent stimulation of antioxidant detoxifying defenses (*58*). Polyphenols may, at least in part, exert their activity in a similar way by providing mild prooxidant challenges through electron transfer reactions leading to moderate formation of ROS. The so-called prooxidant effect of some polyphenols may be in fact the real antioxidant activity. The results presented here on witch hazel bark phenolics, together with our previous studies with homologous fractions from pine and grape (*25–27, 55*), show that the higher the percentage of pyrogallols in the mixtures is, the higher the antiproliferative potency on epithelial cells is. Because the most cytotoxic/antiproliferative mixtures were also those with the highest electron transfer capacity, we hypothesize that tannins may provide the cell with a mild prooxidative challenge through the formation of the superoxide radical and redox cycling to oxidative species, which may stimulate the endogenous detoxifying systems. The prooxidant activity may be, at least in part, responsible for the alleged antioxidant effect of plant phenolics. The new stable radicals HNTTM and TNPTM, which are sensitive only to electron transfer and possess different redox potentials, may help to define the prooxidant and cytotoxic profile of phenolics. The abundance of pyrogallol groups appears to play a major role in the antioxidant/prooxidant effects of hamamelis phenolics.

Acknowledgment. Financial support of the Spanish Ministry of Education and Science (Research Grants PPQ2003-06602-C04-01, -04, and AGL2006-12210-C03-02/ALI and doctoral fellowships to S.T., D.L., and V.U.) is acknowledged. The assistance of Dr. Olga Jáuregui with the mass spectrometry experiments is greatly appreciated.

Supporting Information Available: RP-HPLC chromatograms obtained for all of the fractions before and after thioacidolysis and dose–response curves from the SK-Mel 28 proliferation assay. This material is available free of charge via the Internet at http://pubs.acs.org.

References

(1) Rusznyák, S. P., and Szent-Györgyi, A. (1936) Vitamin P: Flavonols as vitamins. *Nature 138*, 27.
(2) Ross, J. A., and Kasum, C. M. (2002) Dietary flavonoids: Bioavailability, metabolic effects, and safety. *Annu. Rev. Nutr. 22*, 19–34.
(3) Rice-Evans, C. A., Miller, N. J., and Paganga, G. (1996) Structure-antioxidant activity relationships of flavonoids and phenolic acids. *Free Radical Biol. Med. 20*, 933–956.
(4) Yokozawa, T., Chen, C. P., Dong, E., Tanaka, T., Nonaka, G.-I., and Nishioka, I. (1998) Study on the inhibitory effect of tannins and flavonoids against the 1,1-diphenyl-2-picrylhydrazyl radical. *Biochem. Pharmacol. 56*, 213–222.
(5) Brown, J. E., Khodr, H., Hider, R. C., and Rice-Evans, C. A. (1998) Structural dependence of flavonoid interactions with Cu2+ ions: Implications for their antioxidant properties. *Biochem. J. 330*, 1173–1178.
(6) Hider, R. C., Liu, Z. D., and Khodr, H. H. (2001) Metal chelation of polyphenols. In *Flavonoids and Other Polyphenols* (Packer, L., Ed.) pp 190–203, Academic Press Inc., San Diego, CA.
(7) Ishige, K., Schubert, D., and Sagara, Y. (2001) Flavonoids protect neuronal cells from oxidative stress by three distinct mechanisms. *Free Radical Biol. Med. 30*, 433–446.
(8) Alanko, J., Riutta, A., Holm, P., Mucha, I., Vapaatalo, H., and Metsa-Ketela, T. (1999) Modulation of arachidonic acid metabolism by phenols: Relation to their structure and antioxidant/prooxidant properties. *Free Radical Biol. Med. 26*, 193–201.

(9) Lambert, J. D., Sang, S., and Yang, C. S. (2007) Possible controversy over dietary polyphenols: Benefits vs risks. *Chem. Res. Toxicol. 20*, 583–585.
(10) Kondo, K., Kurihara, M., Miyata, N., Suzuki, T., and Toyoda, M. (1999) Mechanistic studies of catechins as antioxidants against radical oxidation. *Archiv. Biochem. Biophys. 362*, 79–86.
(11) Kondo, K., Kurihara, M., Miyata, N., Suzuki, T., and Toyoda, M. (1999) Scavenging mechanisms of (−)-epigallocatechin gallate and (−)-epicatechin gallate on peroxyl radicals and formation of superoxide during the inhibitory action. *Free Radical Biol. Med. 27*, 855–863.
(12) Nutter, L. M., Wu, Y. Y., Ngo, E. O., Sierra, E. E., Gutierrez, P. L., and Abul-Hajj, Y. J. (1994) An o-quinone form of estrogen produces free radicals in human breast cancer cells: Correlation with DNA damage. *Chem. Res. Toxicol. 7*, 23–28.
(13) Boots, A. W., Li, H., Schins, R. P. F., Duffin, R., Heemskerk, J. W. M., Bast, A., and Haenen, G. (2007) The quercetin paradox. *Toxicol. Appl. Pharmacol. 222*, 89–96.
(14) Sang, S., Hou, Z., Lambert, J. D., and Yang, C. S. (2005) Redox properties of tea polyphenols and related biological activities. *Antioxid. Redox Signaling 7*, 1704–1714.
(15) Liang, Y. C., Lin-shiau, S. Y., Chen, C. F., and Lin, J. K. (1997) Suppression of extracellular signals and cell proliferation through EGF receptor binding by (−)-epigallocatechin gallate in human A431 epidermoid carcinoma cells. *J. Cell Biochem. 67*, 55–65.
(16) Ahmad, N., Cheng, P. Y., and Mukhtar, H. (2000) Cell cycle dysregulation by green tea polyphenol epigallocatechin-3-gallate. *Biochem. Biophys. Res. Commun. 275*, 328–334.
(17) Scalbert, A., Morand, C., Manach, C., and Remesy, C. (2002) Absorption and metabolism of polyphenols in the gut and impact on health. *Biomed. Pharmacother. 56*, 276–282.
(18) Halliwell, B. (2006) Reactive species and antioxidants. Redox biology is a fundamental theme of aerobic life. *Plant Physiol. 141*, 312–322.
(19) Linnane, A. W., Kios, M., and Vitetta, L. (2007) Healthy aging: regulation of the metabolome by cellular redox modulation and prooxidant signaling systems: The essential roles of superoxide anion and hydrogen peroxide. *Biogerontology 8*, 445–467.
(20) Halliwell, B., Zhao, K., and Whiteman, M. (2000) The gastrointestinal tract: A major site of antioxidant action? *Free Radical Res. 33*, 819–830.
(21) Cross, C. E., van der Vliet, A., Louie, S., Thiele, J. J., and Halliwell, B. (1998) Oxidative stress and antioxidants at biosurfaces: Plants, skin, and respiratory tract surfaces. *Environ. Health Perspect. 106* (Suppl. 5), 1241–1251.
(22) Azam, S., Hadi, N., Khan, N. U., and Hadi, S. M. (2004) Prooxidant property of green tea polyphenols epicatechin and epigallocatechin-3-gallate: Implications for anticancer properties. *Toxicol. in Vitro 18*, 555–561.
(23) Plumb, G. W., De Pascual-Teresa, S., Santos-Buelga, C., Cheynier, V., and Williamson, G. (1998) Antioxidant properties of catechins and proanthocyanidins: Effect of polymerization, galloylation and glycosylation. *Free Radical Res. 29*, 351–358.
(24) Saint-Cricq de Gaulejac, N., Vivas, N., Freitas, V., and Bourgeois, G. (1999) The influence of various phenolic compounds on scavenging activity assessed by an enzymatic method. *J. Sci. Food Agric. 79*, 1081–1090.
(25) Torres, J. L., Varela, B., García, M. T., Carilla, J., Matito, C., Centelles, J. J., Cascante, C., Sort, X., and Bobet, R. (2002) Valorization of grape (*Vitis vinifera*) byproducts. Antioxidant and biological properties of polyphenolic fractions differing in procyanidin composition and flavonol content. *J. Agric. Food Chem. 50*, 7548–7555.
(26) Touriño, S., Selga, A., Jiménez, A., Juliá, L., Lozano, C., Lizárraga, D., Cascante, C., and Torres, J. L. (2005) Procyanidin fractions from pine (*Pinus pinaster*) bark: Radical scavenging power in solution, antioxidant activity in emulsion and antiproliferative effect in melanoma cells. *J. Agric. Food Chem. 53*, 4728–4735.
(27) Ugartondo, V., Mitjans, M., Touriño, S., Torres, J. L., and Vinardell, M. P. (2007) Comparative antioxidant and cytotoxic effect of procyanidin fractions from grape and pine. *Chem. Res. Toxicol. 20*, 1543–1548.
(28) Torres, J. L., and Bobet, R. (2001) New flavanol-derivatives from grape (*Vitis vinifera*) byproducts. Antioxidant aminoethylthio-flavan-3ol conjugates from a polymeric waste fraction used as a source of flavanols. *J. Agric. Food Chem. 49*, 4627–4634.
(29) Torres, J. L., Varela, B., Brillas, E., and Juliá, L. (2003) Tris(2,4,6Trichloro-3,5-dinitrophenyl)methyl radical: A new stable coloured magnetic species as a chemosensor for natural polyphenols. *Chem. Commun.* 74–75.
(30) Torres, J. L., Carreras, A., Jiménez, A., Brillas, E., Torrelles, X., Rius, J., and Juliá, L. (2007) Reducing power of simple polyphenols by electron-transfer reactions using a new stable radical of the PTM series, tris(2,3,5,6-tetrachloro-4-nitrophenyl)methyl radical. *J. Org. Chem. 72*, 3750–3756.
(31) Dauer, A., Metzner, P., and Schimmer, O. (1998) Proanthocyanidins from the bark of *Hamamelis virginiana* exibit antimutagenic properties against nitroaromatic compounds. *Planta Med. 64*, 324–327.
(32) Deters, A., Dauer, A., Schnetz, E., Fartasch, M., and Hensel, A. (2001) High molecular compounds (polysaccharides and proanthocyanidins) from *Hamamelis virginiana* bark: Influence on human skin keratinocyte proliferation and differentiation and influence on irritated skin. *Phytochemistry 58*, 949–958.
(33) Matito, C., Mastorakou, F., Centelles, J. J., Torres, J. L., and Cascante, M. (2003) Antiproliferative effect of antioxidant polyphenols from grape in murine Hepa-1c1c7. *Eur. J. Nutr. 42*, 43–49.
(34) Torres, J. L., and Selga, A. (2003) Procyanidin size and composition by thiolysis with cysteamine hydrochloride and chromatography. *Chromatographia 57*, 441–445.
(35) Alcolea, J. F., Cano, A., Acosta, M., and Arnao, M. B. (2002) Hydrophilic and lipofilic antioxidant activities of grapes. *Nahrung 46*, 353–356.
(36) Blois, M. S. (1958) Antioxidant determinations by the use of stable free radical. *Nature 181*, 1199–1200.
(37) Brand-Williams, W., Cuvelier, M. E., and Berset, C. (1995) Use of a free radical method to evaluate antioxidant activity. *Lebensm.-Wiss. Technol. 28*, 25–30.
(38) Miki, M., Tamai, H., Mino, M., Yamamoto, Y., and Niké, E. (1987) Free radical chain oxidation of rat red blood cells by molecular oxygen and its inhibition by α-tocopherol. *Arch. Biochem. Biophys. 258*, 373–380.
(39) Ugartondo, V., Mitjans, M., Lozano, C., Torres, J. L., and Vinardell, M. P. (2006) Comparative study of the cytotoxicity induced by antioxidant epicatechin conjugates obtained from grape. *J. Agric. Food Chem. 54*, 6945–6950.
(40) Babich, H., Krupka, M. E., Nissim, H. A., and Zuckerbraun, H. L. (2005) Differential in vitro cytotoxicity of (−)-epicatechin gallate (ECG) to cancer and normal cells from the human oral cavity. *Toxicol. in Vitro 19*, 231–242.
(41) Borenfreund, E. P., and Rapad, J. (1983) A colorimetric assay to cellular growth and survival: Application to proliferation and cytotoxicity assay. *Toxicol. Lett. 24*, 119–124.
(42) Riddell, R. J., Clothier, R. H., and Ball, M. (1986) An evaluation of three in vitro cytotoxicity assays. *Food Chem. Toxicol. 24*, 469–471.
(43) Mosmann, T. (1983) Rapid colorimetric assay for cellular growth and survival: Application to proliferation and cytotoxicity assays. *J. Immunol. Methods* 55–63.
(44) Dauer, A., Rimpler, H., and Hensel, A. (2003) Polymeric proanthocyanidins from the bark of *Hamamelis virginiana*. *Planta Med. 69*, 89–91.
(45) Sun, B. S., Belchior, G. P., Ricardo da Silva, J. M., and Spranger, M. I. (1999) Isolation and purification of dimeric and trimeric procyanidins from grape seeds. *J. Chromatogr. A 841*, 115–121.
(46) Hartisch, C., and Kolodziej, H. (1996) Galloylhamameloses and proanthocyanidins from *Hamamelis virginiana*. *Phytochemistry 42*, 191–198.
(47) Harbowy, M. E., and Balentine, D. A. (1997) Tea chemistry. *Crit. Rev. Plant Sci. 16*, 415–480.
(48) Haberland, C., and Kolodziej, H. (1994) Novel galloylhamameloses from *Hamamelis virginiana*. *Planta Med. 60*, 464–466.
(49) Miller, N. J., and Rice Evans, C. (1997) The relative contributions of ascorbic acid and phenolic antioxidants to the total antioxidant activity of orange and apple fruit juices and blackcurrant drink. *Food Chem. 60*, 331–337.
(50) Pietta, P., Simonetti, P., and Mauri, P. (1998) Antioxidant activity of selected medicinal plants. *J. Agric. Food Chem. 46*, 4487–4490.
(51) Dangles, O., Fargeix, G., and Dufour, C. (2000) Antioxidant properties of anthocyanins and tannins: A mechanistic investigation with catechin and the 3′,4′,7-trihydroxyflavylium ion. *J. Chem. Soc., Perkin Trans. 2* 1653–1666.
(52) Jiménez, A., Selga, A., Torres, J. L., and Juliá, L. (2004) Reducing activity of polyphenols with stable radicals of the TTM series. Electron transfer versus H-abstraction reactions in flavan-3-ols. *Org. Lett. 6*, 4583–4586.
(53) Tan, X. H., Hu, D. R., Li, S. R., Han, Y., Zhang, Y. L., and Zhou, D. Y. (2000) Differences of four catechins in cell cycle arrest and induction of apoptosis in LoVo cells. *Cancer Lett. 158*, 1–6.
(54) Kozikowski, A. P., Tuckmantel, W., Bottcher, G., and Romanczyk, L. J., Jr. (2003) Studies in polyphenol chemistry and bioactivity. 4. (1) Synthesis of trimeric, tetrameric, pentameric, and higher oligomeric epicatechin-derived procyanidins having all-4β,8-interflavan connectivity and their inhibition of cancer cell growth through cell cycle arrest. *J. Org. Chem. 68*, 1641–1658.
(55) Lizárraga, D., Lozano, C., Briede, J. J., van Delft, J. H., Touriño, S., Centelles, J. J., Torres, J. L., and Cascante, M. (2007) The importance of polymerization and galloylation for the antiproliferative properties of procyanidin-rich natural extracts. *FEBS J. 274*, 4802–4811.

(56) Lozano, C., Torres, J. L., Juliá, L., Jiménez, A., Centelles, J. J., and Cascante, M. (2005) Effect of new antioxidant cysteinyl-flavanol conjugates on skin cancer cells. *FEBS Lett. 579*, 4219–4225.
(57) Valko, M., Leibfritz, D., Moncol, J., Cronin, M. T. D., Mazur, M., and Telser, J. (2007) Free radicals and antioxidants in normal physiological functions and human disease. *Int. J. Biochem. Cell Biol. 39*, 44–84.
(58) Ascensao, A., Magalhaes, J. F., Soares, J. M., Ferreira, R. M., Neuparth, M. J., Appell, H. J., and Duarte, J. A. (2005) Cardiac mitochondrial respiratory function and oxidative stress: The role of exercise. *Int. J. Sports Med. 26*, 258–267.

TX700425N

JOURNAL OF NATURAL PRODUCTS

Article

pubs.acs.org/jnp

Hamamelitannin from Witch Hazel (*Hamamelis virginiana*) Displays Specific Cytotoxic Activity against Colon Cancer Cells

Susana Sánchez-Tena,[†] María L. Fernández-Cachón,[†,‡] Anna Carreras,[§] M. Luisa Mateos-Martín,[§] Noelia Costoya,[⊥] Mary P. Moyer,[∥] María J. Nuñez,[⊥] Josep L. Torres,[§] and Marta Cascante*[,†]

[†]Faculty of Biology, Universitat de Barcelona, IBUB, Unit Associated with CSIC, 08028 Barcelona, Spain

[§]Institute for Advanced Chemistry of Catalonia (IQAC-CSIC), 08034 Barcelona, Spain

[⊥]School of Engineering, Universidade de Santiago de Compostela, 15782 Santiago de Compostela, Spain

[∥]INCELL Corporation, San Antonio, Texas 78249, United States

ABSTRACT: *Hamamelis virginiana* (witch hazel) bark is a rich source of condensed and hydrolyzable tannins reported to exert a protective action against colon cancer. The present study characterizes different witch hazel tannins as selective cytotoxic agents against colon cancer. To cover the structural diversity of the tannins that occur in *H. virginiana* bark, the hydrolyzable tannins, hamamelitannin and pentagalloylglucose, together with a proanthocyanidin-rich fraction (F800H4) were selected for the study. Treatment with these compounds reduced tumor viability and induced apoptosis, necrosis, and S-phase arrest in the cell cycle of HT29 cells, with hamamelitannin being the most efficient. Owing to polyphenol-mediated H_2O_2 formation in the incubation media, the antiproliferative effect was determined in the presence and absence of catalase to rule out any such interference. The presence of catalase significantly changed the IC_{50} only for F800H4. Furthermore, at concentrations that inhibit the growth of HT29 cells by 50%, hamamelitannin had no harmful effects on NCM460 normal colonocytes, whereas pentagalloylglucose inhibited both cancerous and normal cell growth. Using the TNPTM assay, we identified a highly reactive phenolic position in hamamelitannin, which may explain its efficacy at inhibiting colon cancer growth.

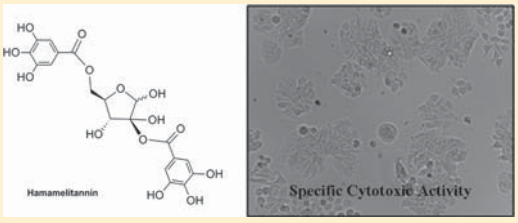

Several epidemiological studies have indicated that tannins may exert a protective effect against colon cancer, one of the most prevalent neoplastic diseases in the developed world.[1,2] Witch hazel (*Hamamelis virginiana*) bark is a rich source of both proanthocyanidins, or condensed tannins, and hydrolyzable tannins (Figure 1) such as hamamelitannin and pentagalloylglucose,[3] whose capacity to regulate cell proliferation, cell cycle, and apoptosis has attracted much attention.[4] An inverse relation has been reported between proanthocyanidins and colorectal cancer.[5] An in vitro study demonstrated that a grape seed proanthocyanidin extract significantly inhibits cell viability and increases apoptosis in Caco-2 colon cancer cells, but does not alter the viability of the normal colon NCM460 cell line.[6] Other results show that proanthocyanidins from different sources are cytotoxic to human colorectal cells.[7−9] In addition, several in vitro and in vivo studies have shown that hydrolyzable tannins from witch hazel bark exhibit multiple biological activities, which may have potential in the prevention and treatment of cancer. In vivo preclinical studies of pentagalloylglucose, one of the major hydrolyzable tannins in witch hazel, demonstrated inhibition of prostate cancer,[10,11] lung cancer,[12] and sarcoma[13] cells. In vitro inhibition of the growth and invasiveness of breast cancer, leukemia, melanoma, and liver cancer cells has also been reported.[14−17] The other major hydrolyzable tannin in witch hazel, hamamelitannin, inhibits TNF-mediated endothelial cell death and DNA fragmentation in EAhy926 endothelial cells.[18] Since TNFα/TNFR1 signaling may act as a tumor promoter for colon carcinogenesis,[19] the anti-TNF activity of hamamelitannin may indicate a protective effect against colon cancer. Furthermore, hamamelitannin has been described to inhibit 5-lipoxygenase (5-LOX),[20] and given that 5-LOX is an inflammatory enzyme involved in malignant transformation,[21] this inhibition could prevent cancer growth.

Moreover, various studies have analyzed the cytotoxicity and scavenging capacity of *H. virginiana* phenolic compounds. It has been reported that different witch hazel polyphenolic fractions are highly active as free radical scavengers against 2,2′-azinobis(3-ethylbenzothiazoline-6-sulfonic acid) (ABTS), 1,1-diphenyl-2-picrylhydrazyl (DPPH), and tris(2,4,6-trichloro-3,5-dinitrophenyl)methyl (HNTTM). They also reduce tris-(2,3,5,6-tetrachloro-4-nitrophenyl)methyl (TNPTM) radical to some extent, which indicates that they contain highly reactive hydroxy groups. In this way, witch hazel fractions protect red blood cells from free radical-induced hemolysis and also inhibit the proliferation of the SK-Mel 28 melanoma tumor cell line.[22] Some of these fractions also inhibited cell proliferation, arrested the cell cycle at the S phase, and induced

Received: May 20, 2011
Published: January 4, 2012

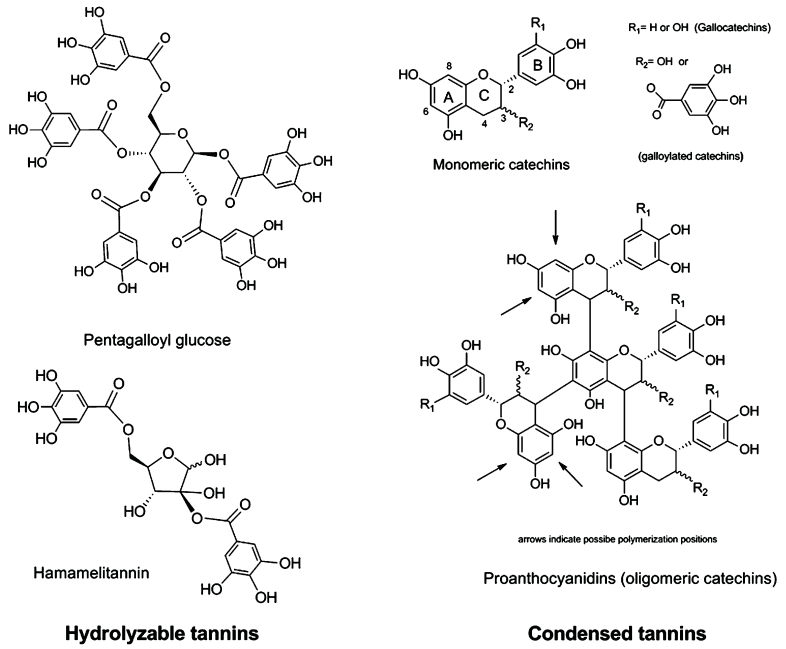

Figure 1. Structures of hydrolyzable and condensed tannins in *Hamamelis virginiana* bark.

apoptosis in HT29 human colon cancer cells.[23] The witch hazel mixtures studied so far include those from highly heterogeneous mixtures containing both hydrolyzable and condensed tannins of low molecular weight, as well as flavan-3-ol monomers;[22,23] however, the activity of oligomeric structures from witch hazel bark has not been evaluated. Furthermore, Masaki et al. reported that hamamelitannin from *H. virginiana* possesses protective activity from cell damage induced by superoxide anion radicals in murine dermal fibroblasts.[24,25]

To advance our understanding of the compounds responsible for the activity of *H. virginiana* bark, we evaluated the behavior of pure hamamelitannin and pentagalloylglucose (hydrolyzable tannins of different size) and a highly purified proanthocyanidin-rich fraction (F800H4). First, we examined the viability, apoptosis, and cell cycle of the human colorectal adenocarcinoma HT29 cell line after treatment with these compounds. To identify products that inhibit cancer cell growth without harming normal cells, the antiproliferative capacity of *Hamamelis* compounds was also measured against the NCM460 cell line (human colonocytes). As several studies have reported that polyphenols can be oxidized under standard cell culture conditions, leading to the production of significant amounts of ROS such as H_2O_2, and that this can modulate cell functions,[26] we supplemented the cell culture medium with catalase, which decomposes polyphenol-generated ROS, thus ruling out this possibility.[27]

RESULTS AND DISCUSSION

Pentagalloylglucose and fraction F800H4 were extracted from the bark of witch hazel, whereas the hydrolyzable tannin hamamelitannin was obtained commercially. Both hydrolyzable tannins presented a purity of 98% or more, as confirmed by HPLC. Once fraction F800H4 was obtained, its polyphenolic composition was characterized to ensure that it possessed a high percentage of condensed tannins. Table 1 summarizes the results of the HPLC analysis after thioacidolysis in the presence of cysteamine (condensed tannins) and direct HPLC analysis (gallic acid, pentagalloylglucose, and hamamelitannin). F800H4 was found to be composed of mostly condensed tannins (83.9% of the total tannins), both monomers and proanthocyanidins [(epi)catechin oligomers and polymers]. It also contained 16.1% hydrolyzable tannins, mainly hamamelitannin. Pentagalloylglucose was not detected in fraction F800H4. The condensed tannins had a mean degree of polymerization (mDP) of 2.6, 35% galloylation and 32% pyrogallol. The total galloylation of the fraction was 45.5%.

Table 1. Polyphenolic Composition of F800H4[a]

Composition of the Condensed Tannins (CTn) 83.9%					
mDP	% G	% P			
2.6	35.0	32.0			
% GC	% EGC	% C	% EC	% EGCG	% ECG
12.4	0.4	29.1	23.0	19.1	15.9
Composition of the Hydrolyzable Tannins (HTn) 16.1%					
% GA		% HT		% PGG	
10.0		90.0		0.0	

[a]mDP, mean degree of polymerization; % G, percentage of galloylation; % P, percentage in pyrogallol; GC, gallocatechin; EGC, epigllocatechin; C, catechin; EC, epicatechin; EGCG, epigallocatechin gallate; ECG, epicatechin gallatel; GA, gallic acid; HT, hamamelitannin; PGG, pentagalloylglucose.

Tannins regulate different cell functions through different actions that may or may not involve redox reactions.[28] Since

dx.doi.org/10.1021/np200426k | J. Nat. Prod. 2012, 75, 26–33

Table 2. Hydrogen Donation and Electron Transfer Capacity

	DPPH			HNTTM			TNPTM		
	EC_{50}[a]	ARP[b]	H/e[c]	EC_{50}[a]	ARP[b]	e[c]	EC_{50}[a]	ARP[b]	e[c]
PGG	23.8	42.0	19.8	54.8	18.2	8.6	2403.9	0.4	0.2
HT	27.8	36.2	8.8	71.2	14.0	3.4	116.2	2.2	1.0
F800H4	39.8	25.1	27.1	66.7	15.0	16.2	1761.6	0.6	0.7

[a]EC_{50}, μg of polyphenol/μmol of radical. [b]ARP, $(1/EC_{50}) \times 10^3$. [c]Number of hydrogen atoms donated or electrons transferred to the stable radical per molecule of polyphenol, calculated as the inverse of 2 × molar EC_{50}.

polyphenols may act as antioxidants and prooxidants, we studied the redox activity of *H. virginiana* compounds and evaluated their free radical scavenging properties using different stable radicals such as DPPH, HNTTM, and TNPTM. DPPH reacts with polyphenols by mechanisms that may include both hydrogen donation and electron transfer,[29] while HNTTM and TNPTM are sensitive only to electron transfer.[30] The reactions with DPPH and HNTTM gave information on the total capacity to scavenge radicals by hydrogen donation or concerted electron proton transfer (DPPH) and by electron transfer (HNTTM). The reaction with TNPTM revealed the presence of highly redox reactive positions. Table 2 summarizes the activities of pentagalloylglucose, hamamelitannin, and the proanthocyanidin fraction F800H4 against the stable free radicals. Overall, pentagalloylglucose, hamamelitannin, and the proanthocyanidin-rich fraction F800H4 showed a similar total scavenging capacity, as their number of phenolic hydroxy groups per unit of mass was similar. Interestingly, differences were detected with TNPTM. While the scavenging capacity of the polyphenols against TNPTM is low because only some of the hydroxy groups are able to donate electrons to this radical, the possible effects of these hydroxy groups may be biologically relevant because they are the most reactive positions. One of the phenolic hydroxy groups in hamamelitannin was reactive enough to transfer its electron to TNPTM, while pentagalloylglucose was much less responsive (Table 2, last column). Hamamelitannin and pentagalloylglucose are structurally similar. In the case of hamamelitannin though, there is a hydroxy moiety geminal to one of the gallate esters, and this might explain the differences detected in the reactivity against the TNPTM radical. The extra hydroxy group might participate in a hydrogen bond with the carbonyl group from the gallate moiety to form a six-membered ring. This could introduce a conformational restriction with loss of planarity and subsequent loss of conjugation within the gallate moiety. The extended conjugation of the carbonyl and aromatic groups is the reason that gallates are less reactive than pyrogallols.[31] The results with TNPTM indicate that hamamelitannin is particularly reactive and may even participate in the formation of ROS through electron transfer to oxygen to form the superoxide radical.

Pentagalloylglucose has been shown to inhibit different malignancies.[10,11,13] Potential mechanisms for its anticancer activity include antiangiogenesis, antiproliferation, S-phase and G1-phase cell cycle arrest, induction of apoptosis, and anti-inflammatory and antioxidative effects . Putative molecular targets include p53, Stat3, Cox-2, VEGFR1, AP-1, SP-1, Nrf-2, and MMP-9. This study reports for the first time the role of pentagalloylglucose in colon cancer. We studied here the viability, the cell cycle, and the apoptosis process in human colorectal adenocarcinoma HT29 cells. In these bioassays, different positive controls were used. Epigallocatechin gallate (EGCG), a major catechin in green tea described to have antitumor activity,[32,33] was used as a standard in the cell viability assays; the cell cycle inhibitor hydroxyurea (HU) was used as a standard in the cell cycle experiments,[34] and staurosporine (ST) was utilized as a positive control in the apoptosis assays.[35] Treatment with pentagalloylglucose reduced the viability of HT29 cells with an IC_{50} value of 28 ± 8.8 μg/mL (Figure 2a) and induced 11% apoptosis compared to control cells, 5% necrosis (Figure 3), and S-phase arrest in the cell cycle with 8% increase in the population of cells in the S phase and a concomitant decrease in the percentage of cells in the G1 and G2 phases (Figure 4). Because pentagalloylglucose inhibits DNA replicative synthesis with greater efficacy than a known DNA polymerase-alpha inhibitor, aphidocolin,[36] this may explain the arrest in the S phase. The antitumor effects of hamamelitannin have not been examined, except for its antigenotoxic action in HepG2 human hepatoma cells reported by Dauer et al.,[37] as well as its anti-TNF[18] and anti-LOX activities.[20] The cellular mechanism that this hydrolyzable tannin induces may be related to the inhibition of the tumor necrosis factor itself and its receptor, which affect apoptosis, necrosis, and cell cycle processes. As a result, after treatment with hamamelitannin, we observed a reduction in the viability of HT29 cells with an IC_{50} of 20 ± 4.5 μg/mL (Figure 2a) and induction of 26% apoptosis, 14% necrosis (Figure 3), and S-phase arrest in the cell cycle with a 16% increase in the population of cells in this phase (Figure 4). With regard to condensed tannins, proanthocyanidins from various sources have been reported to inhibit colon cancer cells.[38,39] Treatment of the human colon adenocarcinoma HT29 cell line with the proanthocyanidin-rich fraction F800H4 extracted from witch hazel bark was less effective at inhibiting cell viability (IC_{50} = 38 ± 4.4 μg/mL; Figure 2a) and inducing apoptosis (9%) and necrosis (6%) (Figure 3) than the same treatment with hydrolyzable tannins. F800H4 had little effect on the normal cell cycle distribution apart from a slight increase in the S and G2 phases (Figure 4).

Overall, the hydrolyzable tannins were more effective than the condensed tannins. Interestingly, hamamelitannin, which includes a highly reactive position, as demonstrated by its reaction with TNPTM (Table 2), showed the strongest inhibition of cell viability, induction of apoptosis and necrosis, and cell cycle arrest in the S phase in HT29 colon cancer cells (Figures 2a, 3, 4). The effect of this reactive position in hamamelitannin may even be prooxidant. The prooxidant effect of some polyphenols has been discussed extensively, and it has been suggested that moderate generation of ROS may produce an antioxidant effect by fostering the endogenous defenses.[40,41] Therefore, in our assays, hamamelitannin may exert its activity, at least in part, by providing mild prooxidant challenges through electron transfer reactions leading to moderate formation of ROS.

On the other hand, since it has been reported that an increase in endogenous ROS levels is required for the transition from the G1 to the S phase of the cell cycle,[42] the cell cycle

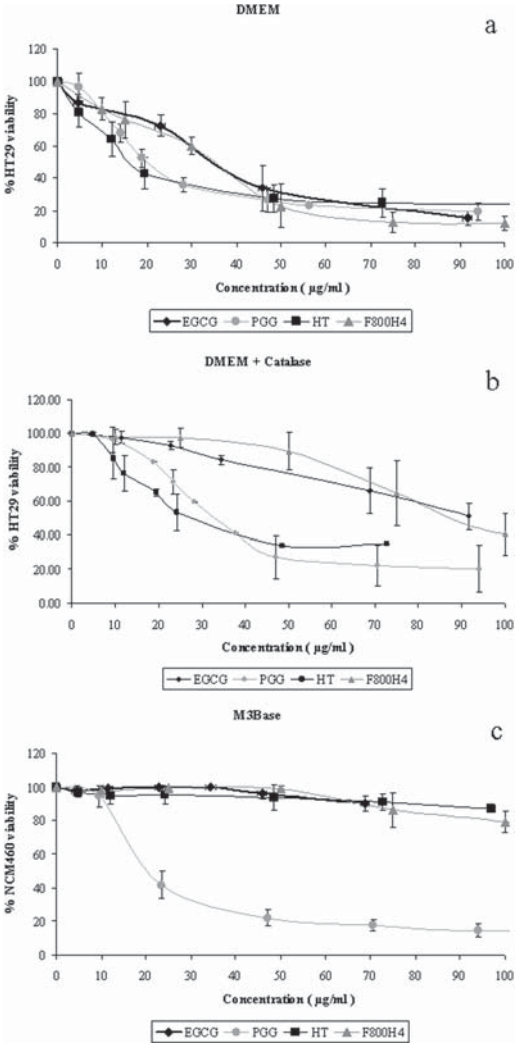

Figure 2. (a) Effect on HT29 cell viability of different concentrations of *Hamamelis virginiana* compounds in DMEM. (b) Effect on HT29 cell viability of witch hazel compounds in DMEM supplemented with catalase (100 U/mL). (c) Effect of Hamamelis products on NCM460 colonocyte growth. In all cases epigallocatechin gallate is used as a standard. Values are represented as mean of percentage of cell viability with respect to control cells ± standard error of three independent experiments.

arrest in the S phase induced by witch hazel compounds may be explained to some extent by its ROS scavenging capacity.

In the search for compounds or fractions that inhibit cancer cell growth without harming normal cells, the antiproliferative capacity of pentagalloylglucose, hamamelitannin, and the proanthocyanidin-rich fraction F800H4 was determined in NCM460 human colonocytes. NCM460 are nontumorigenic cells derived from normal colon mucosa that has not been infected or transfected with any genetic information.[43] This is

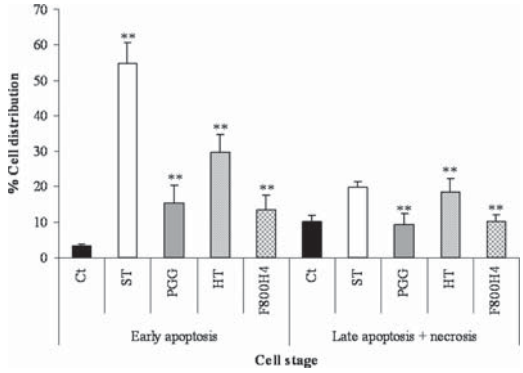

Figure 3. Early apoptotic cells: annexin V+/PI−. Late apoptotic/necrotic cells: annexin V+/PI+ and annexin V−/PI+. Staurosporine is utilized as a positive control. Values are expressed as mean ± standard deviation of three separate experiments. $^{**}p < 0.001$, significant difference with respect to the corresponding value in untreated cells (Ct).

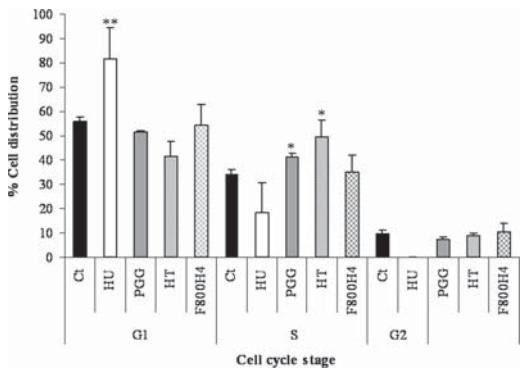

Figure 4. Normalized percentages of cells in different cell stages. Cell phases analyzed: Gl, S, and G2. The cell cycle inhibitor hydroxyurea was used as a standard. Mean ± standard deviation of three separate experiments. $^{*}p < 0.05$; $^{**}p < 0.001$, significant difference with respect to control cells (Ct).

the first comparison of the effects of witch hazel compounds on the growth of nontransformed colonocytes and cancerous colon cells. Our results show that the concentrations of hamamelitannin and F800H4 capable of inducing the death of HT29 cells (Figure 2a) had no harmful effects on normal colon cells (IC_{50} higher than 100 μg/mL for hamamelitannin and F800H4) (Figure 2c), whereas pentagalloylglucose inhibited both cancerous and normal cell growth (Figure 2a, c). Pentagalloylglucose inhibited NCM460 cell viability with an IC_{50} of 23 μg/mL ± 2.4 (Figure 2a, c).

It has been reported that polyphenol-mediated ROS formation in cell culture medium can lead to the artifactual modulation of cytotoxicity attributed to polyphenol exposure. Accordingly, Chai et al. reported that H_2O_2-mediated cytotoxicity, resulting from incubation of PC12 cells with green tea or red wine, was completely prevented by the addition of bovine liver catalase to the culture medium.[44] All *Hamamelis* compounds tested together with the positive

dx.doi.org/10.1021/np200426k | *J. Nat. Prod.* 2012, 75, 26–33

control used (EGCG)[45,46] generated H_2O_2 in a concentration-dependent manner in DMEM (Figure 5a). Hamamelitannin showed the highest H_2O_2 production, at 100 μg/mL. As expected, supplementing the cell culture medium with 100 U/mL catalase resulted in almost complete decomposition of polyphenol-generated H_2O_2 in all cases (Figure 5b). The next step was to study the antiproliferative capacity of *H. virginiana* polyphenolics by co-incubating with catalase. This enzyme had little effect on HT29 cells incubated with hydrolyzable tannins (IC_{50} in DMEM = 28 μg/mL ± 8.8 (Figure 2a)/IC_{50} in DMEM with catalase = 34 μg/mL ± 1.2 (Figure 2b) for pentagalloylglucose and IC_{50} in DMEM = 20 μg/mL ± 4.5 (Figure 2a)/IC_{50} in DMEM with catalase =13 μg/mL ± 4.6 (Figure 2b) for hamamelitannin), whereas F800H4 cytotoxicity was shown to be partially attributable to H_2O_2-mediated modulation (IC_{50} in DMEM = 38 μg/mL ± 4.4 (Figure 2a)/IC_{50} in DMEM with catalase = 95 μg/mL ± 8.7 (Figure 2b)). This effect is probably triggered by the highly reactive pyrogallol moieties in the condensed tannins. Interestingly, the results obtained for the positive control, EGCG, a flavan-3-ol with a pyrogallol B-ring, are in accordance with this hypothesis. Consequently, the difference between the IC_{50} value of F800H4 determined in HT29 cells incubated with catalase (Figure 2b) and the value established in NCM460 cells (Figure 2c) is not as high as when we compared the results obtained for HT29 without catalase (Figure 2a), which were artifactual, with NCM460 (Figure 2c). This demonstrates that, as with pentagalloylglucose, F800H4 is not completely specific against cancer cells. Interestingly, the cytotoxic activity of hamamelitannin was not modified by the addition of catalase to the medium.

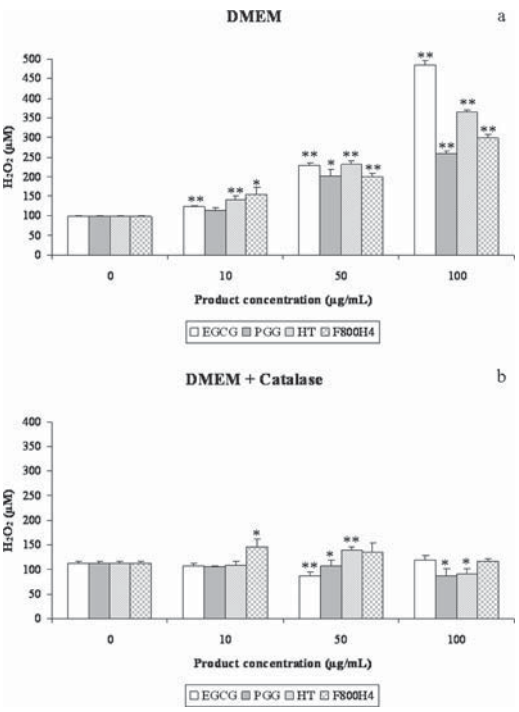

Figure 5. (a) H_2O_2 concentration in cell culture medium (DMEM + 10% FCS + 0.1% streptomycin/penicillin) with pentagalloyl glucose, hamamelitannin, and the proanthocyanidin-rich fraction F800H4 in medium. (b) H_2O_2 concentration produced in DMEM culture medium with catalase (100 U/mL) after incubation with witch hazel compounds. Epigallocatechin gallate is used as a positive control. Mean ± standard deviation of two independent experiments. $^{**}p < 0.001$ and $^{*}p < 0.05$, significant difference with respect to the corresponding value in untreated cells (Ct).

In summary, we conclude that pentagalloylglucose and the proanthocyanidin-rich fraction F800H4 do not show specificity for cancerous cells, whereas hamamelitannin is a promising chemotherapeutic agent, which might be used for the treatment of colon cancer without compromising the viability of normal colon cells. Hamamelitannin appears to contain a highly reactive phenolic position that can be detected by the stable radical TNPTM, which may explain its efficacy at inhibiting colon cancer cell growth. These findings may lead to a better understanding of the structure–bioactivity relationship of tannins, which should be of assistance for formulations of chemopreventive and chemotherapeutic agents.

EXPERIMENTAL SECTION

General Experimental Procedures. UV measurements were made on a Cary 50-Bio UV spectrophotometer (Varian, Palo Alto, CA, USA). Semipreparative chromatography was conducted on a Waters system (Milford, MA, USA) using an X-Terra C_{18} (19 × 250 mm, 10 μm) column. HPLC was carried out on a Hitachi (San Jose, CA, USA) system equipped with a quaternary pump, autosampler, and diode array detector and an analytical Kromasil C_{18} (Teknokroma, Barcelona, Spain) column. All chemicals were purchased from Sigma-Aldrich Co. (St Louis, MO, USA), unless otherwise specified. For extraction, we used deionized water, bulk EtOH (Momplet y Esteban, Barcelona, Spain), bulk acetone (Quimivita, Sant Adrià del Besòs, Spain), and bulk hexane (alkanes mixture) (Quimivita). For purification, deionized water, analytical grade MeOH (Panreac, Montcada i Reixac, Spain), analytical grade acetone (Carlo Erba, Milano, Italy), and preparative grade CH_3CN (E. Merck, Darmstadt, Germany) were used for semipreparative and preparative chromatography; milli-Q water and HPLC grade CH_3CN (E. Merck) were used for analytical RP-HPLC. Analytical grade MeOH (Panreac) was used for thioacidolysis and free radical scavenging assays, and analytical grade CH_3Cl (Panreac) was used for the electron transfer assays. TFA (Fluorochem, Derbyshire, UK) biotech grade was distilled in-house. HCl (37%) and HOAc were from E. Merck. Et_3N (E. Merck) was of buffer grade. Deuterated solvents for NMR were from SDS (Peypin, France). DPPH (95%) was from Aldrich (Gillingham-Dorset, UK), and 6-hydroxy-2,5,7,8-tetramethylchroman-2-carboxylic acid (Trolox) (97%) was from Aldrich (Milwaukee, WI, USA). HNTTM and TNPTM radicals were synthesized as described elsewhere.[30,47] Antibiotics (10 000 U/mL penicillin, 10 000 μg/mL streptomycin) were obtained from Gibco-BRL (Eggenstein, Germany), fetal calf serum (FCS) was from Invitrogen (Paisley, UK), and trypsin EDTA solution C (0.05% trypsin–0.02% EDTA) was from Biological Industries (Kibbutz Beit Haemet, Israel). The annexin V/FITC kit was obtained from Bender System (Vienna, Austria). M3Base medium was purchased from INCELL (San Antonio, TX, USA).

Extraction, Fractionation, and Characterization of F800H4. Polyphenols were obtained from witch hazel bark by extraction with acetone–water (7:3) and fractionation with EtOAc,[22] which produced fraction OWH (polyphenols soluble in EtOAc and H_2O) and fraction AH (polyphenols only soluble in H_2O). To generate fraction F800H4, AH (800 mg) was dissolved in 50% MeOH and fractionated on a Sephadex LH-20 column (50 × 2.5 cm i.d.) using a gradient of MeOH in H_2O and a final step of washing with acetone, as previously reported.[48] Five subfractions (800H1 to 800H5) were collected, and their absorbance was measured at 280 and 400 nm; yield, 8% from

fraction AH; 0.05% from witch hazel bark. Table 1 shows the chemical composition of fraction F800H4, which was estimated as previously described.[22] The content of condensed tannins was estimated by thioacidolytic depolymerization in the presence of cysteamine and HPLC analysis of the cleaved units. The hydrolyzable tannins were determined directly from the fraction by HPLC and standards.

Purification of Pentagalloylglucose. Pentagalloylglucose was purified from fraction OWH by semipreparative chromatography on a Waters system (Milford, MA, USA) using an X-Terra C_{18} (19 × 250 mm, 10 μm) column. A total amount of 2 g of OWH was processed in successive chromatographic runs with loads of 200 mg, 4 mL each, and elution by a binary system [solvent A, 0.1% aqueous TFA; solvent B, 0.08% TFA in H_2O-CH_3CN (1:4)] under the following conditions: 10 min at 16% B and two gradients, 16−36% B over 40 min, and 36−55% B over 5 min, at a flow rate of 10 mL/min with detection at 235 nm. The purity of the pentagalloylglucose was ascertained by HPLC on a Hitachi (San Jose, CA, USA) system equipped with a quaternary pump, autosampler, and diode array detector and an analytical Kromasil C_{18} (Teknokroma, Barcelona, Spain) column under the same elution conditions at a flow rate of 1 mL/min. Pentagalloylglucose was lyophilized, and its identity was confirmed by chromatography coupled to high-resolution mass spectrometry and NMR; purity, 95% by HPLC; yield, 3.8% from fraction OWH, 0.03% from witch hazel bark.

DPPH Assay. The antiradical capacity of the polyphenols was evaluated by the DPPH stable radical method.[49] Fresh MeOH solutions (2 mL) at concentrations ranging from 2 to 30 μM were added to a freshly prepared radical solution (2 mL, 120 μM) in deoxygenated MeOH. The mixture was incubated for 30 min at room temperature in the dark, and the UV absorbance at 517 nm was measured. The results were plotted as the percentage of absorbance disappearance $[(1 - A/A_0) \times 100]$ against the amount of sample divided by the initial concentration of DPPH. Each data point was the result of three independent determinations. A dose−response curve was obtained for every sample. The results are expressed as the efficient concentration, EC_{50}, given as the amount of polyphenols that consumes half the amount of free radical divided by the initial amount of DPPH in micromoles. The results are also expressed as antiradical power (ARP), which is the inverse of EC_{50}. UV measurements were made on a Cary 50-Bio UV spectrophotometer (Varian, Palo Alto, CA, USA).

Electron Transfer Capacity against the Stable Free Radicals HNTTM and TNPTM. Fresh solutions of the polyphenols (2 mL) at concentrations ranging from 2 to 62 μM were added to a freshly prepared solution of HNTTM (2 mL, 120 μM) in deoxygenated $CHCl_3$−MeOH (2:1). The mixture was incubated for 7 h at room temperature in the dark, and the UV absorbance was measured at 384 nm. The results are plotted as the percentage of absorbance disappearance $[(1 - A/A_0) \times 100]$ against the amount of sample divided by the initial amount of the radical in micromoles, as described for DPPH. Each data point was the result of three independent determinations. A dose−response curve was obtained for every sample. The results are expressed as the efficient concentration, EC_{50}, and as ARP. The working conditions with TNPTM were essentially those described for HNTTM[30] with some differences. The concentration range was 10−120 μM, the incubation time was 48 h, and the absorbance was measured at 378 nm. The results are plotted as described for HNTTM.

Cell Culture. Human colorectal adenocarcinoma HT29 cells (obtained from the American Type Culture Collection, HTB-38) were grown as a monolayer culture in Dulbecco's modified Eagle's medium (DMEM) in the presence of 10% heat-inactivated fetal calf serum and 0.1% streptomycin/penicillin in standard culture conditions. NCM460 cells, obtained by a Material Transfer Agreement with INCELL, are from an epithelial cell line derived from the normal colon mucosa of a 68-year-old Hispanic male.[43] They were grown as a monolayer culture in M3Base medium (which contains growth supplements and antibiotics) supplemented with 10% heat-inactivated fetal calf serum and 2.5 mM D-glucose (final concentration 5 mM glucose). The cells were cultured at 37 °C in a 95% air, 5% CO_2 humidified environment.

Determination of Cell Viability. The assay was performed using a variation of the MTT assay described by Mosmann.[50] The assay is based upon the principle of reduction of MTT into blue formazan pigments by viable mitochondria in healthy cells. The cells were seeded at densities of 3×10^3 cells/well (HT29 cells) and 1×10^4 cells/well (NCM460 cells) in 96-well flat-bottom plates. After 24 h of incubation at 37 °C, the polyphenolic samples were added to the cells at different concentrations in fresh medium. Some experiments were performed in the presence of catalase (100 U/mL, from bovine liver) to examine the potential influence on extracellular H_2O_2. The use of an antioxidant enzyme in the cell medium allows us to rule out the effects of exogenous H_2O_2 generated during the incubation with polyphenols. The addition of this enzyme does not affect the cellular markers, since it does not enter the cells and is removed after incubation. In all cases the antitumor agent EGCG was used as standard. The culture was incubated for 72 h. Next the medium was removed, and 50 μL of MTT (1 mg/mL in PBS) with 50 μL of fresh medium was added to each well and incubated for 1 h. The MTT reduced to blue formazan, and the precipitate was dissolved in 100 μL of DMSO; absorbance values were measured on an ELISA plate reader (550 nM) (Tecan Sunrise MR20-301, Tecan, Salzburg, Austria). Absorbance was taken as proportional to the number of living cells. The concentrations that caused 50% cell growth inhibition (IC_{50}) were estimated from the dose−viability curves.

Cell Cycle Analysis by FACS. The cell cycle was analyzed by measuring the cellular DNA content using the fluorescent nucleic acid dye propidium iodide (PI) to identify the proportion of cells in each stage of the cell cycle. The assay was carried out using flow cytometry with a fluorescence-activated cell sorter (FACS). HT29 cells were plated in six-well flat-bottom plates at a density of 87×10^3 cells/well. After 24 h of incubation at 37 °C, the polyphenolic fractions were added to the cells at their respective IC_{50} values. We used the G1/S cell cycle inhibitor HU at 1 mM as standard. The cultures were incubated for 72 h in the absence or presence of the polyphenolic fractions. The cells were trypsinized, pelleted by centrifugation (1500 rpm for 5 min), and stained in Tris-buffered saline containing 50 μg/mL PI, 10 μg/mL RNase free of DNase, and 0.1% Igepal CA-630. They were incubated in the dark for 1 h at 4 °C. Cell cycle analysis was performed by FACS (Epics XL flow cytometer, Coulter Corp., Hialeah, FL, USA) at 488 nm.[51]

Apoptosis Analysis by FACS. Double staining with annexin V-FITC and PI measured by FACS was used to determine the percentage of apoptotic cells. Annexin+/PI− cells were considered early apoptotic cells. Annexin+/PI+ and annexin−/PI+ cells were classed together as late apoptotic/necrotic cells, since this method does not differentiate necrotic cells from cells in late stages of apoptosis, which are also permeable to PI. The cells were seeded, treated, and collected as described in the previous section. ST (1 μM) was utilized as a control of apoptosis induction. After centrifugation (1500 rpm for 5 min), they were washed in binding buffer (10 mM Hepes, pH 7.4, 140 mM NaCl, 2.5 mM $CaCl_2$) and resuspended in the same buffer. Annexin V-FITC was added using the annexin V-FITC kit. Afterward, the cells were incubated for 30 min at room temperature in the dark. Next, PI was added 1 min before the FACS analysis at 20 μg/mL. Fluorescence was measured at 495 nm (annexin V-FITC) and 488 nm (PI).

Determination of H_2O_2 (FOX Assay). H_2O_2 in the cell culture medium was determined using the ferrous oxidation xylenol orange (FOX) assay.[52] After oxidation of Fe(II) to Fe(III) by H_2O_2, the resulting xylenol orange−Fe(III) complex was quantified spectrophotometrically (560 nm). The cells were incubated for 72 h with a range of concentrations of witch hazel compounds in culture medium (DMEM or M3Base) either alone or in the presence of catalase (100 U/mL, from bovine liver) under cell culture conditions (96-well flat-bottom plate, in the absence of cells). EGCG was used as a positive control in this assay given that it has already been reported that this product generates high levels of ROS in cell culture media. Next, 100 μL of medium was transferred to a new 96-well flat-bottom plate. FOX reagent (900 μL) was added to each aliquot: 100 μM xylenol orange, 250 μM ferrous ammonium sulfate, 25 mM H_2SO_4 and 4 mM BHT in

90% (v/v) MeOH. After 30 min, absorbance at 560 nm was measured in a microplate reader (Tecan Sunrise MR20-301, Tecan). Peroxides were quantified by comparing the absorbance to a standard curve (H_2O_2 concentrations: 0−150 μM).

Data Presentation and Statistical Analysis. Data are given as the means ± SD (standard deviation). For each assay, the parametric unpaired two-tailed independent sample *t* test was used for statistical comparison with the untreated control cells, and differences were considered to be significant when $p < 0.05$ and $p < 0.001$.

AUTHOR INFORMATION

Corresponding Author

*Phone: 0034 934021593. Fax: 0034 934021559. E-mail: martacascante@ub.edu.

Present Address

‡Freiburg Institute for Advanced Studies. School of Life Sciences−LifeNet, Freiburg im Breisgau, Germany.

ACKNOWLEDGMENTS

Financial support was provided by grants SAF2008-00164, SAF2011-25726, AGL2006-12210-C03-02/ALI, and AGL2009-12374-C03-03/ALI from the Spanish government Ministerio de Ciencia e Innovación and personal financial support (FPU program); from the Ministerio de Educación y Ciencia; and from the Red Temática de Investigación Cooperativa en Cáncer, Instituto de Salud Carlos III, Spanish Ministry of Science and Innovation & European Regional Development Fund (ERDF) "Una manera de hacer Europa" (ISCIII-RTICC grants RD06/0020/0046). We have also received financial support from the AGAUR-Generalitat de Catalunya (grant 2009SGR1308, 2009 CTP 00026, and Icrea Academia Award 2010 granted to M.C.) and the European Commission (FP7) ETHERPATHS KBBE-grant agreement no. 22263.

REFERENCES

(1) Theodoratou, E.; Kyle, J.; Cetnarskyj, R.; Farrington, S. M.; Tenesa, A.; Barnetson, R.; Porteous, M.; Dunlop, M.; Campbell, H. *Cancer Epidemiol. Biomarkers Prev.* **2007**, *16*, 684−693.

(2) Cutler, G. J.; Nettleton, J. A.; Ross, J. A.; Harnack, L. J.; Jacobs, D. R. Jr.; Scrafford, C. G.; Barraj, L. M.; Mink, P. J.; Robien, K. *Int. J. Cancer.* **2008**, *123*, 664−671.

(3) Vennat, B.; Pourrat, H.; Pouget, M. P.; Gross, D.; Pourrat, A. *Planta Med.* **1988**, *54*, 454−457.

(4) Hu, H.; Chai, Y.; Wang, L.; Zhang, J.; Lee, H. J.; Kim, S. H.; Lu, J. *Mol. Cancer Ther.* **2009**, *8*, 2833−2843.

(5) Mutanen, M.; Pajari, A. M.; Paivarinta, E.; Misikangas, M.; Rajakangas, J.; Marttinen, M.; Oikarinen, S. *Asia Pac. J. Clin. Nutr.* **2008**, *17* (Suppl 1), 123−125.

(6) Engelbrecht, A. M.; Mattheyse, M.; Ellis, B.; Loos, B.; Thomas, M.; Smith, R.; Peters, S.; Smith, C.; Myburgh, K. *Cancer Lett.* **2007**, *258*, 144−153.

(7) Chung, W. G.; Miranda, C. L.; Stevens, J. F.; Maier, C. S. *Food Chem. Toxicol.* **2009**, *47*, 827−836.

(8) Gosse, F.; Guyot, S.; Roussi, S.; Lobstein, A.; Fischer, B.; Seiler, N.; Raul, F. *Carcinogenesis* **2005**, *26*, 1291−1295.

(9) Kolodziel, H.; Heberland, C.; Woerdenbag, H. J.; Konings, A. W. T. *Phytother. Res.* **1995**, *9*, 410−415.

(10) Hu, H.; Lee, H. J.; Jiang, C.; Zhang, J.; Wang, L.; Zhao, Y.; Xiang, Q.; Lee, E. O.; Kim, S. H.; Lu, J. *Mol. Cancer Ther.* **2008**, *7*, 2681−2691.

(11) Kuo, P. T.; Lin, T. P.; Liu, L. C.; Huang, C. H.; Lin, J. K.; Kao, J. Y.; Way, T. D. *J. Agric. Food Chem.* **2009**, *57*, 3331−3339.

(12) Huh, J. E.; Lee, E. O.; Kim, M. S.; Kang, K. S.; Kim, C. H.; Cha, B. C.; Surh, Y. J.; Kim, S. H. *Carcinogenesis* **2005**, *26*, 1436−1445.

(13) Miyamoto, K.; Kishi, N.; Koshiura, R.; Yoshida, T.; Hatano, T.; Okuda, T. *Chem. Pharm. Bull. (Tokyo)* **1987**, *35*, 814−822.

(14) Chen, W. J.; Chang, C. Y.; Lin, J. K. *Biochem. Pharmacol.* **2003**, *65*, 1777−1785.

(15) Chen, W. J.; Lin, J. K. *J. Biol. Chem.* **2004**, *279*, 13496−13505.

(16) Oh, G. S.; Pae, H. O.; Oh, H.; Hong, S. G.; Kim, I. K.; Chai, K. Y.; Yun, Y. G.; Kwon, T. O.; Chung, H. T. *Cancer Lett.* **2001**, *174*, 17−24.

(17) Ho, L. L.; Chen, W. J.; Lin-Shiau, S. Y.; Lin, J. K. *Eur. J. Pharmacol.* **2002**, *453*, 149−158.

(18) Habtemariam, S. *Toxicon* **2002**, *40*, 83−88.

(19) Sakai, H.; Yamada, Y.; Shimizu, M.; Saito, K.; Moriwaki, H.; Hara, A. *Chem. Biol. Interact.* **2010**, *184*, 423−430.

(20) Hartisch, C.; Kolodziej, H.; von Bruchhausen, F. *Planta Med.* **1997**, *63*, 106−110.

(21) Wasilewicz, M. P.; Kolodziej, B.; Bojulko, T.; Kaczmarczyk, M.; Sulzyc-Bielicka, V.; Bielicki, D.; Ciepiela, K. *Int. J. Colorectal Dis.* **2010**, *25*, 1079−1085.

(22) Touriño, S.; Lizarraga, D.; Carreras, A.; Lorenzo, S.; Ugartondo, V.; Mitjans, M.; Vinardell, M. P.; Julia, L.; Cascante, M.; Torres, J. L. *Chem. Res. Toxicol.* **2008**, *21*, 696−704.

(23) Lizarraga, D.; Tourino, S.; Reyes-Zurita, F. J.; de Kok, T. M.; van Delft, J. H.; Maas, L. M.; Briede, J. J.; Centelles, J. J.; Torres, J. L.; Cascante, M. *J. Agric. Food Chem.* **2008**, *56*, 11675−11682.

(24) Masaki, H.; Atsumi, T.; Sakurai, H. *Free Radical Res. Commun.* **1993**, *19*, 333−340.

(25) Masaki, H.; Atsumi, T.; Sakurai, H. *Biol. Pharm. Bull.* **1995**, *18*, 59−63.

(26) Halliwell, B. *FEBS Lett.* **2003**, *540*, 3−6.

(27) Bellion, P.; Olk, M.; Will, F.; Dietrich, H.; Baum, M.; Eisenbrand, G.; Janzowski, C. *Mol. Nutr. Food Res.* **2009**, *53*, 1226−1236.

(28) Sang, S.; Hou, Z.; Lambert, J. D.; Yang, C. S. *Antioxid. Redox Signal.* **2005**, *7*, 1704−1714.

(29) Foti, M. C.; Daquino, C.; Geraci, C. *J. Org. Chem.* **2004**, *69*, 2309−2314.

(30) Torres, J. L.; Carreras, A.; Jimenez, A.; Brillas, E.; Torrelles, X.; Rius, J.; Julia, L. *J. Org. Chem.* **2007**, *72*, 3750−3756.

(31) Sato, M.; Toyazaki, H.; Yoshioka, Y.; Yokoi, N.; Yamasaki, T. *Chem. Pharm. Bull. (Tokyo)* **2010**, *58*, 98−102.

(32) Singh, B. N.; Shankar, S.; Srivastava, R. K. *Biochem. Pharmacol.* **2011**, *82*, 1807−1821.

(33) Yang, C. S.; Wang, H.; Li, G. X.; Yang, Z.; Guan, F.; Jin, H. *Pharmacol. Res.* **2011**, *64*, 113−122.

(34) Iacomino, G.; Medici, M. C.; Napoli, D.; Russo, G. L. *J. Cell. Biochem.* **2006**, *99*, 1122−1131.

(35) Elsaba, T. M.; Martinez-Pomares, L.; Robins, A. R.; Crook, S.; Seth, R.; Jackson, D.; McCart, A.; Silver, A. R.; TomLinson, I. P.; Ilyas, M. *PLoS One.* **2010**, *5*, e10714.

(36) Hu, H.; Zhang, J.; Lee, H. J.; Kim, S. H.; Lu, J. *Carcinogenesis* **2009**, *30*, 818−823.

(37) Dauer, A.; Hensel, A.; Lhoste, E.; Knasmuller, S.; Mersch-Sundermann, V. *Phytochemistry* **2003**, *63*, 199−207.

(38) McDougall, G. J.; Ross, H. A.; Ikeji, M.; Stewart, D. *J. Agric. Food Chem.* **2008**, *56*, 3016−3023.

(39) Maldonado-Celisa, M. E.; Roussia, S.; Foltzer-Jourdainne, C.; Gosse, F.; Lobstein, A.; Habold, C.; Roessner, A.; Schneider-Stock, R.; Raul, F. *Cell. Mol. Life Sci.* **2008**, *65*, 1425−1434.

(40) Ascensao, A. A.; Magalhaes, J. F.; Soares, J. M.; Ferreira, R. M.; Neuparth, M. J.; Appell, H. J.; Duarte, J. A. *Int. J. Sports Med.* **2005**, *26*, 258−267.

(41) Dhakshinamoorthy, S.; Long, D. J. 2nd; Jaiswal, A. K. *Curr. Top Cell Regul.* **2000**, *36*, 201−216.

(42) Havens, C. G.; Ho, A.; Yoshioka, N.; Dowdy, S. F. *Mol. Cell. Biol.* **2006**, *26*, 4701−4711.

(43) Moyer, M. P.; Manzano, L. A.; Merriman, R. L.; Stauffer, J. S.; Tanzer, L. R. *In Vitro Cell Dev. Biol. Anim.* **1996**, *32*, 315−317.

(44) Chai, P. C.; Long, L. H.; Halliwell, B. *Biochem. Biophys. Res. Commun.* **2003**, *304*, 650−654.

(45) Elbling, L.; Weiss, R. M.; Teufelhofer, O.; Uhl, M.; Knasmueller, S.; Schulte-Hermann, R.; Berger, W.; Micksche, M. *FASEB J.* **2005**, *19*, 807−809.
(46) Long, L. H.; Clement, M. V.; Halliwell, B. *Biochem. Biophys. Res. Commun.* **2000**, *273*, 50−53.
(47) Torres, J. L.; Varela, B.; Brillas, E.; Julia, L. *Chem. Commun. (Cambridge, U.K.).* **2003**, 74−75.
(48) Jerez, M.; Touriño, S.; Sineiro, J.; Torres, J. L.; Núñez, M. J. *Food Chem.* **2007**, *104*, 518−527.
(49) Brand-Williams, W.; Cuvelier, M. E.; Berset, C. *LWT−Food Sci. Technol.* **1995**, *28*, 25−30.
(50) Mosmann, T. *J. Immunol. Methods* **1983**, *65*, 55−63.
(51) Lozano, C.; Torres, J. L.; Julia, L.; Jimenez, A.; Centelles, J. J.; Cascante, M. *FEBS Lett.* **2005**, *579*, 4219−4225.
(52) Jiang, Z.-Y.; Hunt, J. V.; Wolff, S. P. *Anal. Biochem.* **1992**, *202*, 384−389.